Final Report

ENVIRONMENTAL EFFECTS ON THE INCUBATION TIME CHARACTERISTICS IN STRESS-CORROSION CRACKING

(N00014-08-1-0646)

Yanyao Jiang
Department of Mechanical Engineering (312)
University of Nevada, Reno
Reno, NV 89557
Phone: 775-784-4510, Fax: 775-784-1701, E-mail: yjiang@unr.edu

Submitted to

Dr. **Asuri K. Vasudevan**

Scientific Officer
Office of Naval Research, Code-332
875 North Randolph Street, Suite 1425, Room- 629
Arlington, VA 22203

April 2011

Final Report

ENVIRONMENTAL EFFECTS ON THE INCUBATION TIME CHARACTERISTICS IN STRESS-CORROSION CRACKING

(N00014-08-1-0646)

Yanyao Jiang
Department of Mechanical Engineering (312)
University of Nevada, Reno
Reno, NV 89557
Phone: 775-784-4510, Fax: 775-784-1701, E-mail: yjiang@unr.edu

Submitted to

Dr. **Asuri K. Vasudevan**

Scientific Officer
Office of Naval Research, Code-332
875 North Randolph Street, Suite 1425, Room- 629
Arlington, VA 22203

April 2011

REPORT DOCUMENTATION PAGE

Form Approved
OMB No. 0704-0188

PLEASE DO NOT RETURN YOUR FORM TO THE ABOVE ADDRESS.

1. REPORT DATE *(DD-MM-YYYY)*	2. REPORT DATE	3. DATES COVERED *(From - To)*
02-05-2011	Final	March 2008-December 2010

4. TITLE AND SUBTITLE

ENVIRONMENTAL EFFECTS ON THE INCUBATION TIME CHARACTERISTICS IN STRESS-CORROSION CRACKING

5a. CONTRACT NUMBER

5b. GRANT NUMBER

N00014-08-1-0646

5c. PROGRAM ELEMENT NUMBER

6. AUTHOR(S)

Yanyao Jiang

5d. PROJECT NUMBER

5e. TASK NUMBER

5f. WORK UNIT NUMBER

7. PERFORMING ORGANIZATION NAME(S) AND ADDRESS(ES)

University of Nevada, Reno
1664 North Virginia Street
204 Ross Hall/Mail Stop 325
Reno, NV 89557-0240

8. PERFORMING ORGANIZATION REPORT NUMBER

9. SPONSORING/MONITORING AGENCY NAME(S) AND ADDRESS(ES)

Office of Naval Research, Code-332
875 North Randolph Street, Suite 1425, Room- 629
Arlington, VA 22203

10. SPONSOR/MONITOR'S ACRONYM(S)

11. SPONSORING/MONITORING AGENCY REPORT NUMBER

12. DISTRIBUTION AVAILABILITY STATEMENT

Approved for Public Release; Distribution is Unlimited

13. SUPPLEMENTARY NOTES

14. ABSTRACT

Stress corrosion cracking (SCC) experiments were conducted on 4340 steel in NaCl aqueous solutions of different concentrations. Despite the differences in controlling conditions, the experiments yielded similar results for the threshold stress intensity factor and the plateau velocity in the 3.5 wt% NaCl solution. Dependence of the plateau velocity on the NaCl concentration was observed. SCC experiments on 7075-T651 Al alloy were conducted in chromate-inhibited, acidic NaCl aqueous solutions with different concentrations. The SCC process consists of three stages: incubation, transient crack growth, and stable crack growth. The incubation time is highly dependent on the load level. For a given NaCl concentration, the relationship between the applied load and the incubation time follows a power law function. A NaCl concentration of 0.1% results in the shortest incubation time and the fastest plateau velocity.

15. SUBJECT TERMS

4340 steel, 7075-T651 aluminum alloy, incubation time, stress corrosion.

16. SECURITY CLASSIFICATION OF:			17. LIMITATION OF ABSTRACT	18. NUMBER OF PAGES	19a. NAME OF RESPONSIBLE PERSON
a. REPORT	b. ABSTRACT	c. THIS PAGE			Yanyao Jiang
UNCLASS	UNCLASS	UNCLASS	UNLIMITED	201	19b. TELEPONE NUMBER *(Include area code)* 775-784-4510

ENVIRONMENTAL EFFECTS ON THE INCUBATION TIME CHARACTERISTICS IN STRESS-CORROSION CRACKING

SUMMARY

The objectives of the research are to (i) explore the incubation time characteristics in stress-corrosion cracking with the influence of the anodic dissolution cracking and hydrogen assisted cracking in different environments and at various applied stresses, and, (ii) quantify the incubation time with respect to the driving force considering the environmental effect.

Extensive stress corrosion cracking (SCC) experiments were conducted on 7075-T651 aluminum alloy and the high strength martensitic steel AISI 4340 (yield stress = 1503 MPa) in sodium chloride (NaCl) aqueous solutions of different concentrations. The experiments on AISI 4340 were conducted under the controls of constant load, constant crack opening displacement (COD), constant loading rate, and constant COD rate. Despite the differences in controlling conditions, the experiments yielded similar results for the threshold stress intensity factor and the plateau velocity in the 3.5 wt% NaCl solution. Dependence of the plateau velocity on the NaCl concentration was observed, while the values of the threshold stress intensity factors appear to be independent of the NaCl concentration in distilled water. Stress corrosion cracking was observed in silicone oil and in paraffin and the general cracking phenomenon was similar to that occurred in water and NaCl solution but at a much lower velocity.

SCC experiments on 7075-T651 aluminum alloy were conducted in a chromate-inhibited, acidic 3.5% NaCl aqueous solution using compact tension specimens with a thickness of 3.8mm under permanent immersion conditions. The effects of loading magnitude, overload, underload, and two-step high-low sequence loading on incubation time and crack growth behavior were investigated. The results show that the SCC process consists of three stages: incubation, transient crack growth, and stable crack growth. The incubation time is highly dependent on the load level. Tensile overload or compressive underload applied prior to SCC significantly altered the initiation time of corrosion cracking. Transition from a high to a low loading magnitude resulted in a second incubation but much shorter or disappearing transient stage. The stable crack growth rate is independent of stress intensity factor in the range of 10 to 22 MPa$\sqrt{m}$. SCC experiments were also conducted in aqueous solution with NaCl concentration ranging from 0.01% (0.0017 M) to 5.0% (0.855 M) to study the influence of NaCl concentration on SSC behavior. For a given NaCl concentration, the relationship between the applied stress intensity factor and the incubation time follows a power law function similar to that of the S-N curve in fatigue. There exists a demarcation NaCl concentration of 0.1% which results in the shortest incubation time and the fastest plateau velocity. Incremental load experiments were conducted to determine the threshold stress intensity factor K_{ISCC} for different NaCl concentrations. It was found that K_{ISCC} decreases with increasing NaCl concentration from 0.03% NaCl to 0.35% NaCl. The K_{ISCC} value is almost identical in the range 4.0~4.5 $MPa\sqrt{m}$ when the NaCl concentration is higher than 0.35%.

TABLE OF CONTENTS

SUMMARY I

TABLE OF CONTENTS II

LIST OF TABLES III

LIST OF FIGURES VIII

I. AISI 4340 STEEL 1

I.1. INTRODUCTION 1

I.2. EXPERIMENT 4

I.3. RESULTS 11

I.3.1. Effect of Loading Rate *12*

I.3.2. Effect of NaCl Concentration *15*

I.4. DISCUSSION 22

I.5 STRESS CORROSION CRACKING EXPERIMENTS OF 4340 STEEL IN SILICON OIL, IN PARAFFIN, AND IN DRY AIR 29

I.6. CONCLUSIONS 33

II. 7075-T651 ALUMINUM ALLOY 35

II.1. INTRODUCTION 35

II.2. EXPERIMENTAL PROCEDURE 36

II.3. RESULTS 44

II.3.1. Typical Features of Stress Corrosion Cracking Behavior *45*

II.3.2. Effect of Loading Magnitude *50*

II.3.3. Effects of Overload and Underload *54*

II.3.4. Effect of High-Low Sequence Loading *56*

II.3.5. Effect of NaCl Concentration on Stress Corrosion of 7075-T651 ..... *59*

II.4. MEASUREMENT OF K_{ISCC} 71

II.5. INFLUENCE OF NACL CONCENTRATION ON FRACTURE STRESS INTENSITY FACTOR 74

II.6. DISCUSSION 77

II.7. CONCLUSIONS 79

ACKNOWLEDEMENTS 80

REFERENCES 81

APPENDIX A EXPERIMENTAL CRACK GROWTH DATA FOR STRESS CORROSION CRACKING OF AISI4340 STEEL 88

APPENDIX B EXPERIMENTAL CRACK GROWTH DATA FOR STRESS CORROSION CRACKING OF 7075T651 143

LIST OF TABLES

Table 1. Chemical composition of AISI 4340, wt% 4
Table 2. Static material properties of AISI 4340 4
Table 3. Constant load experiments 7
Table 4. Constant COD experiments 8
Table 5. Constant displacement at loading point experiments 8
Table 6. Loading rate controlled experiments 9
Table 7. Experiments under COD rate control 10
Table 8. Results of SCC of AISI 4340 in aqueous environments from literature 24
Table 9. Static material properties of 7075-T651 aluminum alloy (E = 72 GPa) 38
Table 10. SCC tests on effect of stress intensity factor on incubation time (3.5% wt NaCl, 0.6 M) 40
Table 11. SCC tests on effect of overload/underload on incubation time (3.5% wt NaCl, 0.6M) 41
Table 12. Effect of high –low sequence loading on SCC (3.5% wt NaCl, 0.6M) 41
Table 13. SCC tests on effect of NaCl concentration and initial stress intensity factor on incubation time and stable crack growth 60
Table 14. Influence of NaCl concentration on incubation time and stable crack growth rate (K_I=10 $MPa\sqrt{m}$) 65
Table 15. Incremental load experiments for K_{ISCC} at different NaCl concentrations 72
Table 16. Fracture stress intensity factor with different NaCl concentrations 75

Table A1. Stress Corrosion Experimental Data for Specimen HT-24 (0% NaCl, Constant Load Control, $P = 3.40kN$) 88
Table A2. Stress Corrosion Experimental Data for Specimen HT-26 (0% NaCl, Constant Load Control, $P = 3.00kN$) 90
Table A3. Stress Corrosion Experimental Data for Specimen HT-27 Step2 (3.5% NaCl, $\delta = 0.042mm$) and Step3 (3.5% NaCl, $P = 1.00kN$) 92
Table A4. Stress Corrosion Experimental Data for Specimen HT-33 Step2 (0% NaCl, $\delta = 0.062mm$) and Step3 (0% NaCl, $P = 0.8kN$) 94
Table A5. Stress Corrosion Experimental Data for Specimen HT-34 step2 (0.35% NaCl, $\delta = 0.070mm$) and step3 (0.35% NaCl, $P = 1.10kN$) 96
Table A6. Stress Corrosion Experimental Data for Specimen HT-40 step2 (0.0035% NaCl, $\delta = 0.051mm$) and step3 (0.0035% NaCl, $P = 1.00kN$) 98
Table A7. Stress Corrosion Experimental Data for Specimen HT-39 step2 (0.0105% NaCl, $\delta = 0.063mm$) and step3 (0.0105% NaCl, $P = 1.10kN$) 100
Table A8. Stress Corrosion Experimental Data for Specimen for HT-37 step1 (0.015% NaCl, $dP/dt = 0.100N/s$) and step2 (0.015% NaCl, $\delta = 0.24mm$) 102
Table A9. Stress Corrosion Experimental Data for Specimen HT-29 (0% NaCl, constant displacement control, $\Delta = 0.191mm$) 105
Table A10. Stress Corrosion Experimental Data for Specimen HT-30 (3.5% NaCl, constant displacement control, $\Delta = 0.141mm$) 109
Table A11. Stress Corrosion Experimental Data for Specimen HT-31 (3.5% NaCl, constant displacement control, $\Delta = 0.122mm$) 112
Table A12. Stress Corrosion Experimental Data for Specimen HT-28 step5 (3.5% NaCl, constant displacement control, $\Delta = 0.121mm$) 114

Table A13. Stress Corrosion Experimental Data for Specimen HT-36 Step2 (3.5% NaCl, constant displacement control, $\Delta = 0.150mm$) 116
Table A14. Stress Corrosion Experimental Data for Specimen HT-38 (0.0228% NaCl, constant loading rate control, $dP/dt = 0.278N/s$) 119
Table A15. Stress Corrosion Experimental Data for Specimen HT-43 (0.012% NaCl, constant loading rate control, $dP/dt = 0.100N/s$) 121
Table A16. Stress Corrosion Experimental Data for Specimen HT-42 (0.0% NaCl, constant loading rate control, $dP/dt = 0.100N/s$) 122
Table A17. Stress Corrosion Experimental Data for Specimen HT-41 (3.5% NaCl, constant loading rate control, $dP/dt = 0.100N/s$) 124
Table A18. Stress Corrosion Experimental Data for Specimen HT-44 step1 (0.0% NaCl, $dP/dt = 0.100N/s$) and step2 (0.0035% NaCl, $dP/dt = 0.100N/s$) and step3 (0.035% NaCl, $dP/dt = 0.037N/s$) 125
Table A19. Stress Corrosion Experimental Data for Specimen HT-47 step1 (0.35% NaCl, $dP/dt = 0.100N/s$) and step2 (0. 35% NaCl, $dP/dt = 0.044N/s$) 127
Table A20. Stress Corrosion Experimental Data for Specimen HT-51 (3.5% NaCl, constant loading rate control, $dP/dt = 0.0325N/s$) 129
Table A21. Stress Corrosion Experimental Data for Specimen HT-52 step2 (3.5% NaCl, constant loading rate control, $dP/dt = 1.000N/s$) 131
Table A22. Stress Corrosion Experimental Data for Specimen HT-54 step1 (3.5% NaCl, $dP/dt = 0.05N/s$) and step2 (3.5% NaCl, $dP/dt = 3.00N/s$) 132
Table A23. Stress Corrosion Experimental Data for Specimen HT-55 step1 (3.5% NaCl, $dP/dt = 3.3N/s$), step2 (3.5% NaCl, $dP/dt = 7.1N/s$), step3 (3.5% NaCl, $dP/dt = 7.5N/s$) and step4 (3.5% NaCl, $dP/dt = 0.68N/s$) 134
Table A24. Stress Corrosion Experimental Data for Specimen HT-45 (3.5% NaCl, constant COD rate control, $d\delta/dt = 1.0e-04mm/s$) 137
Table A25. Stress Corrosion Experimental Data for Specimen HT-48 (3.5% NaCl, constant COD rate control, $d\delta/dt = 2.0e-05mm/s$) 138
Table A26. Stress Corrosion Experimental Data for Specimen HT-49 (3.5% NaCl, constant COD rate control, $d\delta/dt = 2.0e-04mm/s$) 140
Table A27. Stress Corrosion Experimental Data for Specimen HT-50 (3.5% NaCl, constant COD rate control, $d\delta/dt = 1.0e-05mm/s$) 141

Table B1. Stress Corrosion Experimental Data for Specimen SL51 143
Table B2. Stress Corrosion Experimental Data for Specimen SL76 (3.5% NaCl, $K_i = 6.8MPa\sqrt{m}$) 144
Table B3. Stress Corrosion Experimental Data for Specimen SL39 (3.5% NaCl, $K_i = 8MPa\sqrt{m}$) 145
Table B4. Stress Corrosion Experimental Data for Specimen SL33 (3.5% NaCl, $K_i = 9.8MPa\sqrt{m}$) 146
Table B5. Stress Corrosion Experimental Data for Specimen SL41 (3.5% NaCl, $K_i = 10MPa\sqrt{m}$) 147
Table B6. Stress Corrosion Experimental Data for Specimen SL37 (3.5% NaCl, $K_i = 12.2MPa\sqrt{m}$) 148

Table B7. Stress Corrosion Experimental Data for Specimen SL77 (3.5% NaCl, $K_i = 16MPa\sqrt{m}$) 149
Table B8. Stress Corrosion Experimental Data for Specimen SL49 (3.5% NaCl, 25% overload, $K_i = 10MPa\sqrt{m}$) 150
Table B9. Stress Corrosion Experimental Data for Specimen SL45 (3.5% NaCl, Step 1: 50% overload, $K_i = 10MPa\sqrt{m}$, $K_f = 15.34MPa\sqrt{m}$; Step 2: $K_i = 8.27MPa\sqrt{m}$) 151
Table B10. Stress Corrosion Experimental Data for Specimen SL50 (3.5% NaCl, 75% overload, $K_i = 10MPa\sqrt{m}$) 153
Table B11. Stress Corrosion Experimental Data for Specimen SL47 (3.5% NaCl, 100% overload, $K_i = 10MPa\sqrt{m}$) 153
Table B12. Stress Corrosion Experimental Data for Specimen SL46 (3.5% NaCl, 125% overload, $K_i = 10MPa\sqrt{m}$) 154
Table B13. Stress Corrosion Experimental Data for Specimen SL44 (3.5% NaCl, 50% underload, $K_i = 10MPa\sqrt{m}$) 155
Table B14. Stress Corrosion Experimental Data for Specimen SL48 (3.5% NaCl, Step 1: 100% underload, $K_i = 10MPa\sqrt{m}$, $K_f = 12.27MPa\sqrt{m}$; Step 2: $K_i = 10.7MPa\sqrt{m}$) 156
Table B15. Stress Corrosion Experimental Data for Specimen SL66 (5.0% NaCl, $K_i = 10MPa\sqrt{m}$) 158
Table B16. Stress Corrosion Experimental Data for Specimen SL65 (3.0% NaCl, $K_i = 10MPa\sqrt{m}$) 159
Table B17. Stress Corrosion Experimental Data for Specimen SL64 (2.0% NaCl, $K_i = 10MPa\sqrt{m}$) 160
Table B18. Stress Corrosion Experimental Data for Specimen SL62 (1.0% NaCl, $K_i = 10MPa\sqrt{m}$) 161
Table B19. Stress Corrosion Experimental Data for Specimen SL79 (1% NaCl, $K_i = 15MPa\sqrt{m}$) 161
Table B20. Stress Corrosion Experimental Data for Specimen SL102 (0.35% NaCl, $K_i = 6MPa\sqrt{m}$) 162
Table B21. Stress Corrosion Experimental Data for Specimen SL99 (0.35% NaCl, $K_i = 8MPa\sqrt{m}$) 163
Table B22. Stress Corrosion Experimental Data for Specimen SL61 (0.35% NaCl, $K_i = 10MPa\sqrt{m}$) 164
Table B23. Stress Corrosion Experimental Data for Specimen SL78 (0.35% NaCl, $K_i = 15MPa\sqrt{m}$) 165
Table B24. Stress Corrosion Experimental Data for Specimen SL100 (0.35% NaCl, $K_i = 12MPa\sqrt{m}$) 166

Table B25. Stress Corrosion Experimental Data for Specimen SL101 (0.35% NaCl, $K_i = 14MPa\sqrt{m}$) 167
Table B26. Stress Corrosion Experimental Data for Specimen SL63 (0.1% NaCl, $K_i = 10MPa\sqrt{m}$) 168
Table B27. Stress Corrosion Experimental Data for Specimen SL72 (0.1% NaCl, $K_i = 15MPa\sqrt{m}$) 169
Table B28. Stress Corrosion Experimental Data for Specimen SL69 (0.07% NaCl, $K_i = 10MPa\sqrt{m}$) 169
Table B29. Stress Corrosion Experimental Data for Specimen SL67 (0.035% NaCl, $K_i = 10MPa\sqrt{m}$) 170
Table B30. Stress Corrosion Experimental Data for Specimen SL81 (0.035% NaCl, $K_i = 15MPa\sqrt{m}$) 172
Table B31. Stress Corrosion Experimental Data for Specimen SL103 (0.035% NaCl, $K_i = 12MPa\sqrt{m}$) 173
Table B32. Stress Corrosion Experimental Data for Specimen SL104 (0.035% NaCl, $K_i = 14MPa\sqrt{m}$) 175
Table B33. Stress Corrosion Experimental Data for Specimen SL105 (0.035% NaCl, $K_i = 8MPa\sqrt{m}$) 177
Table B34. Stress Corrosion Experimental Data for Specimen SL106 (0.035% NaCl, $K_i = 6MPa\sqrt{m}$) 178
Table B35. Stress Corrosion Experimental Data for Specimen SL114 (0.01% NaCl, $K_i = 8MPa\sqrt{m}$) 180
Table B36. Stress Corrosion Experimental Data for Specimen SL115 (0.01% NaCl, $K_i = 10MPa\sqrt{m}$) 182
Table B37. Stress Corrosion Experimental Data for Specimen SL116 (0.01% NaCl, $K_i = 12MPa\sqrt{m}$) 184
Table B38. Stress Corrosion Experimental Data for Specimen SL70 (0.01% NaCl, $K_i = 10MPa\sqrt{m}$) 186
Table B39. Stress Corrosion Experimental Data for Specimen SL83 (0.01% NaCl, $K_i = 15MPa\sqrt{m}$) 188
Table B40. Incremental load experiment for the determination of K_{ISCC} (Specimen SL92, 3.5% NaCl, $dP/dt = 2.14e-4N/s$) 189
Table B41. Incremental load experiment for the determination of K_{ISCC} (Specimen SL93, 0.1% NaCl, $dP/dt = 2.27e-4N/s$) 189
Table B42. Incremental load experiment for the determination of K_{ISCC} (Specimen SL94, 0.35% NaCl, $dP/dt = 2.26e-4N/s$) 190
Table B43. Incremental load experiment for the determination of K_{ISCC} (Specimen SL95, 1.0% NaCl, $dP/dt = 2.19e-4N/s$) 190

Table B44. Incremental load experiment for the determination of K_{ISCC} (Specimen SL96, 0.035% NaCl, $dP/dt = 2.24e-4N/s$) 191
Table B45. Incremental load experiment for the determination of K_{ISCC} (Specimen SL97, 0.7% NaCl, $dP/dt = 2.25e-4N/s$) 191
Table B46. Incremental load experiment for the determination of K_{ISCC} (Specimen SL98, 5.0% NaCl, $dP/dt = 2.24e-4N/s$) 192

LIST OF FIGURES

Fig.1 Stress-strain curves obtained from experiments for (a) monotonic tension and (b) monotonic torsion 4
Fig. 2 Compact tension specimen used in the SCC experiments (all dimensions are in mm) 5
Fig. 3 Experimental setup for SCC experiments; (a) schematics, (b) photo picture 6
Fig. 4 Multiple step experiment with constant load and constant COD control 10
Fig. 5 Effect of loading rate on (a) threshold stress intensity K_{ISCC} and (b) average plateau crack growth velocity 13
Fig. 6 Variation of stress intensity factor in COD rate controlled experiments 14
Fig. 7 Variation of COD with time in an experiment with constant load rate control 14
Fig. 8 SCC experiments in aqueous NaCl solution of different concentrations 16
Fig. 9 Average plateau crack growth velocity as function of NaCl concentration 17
Fig. 10 Dependence of K_{ISCC} on NaCl concentration 18
Fig. 11 SEM photograph illustrating intergranular SCC in AISI 4340 steel 19
Fig. 12 Photograph of a propagating SCC crack (Specimen HT-43, $dP/dt = 0.1\,N/s$) 20
Fig. 13 Branching of the stress corrosion crack ($dP/dt = 0.1\,N/\sec$, 0.012 wt% NaCl) 21
Fig. 14 Effect of branching on crack growth rate 22
Fig. 15 K_{ISCC} as a function of yield stress for AISI 4340 steel 25
Fig. 16 Plateau velocity as a function of yield stress for AISI 4340 steel 25
Fig. 17 Crack length measured during the experiment and obtained from Eq. [2] 28
Fig. 18 Crack growth rate versus the stress intensity factor for the SCC experiments in silicon oil and paraffin 30
Fig. 19 Comparison of SSC results in aqueous NaCl solution and those in silicon oil and paraffin 30
Fig. 20 Surface crack profile during stress corrosion of 4340 steel in silicon oil 31
Fig. 21 SCC behavior of 4340 steel in dry air at room temperature 32
Fig. 22 Surface crack observation of a CT specimen made of 4340 steel subjected to a constant stress intensity factor (30 $MPa\sqrt{m}$) 33
Fig. 23 Microstructure of 7075-T651 aluminum alloy 37
Fig. 24 Monotonic tensile curves of 7075-T651 aluminum alloy 38
Fig. 25 Compact specimen used in the SCC experiments (all dimensions are in mm): (a) specimen and (b) orientation of the specimens with respect to the rolling axis 39
Fig. 26 Experimental setup for SCC experiments 39
Fig. 27 Schematic representation of the loading system 43
Fig. 28 Variation of stress intensity factor with crack length with and without spring washers 44
Fig. 29 Typical SCC behavior with initial applied stress intensity factor of 14 MPa $\sqrt{m}$ 45
Fig. 30 Typical transient stage for SCC crack growth 46
Fig. 31 Stress corrosion crack observed on specimen surface 47
Fig. 32 Fracture surface during early phase of the stable growth stage 47
Fig. 33 SEM fractographs of SCC zone 49
Fig. 34 Incubation time as a function of initially applied stress intensity factor 50
Fig. 35 Stress corrosion crack growth rate curves under: (a) decreasing and (b) increasing stress intensity factor conditions 51
Fig. 36 Variation of stable crack growth rate with stress intensity factor 52

Fig. 37 Overload effect on incubation time of 7075-T651 aluminum alloy: Comparison with literature data [111] 54
Fig. 38 Effects of overload and underload on plateau crack growth rate of 7075-T651 aluminum alloy 56
Fig. 39 Effect of high-Low sequence loading on SCC of 7075-T651 alloy: (a) stress intensity factor was reduced from 13.7 MPa $\sqrt{m}$ to 10.7 MPa $\sqrt{m}$, (b) stress intensity factor was reduced from 15.3 MPa $\sqrt{m}$ to 8.3 MPa $\sqrt{m}$, and (c, d) variation of crack growth rate with stress intensity factor 59
Fig. 40 Typical SCC behavior in corrosive solutions with different NaCl concentrations with initial applied stress intensity factor of 15 MPa $\sqrt{m}$ 63
Fig. 41 Influence of NaCl concentration of corrosive solution on the plot of crack length versus time 63
Fig. 42 Variation of SCC crack growth rate with stress intensity factor and NaCl concentration 64
Fig. 43 Influence of NaCl concentration on incubation time 65
Fig. 44 Influence of NaCl concentration on incubation time and stable (plateau) crack growth rate 66
Fig. 45 Influence of NaCl concentration on incubation time and stable (plateau) crack growth rate 66
Fig. 46 Comparison of incubation times at two loading magnitudes and different NaCl concentrations 67
Fig. 47 Combined effect of stress intensity factor and NaCl concentration of the solution on the incubation time 68
Fig. 48 NaCl concentration effect on crack profile at stable crack growth stage 69
Fig. 49 Traditional methods to measure K_{ISCC} 71
Fig. 50 Measurement of K_{ISCC} via an incremental load test 73
Fig. 51 Variations of crack length versus stress intensity factor at different NaCl concentrations during the incremental load tests 73
Fig. 52 Dependence of K_{ISCC} on NaCl concentration 74
Fig. 53 Influence of NaCl concentration on the fracture stress intensity factor (the number beside a marker indicates the time to fracture in hours) 76

I. AISI 4340 STEEL

I.1. INTRODUCTION

Environmentally assisted crack growth or stress corrosion cracking (SCC) is one of the major sources of failure in engineering structures and machine components and has been studied over the decades. Significant amount of research including experimental work and modeling efforts has been made on the subject of interaction of the stress and the corrosive environments in metallic materials. It has been established [1-4] that SCC occurs under the influence of tensile stresses and corrosive environments. Despite the generally accepted notion that the tensile stress is a necessary condition for SCC to evolve, it has been shown that SCC can also occur under compressive loads in 7075 aluminum alloy [5]. The mechanism of SCC depends on the material, environment state (gaseous or liquid), and the environmental species. It has been established that high-strength steels with martensitic structures are susceptible to hydrogen-assisted cracking (HAC) [6-11, 12, 13, 14] which is related to embrittlement due to hydrogen diffusion. Experiments with H_2 gas charging revealed the dependence of cracking mechanism on the processes of hydrogen diffusion into the crack tip and the distribution of hydrogen among microstructural sites [4, 7, 15-18]. It was shown that the temperature and pressure of supplied dry hydrogen and H_2S gas have significant effect on the threshold stress intensity of cracking (K_{ISCC}) [14, 19]. It was determined that K_{ISCC} increased with decrease in hydrogen pressure. With an increase in the threshold stress intensity, the fracture mode shifted from intergranular cracking to the microvoid coalescence [19]. Hydrogen embrittlement appears to be a function of the microstructure and loading rate. In materials with higher segregation of impurities at the grain boundaries, intergtanular hydrogen assistsed cracking prevails due to hydrogen trapping at the grain boundaries. On the other hand, hydrogen embrittlement by dislocation motion (plastic strain controlled process) can be achieved in materials with decreased amount of hydrogen traps along the grain boundaries and can lead to transgranular cracking [15].

Low alloy high strength steels have been known to develop SCC in water and saline solutions. Significant amount of work has been directed towards the investigation of SCC in aqueous environments with sodium chloride [2-4, 20-28] as well as other dissolved species [1, 29, 30]. In aqueous environments, the hydrogen atoms become available as a result of electrochemical reactions at the crack tip and are absorbed into the material by the diffusion process [4, 22, 31]. The crack-tip reactions are rather complex and generally consist of anodic and cathodic reactions, and hydrolysis of metal ions [4, 11, 22, 26, 32]. The subsequent hydrogen diffusion occurs under the hydrostatic stress condition. The crack tip processes depend on a variety of factors

which complicate the development of standard testing procedures in stress corrosion cracking experiments [33].

It should be mentioned that, from the historical retrospective, the experimental work on environmentally assisted failure started with utilizing smooth dog-bone shaped specimens subjected to static load in corrosive environments. Later, the concepts of fracture mechanics and use of fatigue pre-cracked specimens were introduced into practice in order to facilitate the SCC process [34]. The first experimental observations on SCC of high strength steels using fatigue pre-cracked specimens revealed the crack growth curves containing the plateau region where the crack extension velocity was virtually independent of the applied stress intensity factor and introduced the concept of threshold stress intensity for stress corrosion cracking [34-37]. A variety of specimen configurations was used in the experiments including standard compact tension (CT), cantilever beam (CB), and wedge opening load (WOL) specimens. Crack extension was typically detected by potential drop, variation in crack opening displacement (COD), or acoustic emission techniques [38, 39]. Each specimen configuration enabled testing under control of constant load or constant displacement, thus adding more variables into the experimental practice [40]. In addition, the effect of loading history (pre-cracking stress intensity in particular) became evident and resulted in significant experimental research [41-44]. Of particular interest is the result produced by Rieck and co-workers [44] who showed the possibility of complete inhibition of SCC by introducing creep in dry non-cracking environment prior to stress corrosion testing. Fracture mechanics aspects [45] as well as material-stress-electrochemistry coupling effects [46-50] were investigated and considered in the experimental programs. Among the multitude of factors affecting the environmentally assisted cracking in aqueous environments, the effect of polarization received a significant attention. It was determined that the application of anodic potential significantly reduced the crack growth rate as compared to the application of cathodic potential [50]. X-ray analysis of residual stresses near the SCC fracture surfaces revealed existence of tensile residual stresses under applied cathodic potential while compressive residual stresses were found in the specimens to which anodic potential was applied [47].

The strain rate at the crack tip is associated with the dislocation motion and influences the transport of the hydrogen into the metal matrix [15]. When cracking occurs in water, the only source of hydrogen is the cathodic reduction. Since the cathodic reduction is a function of the anodic dissolution, which in turn is a crack tip strain controlled process, the hydrogen diffusion and hydrogen embrittlement appear to be a strain rate dependent process [25]. It was observed that under very high strain rates at the crack tip, SCC did not occur due to insufficient time for electrochemical reactions to develop [51]. At the same time, very low strain rates allowed for the complete formation of the passive film at the crack tip which restricts the SCC process [2]. Therefore, a balance between the development of fresh crack and the corrosion

processes needs to be maintained in order for the crack to grow. Such a balance was one of the primary subjects of investigation with the introduction of rising load and rising displacement conditions into experimental practice [52-55]. Significant amount of work on loading rate related processes in SCC of high-strength steels has been done by Dietzel and co-workers [16, 27, 56-58] in an effort to develop a new technique for a faster determination of the threshold stress intensity factor (K_{ISCC}). It was shown that the displacement rate and the loading rate controlled experiments yielded the same values of K_{ISCC} as the one traditionally obtained from the constant load experiments [20, 56]. The extensive experimental work on fatigue pre-cracked SCC specimens under loading rate conditions led in the year 2003 to a new ISO standard governing the use of rising load or rising displacement controls in the SCC experiments for various materials [59].

Anodic dissolution plays an important role in the SCC process by dissolving the metal generally along a specific path which for high strength steels coincides with the prior austenite grain boundaries [25]. Therefore, the effect of prior austenite grain size on the SCC rate has been a subject of study [24, 60, 61]. It was shown experimentally that the prior austenite grain size has no effect on K_{ISCC} when cracking occurred in the 3.5% aqueous NaCl solution and in distilled water [24, 25]. At the same time, it was observed that a decrease in prior austenite grain size led to a decrease in the crack growth rate.

Apparently, the SCC growth is influenced by the concentration of the chloride ions in the solution. It was shown that an increase in the NaCl concentration in saline solutions decreased the crack growth rate [22, 62] under otherwise identical conditions. While chloride ions did not enter the hydrolysis process and were irrelevant to the hydrogen reduction, they degrade passive films on the crack flanks during SCC [26]. It should be mentioned that, to the best knowledge of the authors, the effect of the concentration of Cl^- on SCC in the high-strength steels has not been investigated in detail and deserves an additional consideration. Most of the available experimental work was done either in distilled water or in simulated seawater with 3.5% NaCl concentration.

The current investigation is an experimental study of the environmentally assisted cracking in AISI 4340 steel in aqueous solutions of different NaCl concentrations. A series of experiments were designed and conducted using the compact tension (CT) specimens in an effort to understand the effect of NaCl concentration on the threshold stress intensity factor and the plateau crack growth velocity. Experiments with different loading rates were conducted in order to study the loading rate effect on the SCC of the material under investigation. The experimental set-up was so designed such that a real-time in situ observation of the crack extension can be made to produce accurate first-hand data.

I.2. EXPERIMENT

The material under investigation is AISI 4340 steel which has been used in aeronautic applications including landing gears and reductors. The chemical composition of the material is shown in Table I. Prior to final machining of the testing specimen, the material was heat treated at 860^0C for one hour followed by quenching in agitated warm oil, then tempered at 300^0C for two hours and air cooled.

Table 1. Chemical composition of AISI 4340, wt%

C	Cr	Mn	Mo	Ni	Fe
0.37	0.70	0.70	0.20	1.83	Balance

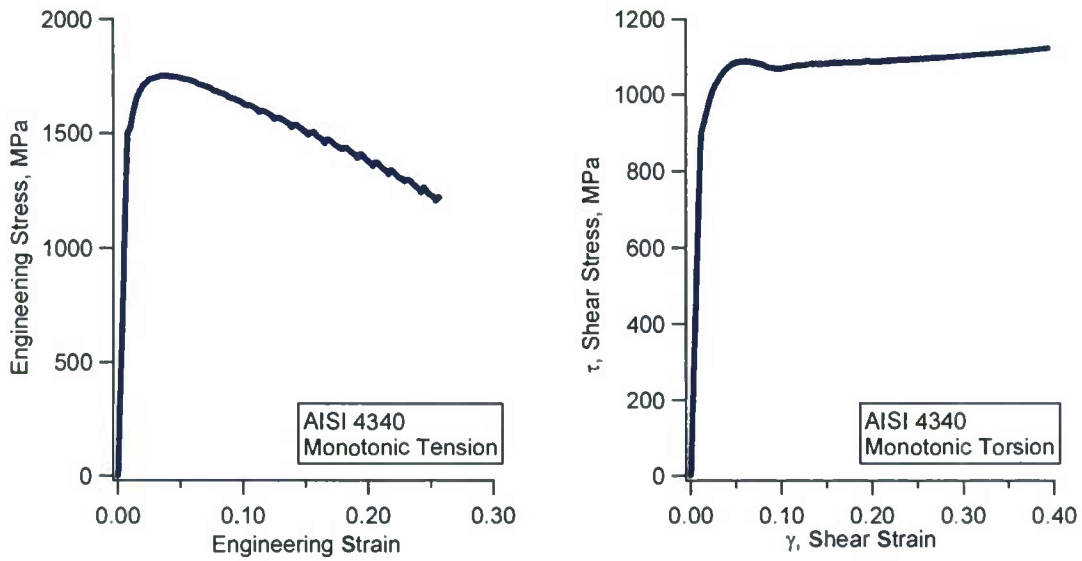

Fig.1 Stress-strain curves obtained from experiments for (a) monotonic tension and (b) monotonic torsion

Table 2. Static material properties of AISI 4340

Elasticity Modulus E (GPa)	207	Ultimate Strength S_u (MPa)	1754
Shear Modulus G (GPa)	80.86	Engineering fracture stress (MPa)	2183
Poisson's Ratio μ	0.28	Engineering Fracture Strain e_f	0.257
Yield Stress σ_y (MPa)	1503	Reduction in Area R_A (%)	44.1

In order to determine the static material properties, one smooth dog-bone shaped specimen was tested under monotonic tension. The gage length of the specimen was 12.7mm and the diameter was 8.0 mm. The stress-strain curve obtained from the monotonic tension test is shown in Fig. 1(a). Another smooth dog-bone shaped

specimen was subjected to pure monotonic torsion loading. The gage length was 25.4 mm and the diameter within the gage length was 12.0 mm. The surface strain was measured by using an extensometer with 3% shear strain range. The extensometer was removed from the specimen after the surface strain reached its range. The surface shear strain higher than 3% was determined by the measured rotational angle of the actuator through a relationship between the surface shear strain and the rotational angle established before the removal of the extensometer from the specimen. The surface shear stress was determined following the Nadai's formula [63]. The shear stress-shear strain curve obtained from monotonic torsion is shown in Fig. 1(b). All the static material properties of the 4340 steel are listed in Table 2. It is noticed that the monotonic torsion experiment is advantageous to monotonic tension because it eliminates the process of necking and enables to obtain the true fracture stress and strain of the material.

Round compact tension (CT) specimens, as shown in Fig. 2, were machined from commercially obtained 4340 steel round bar with a diameter of 44.44 mm in the transversal direction (CR orientation [21]). The heat treatment procedure described previously was done to the specimens prior to testing. The thickness of the specimens was 3.8 mm. Notches were cut using the EDM (electro-discharge machine) process in order to eliminate cold work associated with the traditional saw cutting and drilling. One side of the specimens was polished in order to facilitate the observation of crack growth. The specimens were placed into ultrasonic cleaner prior to testing to remove the residual materials from machining and polishing.

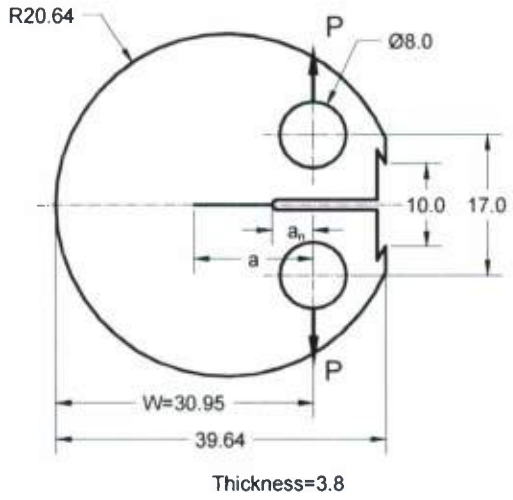

Fig. 2 Compact tension specimen used in the SCC experiments (all dimensions are in mm)

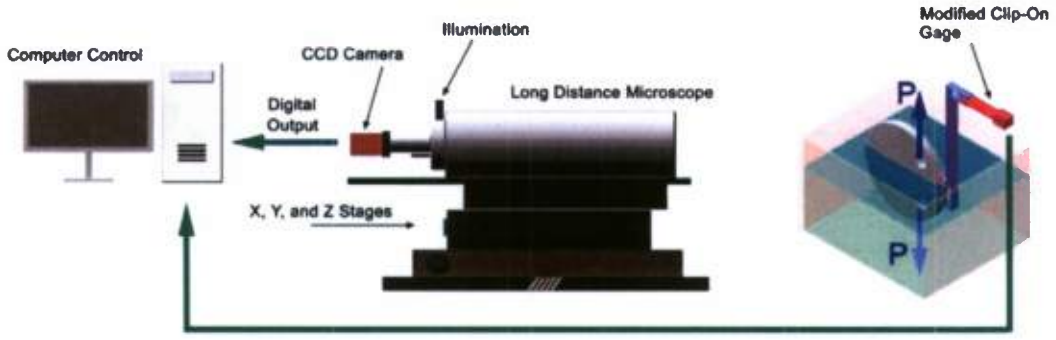

(a)

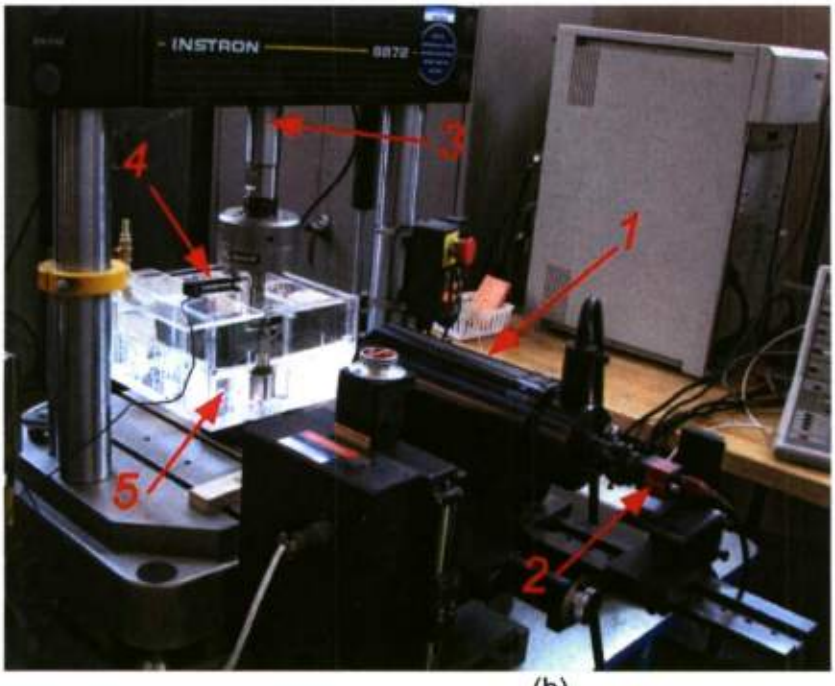

① Long-Distance Microscope QM100
② CCD Camera
③ Instron 8872 Servo-hydraulic Frame
④ Modified Clip-on Extensometer
⑤ Transparent Chamber Containing the Solution

(b)

Fig. 3 Experimental setup for SCC experiments; (a) schematics, (b) photo picture

The crack growth experiments were conducted using an Instron 8870 material testing machine with a 25 kN capacity load cell. Schematics of the experimental setup are shown in Fig. 3. The specimen was placed into a transparent acrylic chamber containing the solution and the crack extension was measured with help of a long-distance optical microscope QM100 (working distance from 150 to 380 mm). The volume of the chamber was 6L and the specimen was installed in such a way that the solution covered approximately 2/3 of the specimen (Fig. 3). The chamber remained naturally aerated during the experiment. The microscope was mounted on a stage allowing for horizontal and vertical motions. The microscope was equipped with a CCD

camera and a direct real-time observation of the crack was done using the computer output and position digital display. A modified clip-on gage was attached to the knife edges of the specimen (Fig. 2) and connected to the Instron electronic control channel which allowed for the acquisition of the data and the control of the crack opening displacement (COD). All of the experiments were conducted at a free potential. In all of the experiments in saline solution, the bulk pH value of the solution was equal to 7 and all the experiments were conducted at room temperature.

With the configuration of the setup described, several types of experiments were conducted with different controlled variables. The experiments were performed under the following controlling conditions: constant load ($P = const$), constant COD ($\delta = const$), constant displacement of the loading point of the specimen ($\Delta = const$), loading rate control ($dP/dt = const$), and COD rate control ($d\delta/dt = const$). The details of the experiments are listed in Tables 3-7. Pre-cracking with decreasing loading amplitude was performed on all of the specimens prior to SCC testing in the solution with the maximum stress intensity factor in a loading cycles being less than 7.0 MPa $m^{1/2}$.

Table 3. Constant load experiments

Spec.#	NaCl %	Step#	P, kN	K_{pr}, MPa $m^{1/2}$	K_{in}, MPa $m^{1/2}$	K_f, MPa $m^{1/2}$	a_i, mm	a_f, mm	t_{inc}, sec	$(da/dt)_p$ mm/sec
HT-24	0	...	3.40	25.70	25.70	90.80	8.004	19.846	203	1.61e-2
HT-26	0	...	3.00	25.80	22.80	76.13	8.006	19.473	631	1.90e-2
HT-36	3.5	1	2.80	4.91	18.00	19.90	6.276	7.338	180	-
HT-27	3.5	1	1.80	5.48	15.00	15.70	9.140	10.153	83	-
		3	1.00	...	14.20	61.13	14.562	24.277	...	4.02e-3
HT-33	0	1	2.97	5.22	20.00	22.70	6.807	7.818	127	-
		3	0.80	...	14.80	72.60	16.952	25.700	...	1.69e-2
HT-34	0.35	1	2.36	5.48	18.00	19.00	7.996	8.559	246	-
		3	1.10	...	16.80	59.27	15.187	23.755	...	4.25e-3
HT-40	0.0035	1	2.25	5.98	14.20	15.08	6.245	6.826	159	-
		3	1.00	...	12.60	58.77	13.405	24.125	...	6.86e-3
HT-39	0.0105	1	2.20	5.25	13.60	21.37	6.064	10.154	171	-
		3	1.10	...	24.80	42.90	18.621	22.163	...	5.36e-3

P – Applied load
K_{pr} – Maximum stress intensity factor at the end of fatigue pre-cracking
K_{in} – Stress intensity factor at the beginning of the experiment
K_f – Stress intensity factor at the termination of the experiment
a_i – Crack length at the beginning of the experiment measured from the line of applied load
a_f – Crack length at the termination of the experiment measured from the line of applied load
t_{inc} – Crack incubation time based on 0.5 mm crack length
$(da/dt)_p$ -average plateau velocity

Table 4. Constant COD experiments

Spec.#	NaCl %	Step#	δ, mm	K_{in}, MPa $m^{1/2}$	K_f, MPa $m^{1/2}$	a_i, mm	a_f, mm
HT-27	3.5	2	0.042	15.70	11.80	10.153	14.325
HT-33	0	2	0.062	23.90	13.40	7.994	16.953
HT-34	0.35	2	0.070	18.33	12.39	8.586	15.188
HT-40	0.0035	2	0.051	16.93	11.12	7.223	13.267
HT-39	0.0105	2	0.063	21.38	11.83	10.155	18.517
HT-37	0.015	2	0.240	39.17	17.29	18.881	28.138

δ – Displacement of the notch flanks at the edge of the specimen (COD displacement)

K_{in} – Stress intensity factor at the beginning of the experiment

K_f – Stress intensity factor at the termination of the experiment

a_i – Crack length at the beginning of the experiment measured from the line of applied load

a_f – Crack length at the termination of the experiment measured from the line of applied load

Table 5. Constant displacement at loading point experiments

Spec.#	NaCl %	Step#	Δ, mm	K_{pr}, MPa $m^{1/2}$	K_{in}, MPa $m^{1/2}$	K_f, MPa $m^{1/2}$	a_i, mm	a_f, mm	t_{inc}, sec	$(da/dt)_p$ mm/sec
HT-29	0	...	0.191	26.2	26.20	14.58	8.048	28.56	245	8.91e-3
HT-30	3.5	...	0.141	19.75	21.60	13.50	8.000	26.75	265	3.48e-3
HT-31	3.5	...	0.122	19.82	18.05	14.96	8.009	27.66	288	3.15e-3
HT-28	3.5	5	0.121	...	17.44	11.85	9.715	26.27	...	3.79e-3
HT-36	3.5	2	0.150	...	16.02	12.30	8.041	25.23	...	4.51e-3

Δ – Displacement of the actuator at the point of load application

K_{pr} – Maximum stress intensity factor at the end of fatigue pre-cracking

K_{in} – Stress intensity factor at the beginning of the experiment

K_f – Stress intensity factor at the termination of the experiment

a_i – Crack length at the beginning of the experiment measured from the line of applied load

a_f – Crack length at the termination of the experiment measured from the line of applied load

t_{inc} – Crack incubation time based on 0.5 mm crack length

$(da/dt)_p$-average plateau velocity

Table 6. Loading rate controlled experiments

Spec.#	NaCl %	Step#	dP/dt, N/sec	K_{pr}, MPa $m^{1/2}$	K_{in}, MPa $m^{1/2}$	K_f, MPa $m^{1/2}$	a_i, mm	a_f, mm	K_{ISCC} MPa $m^{1/2}$	$(da/dt)_p$ mm/sec
HT-38	0.0228	...	0.278	5.54	8.33	57.31	6.02	18.33	9.48	3.78e-3
HT-37	0.015	1	0.100	5.22	8.34	39.17	6.04	18.69	10.9	4.50e-3
HT-43	0.012	...	0.100	4.80	7.9	41.21	5.94	18.19	9.75	3.90e-3
HT-42	0.0	...	0.100	4.73	8.0	58.0	6.22	20.16	9.41	1.02e-2
HT-41	3.5	...	0.100	4.73	7.97	32.94	6.00	16.05	10.9	4.18e-3
HT-44	0.0	1	0.100	4.28	9.17	12.95	5.95	8.03	10.35	4.45e-3
	0.0035	2	0.100	5.07	8.56	19.37	8.29	13.85	9.90	4.45e-3
	0.035	3	0.037	8.51	10.11	18.12	14.13	18.32	10.27	4.45e-3
HT-47	0.35	1	0.100	4.08	8.14	20.32	6.05	13.61	8.30	3.20e-3
		2	0.044	6.78	8.14	58.45	14.32	24.44	9.59	3.20e-3
HT-51	3.5	...	0.0325	3.60	8.97	64.35	6.28	20.43	12.83	3.16e-3
HT-52	3.5	2	1.000	6.60	3.10	53.69	8.19	14.85	10.84	3.39e-3
HT-54	3.5	1	0.050	5.37	6.33	22.20	6.18	11.76	12.18	2.80e-3
		2	3.000	6.04	7.09	90.95	13.59	18.02	11.58	2.80e-3
HT-55	3.5	1	3.300	5.20	0.61	30.08	5.96	7.86	11.55	3.02e-3
		2	7.100	6.77	0.85	44.28	9.14	10.51	12.99	3.02e-3
		3	7.500	7.12	1.06	52.22	11.55	12.61	12.64	3.02e-3
		4	0.680	7.96	6.54	32.58	14.78	18.55	9.83	3.02e-3

dP/dt - Rate of applied external load

K_{pr} – Maximum stress intensity factor at the end of fatigue pre-cracking

K_{in} – Stress intensity factor at the beginning of the experiment

K_f – Stress intensity factor at the termination of the experiment

a_i – Crack length at the beginning of the experiment measured from the line of applied load

a_f – Crack length at the termination of the experiment measured from the line of applied load

K_{ISCC} – Threshold stress intensity factor in stress corrosion

$(da/dt)_p$-average plateau velocity

Table 7. Experiments under COD rate control

Spec.#	NaCl %	$d\delta/dt$, mm/sec	K_{pr}, MPa $m^{1/2}$	K_{in}, MPa $m^{1/2}$	K_f, MPa $m^{1/2}$	a_i, mm	a_f, mm	K_{ISCC} MPa $m^{1/2}$	$(da/dt)_p$ mm/sec
HT-45	3.5	1.0e-04	4.90	6.97	51.49	5.92	14.01	9.96	3.33e-3
HT-48	3.5	2.0e-05	4.36	4.37	19.56	6.01	18.24	12.06	3.86e-3
HT-49	3.5	2.0e-04	3.56	1.94	53.94	6.41	7.61	12.91	2.26e-3
HT-50	3.5	1.0e-05	4.49	4.49	13.89	6.32	16.24	11.54	3.12e-3

$d\delta/dt$ - Rate of crack opening displacement

K_{pr} – Maximum stress intensity factor at the end of fatigue pre-cracking

K_{in} – Stress intensity factor at the beginning of the experiment

K_f – Stress intensity factor at the termination of the experiment

a_i – Crack length at the beginning of the experiment measured from the line of applied load

a_f – Crack length at the termination of the experiment measured from the line of applied load

K_{ISCC} – Threshold stress intensity factor in stress corrosion

$(da/dt)_p$ -average plateau velocity

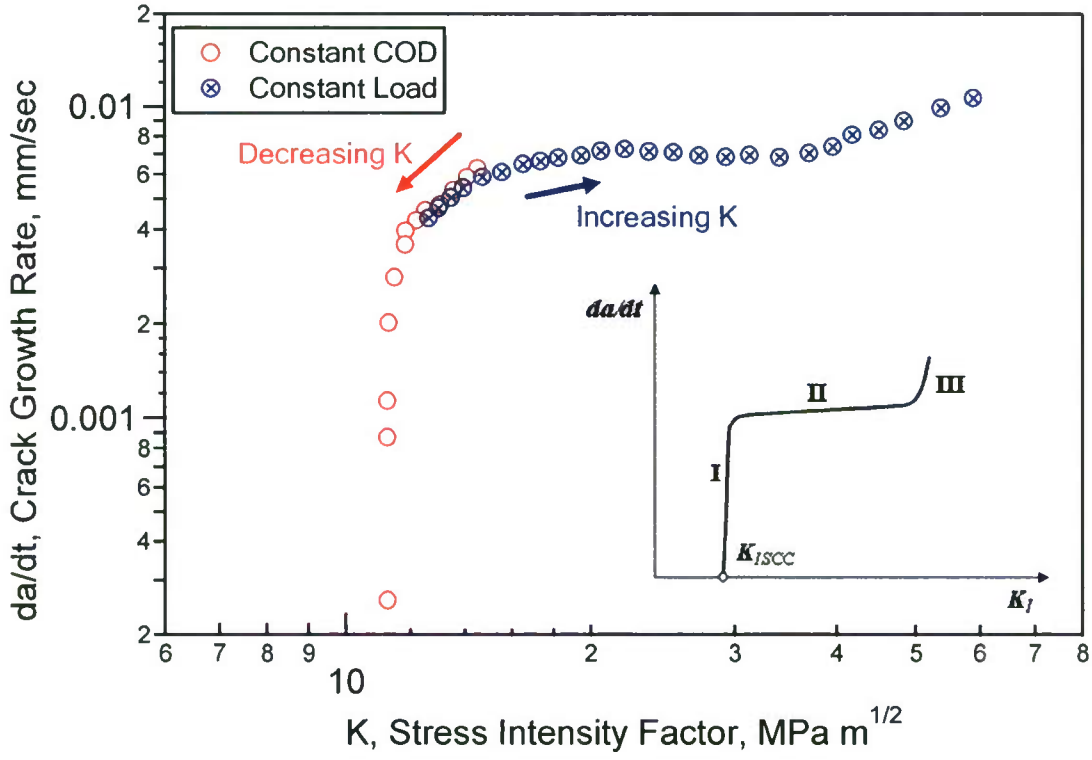

Fig. 4 Multiple step experiment with constant load and constant COD control

As can be seen in Tables 3-7, a majority of the specimens was tested in multiple-step experiments. When the applied load is kept constant, the stress intensity factor increases with the crack extension. When the COD is fixed, the K value decreases with increasing crack length. Therefore, the crack growth curve can be obtained in several steps using a single specimen with different controlled loading conditions. The approach is illustrated in Fig. 4 using the results from Specimen HT-40 tested in 0.0035% NaCl solution. It can be seen that the combination of two controls, constant COD and constant load, can yield a crack growth curve covering all the three stages typically observed in the SCC experiments as illustrated in the insert in Fig. 4.

The multi-step experiments under loading rate control were designed to maximize the experimental data that can be obtained from one single specimen. When the same specimen was tested in several loading steps under different loading rates, fatigue pre-cracking with decreasing amplitude was performed between two loading steps in order to produce a fresh fatigue crack tip each time before the SCC test. The same was done in the case when the experiments were conducted with different NaCl concentrations. Using the loading rate control, the whole crack growth rate curve can be obtained starting from the threshold stress intensity value.

I.3. RESULTS

The current section describes the experimentally obtained results of SCC growth of the 4340 steel. The section is arranged into sub-sections with an emphasis on a particular phenomenon being investigated. The presentation of the crack growth curves is made following the accepted format of the crack growth rate versus the stress intensity factor on a log-log scale. The stress intensity factor was calculated using the following formula [64] for the round CT specimen,

$$\begin{cases} K = P \cdot C \cdot F(\alpha), \\ C = \dfrac{1}{\sqrt{W} \cdot B}, \alpha = \dfrac{a}{W}, \\ F(\alpha) = \dfrac{(2+\alpha)(0.76 + 4.8\alpha - 11.58\alpha^2 + 11.43\alpha^3 - 4.08\alpha^4)}{(1-\alpha)^{3/2}} \end{cases} . \quad (1)$$

where a is the crack length measured from the line of externally applied load P and W and B are the width and the thickness of the specimen, respectively (Fig. 2). Eq. [1] was obtained by the boundary collocation method and has an accuracy of 0.3% when $0.2 \le \alpha \le 1.0$ [64].

The primary data collected as a result of the experiment were the crack length and the elapsed time. A parabolic curve was adopted to best fit a set of seven successive data points in the experimentally obtained relationship between the crack length and

time. The crack growth rate at the middle point was determined from the derivative of the parabola. Detailed experimental results are tabulated for each specimen tested in Appendix A for the 4340 steel.

I.3.1. Effect of Loading Rate

The effect of loading rate on SCC for the 4340 steel was investigated in 3.5% NaCl aqueous solution. Two types of experiments were employed: load rate controlled and COD rate controlled. In all of the experiments, the rate of controlling variable was kept constant. The primary interest was the effect of the loading rate (crack tip strain rate) on the average plateau velocity and the threshold stress intensity factor. The results are shown in Fig. 5. The first plot (Fig. 5(a)) represents the dependence of the SCC threshold stress intensity factor on the rates of COD and the applied load. The loading and COD rates at the onset of cracking are represented as the rate of stress intensity factor on the horizontal axis in Fig. 5(a). Figure 5(b) shows the average plateau velocities corresponding to different values of applied dP/dt and $d\delta/dt$. The markers in Fig. 5 represent the experimentally obtained data points and the thick dotted lines are placed on the graphs to indicate the mean value of the measured quantity.

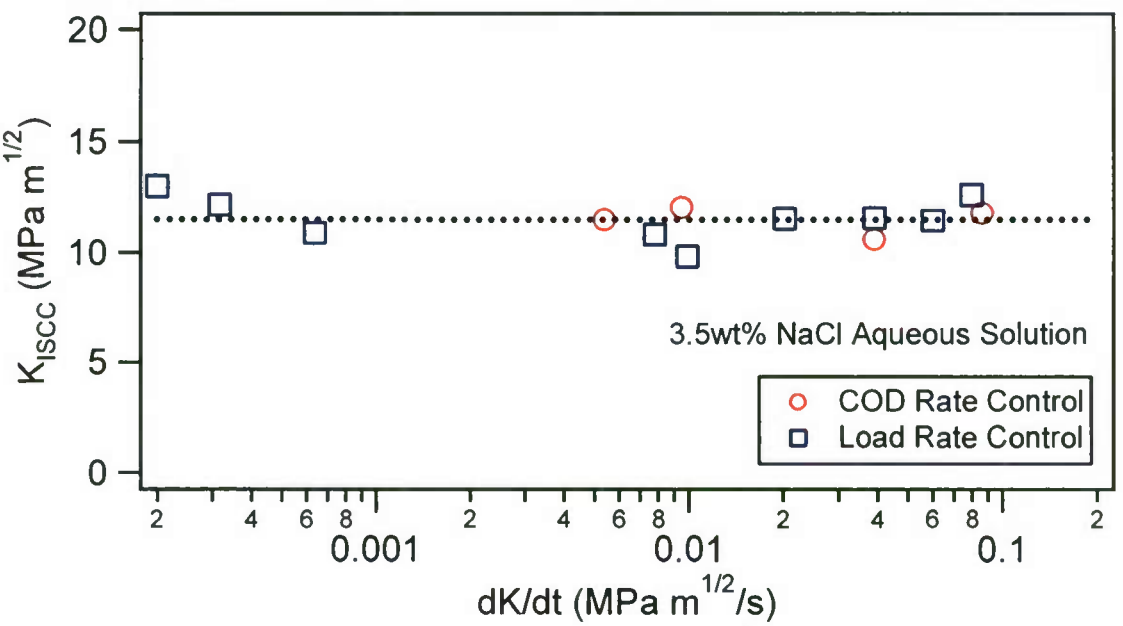

(a)

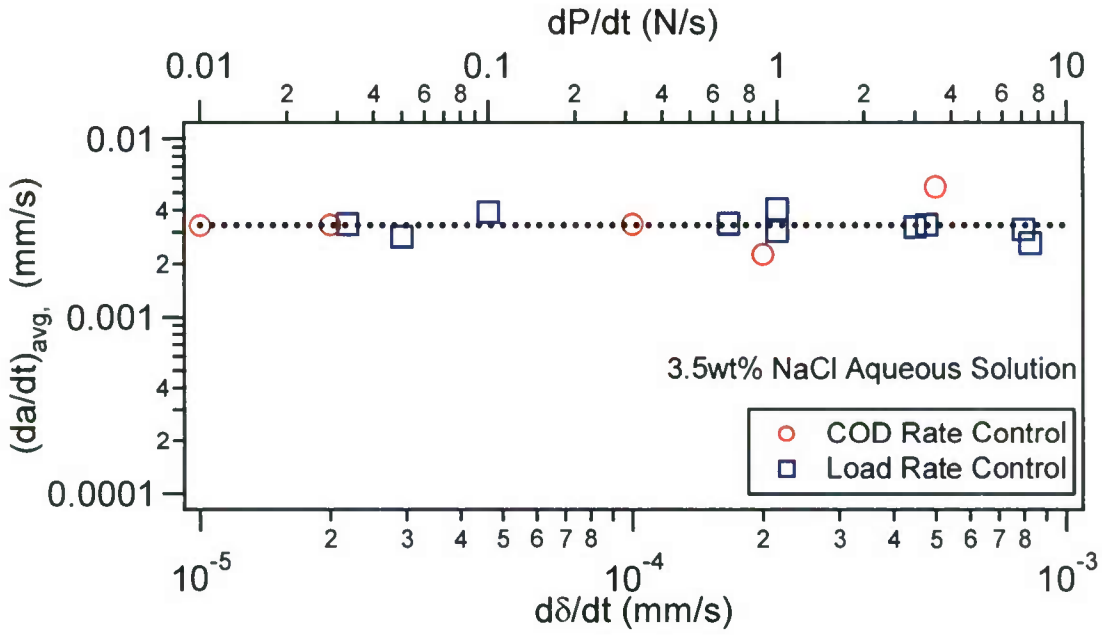

(b)

Fig. 5 Effect of loading rate on (a) threshold stress intensity K_{ISCC} and (b) average plateau crack growth velocity

It can be seen from Fig. 5 that within the range of the applied COD and loading rates used in the experiments, the values of the SCC threshold intensity factors and the plateau crack growth velocities are not practically influenced by the loading rate nor the controlled loading mode (load versus COD). This observation confirms the results previously obtained by Dietzel and co-workers [16, 27, 58].

It should be mentioned that a complete SCC crack growth curve can be obtained only with certain values of COD rates. The variation of the stress intensity factor with the crack length in a constant COD rate controlled experiment in 3.5% NaCl aqueous solution is shown in Fig. 6. It can be seen that under very low rates of COD, the stress intensity factor remains practically constant with the crack extension. In such a case, only the threshold value of the stress intensity factor can be determined from the experiment and the rest of the crack growth curve cannot be obtained.

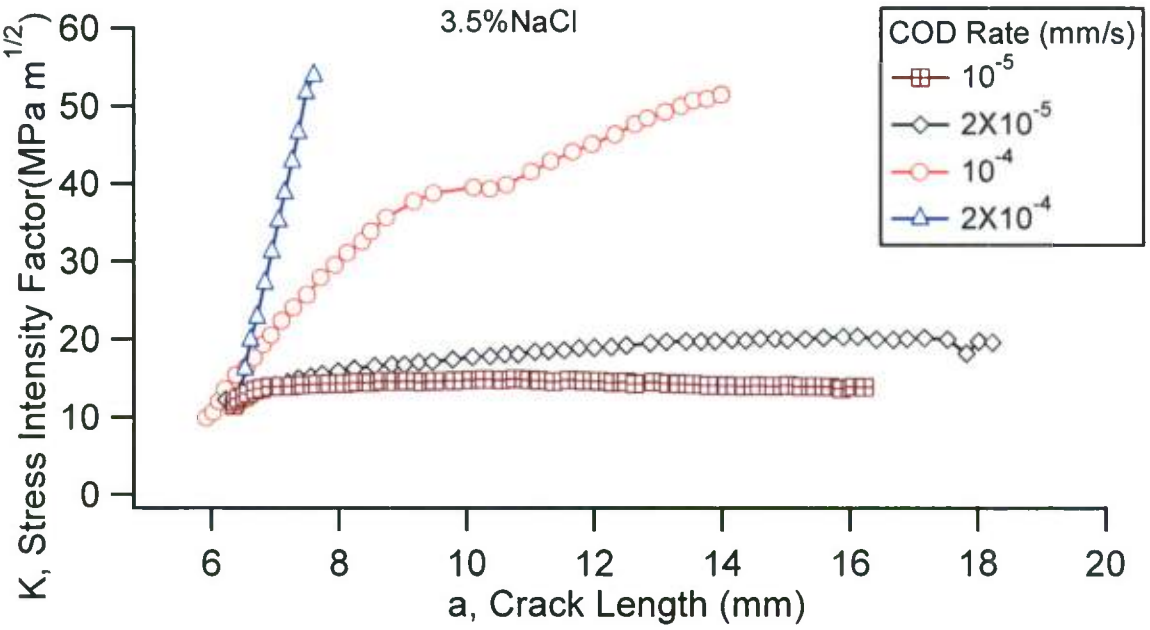

Fig. 6 Variation of stress intensity factor in COD rate controlled experiments

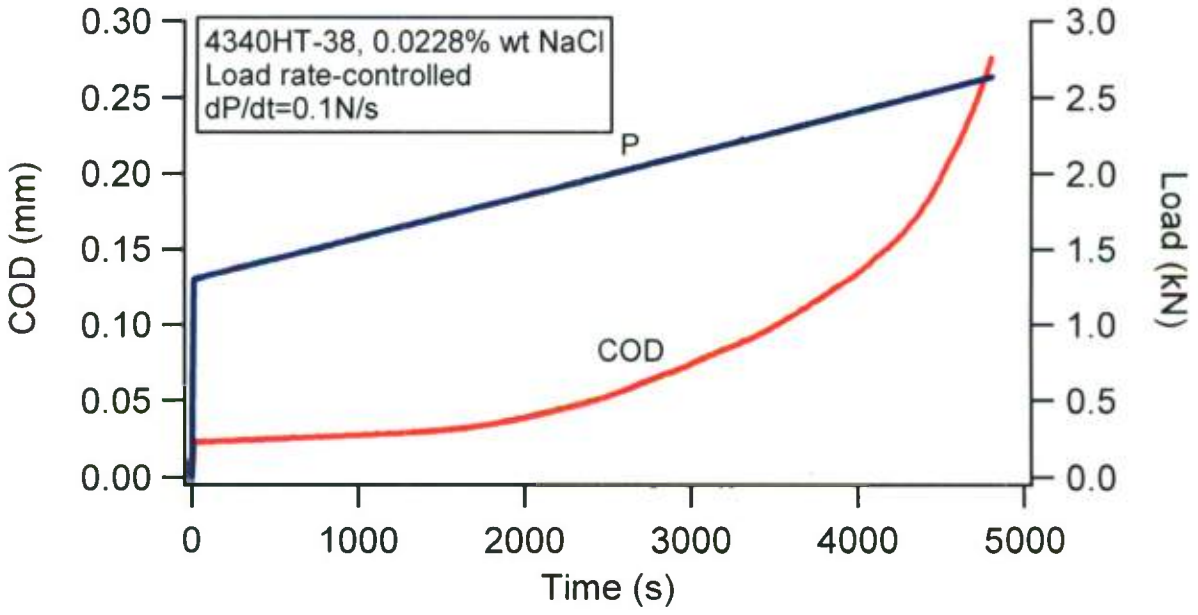

Fig. 7 Variation of COD with time in an experiment with constant load rate control

The experiment with linearly increasing applied load, on the other hand, results in a continuously increasing K, which allows for the determination of all of the stages in the crack growth curve within one experiment. Figure 7 shows the variation of the applied

load and the corresponding COD as a function of time in a load rate controlled experiment. The experiment was performed at a constant loading rate (linearly increasing load) of $dP/dt = 0.1\,N/s$ and produced a complete crack growth curve for the material. It can be seen from Fig. 7 that while the load is changing linearly with time, the COD vs time relationship is similar to a parabolic curve. Therefore, in order to obtain the results corresponding to a constant loading rate experiment, the COD rate should not be constant.

I.3.2. Effect of NaCl Concentration

Nine different concentrations of sodium chloride (NaCl) in water solution were used in the current investigation. The NaCl concentration ranged from 0% (distilled water) to 3.5% (simulated seawater). The values of the threshold stress intensity factors were determined from the load rate controlled experiments and correspond to a first observed crack extension of 0.01mm from the crack tip formed by fatigue pre-cracking prior to the SCC test. All the results for the effect of NaCl concentration are shown in Fig. 8. Experiments were conducted with constant load, constant COD, and constant load rate controls. All of the experiments were performed at free potential and at the room temperature without aeration.

The crack growth results in Fig. 8 display typical SCC behavior with the crack growth curve consisting of three stages, as depicted schematically in the insert in Fig. 4. Stage I is the near threshold (subcritical) crack growth where the velocity of crack propagation strongly depends on stress intensity factor K. Stage II is often called a plateau crack growth and within this range the rate of crack extension is nearly independent of K. Finally, the third stage represents the catastrophic failure of the specimen and is not represented in Fig. 8 because most of the specimens in the current investigation were not loaded until complete separation.

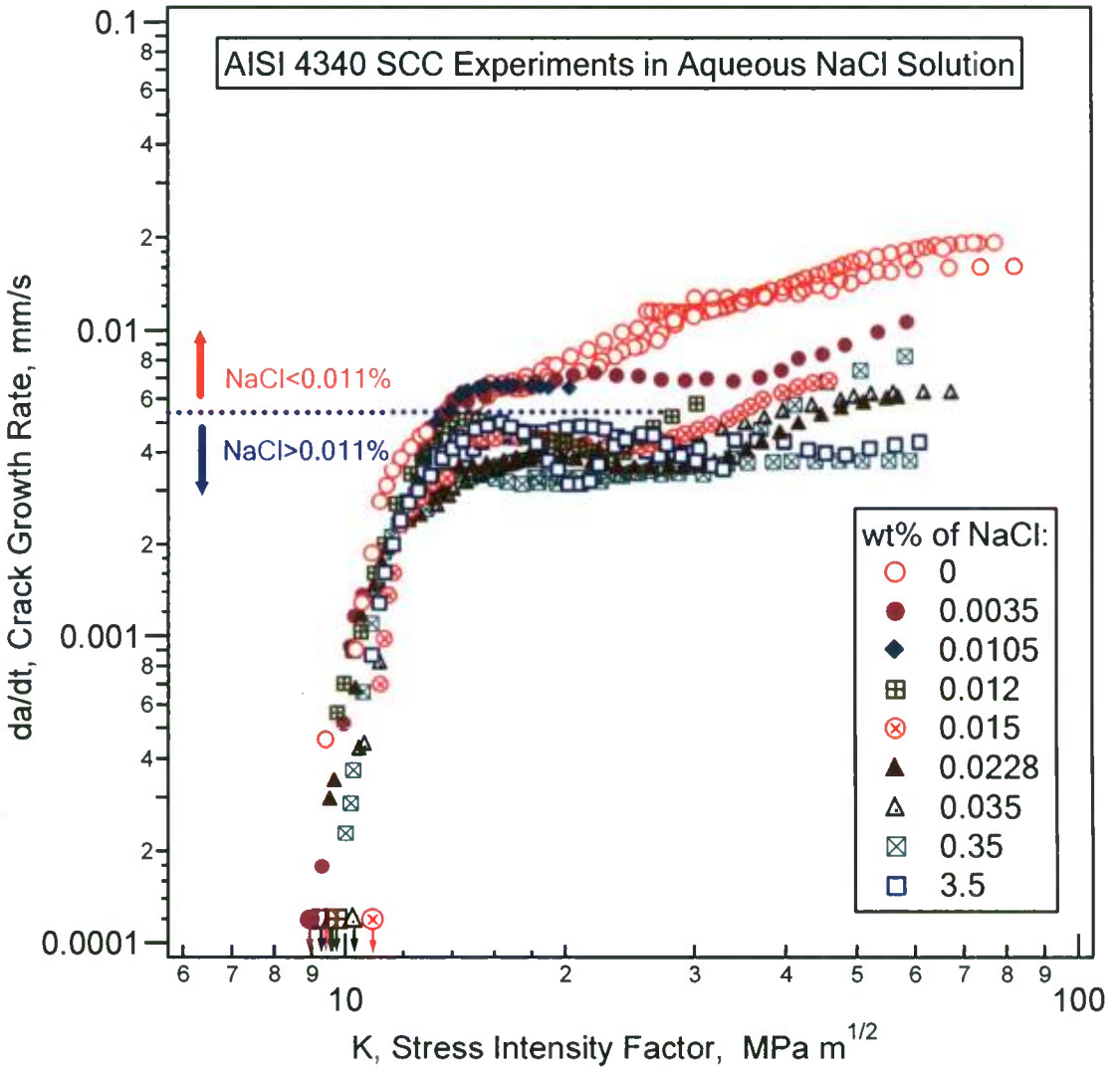

Fig. 8 SCC experiments in aqueous NaCl solution of different concentrations

It can be seen from Fig. 8 that the change in the NaCl concentration has practically no effect on the threshold values of the stress intensity factor and the near-threshold crack growth. At the same time, it can be found that an addition of NaCl to the solution slows down the plateau crack growth as was observed earlier [22, 62]. The highest values of da/dt are reached in pure distilled water. With the addition of sodium and chloride ions, the crack growth rate within the plateau region decreases. It should be noticed that the crack growth rate curve in pure water is distinguishable from the SCC growth curves in saline solutions by the absence of the pronounced plateau in Stage II. In other words, the velocity of crack extension in pure water is dependent on the stress intensity in all three stages of crack growth.

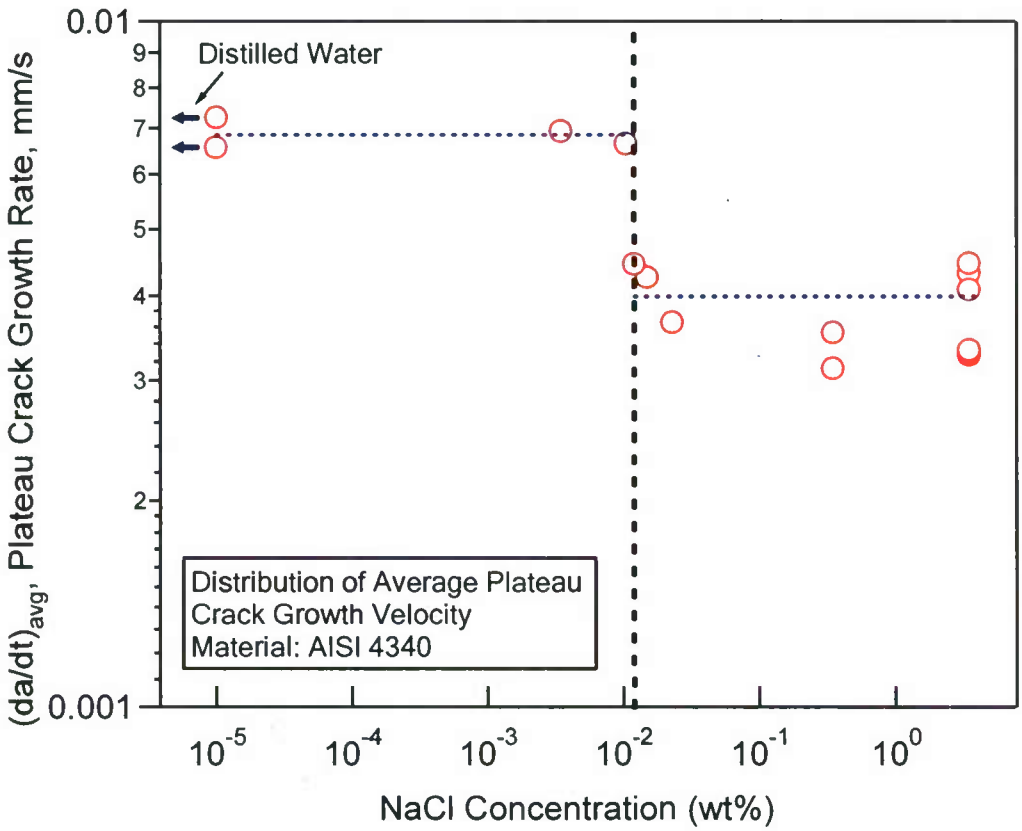

Fig. 9 Average plateau crack growth velocity as function of NaCl concentration

One particular phenomenon regarding plateau crack propagation velocity can be observed from Fig. 8. A decrease in the plateau crack growth rate does not occur continuously with increasing NaCl concentration. Two groups of crack growth curves, one corresponding to the NaCl concentration lower than 0.011% and one with the NaCl concentrations higher than 0.011% can be distinguished in Fig. 8. A further illustration of this phenomenon is shown in Fig. 9 which depicts the average plateau velocity of crack growth as a function of the NaCl concentration. It can be seen from Fig. 9 that the NaCl concentration of 0.011% can be viewed as a "critical concentration" separating two groups of crack growth curves (dashed vertical line in Fig. 9). The first group with the NaCl concentrations being lower than the critical number behaves close to the SCC in pure water. If the NaCl content is increased by 1.5×10^{-3} wt%, the plateau velocity decreases to the values characteristic for the SCC in the 3.5% saline solution.

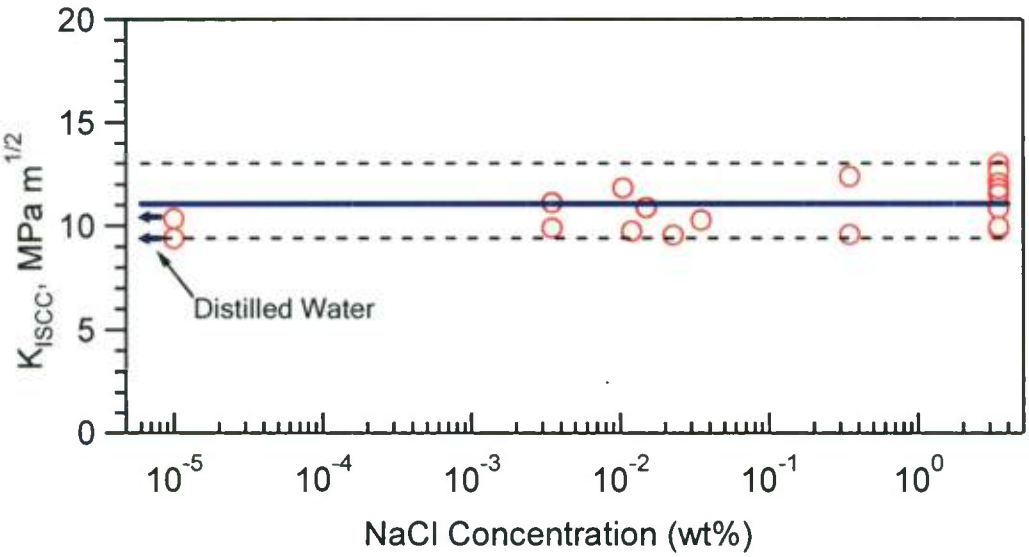

Fig. 10 Dependence of K_{ISCC} on NaCl concentration

Figure 10 is a plot of K_{ISCC} versus the NaCl concentration in the distilled water solution. As was stated earlier, the NaCl concentration has no practical influence on the threshold stress intensity factor. The K_{ISCC} values are confined within the range of 9.4~13.0 $MPa\sqrt{m}$, as being indicated by the dashed lines in Fig. 10. The K_{ISCC} distribution has no correlation with the NaCl concentration. The average K_{ISCC} value was found to be 11.07 $MPa\sqrt{m}$ (thick blue line in Fig. 10).

I.3.3. Microscopic Observations and Crack Morphology

An examination of the fracture surfaces under the scanning electron microscope (SEM) revealed the intergranular cracking mechanism typical for heat treated 4340 steel [65, 66] in all of the specimens subjected to environmentally assisted cracking (Fig. 11). The mechanism is not influenced by the loading rate or the NaCl concentration and there was no significant differences observed in fracture morphologies of the specimens tested under different loading conditions.

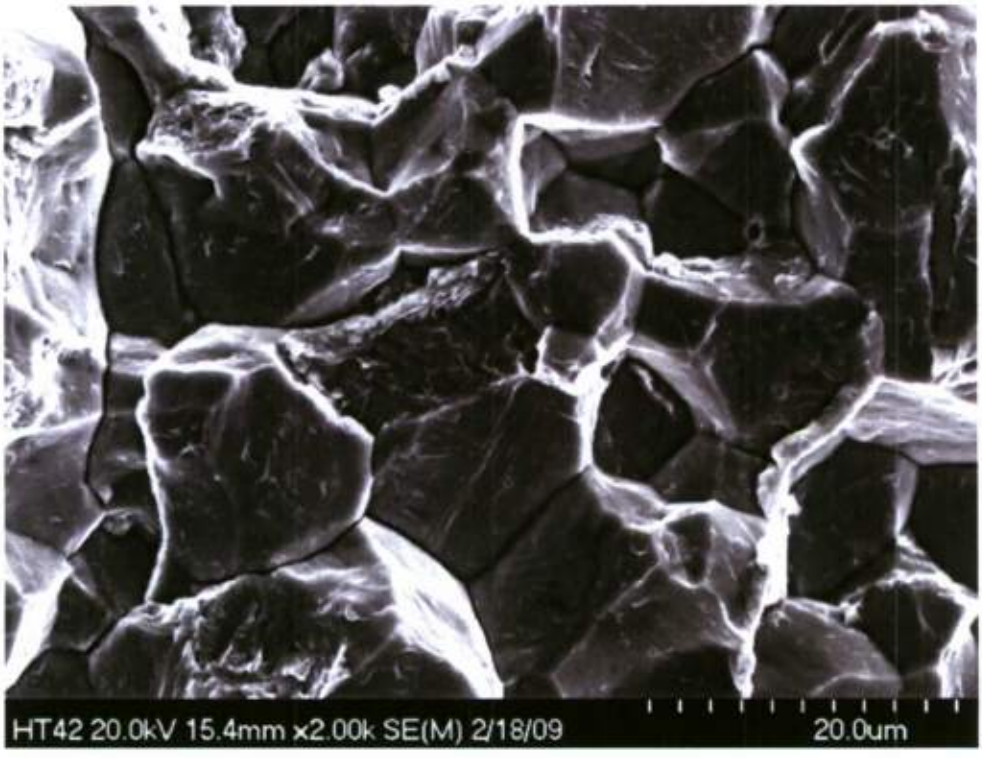

Fig. 11 SEM photograph illustrating intergranular SCC in AISI 4340 steel

It has been generally accepted that the yield strength influences the threshold value of the stress corrosion and hydrogen assisted cracking [7, 4, 25, 62] while the plateau velocity is not significantly dependent on the strength of an alloy [25]. The particular microstructural cracking mechanism, however, is a function of a rate limiting process, i.e., anodic dissolution or hydrogen embrittlement. In the case of hydrogen assisted cracking, the transgranular or intergranular path of a crack is dependent on segregation of impurities, which serves as hydrogen trapping sites, along the grain boundaries [15]. At the same time, experimental observations point to a connection between hydrogen induced cracking and plastic deformation by slip on the {110} planes [4, 15]. Such a deformation mechanism leads to transgranular cracking induced by a local process of plastic strain due to the motion of dislocations. Both mechanisms can be activated during the SCC and the final fracture mode depends on the hydrogen distribution among the trapping sites.

In the present investigation, *in situ* observation of the SCC crack extension through the optical microscope allowed for the acquisition of rather peculiar cracking behavior of AISI 4340. Figure 12 shows the photograph of a growing SCC crack captured with the CCD camera attached to the microscope. It can be seen that the crack propagation consists of a number of small steps ("cells") in which the crack is separated in two branches which later tend to merge together. While the overall plateau velocity remains

constant, the crack propagation is slower when the new "cell" is being formed by crack deviation in two branches. Once the "cell" has started to form, the crack extension becomes faster until the branches come together and the new step is starting to emerge. The schematic representation of the crack growth process is shown in the drawing in Fig. 12. The average vertical distance between the two branches forming a cell is approximately 30 μm which is comparable to the size of two grains of the pre-eutectoid austenite. Such a mechanism was observed in all of the specimens regardless of the NaCl content and loading control mode. It should be mentioned that fatigue cracking of the material under investigation was observed to be also intergranular. However, one clearly distinguishable main crack was observed in fatigue cracking. Therefore, the "cellular" structure of SCC can be attributed to the combined effect of the environment and the static load.

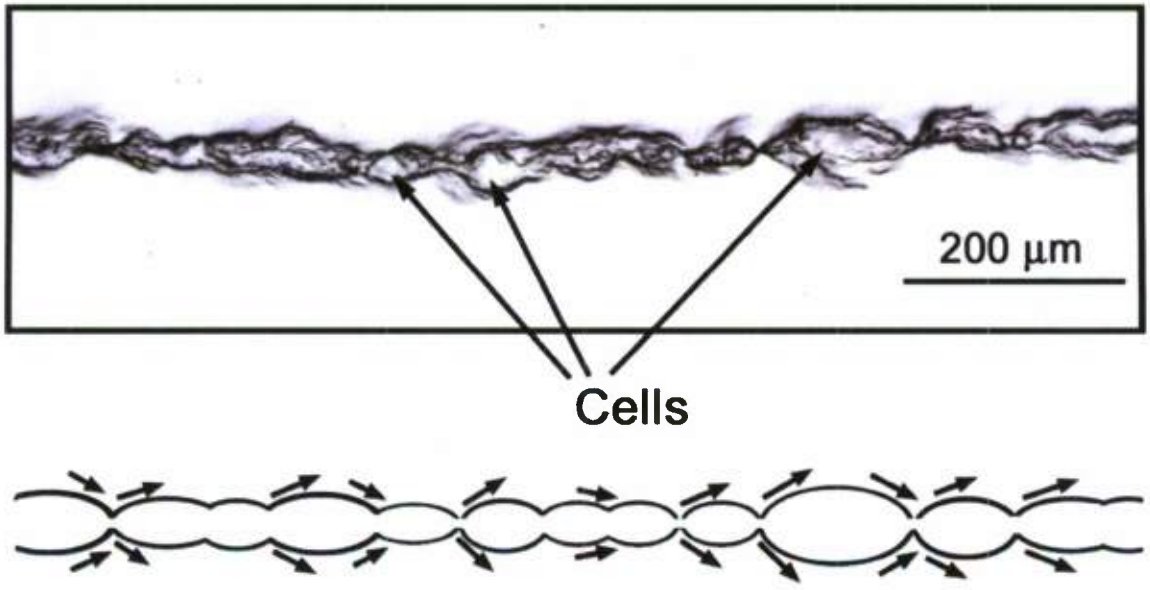

Fig. 12 Photograph of a propagating SCC crack (Specimen HT-43, $dP/dt = 0.1N/s$)

Out of 27 specimens tested in the current investigation, seven specimens developed branching of the main crack during the stress corrosion experiments. Multiple macroscopic branches were observed as illustrated by the photograph in Fig. 13 ($dP/dt = 0.1N/\sec$, 0.012 wt% NaCl). The branching features were not dependent on NaCl concentration in distilled water and were observed in specimens subjected to constant load as well as linearly increasing load conditions. Crack branching has been previously observed in high strength steels subjected to stress corrosion cracking [30, 67, 68-70]. It should be mentioned that the propagation mechanism described above

(Fig. 12) can be considered as microscopic branching since the main crack essentially consists of two propagating branches forming the "cells" and separated by 30 □m vertically. The formation of such "cells" on the microscopic level, however, does not influence the overall plateau velocity of SCC. When the macroscopic branching occurs, the propagation rate of the main horizontal crack significantly slows down as illustrated in Fig. 14. It should be mentioned that the onset of macroscopic branching was observed to occur at specific values of the stress intensity factor ranging from 29.4 $MPa\sqrt{m}$ to 34.7 $MPa\sqrt{m}$. Previous work on SCC of 4340 steel with yield stress equal to 1530 MPa in 0.1N H_2SO_4 solution [30] showed occurrence of branching at stress intensity approximately equal to 2.5 times K_{ISCC}. With the average threshold stress intensity of 11.07 $MPa\sqrt{m}$ determined in current investigation, the onset of branching can be expected at $K = 28\,MPa\sqrt{m}$ which is close to the observed range indicated above.

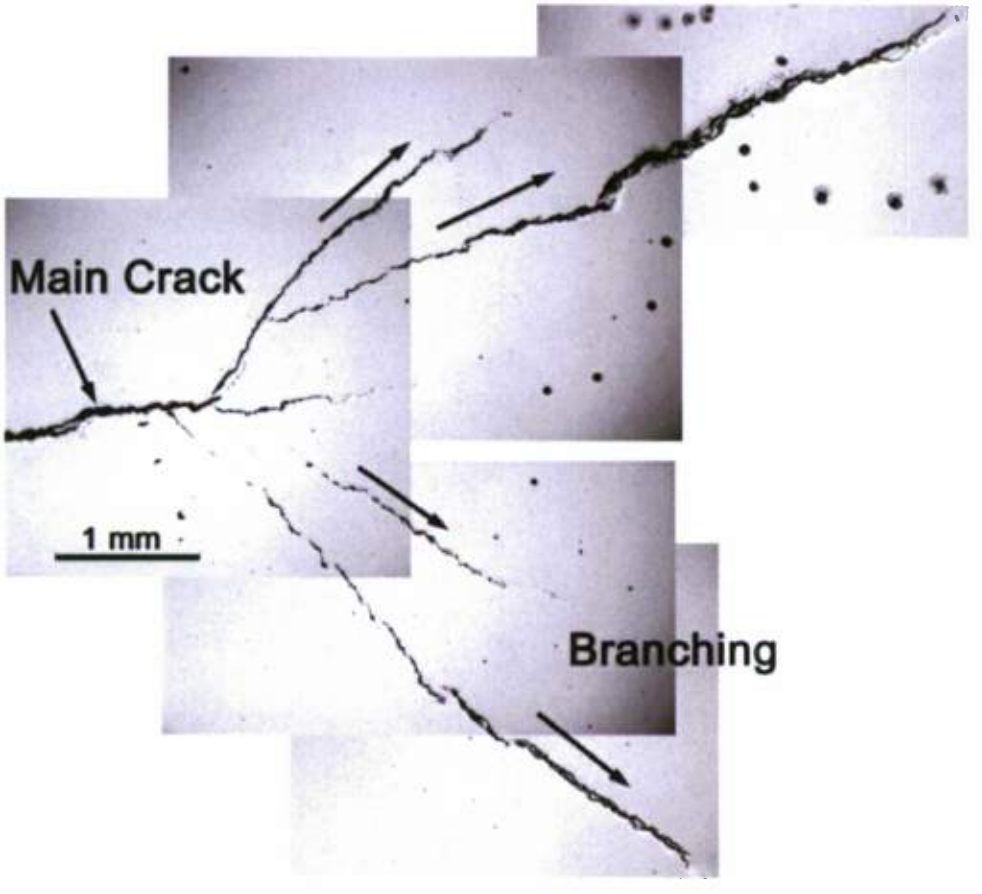

Fig. 13 Branching of the stress corrosion crack ($dP/dt = 0.1\,N/\sec$, 0.012 wt% NaCl)

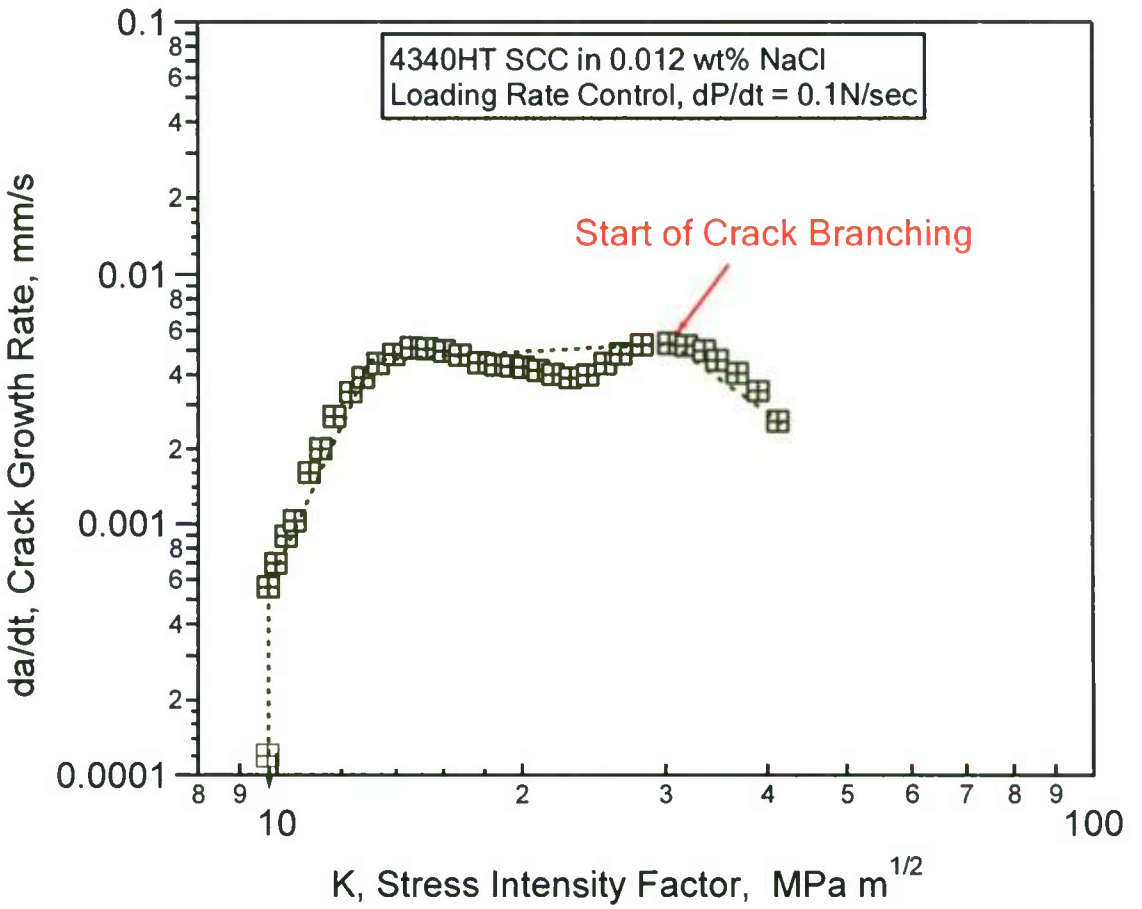

Fig. 14 Effect of branching on crack growth rate

I.4. DISCUSSION

Stress corrosion cracking (SCC) of metallic materials is a rather complex phenomenon involving processes of both metallurgical – electrochemical interactions as well as stresses and strains in the material. The real difficulty is presented when characterization of the mechanism of interaction between the environment and mechanical processes is required. The rate and mechanism of environmentally assisted cracking for a given material depends on many parameters including not only the chemical species in the environment but also the physical state of the media and the temperature [26]. Therefore, it has been accepted [21] that the formulation of a general model for the mechanism of SCC is rather an unreasonable goal since the specific processes operate depending on the details of the environmental and metallurgical conditions. In aqueous environments, a general statement can be made that the stress

corrosion cracking is influenced by the crack tip slip processes, the anodic dissolution, the electrochemical reduction, and the subsequent hydrogen absorption leading to hydrogen embrittlement [7, 21, 22, 26, 48, 71]. The critical combination of these processes leading to SCC can be considered as a mechanism of environmentally assisted crack growth [3, 21].

The first systematic collaborative experimental studies of the SCC behavior of the 4340 steel probably started with the Round Robin test program using the wedge opening load (WOL) specimens initiated in 1974 [20, 72] and involved 20 participating laboratories. The objective of this research was to develop a standard test procedure for the determination of the threshold stress intensity factor using the WOL specimens. Large amount of data from the experiments on 4340 steel with $\sigma_y = 1254\,MPa$ showed values of K_{ISCC} ranging from 23.3 to 26.8 $MPa\sqrt{m}$. Experiments conducted by the researchers employing the WOL and CT specimens later yielded the range of K_{ISCC} from 9.7 $MPa\sqrt{m}$ ($\sigma_y = 1682\,MPa$) [73] to 116 $MPa\sqrt{m}$ ($\sigma_y = 985\,MPa$) [74]. Resent research by Raman et al [75, 76] using circumferential notch tensile (CNT) specimens as a substitute for traditional CT geometry produced values of K_{ISCC} close to 15 $MPa\sqrt{m}$ ($\sigma_y = 1470\,MPa$). In the present work, the average value of K_{ISCC} for AISI 4340 with $\sigma_y = 1503\,MPa$ was determined to be 11.07 $MPa\sqrt{m}$ which is very close to $K_{ISCC} = 11.9\ MPa\sqrt{m}$ determined by Hirose and co-workers for the AISI 4340 steel with the yield stress equal to 1530 *MPa* [46]. The values of threshold stress intensity and plateau crack growth velocity available from the research results reported in literature are arranged in Table 8. In addition to yield stress values, the controlling conditions during the experiment and the specimen types are specified in Table 8. The values of threshold stress intensity factors obtained in the current investigation are compared to the data from the literature in Fig. 15. The results taken from the literature are represented by open circles and the results of the present experiments are shown with filled markers. The solid line represents the reference exponential fit of the data and the dashed lines show the 100% spread from the reference line. Significant amount of scatter can be observed in Fig. 15 and there is a rather large variation in K_{ISCC} values for an identical yield stress. An overall tendency of decreasing threshold stress intensity with increase in σ_y can be observed despite the scatter. It can be seen that the data obtained in the present investigation falls within the scattering band in Fig. 15.

Table 8. Results of SCC of AISI 4340 in aqueous environments from literature

σ_y (MPa)	K_{ISCC} $(MPa\cdot\sqrt{m})$	$(da/dt)_p$ (mm/s)	Testing Method	Specimen Type	NaCl%	Ref.
1530 1330	11.9 20.6	4.0×10^{-02} 1.5×10^{-02}	CL, CD	CT	3.5	[46]
1201	21.0	...	RD	CT	SS	[45]
1700	...	8.0×10^{-02}	CL	DCB	0	[44]
1240	21.7 ~34.5	...	CD	WOL	3.5	[20]
1240	27.9 ~33.4	1.01×10^{-03} $\sim 1.35\times10^{-03}$	CL, CD	CB, WOL	3.5	[40]
1379	27.47	1.35×10^{-03} $\sim 4.66\times10^{-03}$	CL	CB	3.5	[36]
1103, 1240	95.6, 40.7		CD	WOL	SS	[52]
1379~1682	9.7~ 33	...	CD	WOL	3.5	[73]
1312 ~ 1475	16 ~ 22	8.1×10^{-03}	CL	SEN	3.5	[31]
1388 ~ 1554	21.14 ~ 29.1	1.33×10^{-03} $\sim 3.8\times10^{-03}$	CL	...	3.5	[52]
970~1700	...	3.4×10^{-02} $\sim 1.0\times10^{-01}$	CD	DCB	0	[25]
1034, 1379	12.1 ~ 60.4	...	CL	CB	3.5	[49]
1420	...	2.5×10^{-02} 1.4×10^{-02}	CD	WOL	0, 3.5	[22]
1163	35, 37.5	1.1×10^{-06}	RD	CT	SS	[58]
1095	83~89	6.7×10^{-06} $\sim 1.4\times10^{-05}$	RL	CT	SS	[55]
1027 ~1573	8.57 ~58.10	...	RL, CD	CT, WOL	3.5	[53]
1689 ~1827	15.38 ~ 17.58	...	CL	CB	3.5	[60]
1470	15	...	CL	CNT	3.5	[75]
1612 1498	16.6	6.0×10^{-03} 1.6×10^{-02}	CL	CT	0	[23]

$(da/dt)_p$ - Average plateau crack growth rate

CD – Constant displacement (decreasing *K*) control during the experiment

CL – Constant load (increasing *K*) control during the experiment

CK – Constant *K* control; RL – Rising load experiment

RD – Rising displacement (constant rate of COD) control

SS – Simulated seawater

SEN – Single edge-notched specimen; CNT – Circumferential-notched specimen

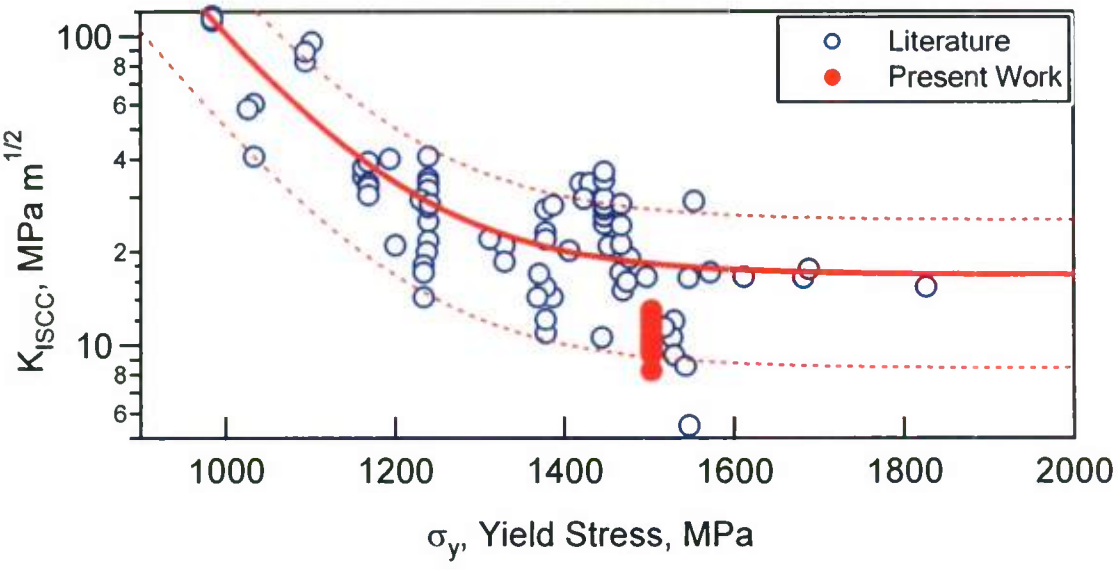

Fig. 15 K_{ISCC} as a function of yield stress for AISI 4340 steel

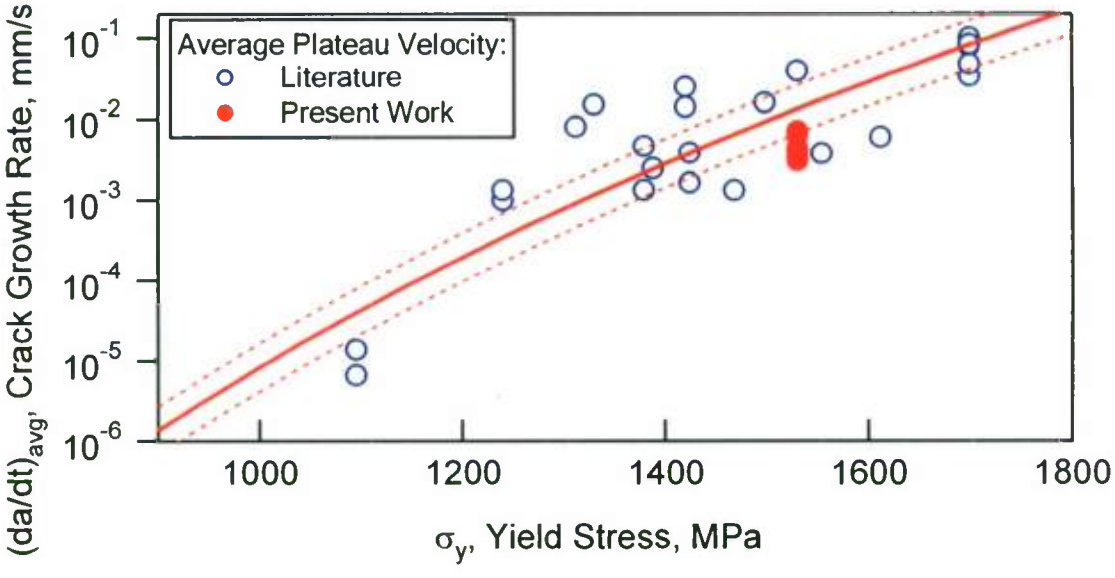

Fig. 16 Plateau velocity as a function of yield stress for AISI 4340 steel

The average plateau velocity as a function of the yield stress is shown in Fig. 16 for the 4340 steel. The detailed values of the plateau velocities are listed in Table 8 under the column "$(da/dt)_p$." The open circles represent the results from the literature and the solid markers are the results obtained from the current study. It is clear that, as a general tendency, a higher yield stress results in a higher plateau velocity.

In addition to the threshold values, the constant load experiments provide the information regarding the crack incubation time. In the present investigation, the experiments under constant load control revealed that the incubation time is practically zero when $K > K_{ISCC}$ if pre-cracking is done with a low K_{max} and crack growth is observed directly at a microscopic level (Table 3). Previous investigations on 4340 with a yield strength $\sigma_y = 1654\,MPa$ [66], however, demonstrated the existence of rather prolonged incubation times (from 11 to 3000 minutes) even when the fatigue pre-cracking was done with maximum stress intensities lower than the initial values of *K* in stress corrosion cracking. The difference most likely can be explained by different definitions of the incubation time concept. While in the current investigation the incubation time is defined as a time required for a crack to extend by 0.01 mm, the incubation time in [66] was treated as time when the crack growth rate reaches the plateau regime.

The constant COD experiments used for the threshold intensity factor determination can take very long time (up to 7,000 hours) when the low initial values of *K* are applied [20]. Therefore, efforts were directed towards developing techniques to accelerate the determination of the threshold [52-55]. Three fracture mechanics based testing approaches (constant load, constant displacement, and constant displacement rate) were applied and compared by Dietzel and co-workers [56] in the experiments on 2024 aluminum alloy. The resulted values of K_{ISCC} and the plateau crack growth velocities were very similar in all of the three applied testing techniques [56]. The applicability of rising COD control to the SCC experiments was further investigated with other metallic materials including AISI 4340 [16, 27, 54, 57, 58] and the results confirmed that the experiments with faster constant displacement rates can be used in place of time-consuming constant load tests. It should be mentioned that the degree of influence of the loading rate on the threshold stress intensity, however, depends on the manufacturing process applied to the material. Research on Ti alloys [77, 78] demonstrated that within the same range of dK/dt , age hardened and cold worked materials exhibit different behavior of K_{ISCC} as a function of loading rate.

In the present investigation, independence of both the threshold stress intensity factor and the plateau velocity of AISI 4340 of the testing technique was confirmed with the experiments in the 3.5wt% NaCl solution. It was observed, however, that the linearly increasing COD controlled experiments may not provide a complete crack growth curve due to the nature of variation of stress intensity factor in such experiments. In the experiments with low rates of COD, the value of *K* stays almost constant with the crack extension, which restricts the results to the region of Stage I in the crack growth curve. Under higher values of displacement rates, Stage I is missed and the experiment can yield the growth data starting from the plateau regime which may give an erroneous estimation of the threshold stress intensity. In order to maintain an

increasing K with time, the crack opening displacement should be increased parabolically (Fig. 7). Based on the results obtained in the present investigation, it can be stated that the experiments under linearly increasing loading are preferable when the complete description of the three stages of crack growth curve is required.

It has been observed that, in general, addition of NaCl to solution decreases the Stage II crack growth rate in high strength steels [22, 62]. This conclusion is based on the results of vast amount of experiments conducted in distilled water and in seawater substitute (3.5% NaCl concentration). To the best of authors' knowledge, a comprehensive research of the chloride ions concentration influence on the SCC growth had not been explored. In the present investigation, it was determined that a minor difference in sodium chloride concentration can cause a sudden change in the plateau crack growth rate. The experimental results obtained from nine different NaCl concentrations in distilled water reveal that the crack growth curves can be divided in two major groups, with each group having a similar Stage II crack growth velocity (Fig. 8). The first group behaves close to SCC in distilled water and corresponds to the concentrations lower than 0.011 wt% NaCl. The SCC behavior of the second group with concentrations higher than 0.011 wt% is similar to that in seawater. Therefore, the 0.011 NaCl wt% concentration can be considered as a critical concentration that influences the plateau crack growth rate in the high strength 4340 steel under investigation. The mechanism of such an influence remains unclear, as it is known that an increase in the chloride content in aqueous solutions enhances the growth rates in steels with a yield stress less than 1241 MPa [79]. Therefore, the effect of the chloride ions concentration depends on the strength and/or heat treatment of the material. The chloride ions in the solution do not enter the hydrolysis reaction and are not responsible for hydrogen reduction [26]. As a result, the amount of hydrogen available for absorption is dependent on the metal ions from the electrochemical reaction at the crack tip and not on the chloride content. The critical concentration phenomenon observed in present work requires further investigations with possible physical explanation.

While the plateau velocity depends on the chloride concentration, the intergranular fracture mechanism was observed to be independent of both the NaCl content and the loading mode. It is known that the high strength steels are susceptible to hydrogen assisted cracking [6-10, 15, 80]. Two possible mechanisms of hydrogen embrittlement have been suggested: influence of hydrogen on crack tip plasticity and grain boundary decohesion due to hydrogen trapping [15, 80-82]. Most likely, both of the mechanisms are present in the SCC of the high strength steels, but the dominance of one of them depends primarily on the amount of hydrogen traps at the grain boundaries, i.e., the degree of phosphorus or sulfur segregation [80]. Experiments on double vacuum arc melted Aermet 100 alloy, which is free of grain boundary impurities, revealed transgranular fracture mode [7, 83]. In addition, unlike air melted 4340 steel, Aermet

100 displayed sensitivity of K_{ISCC} to the chloride concentration [83]. Intergranular cracking in 4340 steel together with rather high crack growth velocities observed in the present experiments suggest that the stress-controlled and brittle cracking mode due to reduced inergranular cohesion dictate the fracture in the material under investigation.

For the geometry of the specimen (Fig. 2) with $2R/W = 1.33$, the following formula [84] can be used to theoretically determine the crack opening displacement (δ),

$$\ln\left(\frac{BE\delta}{2P}\right) = 1.742 - 0.495\alpha + 14.71\alpha^2 - 22.06\alpha^3 + 14.44\alpha^4$$
$$\alpha = \frac{a}{W} \qquad (2)$$

where E is the modulus of elasticity, a is the crack length measured from the line of externally applied load P, and W and B are the width and the thickness of the specimen, respectively. In experimental practice, the crack length can be obtained from Eq. [2] when the COD and applied load are recorded during the experiment.

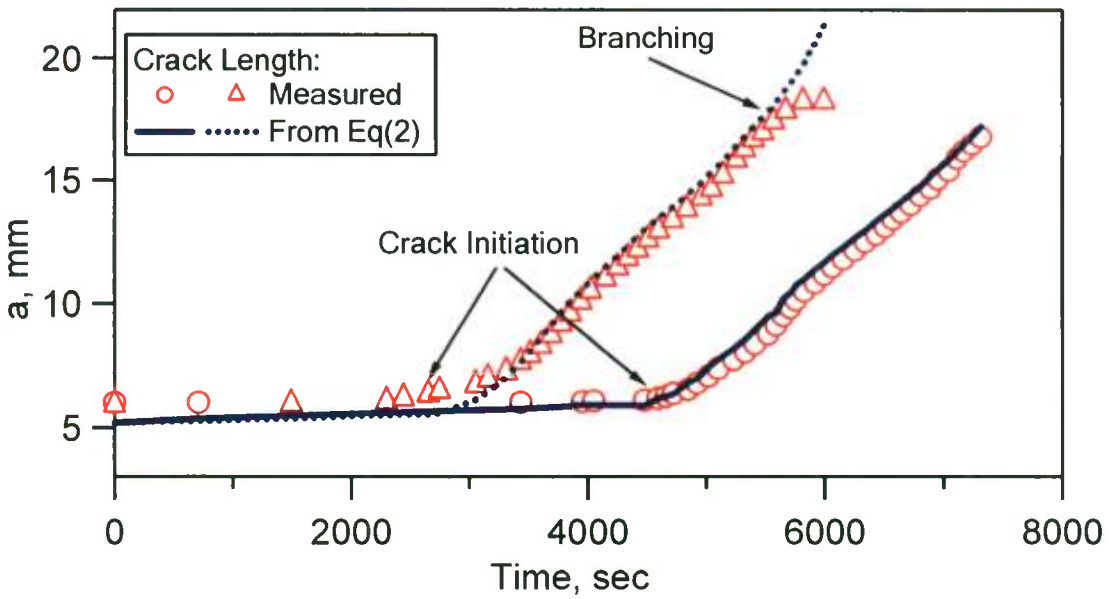

Fig. 17 Crack length measured during the experiment and obtained from Eq. [2]

Comparison between measured and calculated crack length is made in Fig. 17 using the data from the two specimens tested under $dP/dt = 0.1\,N/\sec$ control. Markers represent the experimentally measured crack extension using the optical microscope and the lines represent the solution of Eq. [2] based on the recorded values of the

applied load and the measured COD. It can be seen that overall the crack length calculated based upon the stress intensity factor using Eq. [2] is in the good agreement with the values obtained by direct observation using a reading microscope, especially in the plateau region. However, Eq. [2] is based on the assumption of single main crack in the specimen. When the crack extension is deduced from Eq. [2], the phenomenon of branching can be overlooked and rather erroneous results are obtained (Fig. 17). Optical *in situ* measurement of crack growth provides unique and valuable information allowing registration of every minor detail in crack growth behavior and thus providing accurate results. The above arguments can be also extended to the case of potential drop technique.

I.5 STRESS CORROSION CRACKING EXPERIMENTS OF 4340 STEEL IN SILICON OIL, IN PARAFFIN, AND IN DRY AIR

Experiments were conducted for possible stress corrosion of the 4340 steel in silicon oil and in paraffin. Both silicon oil and paraffin were chemically pure (100% pure, insoluble in water). The specimens used were identical to those shown in Fig.2 and the experimental setup shown in Fig. 3 was used for the stress corrosion experiments in silicon oil and in paraffin. In silicone oil, the specimens were loaded at two different loading rates: 0.1N/s and 0.2 N/s until the load reached 0.5 kN. Thereafter, the load was controlled constant. In paraffin, the initial loading rate was 0.1N/s. The load was kept constant during the stress corrosion experiment after reaching 0.4 kN. K_{ISCC} was determined when the crack started to propagate for approximately 0.01 mm.

Environmentally assisted crack growth in 4340 steel occurred in both silicone oil and paraffin. Figure 18 shows the crack growth rate as a function of stress intensity factor. K_{ISCC} was found to be 16.5 $MPa\sqrt{m}$ and 12.0, respectively, in silicon oil and in paraffin. General cracking phenomenon is similar to that occurs in water and NaCl solution but at a much lower velocity (Fig. 19). Right after K_{ISCC}, the crack growth rate reached a high value. This velocity gradually decreased with increasing K. It was found that the surface crack profile (refer to Fig. 20) of SSC in silicon oil is also very similar to that in NaCL solution: the crack propagation consists of a number of small steps ("cells") in which the crack is separated in two branches which later tend to merge together(compare to Fig.12 for experiments in NaCl solution).

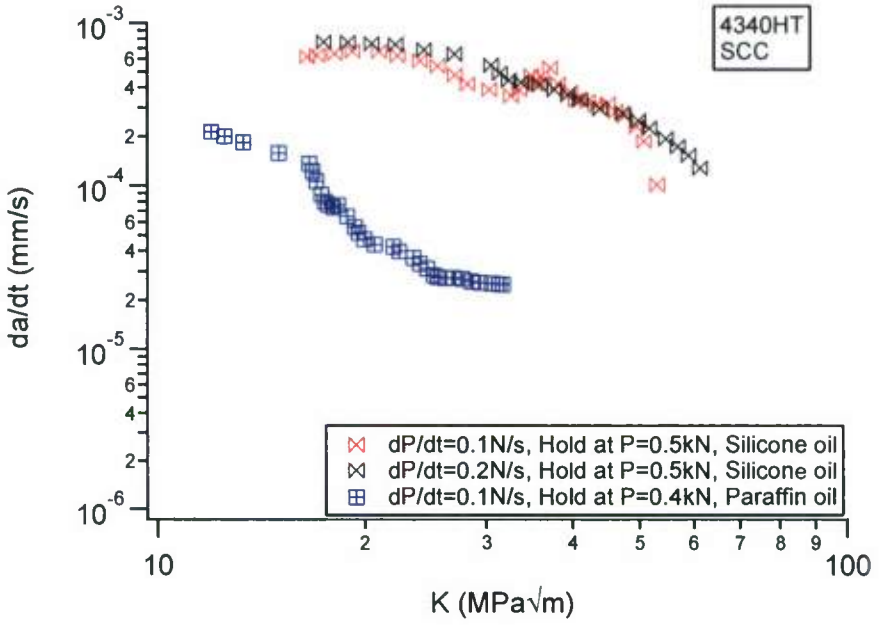

Fig. 18 Crack growth rate versus the stress intensity factor for the SCC experiments in silicon oil and paraffin

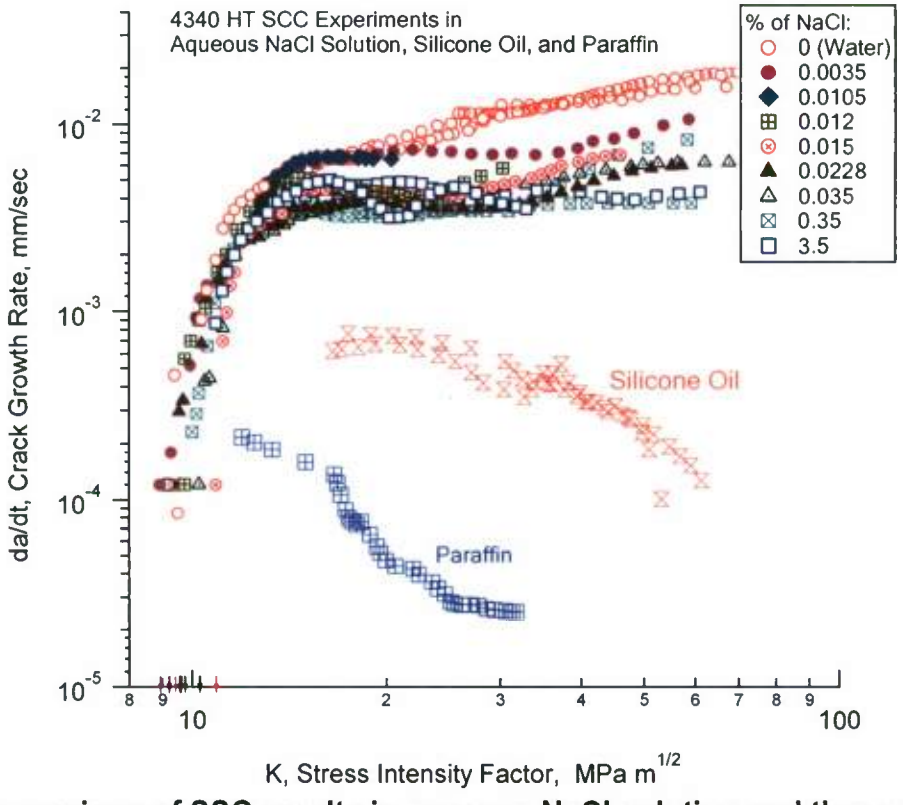

Fig. 19 Comparison of SSC results in aqueous NaCl solution and those in silicon oil and paraffin

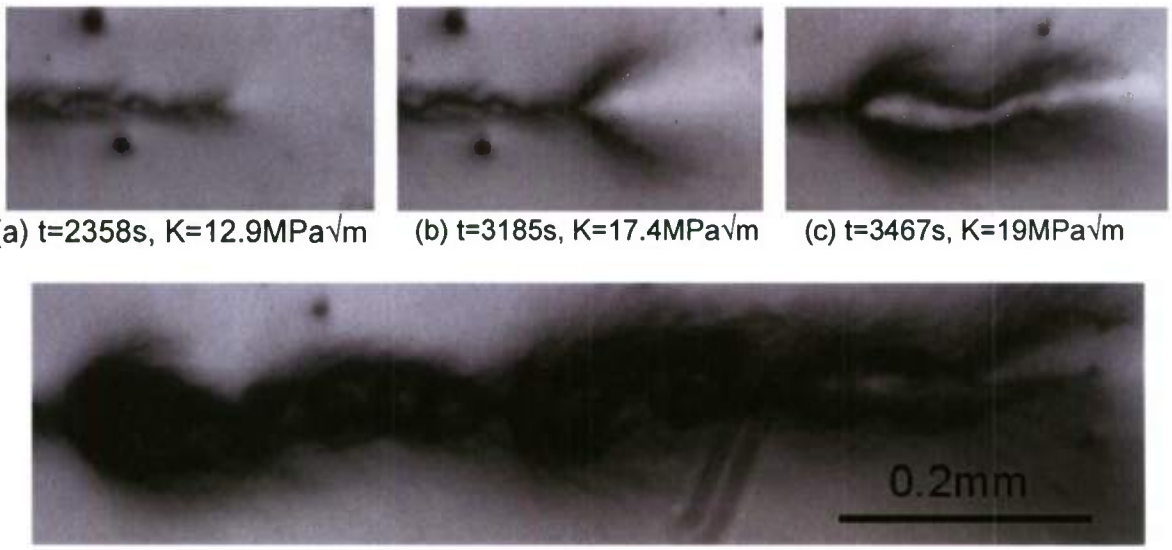

(a) t=2358s, K=12.9MPa√m (b) t=3185s, K=17.4MPa√m (c) t=3467s, K=19MPa√m

(d) t=4482s, K=30MPa√m

Fig. 20 Surface crack profile during stress corrosion of 4340 steel in silicon oil

Experiments were also conducted to check whether or not stress corrosion occurred in dry air (relative humidity =12%) at room temperature. A specimen was loaded at a rate of 2.0 N/s until the load reached 4.8 kN, and the load was then kept constant in the rest of the experiment (refer to Fig. 21). Corresponding to an applied load of 4.8 kN, the stress intensity factor is 67 $MPa\sqrt{m}$. Figure 21 shows the loading history and the photographs taken on the specimen surface at different values of the stress intensity factor. It can be found that the crack tip experienced plastic deformation as the load increased. No crack advance was detected after holding the specimen at a constant K of 67 $MPa\sqrt{m}$ for more than 15 hours. It should be noticed that a stress intensity factor of 67 $MPa\sqrt{m}$ is close to the fracture stress intensity factor of the material.

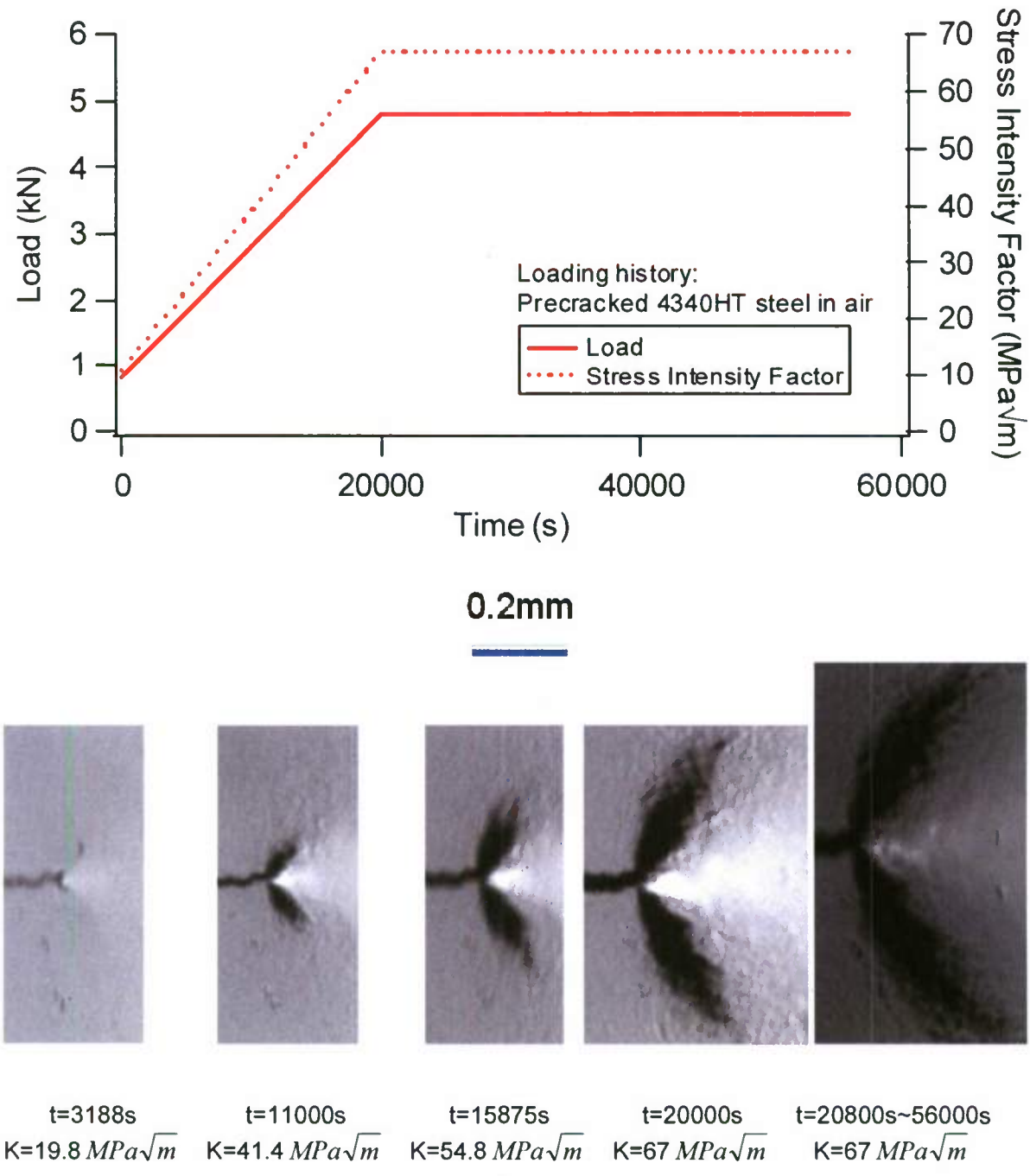

Fig. 21 SCC behavior of 4340 steel in dry air at room temperature

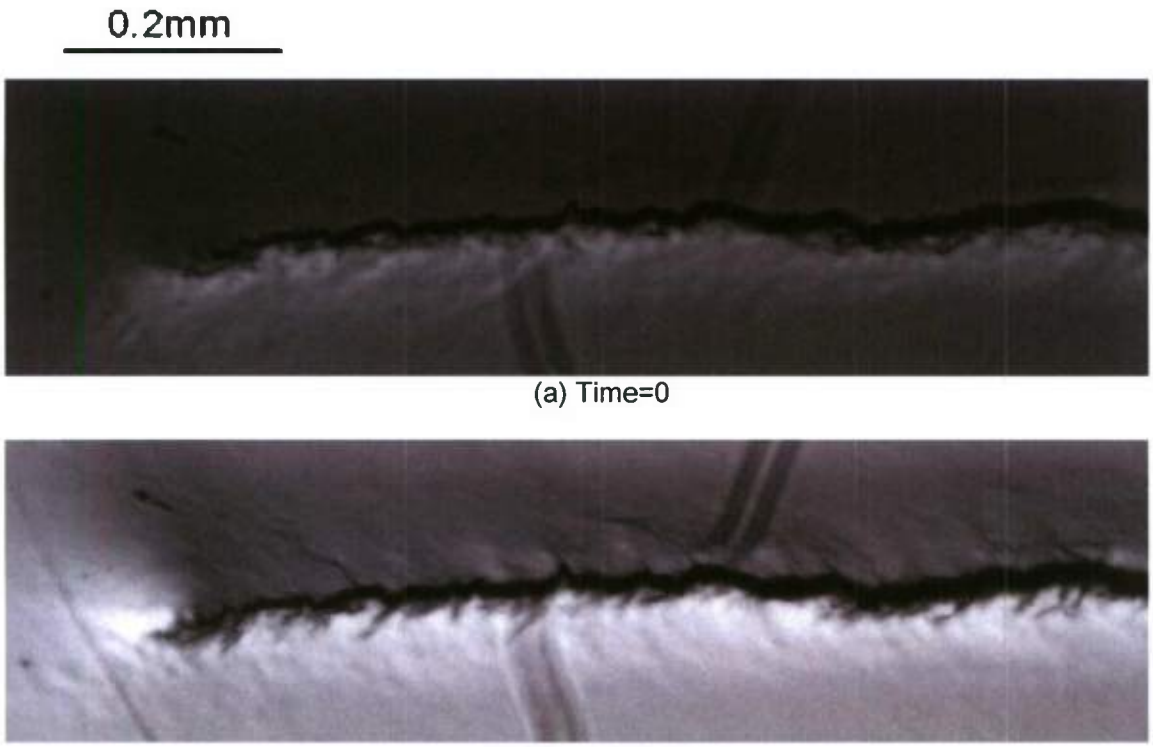

(a) Time=0

(b) Time=150 days

Fig. 22 Surface crack observation of a CT specimen made of 4340 steel subjected to a constant stress intensity factor (30 $MPa\sqrt{m}$)

Another stress corrosion cracking experiment in dry air (12% relative humidity, room temperature) was conducted at a constant K using a specially designed loading fixture. The specimen was pre-cracked. A constant stress intensity factor of 30 $MPa\sqrt{m}$ was applied to the specimen. No crack advance was detected after three months (see Fig. 22). In fact, the specimen was checked recently after more than two years and no crack propagation was found. It can be concluded that no stress corrosion occurs in 4340 steel in dry air (12% relative humidity) at room temperature.

I.6. CONCLUSIONS

Based on the experimental results of the stress corrosion cracking (SCC) experiments on the AISI 4340 steel (yield stress=1503 MPa), the following conclusions can be drawn,

1. K_{ISCC} and the plateau velocity are not significantly influenced by the loading rate.
2. Stage I crack growth can be obtained only when the loading rate is low.
3. COD rate control does not provide an avenue for the experimental determination of

a complete stress corrosion (*da/dt-K)* curve.

4. For 4340 steel, a load-control experiment can provide reasonable stress corrosion results.
5. While the threshold stress intensity is not influenced by NaCl concentration, the plateau crack growth velocity depends on concentration of chloride ions. A critical concentration of 0.011% was found to be a demarcation line between plateau velocities close to distilled water and plateau behavior similar to that in 3.5% saline solution.
6. The cracking mechanism was observed to be intergranular and does not depend on loading type or NaCl concentration.
7. Stress corrosion cracking was observed in silicone oil and paraffin and the general cracking phenomenon was similar to that occurred in water and NaCl solution but at a much lower velocity. Right after K_{ISCC}, the crack growth rate reached a high value. This velocity gradually decreased with increasing K.
8. No stress corrosion cracking occurred in 4340 steel in dry air (12% relative humidity) at room temperature.

II. 7075-T651 ALUMINUM ALLOY

II.1. INTRODUCTION

High strength Al-Zn-Mg-Cu aluminum alloys (7XXX series) are widely used in heavily loaded aircraft structures due to their high strength-to-density ratio. However, this series of aluminum alloys is potentially susceptible to stress corrosion cracking (SCC), particularly in aqueous solutions containing chloride ions. The susceptibility of aluminum alloys to SCC in a corrosive environment can be evaluated using the pre-cracked specimens in terms of the threshold stress intensity factor for SCC (K_{ISCC}) and the crack growth rate (da/dt) [85]. For a pre-cracked specimen of a commercial high strength aluminum alloy, the curve of the crack growth rate (da/dt) versus stress intensity factor (K) generally exhibits two distinguishable stages [86-88]. The crack propagation rate increases sharply with stress intensity factor in stage I while is independent of stress intensity in stage II. Lee et al. [88] suggested that SCC was dominated by anodic dissolution (AD) in stage I and by hydrogen embrittlement (HE) in Stage II. Endo et al. [89] pointed out that K_{ISCC}, the crack growth rate in stage II, and SCC mechanism depended on specimen thickness which determined the constraint condition (plane stress or plane strain condition) at the crack tips. With the increase of specimen thickness, K_{ISCC} decreased, while the crack growth rate in Stage II increases and became dependent on the stress intensity factor [89].

SCC of aluminum alloys is strongly sensitive to environmental, metallurgical, and mechanical factors. The influence of various environmental variables, such as the humidity of air, viscosity, temperature, acidity of the corrosive medium, and the type and concentration of anions, on the SCC behavior of high strength aluminum alloys has been studied [86-88, 90-93]. Speidel [86] reported that the rate of SCC growth in an aluminum alloy in air increased monotonically as humidity of air was increased. Different effects of various anions on SCC kinetics in aluminum alloys were also demonstrated [87]. Le et al. [91-92] investigated the SCC behavior of 7075-T651 in various electrolytes. It was found that an increase in the chloride ion content of environment up to 0.6M enhanced the SCC growth rate, and the cracking was slower at higher concentrations. Great efforts have been made to increase the stress corrosion resistance (SCR) of high strength aluminum alloys by optimization of microstructure via heat treatment [93-109]. Over-aging of 7xxx series showed high SCR but a considerable loss in strength [93]. The retrogression and re-aging (RRA) applied to 7075-T6 aluminum alloy can result in the highest improvement in SCR with negligible reduction in strength [96-97].

It was generally accepted that a tensile stress is a necessary condition for onset of stress corrosion cracking. However, it has been shown that SCC can also occur under compressive loads in aluminum alloys [110]. The threshold stress intensity nucleating

SCC from the notched 7075 aluminum alloy in a 3.5% NaCl aqueous solution under the compressive applied stress is much higher than that under tensile stress. At the same stress intensity factor, the incubation period for SCC under compressive stress is one order of magnitude longer than the corresponding value under tensile stress [110]. Pre-straining or pre-stressing which introduces a residual tensile or compressive stress can also have a significant effect on subsequent stress-corrosion behavior. It was observed that tensile overloads generally resulted in an increased incubation time in the case of 7075-T651 aluminum alloy. Moreover, incubation time increases with increasing overload magnitude [111]. At the same time, the experiments in 3.5% NaCl seawater substitute solution with periodic overloads display a great decrease in corrosion fatigue life of 7075-T651 alloy [112]. It was observed that in 7017-T651 aluminum alloy the tensile residual stress developed at the notch tip after compressive pre-stressing resulted in SCC in moist air even though no external load was applied [113]. Clark [114] reported that notched specimens of 4340 steel exhibited an increased resistance to SCC initiation when preloaded in tension and a decreased resistance when preloaded in compression. As a practical technique, pre-stressing by controlled shot peening to induce compressive residual stress at the surface material can improve the fatigue resistance and stress corrosion resistance of 5000 and 7000 series aluminum alloys [115]. Transient effects are observed following low-high "step" load changes during stress corrosion tests [116]. It was reported that the SCC resistance of a notched specimen can be increased by initially stressing it below the K_{ISCC} level. It is best not to increase the load stepwise during SCC tests in order to determine the K_{ISCC} accurately [117-118].

Structural members typically experience a spectrum of loads in service. Therefore, it is of interest to know how complicated loading history affects the subsequent SCC behavior. The aim of this work is to present a set of experimental results which describe the effects of load level in terms of stress intensity factor (K) and overload/underload percentage on incubation time and stress corrosion crack velocity of 7075-T651 aluminum alloy. Also, the effect of high-low sequence loading on the SCC behavior of the material was investigated.

II.2. EXPERIMENTAL PROCEDURE

The material used for SCC tests was hot-rolled plate of 7075-T651 aluminum alloy with a thickness of 52.7mm. The microstructure of as-received rolled alloy under investigation is shown in Fig. 23 as a 3D image illustrating the directionality of grains. The etchant used in microscopic examination was Keller's reagent (2ml HF (48%), 3ml HCl, 5ml HNO_3, and 190 ml H_2O). The dark particle-like precipitates in the microstructure are $Cr_2Mg_3Al_{18}$ and $(Fe,Mn)Al_6$. Fibrous grains were observed along the direction of rolling. The average thickness of grains was approximately seven microns.

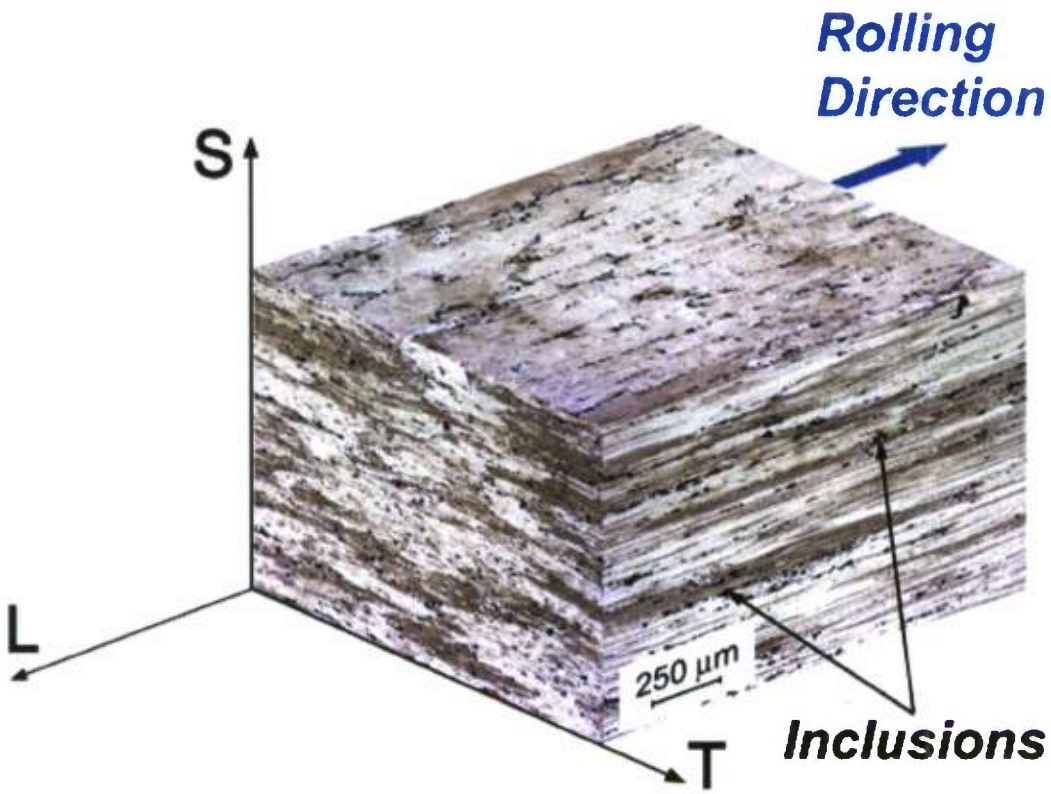

Fig. 23 Microstructure of 7075-T651 aluminum alloy

Static material properties were determined from the monotonic loading experiments performed on the dog-bone shaped plate specimens. The experiments were conducted on the specimens cut in three directions of the rolled plate following the designation shown in Fig. 23. Three specimens were tested in each direction and the average values of the material properties are listed in Table 9. The monotonic curves are displayed in Fig. 24. It can be seen that the lowest ductility and the lowest yield stress are observed in short transverse direction (S), which corresponds to the axis of loading in the CT specimens shown in Fig. 25. SCC sensitivity of metals depends on grain boundary orientation [119] and rolling direction. In 7075 alloy, S-L specimens show intergranular SCC and higher sensitivity to SCC [120] while T-L specimens show much less sensitivity to SCC [121]. In addition, it has been determined that variation of the precipitates and dislocation structures does not influence directional sensitivity to stress corrosion [122].

Table 9. Static material properties of 7075-T651 aluminum alloy (E = 72 GPa)

	S	L	T
Yield Stress (0.2% offset) σ_y *(MPa)*	421.0	494.0	487.0
Ultimate Strength σ_u *(MPa)*	462.7	563.0	540.0
Engineering Fracture Strain ε_f	0.018	0.088	0.064
Monotonic Strength Coefficient K *(MPa)*	601.2	638.3	595.7
Monotonic Strength Hardening Exponent n	0.058	0.047	0.032

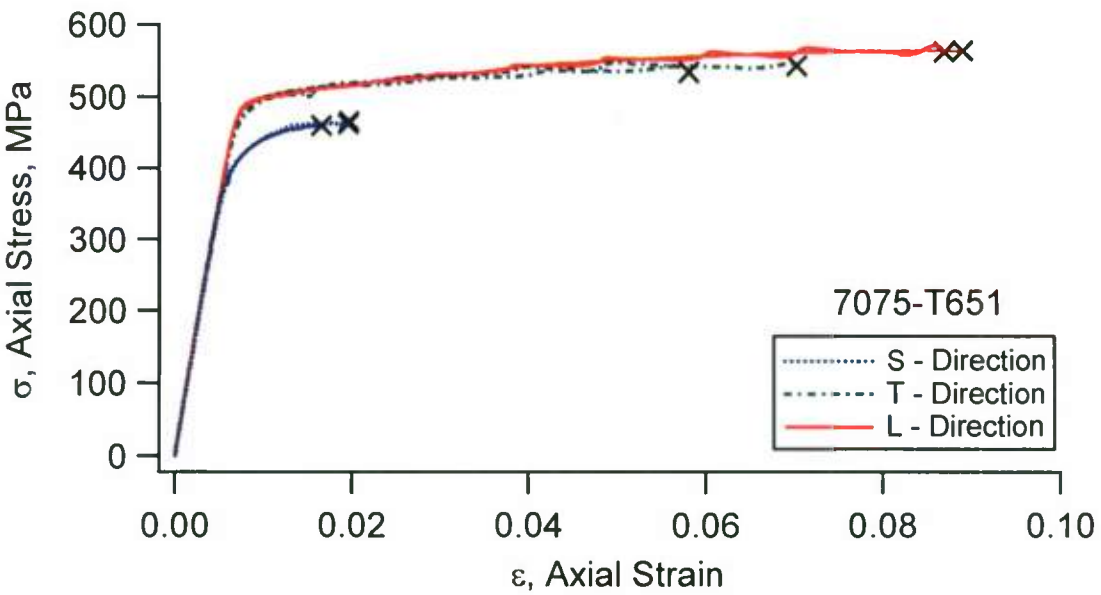

Fig. 24 Monotonic tensile curves of 7075-T651 aluminum alloy

Compact tension (C(T)) specimens of 7075-T651 aluminum alloy were used in SCC experiments. The specimen dimensions are shown in Fig. 25(a). The specimens were cut from the rolled plate in the S-L (Short Transverse - Longitudinal) direction as shown in Fig. 25(b). In the SCC experiments, the stress was applied in the short transverse direction to the grain structure, and SCC growth was in the longitude direction. The thickness of the specimens was 3.8 mm. Notches were cut using the EDM (electro-discharge machine) process in order to investigate the notch effect on fatigue crack initiation, which is not reported in the current study. One side of the specimens was polished in order to facilitate the observation of crack growth. The specimens were placed into ultrasonic cleaner prior to testing to remove the residual materials from machining and polishing.

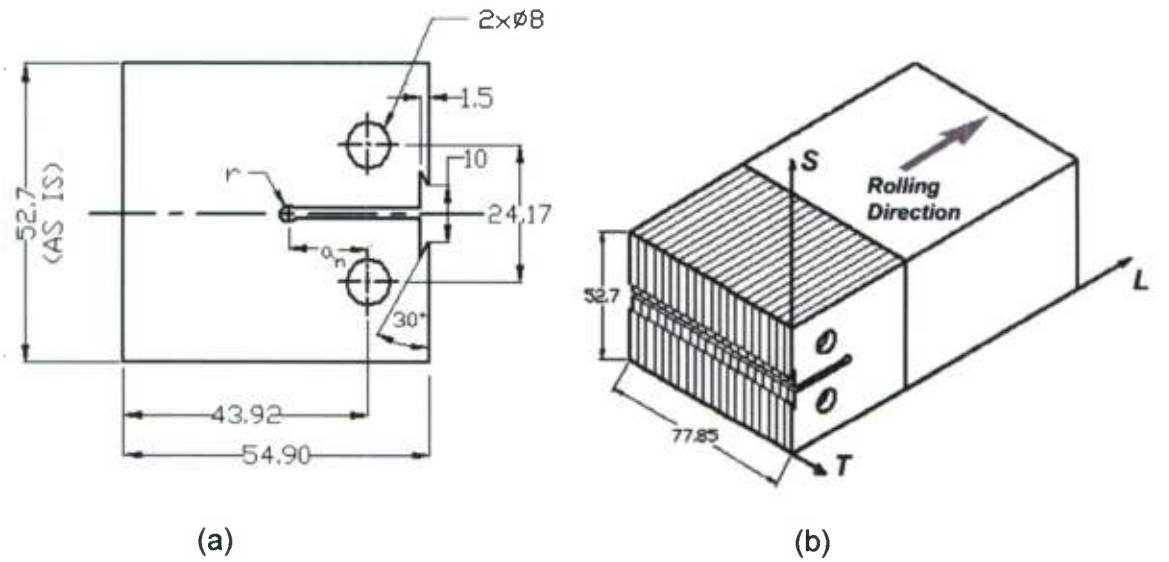

(a) (b)

Fig. 25 Compact specimen used in the SCC experiments (all dimensions are in mm): (a) specimen and (b) orientation of the specimens with respect to the rolling axis

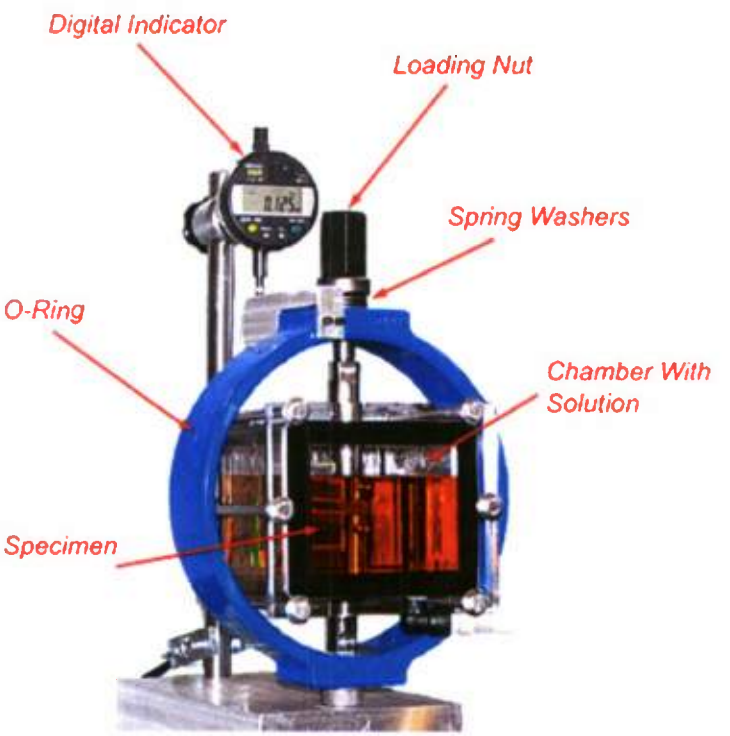

Fig. 26 Experimental setup for SCC experiments

The SCC experiments were performed in the aqueous solution containing 0.6M (3.5 wt%) sodium chloride, 0.02M sodium dichromate, 0.07M sodium acetate, plus 0.389M acetic acid to pH=4. The solution can prevent formation of corrosion products and facilitate observation of cracks [123-124]. Load was applied to the specimens via the commercially supplied and calibrated load-rings (O-rings). The deflection of the loading ring was measured with digital indicator mounted on the stand. The experimental setup is shown in Fig.. 26. The specimen was placed into a transparent acrylic chamber containing the corrosive solution. The volume of the chamber was one liter. To measure the crack length, a long-distance traveling microscope with an accuracy of readings of 0.001 mm was used. Measurements were done by an eight-hour interval. The crack length was measured on one side of the specimen. No aeration was supplied during the experiments. Solution in the chamber was replaced weekly. During the SCC experiments, no protective coating was applied to the surfaces of the specimens, and the specimens were not deliberately isolated from the loading system. Although galvanic coupling between the testing specimen and the loading system was inevitable, the crack growth at the crack tip was not observed after three months when the applied load was much lower than K_{ISCC}. Therefore, the influence of galvanic corrosion on the SCC results (incubation time and crack growth rate) in this study was insignificant. All the experiments were conducted at room temperature under free corroding conditions. Details of the experiments are summarized in Tables 10-12.

Table 10. SCC tests on effect of stress intensity factor on incubation time (3.5% wt NaCl, 0.6 M)

Spec. #	$P_i\,(kN)$	$a_i\,(mm)$	$a_f\,(mm)$	$K_i\,(MPa\sqrt{m})$	$t_{inc}\,(s)$	$t_{frac}\,(s)$	$(da/dt)_p$ (mm/s)
SL51	0.76	14.07	38.702	5.8	407,850	1,679,140	1.61e-5
SL76	0.90	14.04	37.623	6.8	323,902	4,197,683	1.69e-6
SL39	1.02	14.21	26.520	8.0	190,834	1,307,914	1.81e-5
SL33	1.28	14.01	>23.58	9.8	132,374	>1,716,794	4.05e-6
SL41	1.28	14.18	21.812	10.0	118,874	853,062	1.44e-5
SL37	1.58	14.37	28.525	12.2	87,197	785,529	2.10e-5
SL77	2.08	14.16	>17.363	16.0	36,442	604,391	9.10e-6

Note: P_i -Initial applied load K_i -Initial applied stress intensity factor

a_i -Initial crack length a_f -Crack length at failure of specimen or termination of test

t_{inc} -Incubation time t_{frac} -failure time $(da/dt)_p$ -average plateau velocity

Table 11. SCC tests on effect of overload/underload on incubation time (3.5% wt NaCl, 0.6M)

Spec. #	OL/UL (%)	$P_i\,(kN)$	$a_i\,(mm)$	$a_f\,(mm)$	K_i $(MPa\sqrt{m})$	$t_{inc}\,(s)$	$t_{frac}\,(s)$	$(da/dt)_p$ (mm/s)
SL49	OL25%	1.30	13.99	23.12	9.97	160,554	1,185,560	3.41e-5
SL45	OL50%	1.32	14.08	25.61	10.10	432,100	-	1.51e-5
SL50	OL75%	1.27	14.19	27.49	9.83	332,848	1,298,675	2.06e-5
SL47	OL100%	1.31	14.18	17.41	9.93	913,099	1,065,827	1.85e-5
SL46	OL125%	1.13	17.08	25.86	10.32	940,051	1,322,839	2.75e-5
SL44	UL50%	1.32	14.07	30.24	9.93	102,644	1,059,503	2.34e-5
SL48	UL100%	1.30	14.11	26.35	9.84	79,423	-	1.48e-5

Note: OL/UL –Overload or underload percentage $(da/dt)_p$-average plateau velocity

Table 12. Effect of high –low sequence loading on SCC (3.5% wt NaCl, 0.6M)

Spec. #	Step 1 (High load)						Step 2 (Low load)					
	P_i (kN)	a_i (mm)	K_i $MPa\sqrt{m}$	$t_{inc}\,(s)$	K_f $MPa\sqrt{m}$	(da/dt) (mm/s)	$P_i\,(kN)$	$a_i\,(mm$	K_i $MPa\sqrt{m}$	$t_{inc}\,(s)$	$t_{frac}\,(s)$	$(da/dt)_p$ (mm/s)
SL45	1.316	14.08	10.10	432,100	15.34	1.51e-5	0.66	22.01	8.27	466,389	923,880	8.26e-6
SL48	1.299	14.11	9.84	79,423	12.27	1.48e-5	0.942	20.77	10.7	174,140	521,279	1.34e-5

Note: K_f-stress intensity factor when the first step is terminated

$(da/dt)_p$-average plateau velocity

Three types of SCC tests were designed to investigate the influences of loading level and loading history on the SCC behavior of 7075-T651 aluminum alloys: (1) SCC at different initial loading levels, represented by stress intensity factor (Table 10); (2) the effect of overload/underload on SCC behavior at the same initially applied loading level (Table 11); and (3) effect of high-low sequence loading on SCC behavior (Table 12). In a high-low sequence loading test, the SCC test was interrupted when the stable crack growth was established, followed by a load level reduction to a pre-selected level as listed in Table 12.

Prior to SCC testing, the specimens were pre-cracked to 4 mm using a servo-hydraulic machine in tension-tension loading. Pre-cracks were formed in ambient air by fatigue loading. After pre-cracking, tensile or compressive overloads were applied to selected specimens to study the effect of loading history on subsequent stress corrosion cracking behavior. The rest of the specimens were tested in corrosive environments

without application of overloading. In this case, the initial applied stress intensity factor for SCC experiments was always 2 $MPa\sqrt{m}$ higher than the maximum stress intensity factor applied during pre-cracking. The primary result was recorded as experimental data containing values of load calculated from the ring deflection, crack length, and time. The crack growth rate was determined from the experimentally obtained measurement of the crack length as a function of time. A parabolic curve was used to best fit seven consecutive points in the crack length versus time curve. The crack growth rate was obtained by taking the derivative of the fitting curve for the middle point.

For the geometry of the specimen shown in Fig. 25, the stress intensity factor was calculated using the following equation [125]:

$$K = \frac{P(2+\xi)}{B\sqrt{W}(1-\xi)^{3/2}}\left(0.886 + 4.64\xi - 13.32\xi^2 + 14.72\xi^3 - 5.6\xi^4\right) \tag{3}$$

where:

$$\xi = \frac{a}{W} \tag{4}$$

The symbol B in Eq. (1) denotes the thickness of the C(T) specimen and W is the distance between the applied force P and the left edge of the specimen (refer to Fig. 25). The symbol a in Eq. (2) is the crack length measured from the line of the application of the external load, P [125].

It should be mentioned that the compressive deflection of the loading ring changes (decreases) with the crack extension during the stress corrosion experiment, thus decreasing the applied load. Under this loading condition, the stress intensity factor initially keeps approximately constant and later decreases continuously with the crack extension. In order to conduct experiments with increasing K condition, spring washers with the spring constant equal to 2~4 kN/mm were placed in series with the loading ring. With a different combinations of the spring washers, both increasing K and decreasing K can be achieved with the extension of the crack length.

The mechanical system shown in Fig. 26 can be schematically modeled by Fig. 27. k_1, k_2, and k_3 represent the stiffness values of the spring washers, O-ring, and cracked specimen, respectively. ΔL_1, ΔL_2, and ΔL_3 are their extensions under load P. ΔL_2 is experimentally measured and the total deflection ΔL ($\Delta L_1 + \Delta L_2 + \Delta L_3$) is controlled constant in a test. Therefore,

$$P = k_1\Delta L_1 = k_2\Delta L_2 = k_3\Delta L_3 \tag{5}$$

$$\Delta L = \Delta L_1 + \Delta L_2 + \Delta L_3 \tag{6}$$

Assuming that ΔL_3 is equal to the COD through the loading line, k_3 can be expressed as [125],

$$k_3 = \frac{P}{\Delta L_3} = \frac{E}{BV_2(a/w)} \tag{7}$$

$$V_2(a/w) = \left(\frac{1+a/w}{1-a/w}\right)^2 \left[2.163 + 12.219\frac{a}{w} - 20.065\left(\frac{a}{w}\right)^2 - 0.9925\left(\frac{a}{w}\right)^3 + 20.609\left(\frac{a}{w}\right)^4 - 9.9314\left(\frac{a}{w}\right)^5\right] \tag{8}$$

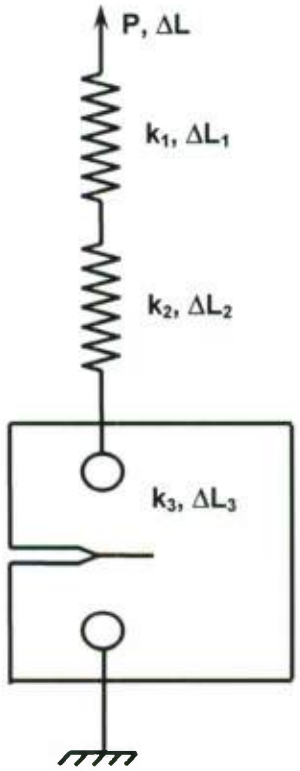

Fig. 27 Schematic representation of the loading system

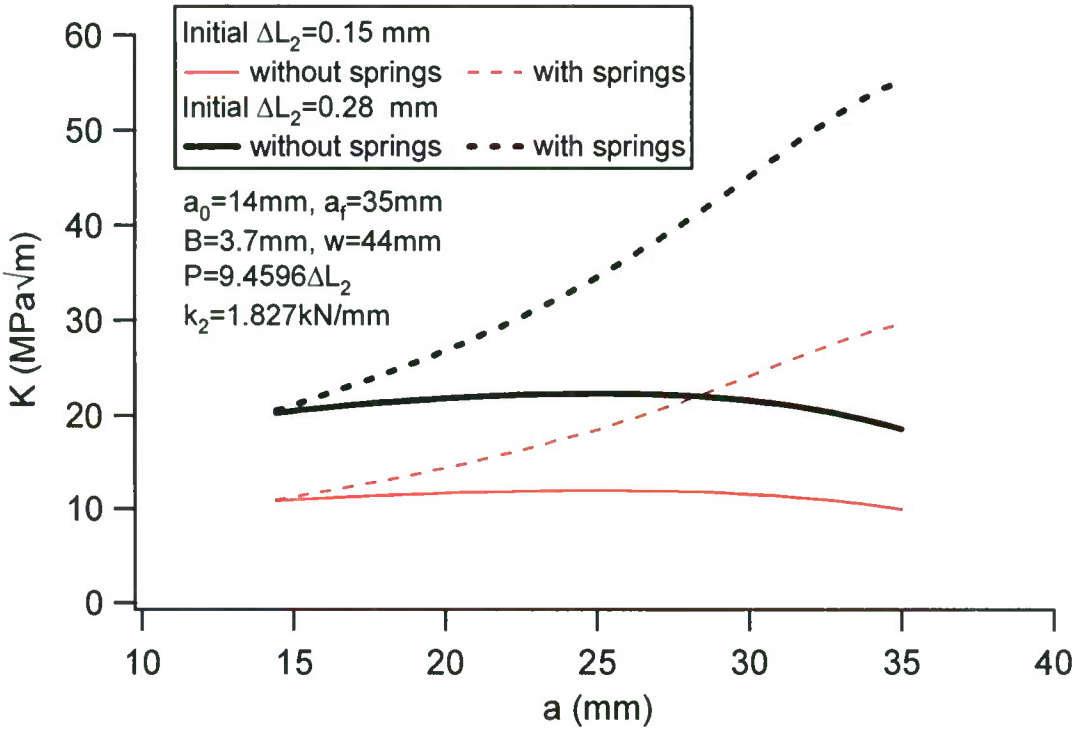

Fig. 28 Variation of stress intensity factor with crack length with and without spring washers

where E is the elasticity modulus of the specimen. dP/dk_3 can be calculated by using,

$$dP/dk_3 = \left(\frac{k_{12}}{k_{12}+k_3}\right)^2 \Delta L \tag{9}$$

where k_{12} is the effective stiffness of the spring washers and O-ring. The smaller k_{12} value, the smaller dP/dk_3. With spring washers, the overall stiffness of the system was reduced, allowing for continuous increase in stress intensity factor within the duration of experiment. A comparison of the relationship between stress intensity factor and crack length with and without spring washers is shown in Fig. 28.

II.3. RESULTS

The primary data collected as a result of the experiment were the applied load, the crack length, and the elapsed time. Equation (3) was used to determine the stress intensity factor for a given time with known applied load and crack length. To determine the crack growth rate, a parabolic curve was adopted to best fit a set of seven successive data points in the experimentally obtained relationship between the crack length and time. The crack growth rate at the middle point was determined from the

derivative of the parabola. Detailed experimental results are tabulated for each specimen tested in Appendix B for 7075T651 aluminum alloy.

II.3.1. Typical Features of Stress Corrosion Cracking Behavior

A photograph of a typical cracking scenario observed in the present work is shown in Fig. 29 together with the crack extension data collected during the experiment. Three crack growth stages can be identified during SCC of 7075 aluminum alloy: incubation, transient growth, and stable growth. During incubation stage load was applied but crack growth was not detected. In the transient (slow) growth stage, the crack growth rate was slow with an average value of approximately 10^{-6} mm/s. During stable (fast) growth stage, crack extended at an approximately constant rate of approximately 2×10^{-5} mm/s until fracture. Similar observations of three distinct stages in the stress corrosion cracking of aluminum alloys in bulk chloride containing solutions were observed by Lifka [126] and Dorward and Hasse [127].

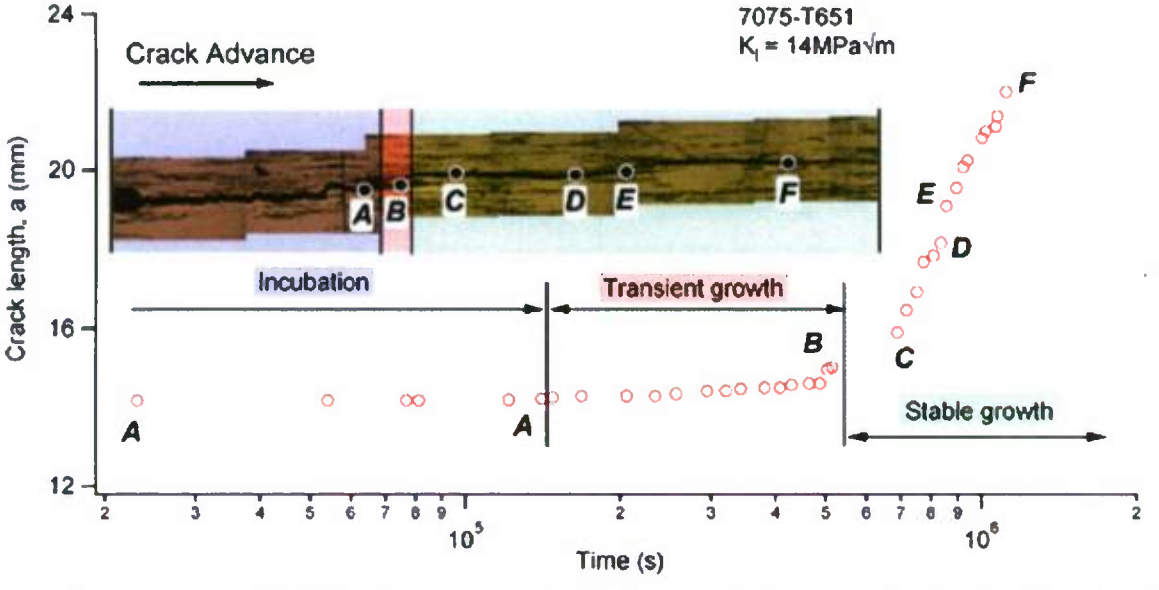

Fig. 29 Typical SCC behavior with initial applied stress intensity factor of 14 MPa$\sqrt{m}$

Generally, stress corrosion crack initiates at the crack tip produced by fatigue pre-cracking. Sometimes the stress corrosion crack may nucleate in the vicinity of fatigue crack tip and form an "attached" crack, which with subsequent growth becomes the main crack connected to the tip of the pre-crack. In order to determine an accurate incubation time in this study, the pictures of the region around the fatigue crack tip were captured periodically and compared. Detailed study of SCC incubation behavior has been performed by Dorward and Hasse [127] and it has been noticed that the values of

incubation time depended on the definition of the crack incubation period. In the present study, the incubation time is defined as the average of two time intervals during which initial pre-crack started to grow by approximately 0.05 mm.

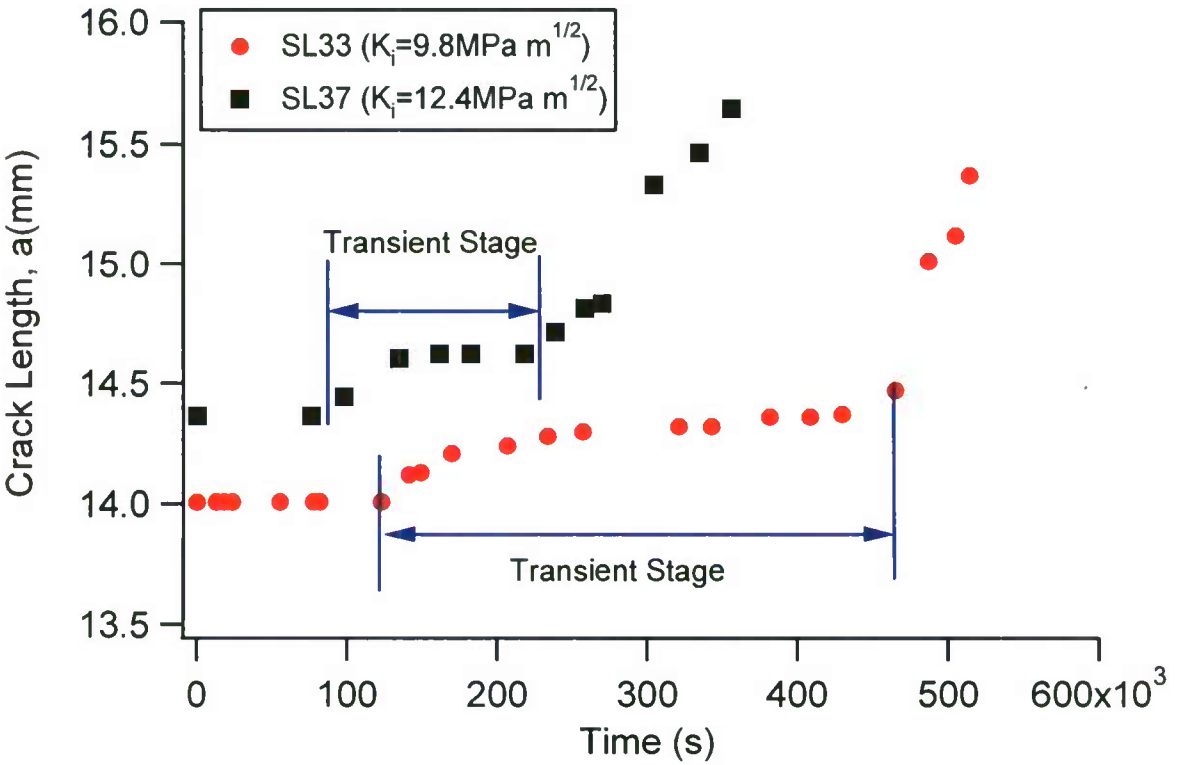

Fig. 30 Typical transient stage for SCC crack growth

After a stress corrosion crack was initiated, the crack propagated slowly, sometime advanced with a decreasing growth rate, or even stopped growth temporally, forming a so-called "transient stage", as shown in Fig. 30. It is highly probable that the SCC nucleates first on the specimen surface but does not penetrate through the thickness of the specimen. The local stress at the crack tip relaxes, resulting in a reduction in the crack growth rate. During this stage, the stress corrosion crack does not advance significantly, but sweeps along the thickness direction until it penetrates the thickness. In the SCC of high strength Al-Zn-Mg-Cu alloys in NaCl aqueous solutions, Dorward and Hasse [124, 127] observed a similar slow transient process by which the intergranular stress corrosion crack develops from the predominantly transgranular mechanical pre-crack. Connolly et al. [128] pointed out that the transition from the cracking incubation stage to the high rate crack growth stage is dependent on the development of a critical crack tip chemistry. Further investigations are necessary to elucidate the electrochemical and mechanical processes governing the cracking behavior during the transient stage.

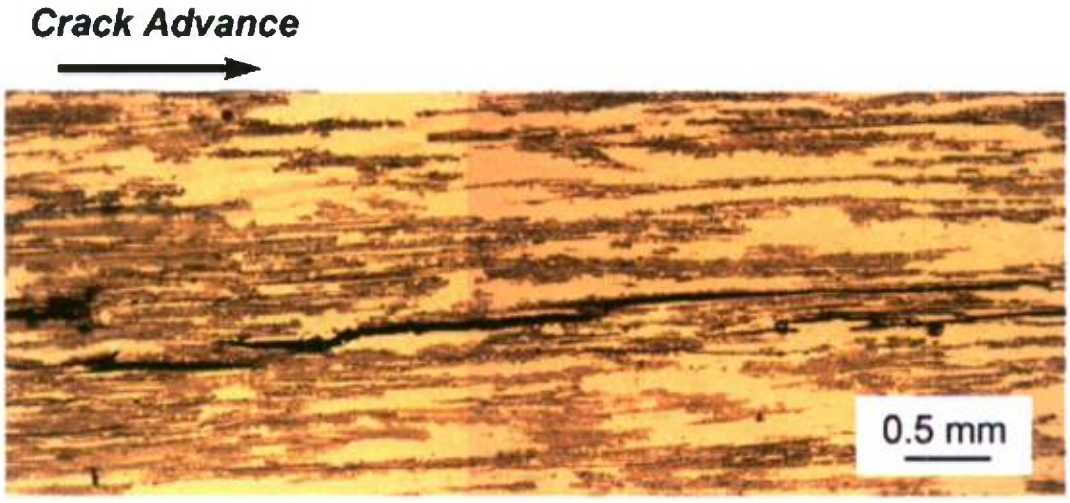

Fig. 31 Stress corrosion crack observed on specimen surface

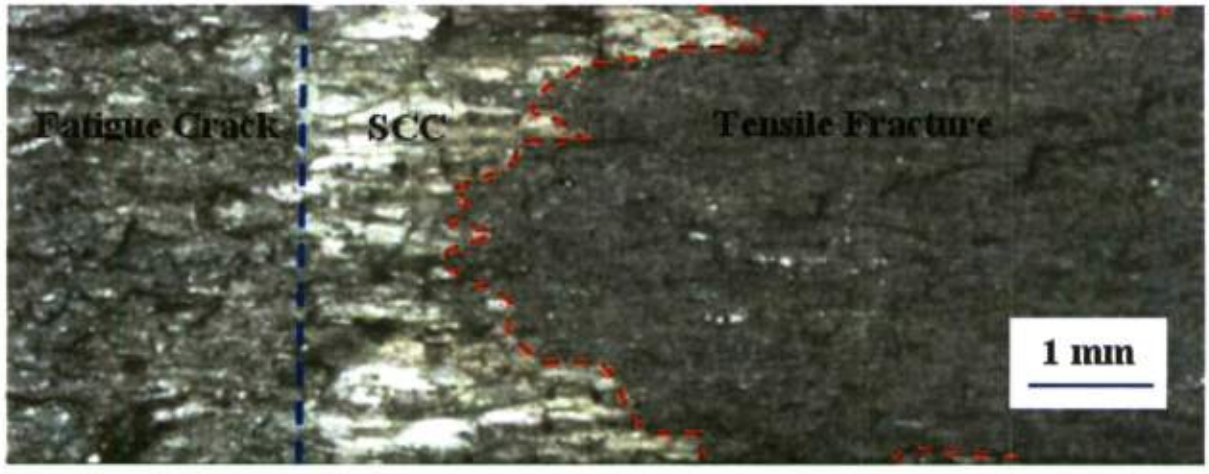

Fig. 32 Fracture surface during early phase of the stable growth stage

After the transient stage, a stable SCC growth can be established with the main crack penetrating completely through the thickness of the specimen. As shown in Fig. 31, stress corrosion crack propagates in a jump manner along grain boundary in the L direction. Figure 32 shows a typical fracture surface during an early phase of the stable growth stage, with a stress corrosion crack length of 3 mm measured from the pre-cracking tip on specimen surface. A clear interface (red dashed line) exists between the SCC zone and the tensile fracture zone under monotonic tension. The profile of the main crack front appears a "C" shape, and generally such a shape persists until final fracture. This indicates that stress corrosion cracks start on the specimen surface and

penetrate the thickness of the specimen. The C-shaped crack front profile is different from that generally found in thick specimens by other researchers who reported either "bowed" crack fronts with crack being longer in the center of the specimen or relatively straight crack front. In the current study, the crack length measured on one side of the specimen surface was used to calculate the crack growth rate and the stress intensity factor. As can be observed in Fig. 32, even during the stable growth stage, a new crack can appear ahead of the existing main crack and grows independently and later combines into the main crack. This may cause the growth rate of the main crack to slow down. The nature of cracking to form jogs along parallel grain boundaries and the morphology of the main crack front lead to the conclusion of limited applicability of the apparent stress intensity factor concept [124]. The local effective stress intensities at the crack tip can significantly differ from the macroscopic values calculated based on the total crack length measured on the specimen surface [124]. Multiple cracks and branches along the grain boundaries were observed and these cracks tend to merge with time to form one main crack [86, 124, 127, 129].

The SEM photographs of the stress corrosion fracture surface are shown in Fig. 33. The fracture mechanism is observed to be a mixture of intergranular and transgranular modes. The stress corrosion crack surface is predominantly intergranular with relatively flat grain boundaries (Fig. 33(a)). In the remaining area, ductile transgranular cracking with the presence of dimples typical for mechanical fracture is frequently observed (Fig. 33 (b)). In the central region of crack profile, the portion of the transgranular mode increases. The present observations are in agreement with earlier fractographies observed for a similar material [86, 111,130].

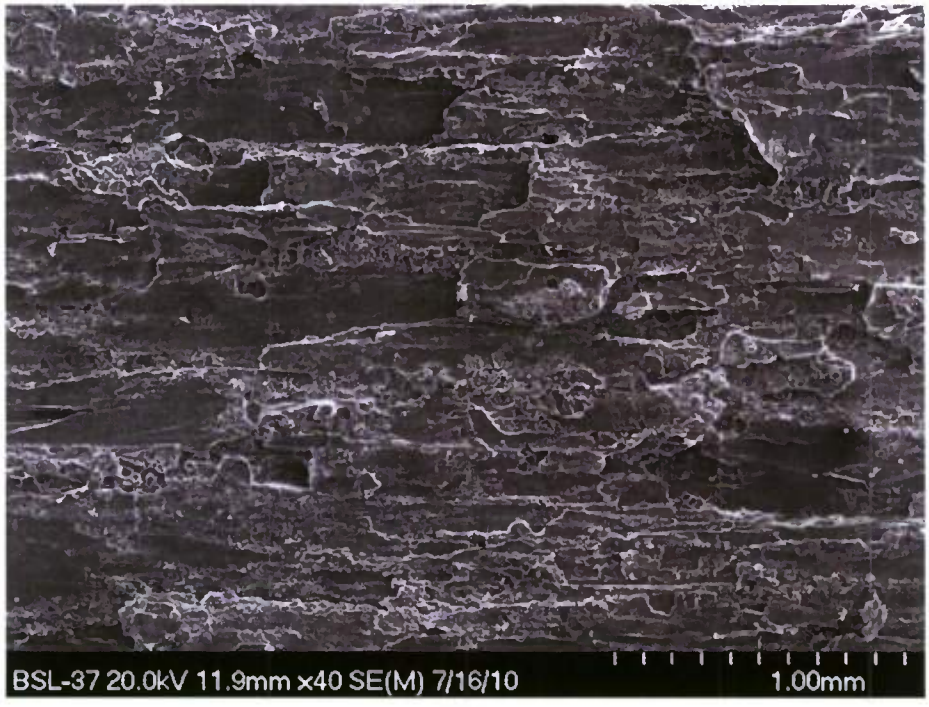

(a)

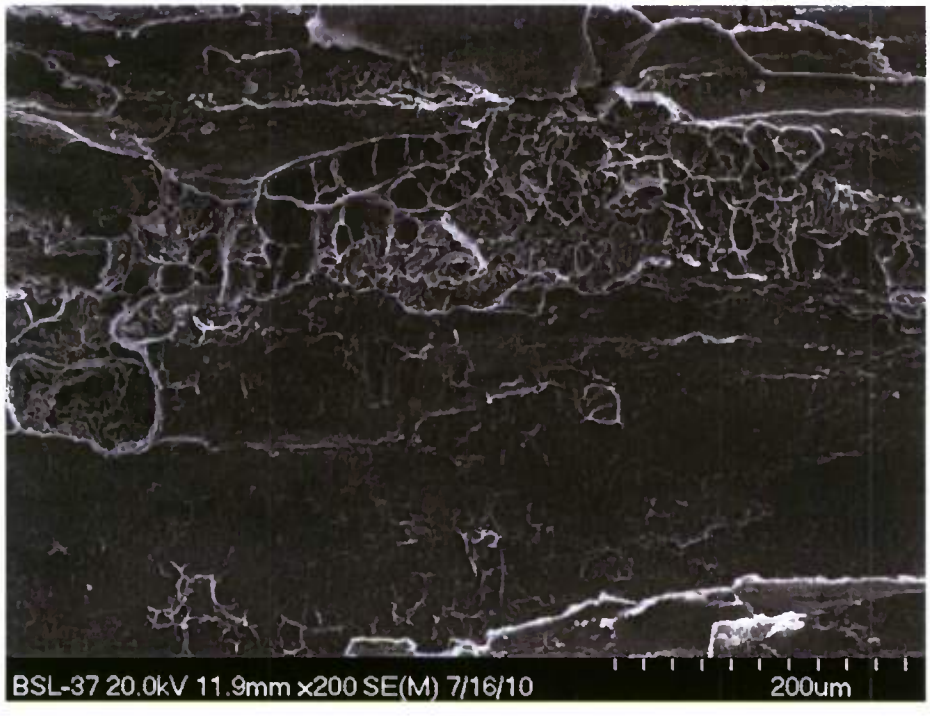

(b)

Fig. 33 SEM fractographs of SCC zone

II.3.2. Effect of Loading Magnitude

The influence of initially applied stress intensity factor, ranging from 6 to 21.5 MPa $\sqrt{m}$, on SCC behavior was investigated using the specimens with fatigue pre-cracks. For each specimen, the initially applied stress intensity factor in SCC test was higher than that applied during fatigue pre-cracking to avoid the possible overloading effect on SCC behavior. Results shown in Fig. 34 suggest that a power law relationship exists between the incubation time and the applied load level. With the decrease in the applied stress intensity factor, the incubation time increases significantly. In a latter section, the determinations of the threshold stress intensity factor (K_{ISCC}) and the fracture stress intensity factor (K_{IC}) will be discussed. In Fig.34, these two limiting stress intensity factors for 3.5% NaCl concentration were added. In addition, the incubation time of the specimen shown in Fig.29 and the incubation times for the first step loading in the high-low step loading experiments were also included in Fig.34. A similarity between the S-N (stress-life) curve in fatigue and the K – incubation time curve in stress corrosion can be noticed. Data scatter similar to that in fatigue curve can be also observed in Fig.34.

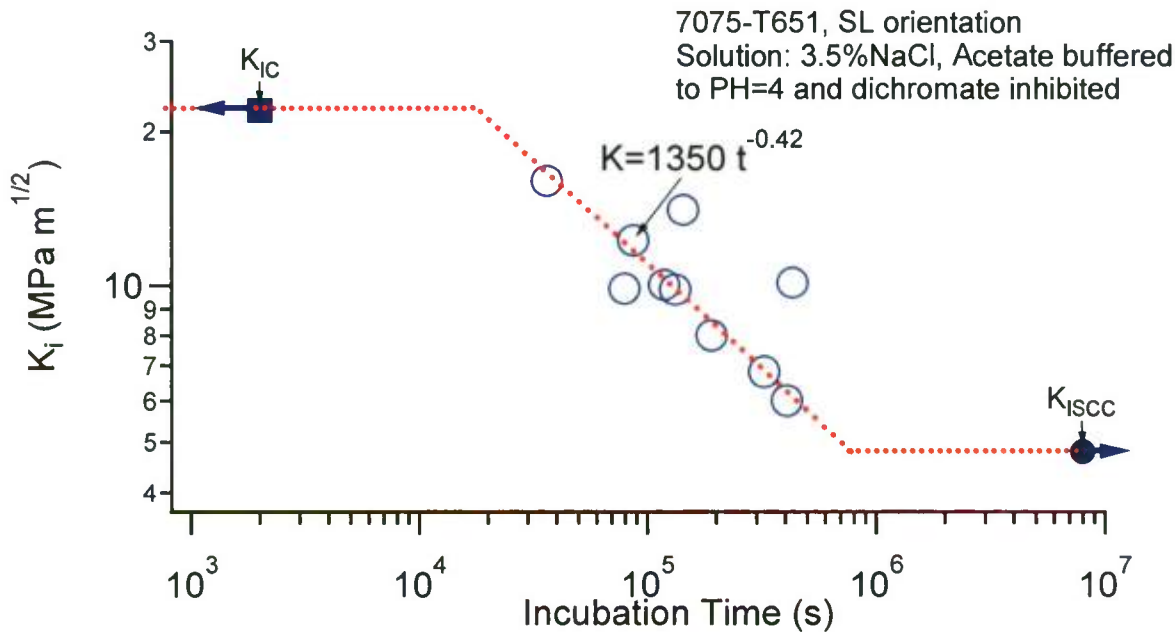

Fig. 34 Incubation time as a function of initially applied stress intensity factor

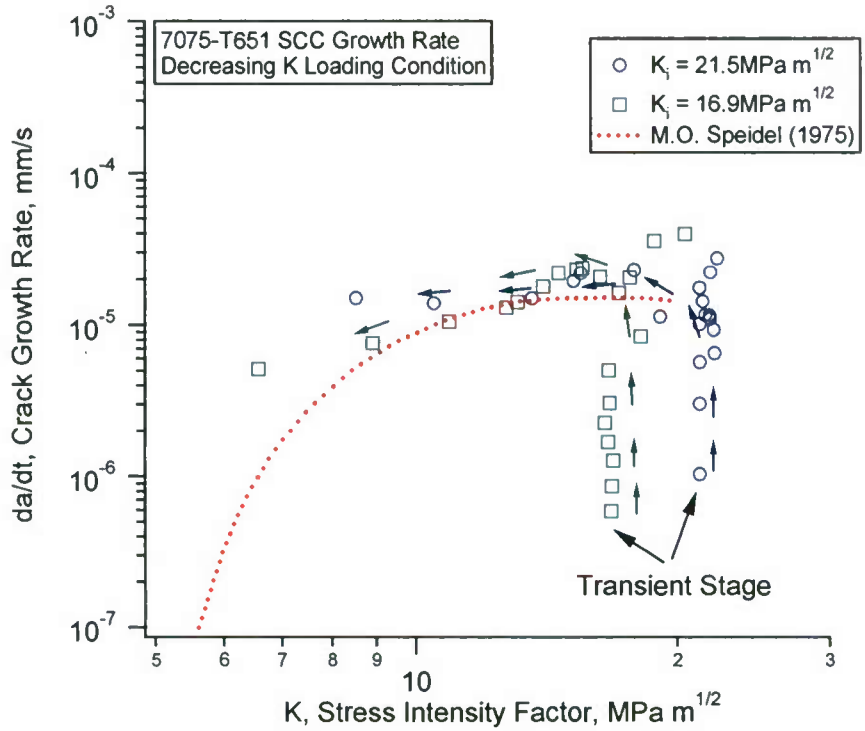

(a)

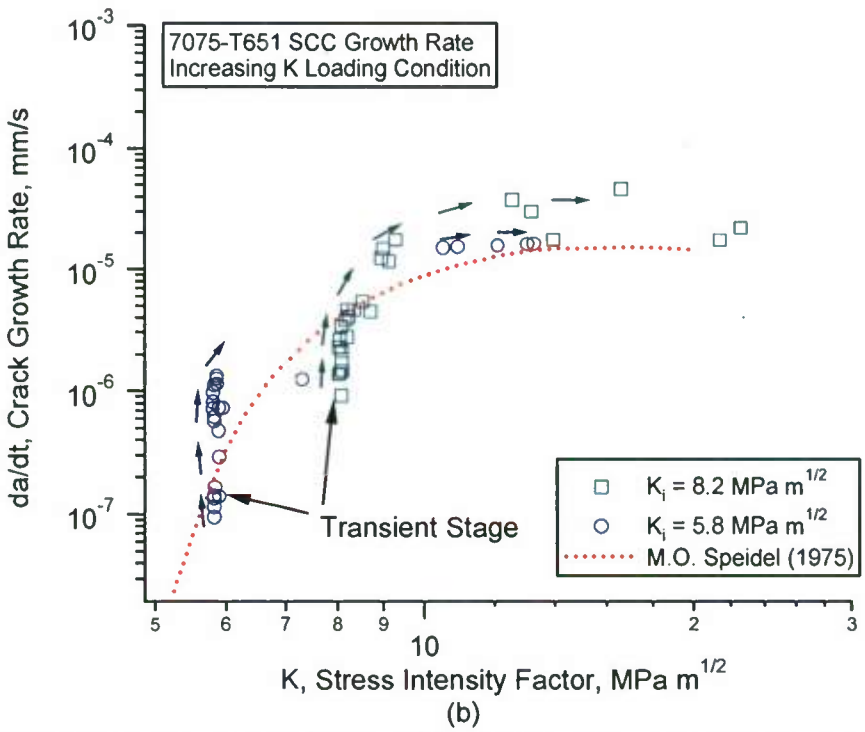

(b)

Fig. 35 Stress corrosion crack growth rate curves under: (a) decreasing and (b) increasing stress intensity factor conditions

By adding or removing the spring washers in the loading system shown in Fig. 26, the tendency of the variation of stress intensity factor with crack length can be adjusted. In such a way, the crack propagation behavior in a wide range of stress intensity factor values can be conveniently investigated. Figure 35 exhibits the crack growth behavior of stress corrosion crack represented in traditional da/dt versus K axes in the log-log scale. For the SCC tests in Fig. 35(a), the spring washers were not employed and the stress intensity factor decreased with crack extension. For the SCC tests in Fig. 35(b), the application of spring washers resulted in an increased stress intensity factor with crack propagation. Data scatter on the plot can be observed, which can be attributed to step-wise nature of stress corrosion crack propagation by advancing cracks along the parallel grain boundaries. It should be noticed that the degree of crack growth data scatter is considerably lower in the experiments with increasing stress intensity factor (Fig. 35 (b)) as compared to those obtained from the decreasing K experiments (Fig. 35(a)).

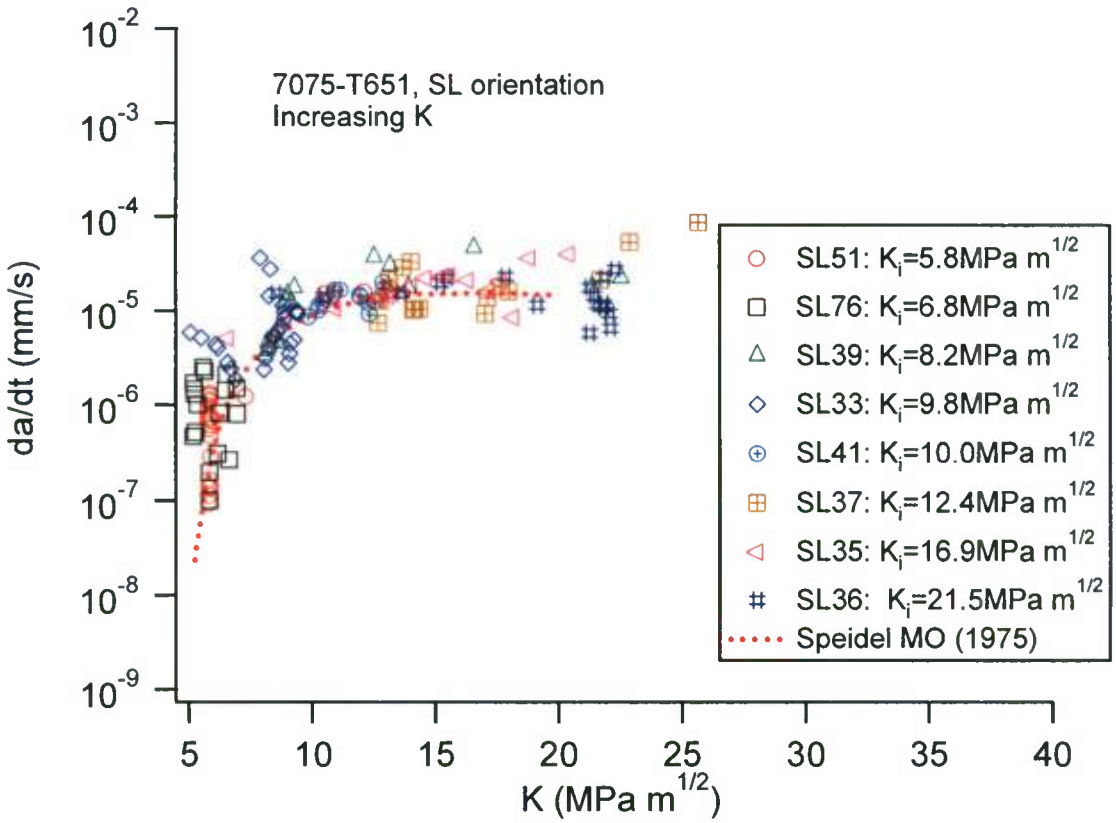

Fig. 36 Variation of stable crack growth rate with stress intensity factor

Excluding the crack growth rate in transient stage, the relationship between the stable crack growth rate and the stress intensity factor is plotted in Fig. 36. As generally observed in commercial high strength aluminum alloys [86], the da/dt - K curve in Fig.

36 consists of two regions. In region I, at relatively low stress intensities (K <10 MPa $\sqrt{m}$), the crack growth rate increases with increasing stress intensity factor. Region II exhibits a plateau and the SCC growth rate is independent of stress intensity factor in the range of 10 to 22 MPa $\sqrt{m}$. The plateau velocity of Region II has an approximate value of 2×10^{-5} mm/s for all specimens, which is in good agreement with the previous data reported by Speidel [86]. It should be mentioned that the experimental conditions in Speidel's SCC tests on S-L oriented 7075-T651 plates were quite different from those in the current investigation. For example, Speidel [86] employed double cantilever beam (DCB) specimens under alternate immersion conditions in 3.5% NaCl solution. Despite these differences, the electrochemical environment in the vicinity of the crack tip during the stable crack growth stage in Speidel's SCC tests was similar to that in the present study. For the stress corrosion of an aluminum alloy in aqueous solution, the pH value of the solution at the tip of a growing SC crack is typically around 3.5, independent of the pH value of the bulk solution [86, 88, 91, 131]. As a result, the solution pH in a wide range has no effect on the region II crack propagation rate. Hartman et al. [132] investigated the effect of corrosion medium on the growth of stress corrosion cracks in aluminum alloy 7075 and they found that in 3% NaCl solution the SCC behavior was neither significantly affected by the pH in the range 3-10 nor in almost neutral solution by addition of chromate. Insignificant effects of chromate on crack kinetics were also observed in other studies [123, 133]. However, Connolly et al. [134] reported that the chromate-inhibited acidified bulk chloride environment identical to that in the current study resulted in a lower Stage II crack growth rate. Landkof and Gal-or [135] reported that the addition of 2 wt% sodium dichromate to a 3.5 wt% NaCl solution led to significant increase in crack growth rate.

Transient and stable growth can be observed in all of the experiments (Fig. 35). The fact that transient crack growth is found under different initial values of applied stress intensity may lead to an erroneous interpretation of threshold stress intensity factor. Indeed, a threshold-like behavior can be observed in all of the experiments shown in Fig. 35. However, the crack growth behavior during the transient stage is completely different from the threshold behavior. When the stress intensity factor approaches the threshold value, the crack growth rate is consistently low. A careful analysis of the crack growth behavior during the transient stage of SCC test indicates that the initial crack growth rate is relatively high, then decreases gradually to a minimum value or even zero, and holds for a period of time, then resumes to the stable crack growth rate. In the transient stage of SCC test, the crack extension is small and the load is reduced slightly, resulting in an approximately constant stress intensity factor. As a result, the transient stage appears to be a vertical line on the curve of crack growth rate versus stress intensity factor. In the experimental practice, the threshold stress intensity is usually determined as the minimal value of K from the plot of applied stress intensity

versus time to failure. Such experiments are typically time consuming and can last for more than 10,000 hours [136].

II.3.3. Effects of Overload and Underload

Similar to overload/underload effects on fatigue crack growth, the spikes of a tensile or compressive load applied prior to stress corrosion testing have a significant effect on SCC incubation time due to residual compressive or tensile stress ahead of the crack tip created during overloading/underloading. To study the effects of overload and underload, a series of SCC experiments were conducted in 3.5wt% NaCl aqueous solution on the specimens previously subjected to overloading or underloading at the end of the pre-cracking. Seven specimens were pre-cracked with a maximum stress intensity factor in the loading cycle $K_{max} = 10MPa\sqrt{m}$, then for each specimen a selected overload or underload was applied. Five overloads (25%, 50%, 75%, 100%, and 125% higher than $10MPa\sqrt{m}$) and two underloads (50% and 100% lower than $-10MPa\sqrt{m}$) were selected. The subsequent stress corrosion testing was done with the initial stress intensity factor identical to the maximum stress intensity factor in the last cycle of the fatigue pre-cracking ($K_i = 10MPa\sqrt{m}$).

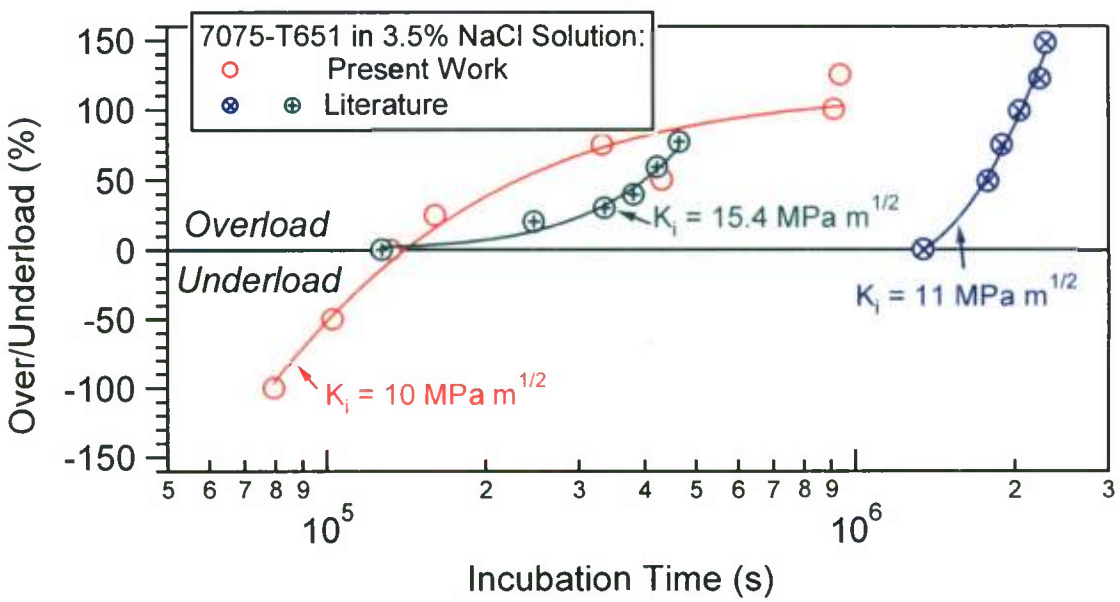

Fig. 37 Overload effect on incubation time of 7075-T651 aluminum alloy: Comparison with literature data [111]

Figure 37 shows how incubation time is significantly affected by the overload/underload application. The markers in Fig. 37 represent the experimentally obtained data points and the lines are shown as a reference fit of the data. It can be seen that the effect on crack incubation depends on whether the applied overload is tensile or compressive. When the incubation time corresponding to zero overload is taken as a reference, it can be seen that the compressive overloading (underloading) tends to accelerate the crack incubation due to a tensile residual stress while tensile overloads prolong the onset of stress corrosion cracking due to a compressive residual stress (Fig. 37). A similar phenomenon of crack growth retardation upon tensile overloading and acceleration following compressive underloading have been observed in fatigue crack propagation of metallic materials and can be attributed to formation of large plastic deformation zones at the crack tip due to application of overloads. It should be also noticed in Fig. 37 that the tensile overloads higher than 50% tend to produce much greater delays in the incubation time.

As a comparison, the experimental results by Hanisch and Burck [111] on the overload effect on SCC behavior of S-L oriented 7075-T651 aluminum alloy specimens are also exhibited in Fig. 37. Similar to the current study, Hanisch and Burck [111] found that the incubation time increased with increasing overload percentage. However, several major differences can be observed in Fig. 37. The overall shape of the curve obtained in the current investigation and those reported in [111] is very different. In the range of high overload percentage (greater than 50%), the small increase in pre-stressing results in significant increase in incubation time as can be seen from the data obtained in the present work. At the same time, the results from [111] demonstrate the tendency of overloads to become less effective as they get higher. In addition to the principal differences in post-overload incubation behavior, the incubation times reported in [111] are much higher for similar levels of initially applied stress intensity factor (Fig. 37).

Such discrepancies can be probably attributed to the differences in specimen geometry and testing technique with the other variables such as material treatment, mechanical properties, and the solution pH. Much thicker (12.7 mm) DCB specimens were used by Hanisch and Burck [111] as compared to the 3.8 mm thick C(T) specimens used in the current study. In addition, alternate immersion tests were performed in [111]. The specimens were immersed in the solution three times per day otherwise being kept exposed to 50% relative humidity air [111]. The engineering recommendation states that there is no significant difference between region II crack propagation rate obtained from alternate immersion and continuous immersion tests [131]. However, these differences can vastly affect the incubation time and the region I crack propagation rate [131].

It is well established that overload retards fatigue crack growth while underload accelerates fatigue crack growth. However, tensile or compressive overloading has no

obvious influence on the subsequent transient crack growth and stable crack propagation in SCC test, as being illustrated in Fig. 38. During the initial crack growth stage, the crack tip needs to pass through the plastic zone caused by the overload or underload. It seems that prior loading history does not affect the stable stress corrosion cracking behavior. Results shown in Fig. 38 suggest that the average plateau crack velocity does not change practically as a function of the applied overloading/underloading. The average plateau velocity is confined to a narrow band around $da/dt = 2\times10^{-5}\ mm/s$ which is identical to the plateau crack growth rate in specimens without overloading.

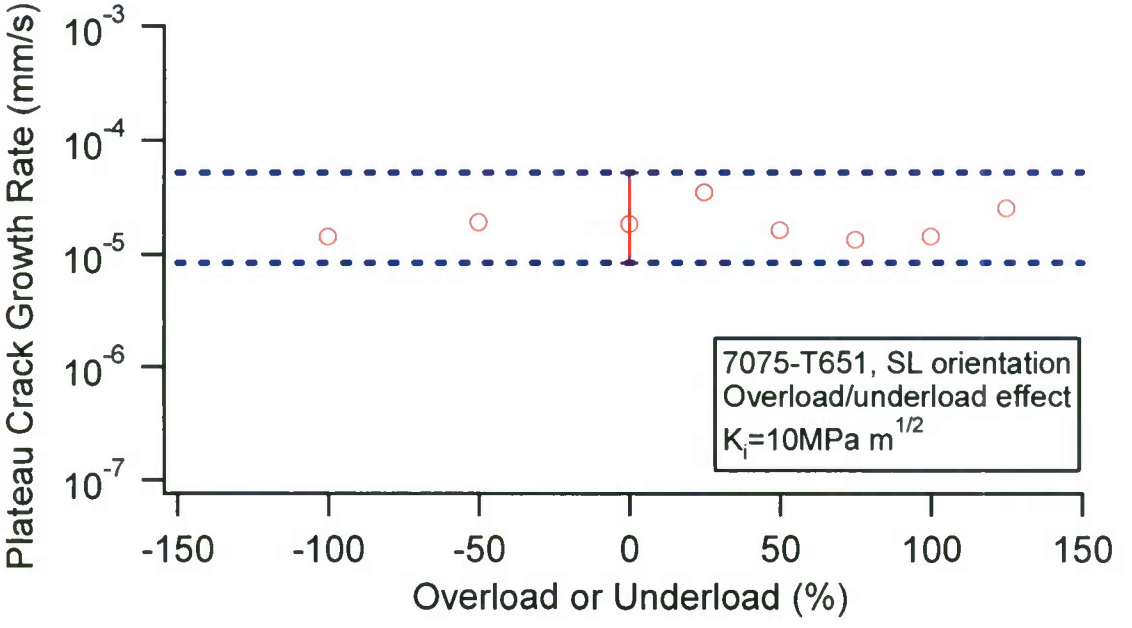

Fig. 38 Effects of overload and underload on plateau crack growth rate of 7075-T651 aluminum alloy

II.3.4. Effect of High-Low Sequence Loading

The effect of variable loading on the stress corrosion crack growth was investigated in two high-low loading sequence experiments conducted in 3.5% NaCl aqueous solution. Each experiment consisted of two loading steps with the load being reduced by a specific percentage at the beginning of the second step. In the first experiment, SCC test was conducted on specimen SL 48, which was underloaded by 100% before SCC test. After the stable crack growth was established at a = 20.765mm and K = 13.7MPa $\sqrt{m}$ (Step 1), the stress intensity factor was reduced to 10.7 MPa $\sqrt{m}$ and SCC test was continued until fracture occurred (Step 2). In the second experiment,

SCC test was performed on specimen SL 45, which was overloaded by 25% before SCC test. After the stable crack growth was established at a = 22 mm and K = 15.3 MPa$\sqrt{m}$ (Step 1), the stress intensity factor was reduced to 8.3 MPa$\sqrt{m}$ and SCC test was continued until specimen fractured (Step 2). The details of the high-low sequence loading experiments can be found in Table 12. The results of the experiments are summarized in Fig. 39. After reducing the load from a higher value to a lower value, the previous stable crack growth was terminated, and a second incubation time and corresponding transient period of crack growth were observed (Fig. 39 (a-b)). Compared to Step 1, the transient stage in Step 2 was greatly shortened or even disappeared. This is possibly because the penetration of the stress corrosion crack tip through the thickness of specimen has been completely established in Step 1. Figure 39(c-d) represents the crack growth rate as a function of applied stress intensity for the experimental scenarios shown in Fig. 39(a-b). It should be mentioned that the second step in specimen SL 45 was performed under the decreasing K condition. As can be seen, after the second period of incubation and transient growth, the velocity of crack extension returns to the characteristic value of the stable crack growth observed in the experiments on the alloy under investigation (Fig. 39(c-d)).

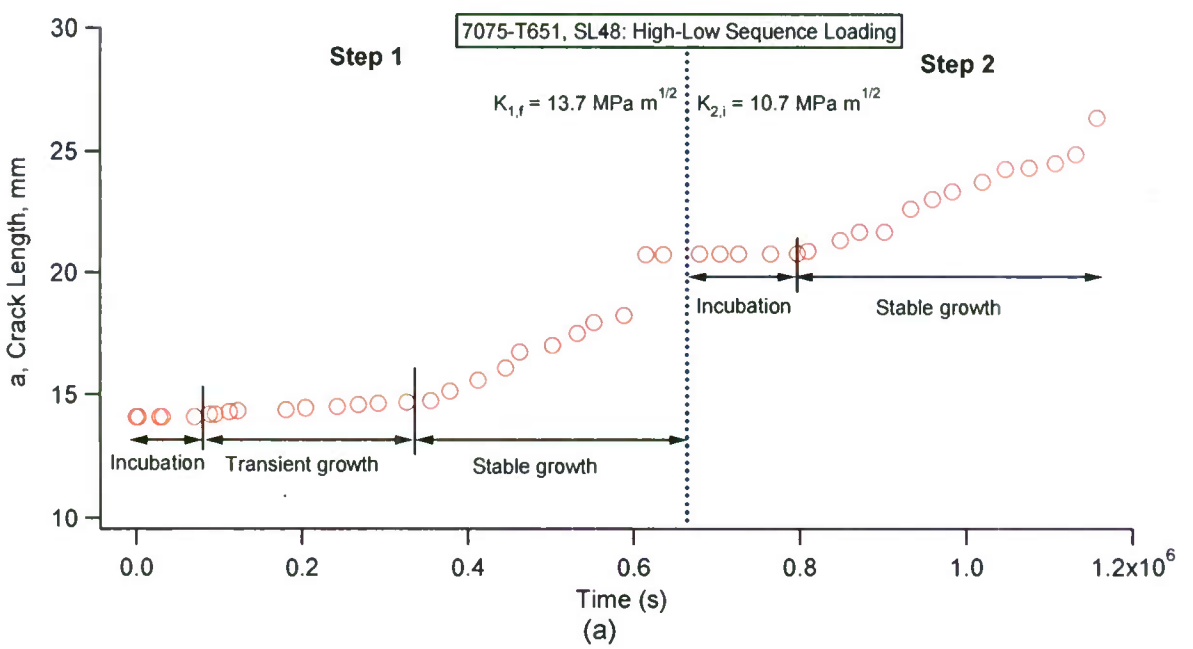

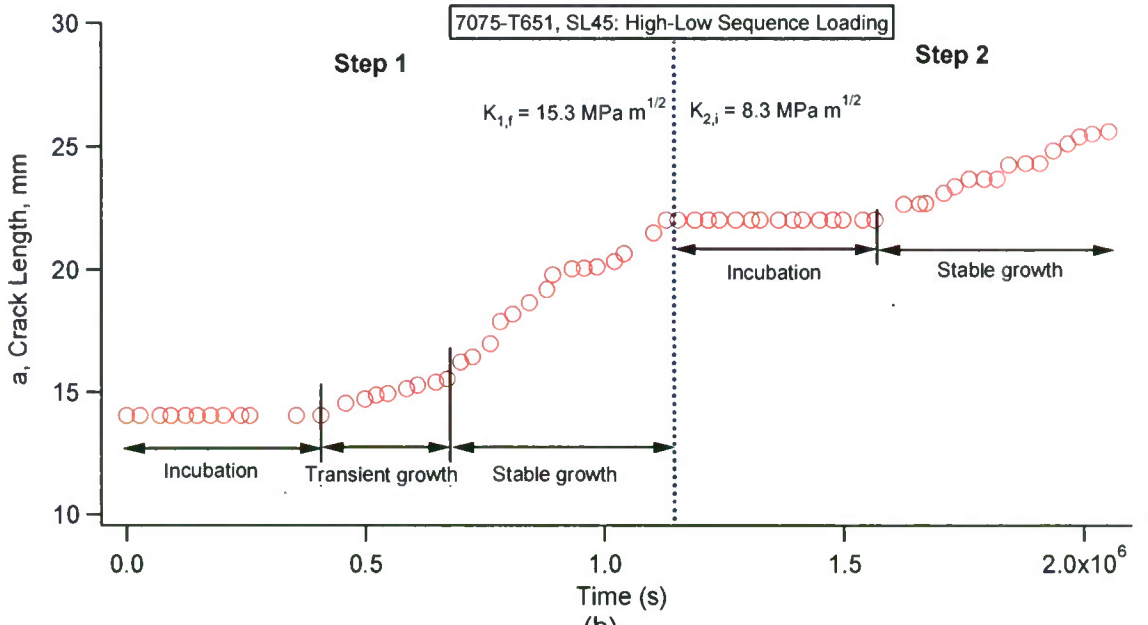
7075-T651, SL45: High-Low Sequence Loading
Step 1
Step 2
$K_{1,f}$ = 15.3 MPa m$^{1/2}$
$K_{2,i}$ = 8.3 MPa m$^{1/2}$
Incubation
Transient growth
Stable growth
Incubation
Stable growth
a, Crack Length, mm
Time (s)
30
25
20
15
10
0.0
0.5
1.0
1.5
2.0x10^6

(b)

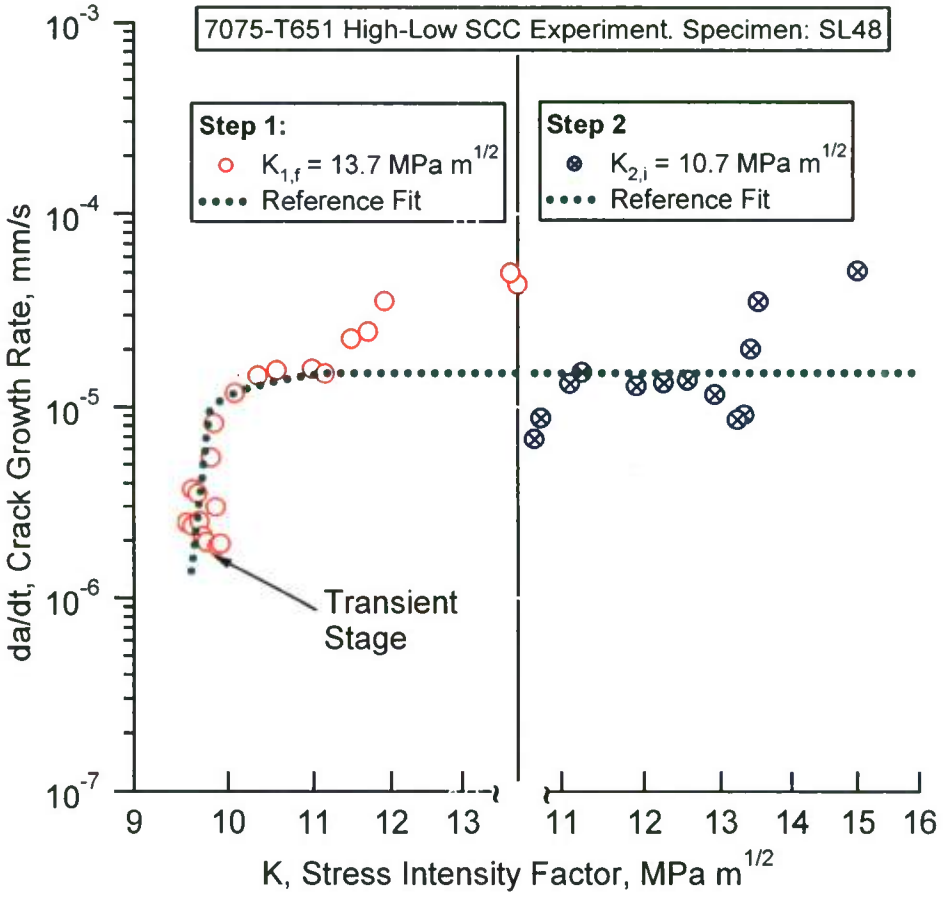
7075-T651 High-Low SCC Experiment. Specimen: SL48
Step 1:
$K_{1,f}$ = 13.7 MPa m$^{1/2}$
Reference Fit
Step 2
$K_{2,i}$ = 10.7 MPa m$^{1/2}$
Reference Fit
Transient Stage
da/dt, Crack Growth Rate, mm/s
10^{-3}
10^{-4}
10^{-5}
10^{-6}
10^{-7}
9
10
11
12
13
11
12
13
14
15
16
K, Stress Intensity Factor, MPa m$^{1/2}$

(c)

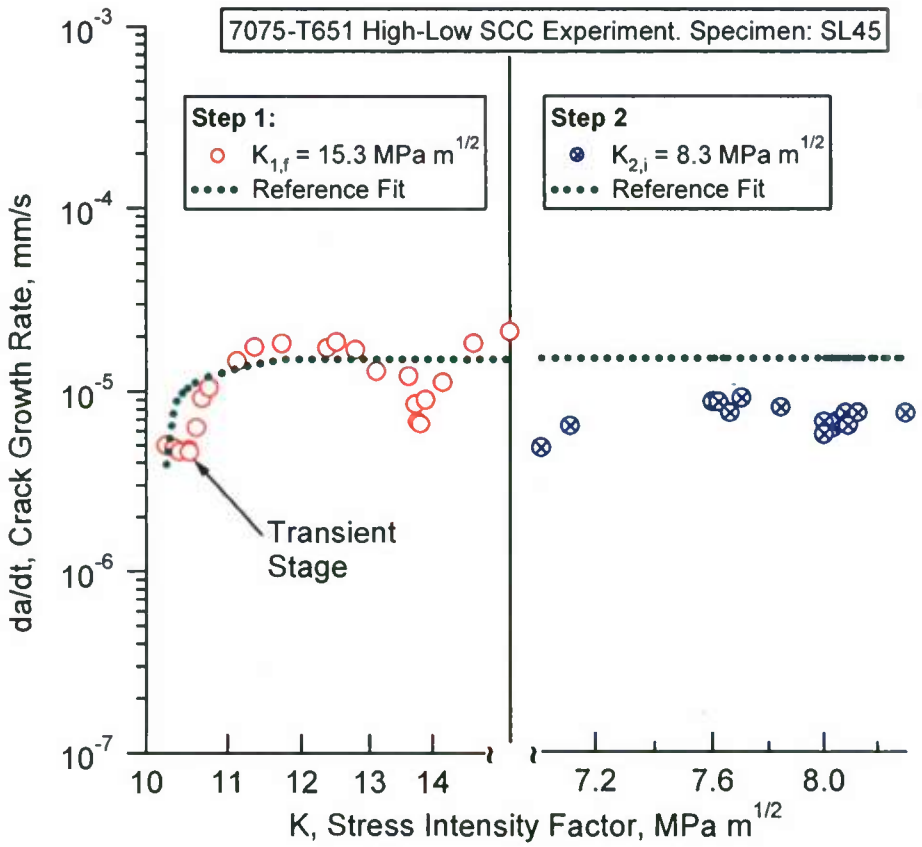

(d)

Fig. 39 Effect of high-Low sequence loading on SCC of 7075-T651 alloy: (a) stress intensity factor was reduced from 13.7 MPa $\sqrt{m}$ to 10.7 MPa $\sqrt{m}$, (b) stress intensity factor was reduced from 15.3 MPa $\sqrt{m}$ to 8.3 MPa $\sqrt{m}$, and (c, d) variation of crack growth rate with stress intensity factor

II.3.5. Effect of NaCl Concentration on Stress Corrosion of 7075-T651

The SCC experiments were performed in the aqueous solution containing sodium chloride, 0.02M sodium dichromate, 0.07M sodium acetate, plus 0.389M acetic acid to pH=4. The concentration of sodium chloride ranged from 0.01 wt% to 5.0 wt% NaCl (0.0017M to 0.85 M). The solution can prevent the formation of corrosion products and avoid product wedging and facilitate observation of cracks [123-124]. The schematic of the experimental setup is shown in Fig. 26. No aeration was supplied during the experiments. Solution in the chamber was replaced weekly. During the SCC experiments, no protective coating was applied to the surfaces of the specimens, and the specimens were not deliberately isolated from the loading system.

Table 13. SCC tests on effect of NaCl concentration and initial stress intensity factor on incubation time and stable crack growth

Spec. #	NaCl (%/M)	P_i (kN)	a_i (mm)	a_f (mm)	K_i $(MPa\sqrt{m}$	t_{inc} (s)	t_{frac} (s)	$(da/dt)_p$ (mm/s)
SL66	5.0/0.85	1.28	14.20	32.23	10.0	188,170	1,159,035	2.17e-5
SL65	3.0/0.51	1.32	14.14	26.07	10.0	94,968	1,097,075	2.26e-5
SL64	2.0/0.34	1.29	14.24	29.38	10.0	87,476	903,583	4.26e-5
SL62	1.0/0.17	1.32	14.06	26.64	10.0	103,458	743,889	4.21e-5
SL79	1.0/0.17	1.96	14.11	15.54	15.0	40,606	278,019	7.65e-6
SL102	0.35/0.06	0.79	13.91	33.75	6.0	534,542	1,146,786	9.06e-5
SL99	0.35/0.06	1.06	14.31	32.38	8.0	100,849	1,340,912	5.67e-5
SL61	0.35/0.06	1.28	14.04	32.12	10.0	63,004	731,262	7.61e-5
SL78	0.35/0.06	1.95	14.10	15.58	15.0	40,950	365,681	9.69e-6
SL100	0.35/0.06	1.53	14.58	27.22	12.0	63,264	961,371	6.41e-5
SL101	0.35/0.06	1.80	14.31	24.32	14.0	61,453	642,352	4.76e-5
SL63	0.10/0.017	1.34	14.06	26.50	10.0	40,507	619,150	1.40e-4
SL72	0.10/0.017	1.98	14.35	22.10	15.0	22,614	173,729	1.74e-4
SL69	0.07/0.012	1.29	14.34	28.57	10.0	102,204	1,160,053	2.49e-5
SL67	0.035/0.006	1.31	14.22	26.48	10.0	229,260	8,722,204	2.12e-6
SL81	0.035/0.006	2.00	13.94	17.08	15.0	63,097	1,681,266	2.68e-6
SL103	0.035/0.006	1.57	14.22	18.28	12.0	300,896	6,054,922	8.45e-7
SL104	0.035/0.006	1.74	14.35	20.64	14.0	55,018	3,991,148	1.38e-6
SL105	0.035/0.006	1.04	14.49	31.90	8.0	492,008	3,990,159	5.21e-6
SL106	0.035/0.006	0.79	14.09	15.69	6.0	2,955,600	23,026,500	6.41e-7
SL114	0.01/0.0017	1.05	14.10	18.41	8.0	1,630,747	15,723,724	4.08e-7
SL115	0.01/0.0017	1.30	14.24	n/a	10.0	1,269,220	n/a	2.01e-7
SL116	0.01/0.0017	1.62	14.02	19.15	12.0	845,038	12,505,887	2.11e-6
SL70	0.01/0.0017	1.32	14.05	16.41	10.0	2,044,745	11,464,752	4.42e-7
SL83	0.01/0.0017	2.00	14.00	20.16	15.0	1,149,153	11,663,520	7.24e-7

Note: P_i -Initial applied load K_i -Initial applied stress intensity factor

a_i-Initial crack length a_f-Crack length at failure of specimen or termination of test .

t_{inc} -Incubation time t_{frac} -failure time K_f - stress intensity factor at failure of specimen or termination of test

$(da/dt)_p$-average plateau velocity

Although galvanic coupling between test specimen and loading system was inevitable, the crack growth at the crack tip was not observed within three months when the applied stress intensity factor (K) was much lower than K_{ISCC} . Therefore, the influence of galvanic corrosion on the SCC results (incubation time and crack growth rate) in this study was insignificant. Details of the experiments and results are summarized in Table 13.

The following SCC tests were designed to investigate the influences of loading level and concentration of sodium chloride on the SCC behavior of 7075-T651 aluminum alloys: (1) SCC tests at different initial loading levels in corrosive solutions with different NaCl concentrations (Tables 10, 13); (2) incremental load tests for K_{ISCC} in corrosive solutions with different NaCl concentrations.

Prior to SCC testing, the specimens were pre-cracked to 4 mm using a servo-hydraulic machine in tension-tension loading. Pre-cracks were formed in ambient air by fatigue loading. The final stress intensity factor applied during pre-cracking was less than 3.0 $MPa\sqrt{m}$.

Figure 40 shows the SCC crack growth behavior of the materials at four different NaCl concentrations: 0.01% (0.0017M), 0.1% (0.017M), 0.35% (0.06 M), and 1% (0.17M). The initial applied stress intensity factor was 15 MPa$\sqrt{m}$. Similar to the SCC crack growth behavior observed in the corrosive solution with 3.5% NaCl, three crack growth stages can be identified: incubation, transient growth, and stable growth. Among the four NaCl concentrations, the incubation time and transient stage were the shortest when the NaCl concentration of the solution was 0.1%.

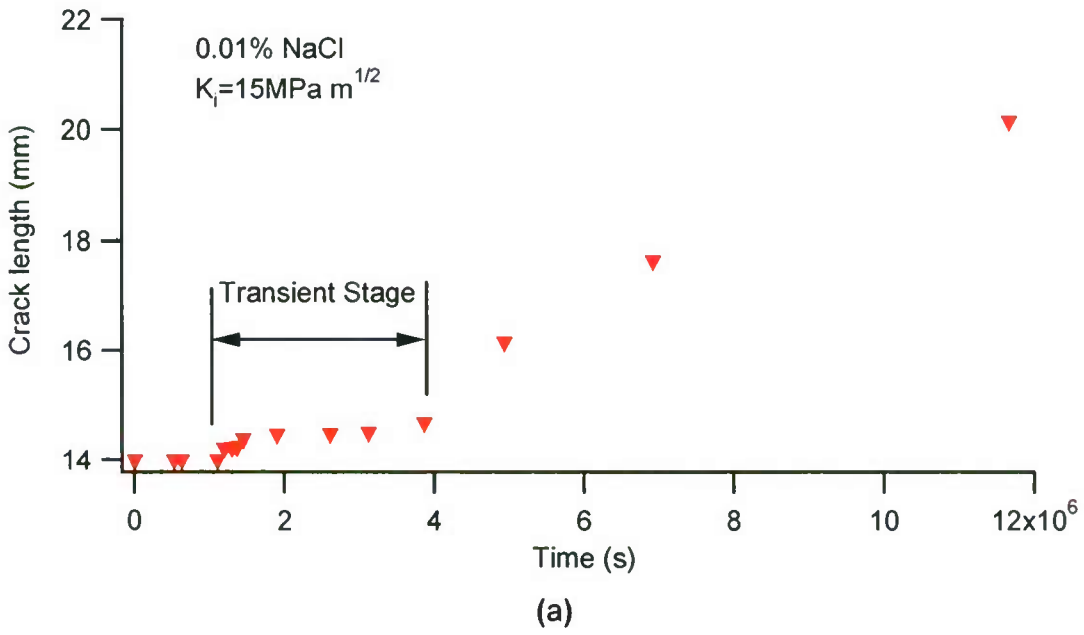

(a)

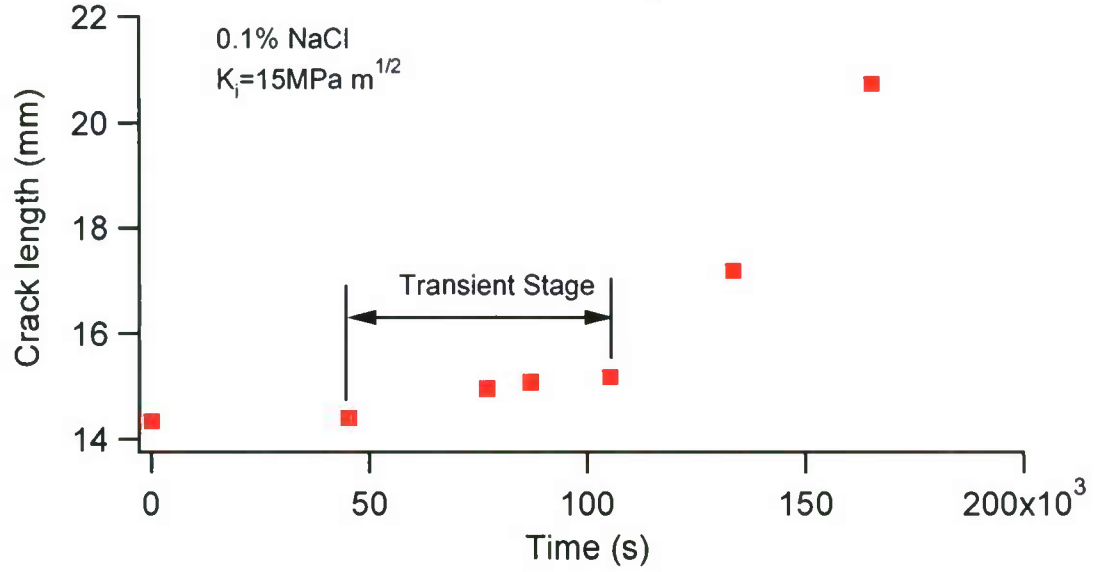
0.1% NaCl
K_i=15MPa $m^{1/2}$
Crack length (mm)
22
20
18
16
14
Transient Stage
0
50
100
150
200x10^3
Time (s)

(b)

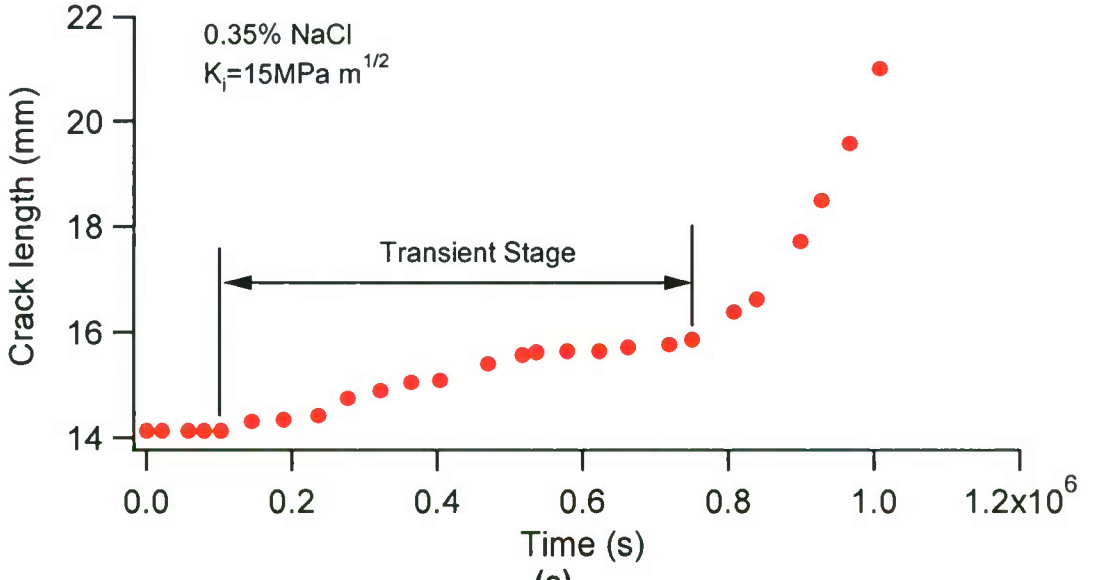
0.35% NaCl
K_i=15MPa $m^{1/2}$
Crack length (mm)
22
20
18
16
14
Transient Stage
0.0
0.2
0.4
0.6
0.8
1.0
1.2x10^6
Time (s)

(c)

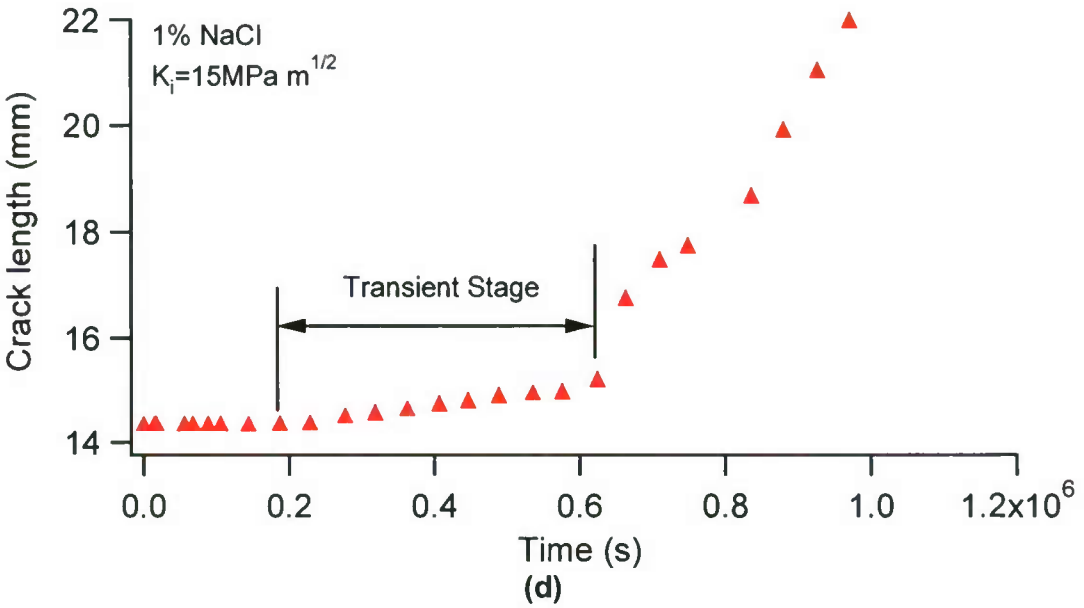

Fig. 40 Typical SCC behavior in corrosive solutions with different NaCl concentrations with initial applied stress intensity factor of 15 MPa $\sqrt{m}$

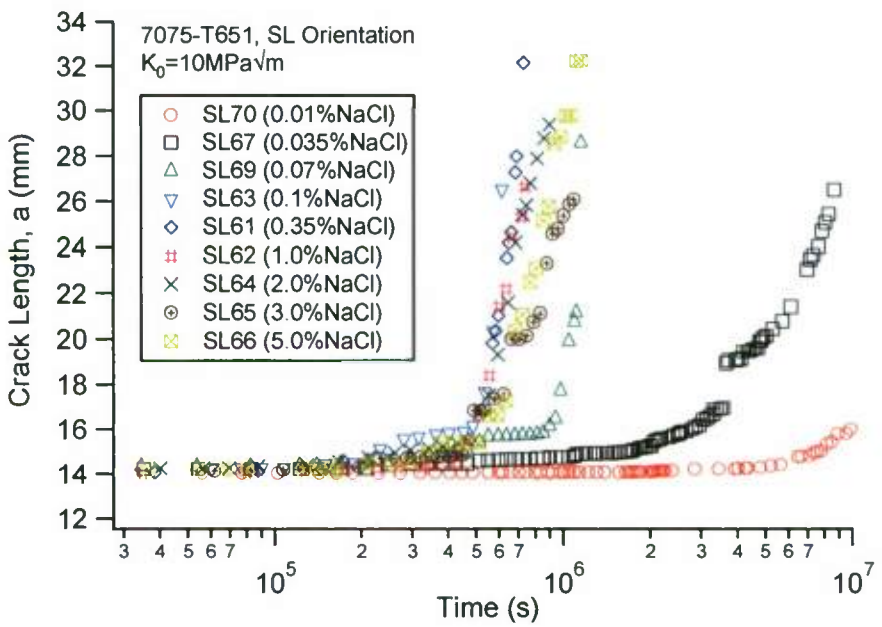

Fig. 41 Influence of NaCl concentration of corrosive solution on the plot of crack length versus time

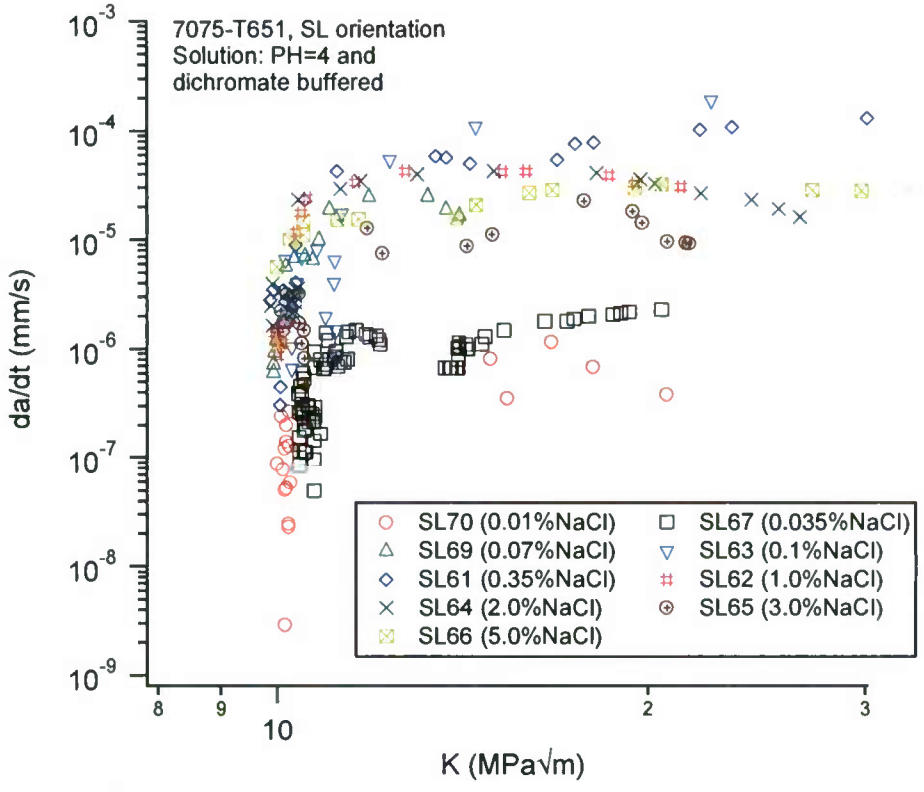

Fig. 42 Variation of SCC crack growth rate with stress intensity factor and NaCl concentration

Figure 41 shows the variations of crack length with time in corrosive solutions with different NaCl concentrations. The initial applied stress intensity factor was 10 MPa $\sqrt{m}$ for all the SCC tests. The stress intensity factor increased with the extension of the crack (increasing K tests). It can be observed that the NaCl concentration has significant influence on the incubation time and the stable crack growth rate of the material.

Figure 42 summarizes the variations of SCC crack growth rate with stress intensity factor for all the NaCl concentrations under investigation. Transient and stable growth can be observed in all of the experiments. A threshold-like behavior corresponding to the transient stage can be observed in all of the experiments shown in Fig. 42. However, the crack growth behavior during the transient stage is completely different from the threshold behavior. When the stress intensity factor approaches the threshold value, the crack growth rate is consistently low.

After the transient stage, the curves of crack growth rate versus stress intensity factor at all the investigated NaCl concentrations exhibit approximately a plateau. The maximum crack growth rate was observed at 0.1% NaCl concentration. When the concentration of NaCl ranges from 0.35% to 5%, the plateau crack growth rate was in a

band between 10^{-5} mm/s to 10^{-4} mm/s. When the concentrations of NaCl solutions were 0.035% and 0.01%, the crack growth rates were significantly reduced.

Table 14. Influence of NaCl concentration on incubation time and stable crack growth rate (K_i=10 $MPa\sqrt{m}$)

Specimen #	NaCl Concentration (%/M)	Incubation Time (hours)	Average Plateau Velocity (mm/s)
SL70	0.01%/0.0017M	568.0	4.42×10^{-7}
SL115	0.01%/0.0017M	352.6	2.01×10^{-7}
SL67	0.035%/0.006M	63.7	2.12×10^{-6}
SL69	0.07%/0.012M	28.4	2.49×10^{-5}
SL63	0.10%/0.017M	11.3	1.40×10^{-4}
SL61	0.35%/0.06M	17.5	7.61×10^{-5}
SL62	1.00%/0.17M	28.7	4.21×10^{-5}
SL64	2.00%/0.34M	24.3	4.26×10^{-5}
SL65	3.00%/0.51M	26.4	2.26×10^{-5}
SL41	3.5%/0.60M	33.0	1.44×10^{-5}
SL66	5.00%/0.85M	52.3	2.17×10^{-5}

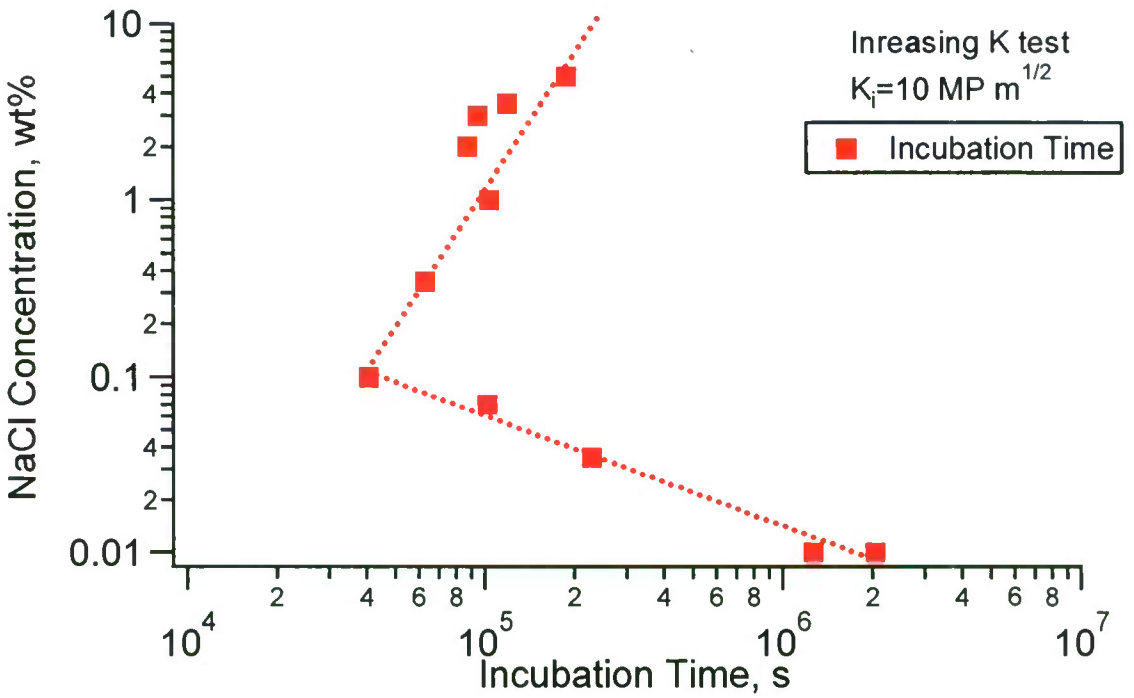

Fig. 43 Influence of NaCl concentration on incubation time

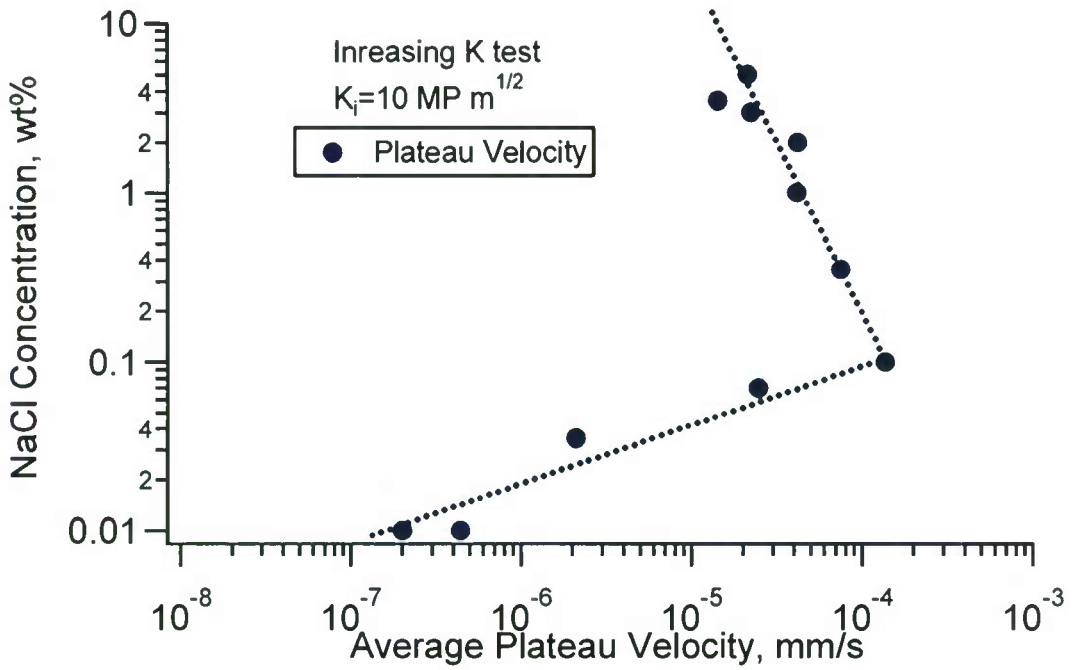

Fig. 44 Influence of NaCl concentration on incubation time and stable (plateau) crack growth rate

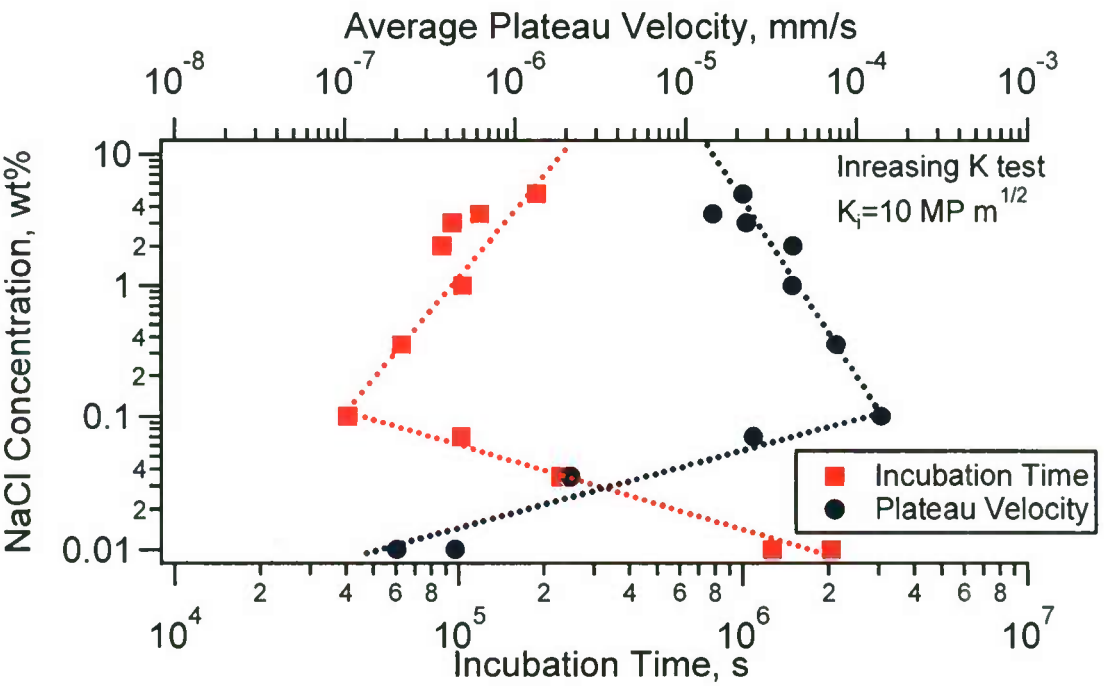

Fig. 45 Influence of NaCl concentration on incubation time and stable (plateau) crack growth rate

Table 14 and Figs. 43-45 summarize the effect of different NaCl concentrations of corrosive solution on the incubation time and the average stable crack growth rate when the initial applied stress intensity factor was 10 $\mathrm{MPa}\sqrt{m}$. Results in Fig.43 are the incubation time as a function of the NaCl concentration in wt%. When the NaCl concentration of solution was less than 0.1%, the incubation time increased significantly with the decrease of NaCl concentration. When the NaCl concentration increases from 0.01% to 0.1%, the incubation time decreases from 568 hours to 11.3 hours. However, when the NaCl concentration further increases from 0.1% to 5.0%, the incubation time increases from 11.3 hours to 52.3 hours. Clearly, the shortest incubation time occurs in 0.1% NaCl solution.

The influence of the NaCl concentration on the average plateau velocity is shown in Fig.44. It can be found that the plateau velocity increases significant with increasing NaCl concentration when the NaCl concentration is less than 0.1%. When the NaCl concentration is larger than 0.1%, the plateau velocity decreases with increasing NaCl concentration.

Figure 45 combines the results shown in Fig.43 and Fig.44 to facilitate a direct comparison of the influences of NaCl concentration on the incubation time and the stable crack growth rate. A shorter incubation time is accompanied by a larger stable crack growth rate. The largest stable crack growth rate and the shortest incubation time occur when the NaCl concentration is 0.1%. .

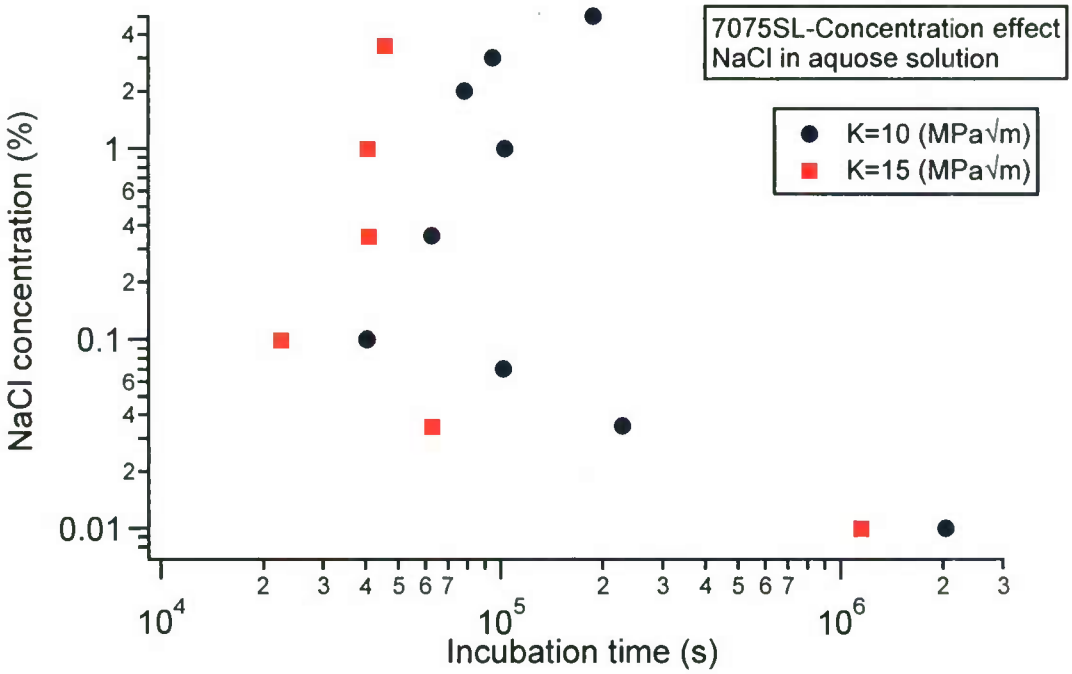

Fig. 46 Comparison of incubation times at two loading magnitudes and different NaCl concentrations

Figure 46 compares the incubation time at two stress intensity factors (K=10 MPa $\sqrt{m}$ and 15 MPa $\sqrt{m}$) and at different NaCl concentrations. At each NaCl concentration level, the incubation time increased with the decrease of stress intensity factor. At the same stress intensity factor, the shortest incubation time occurred in 0.1% NaCl solution. When the NaCl concentration of solution was less than 0.1%, the incubation time increased significantly with the decrease of NaCl solution. At K=15 MPa $\sqrt{m}$ and the NaCl concentration of the solution was in the range of 0.35% to 3.5%, no significant difference in incubation time was observed. At K=10 MPa $\sqrt{m}$ and the NaCl concentration of the solution was in the range of 0.35% to 3.5%, the incubation time exhibited a tendency to increase with increasing NaCl concentration.

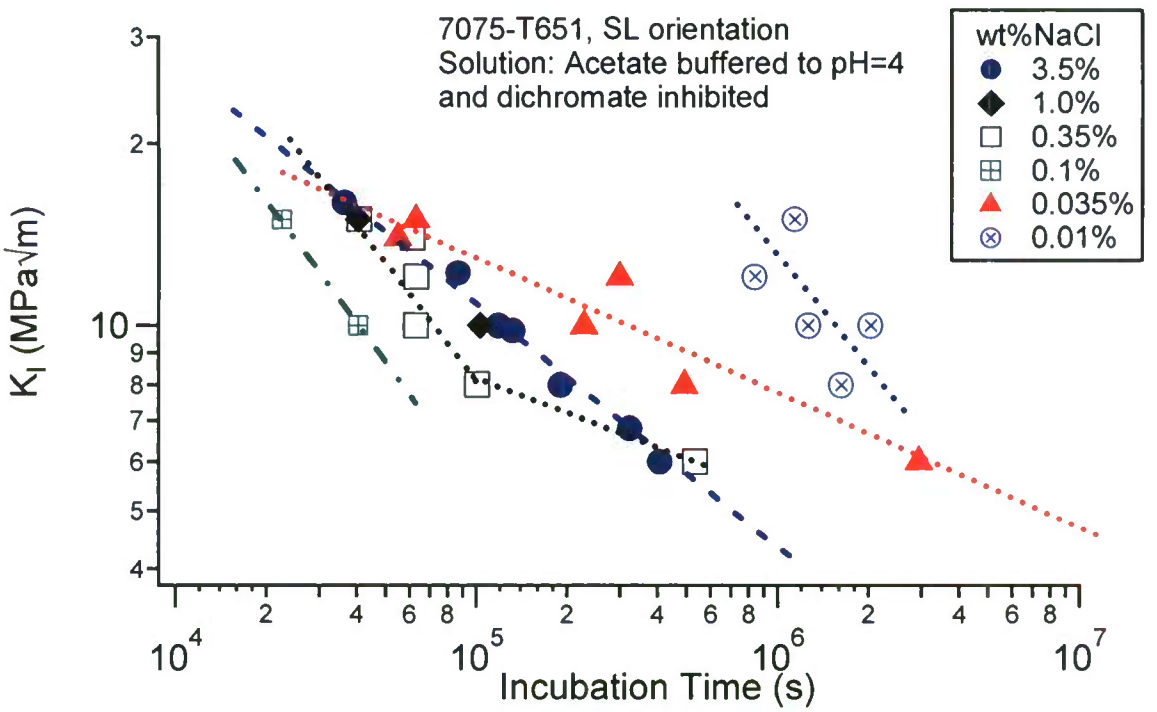

Fig. 47 Combined effect of stress intensity factor and NaCl concentration of the solution on the incubation time

The experimentally obtained relationships between the incubation time and the applied stress intensity factor at six (6) different NaCl concentrations are shown in Fig. 47. At each NaCl concentration, the relationship between the applied stress intensity factor and incubation time can be approximately described by a power law, which is very similar to S-N curve in fatigue. The influence of NaCl concentration on the incubation time becomes more significant with the decrease of stress intensity factor.

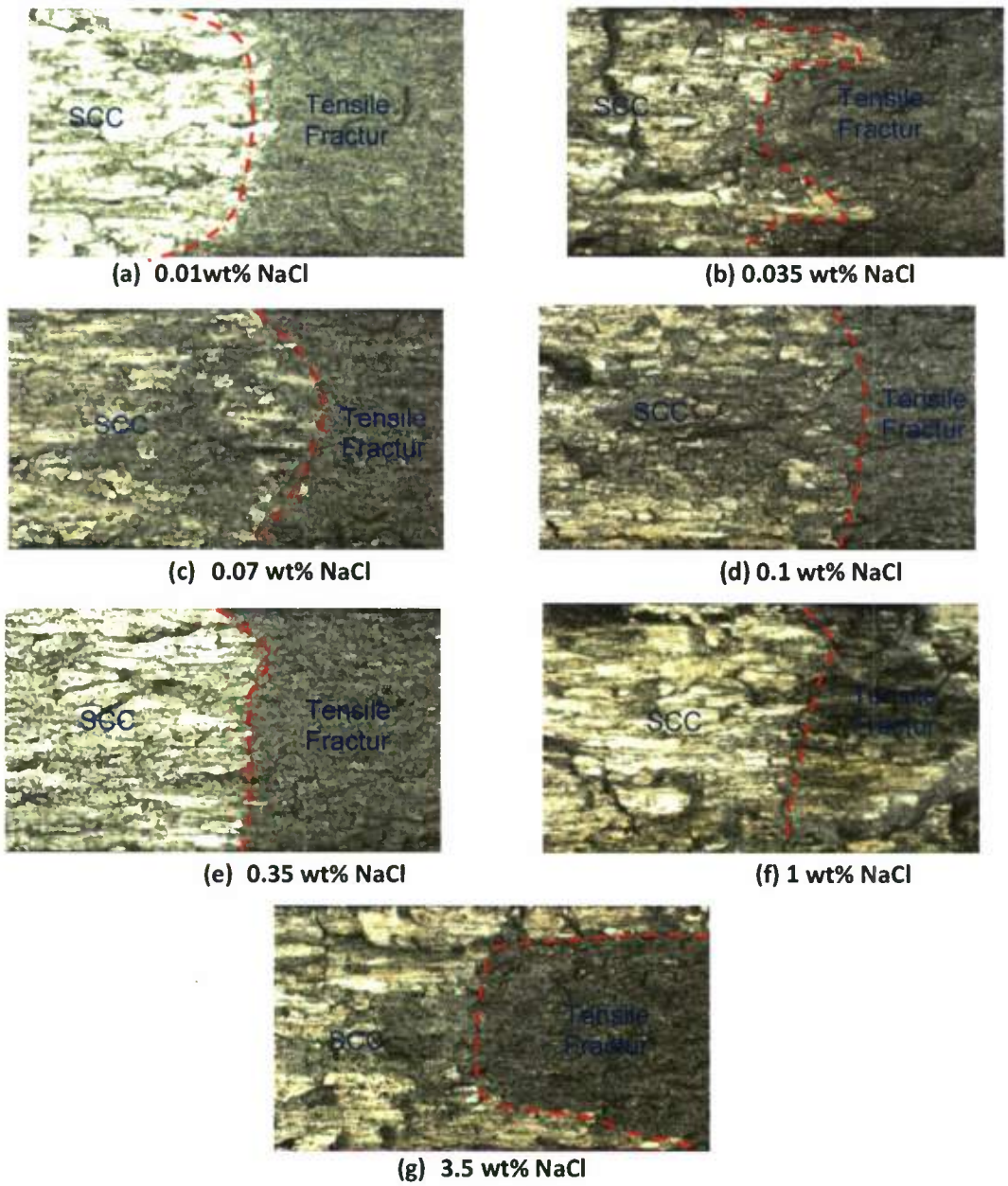

Fig. 48 NaCl concentration effect on crack profile at stable crack growth stage

Figure 48 shows the typical SCC crack front profiles during the stable crack growth stage in the corrosive solutions with different NaCl concentrations. The crack front appears a "C" shape in 3.5% NaCl aqueous solution. When the NaCl concentration of the solution ranges from 0.1% to 1%, the crack front profile is almost straight. When the NaCl concentration of the solution ranges from 0.01% to 0.07%, "bowed" crack fronts with crack being longer in the center of the specimen is observed. Either "bowed" crack fronts with crack being longer in the center of the specimen or relatively straight crack

front is frequently observed in thick specimens satisfying plane strain state. However, such crack front profile can appear in thin specimens under plane stress state when the concentration of NaCl of the corrosive solution is lower than 1%. The change of the crack front profile with NaCl concentration reflects the transition of SCC mechanisms with NaCl concentration, and 0.1% NaCl can be considered as a limiting concentration. Further studies on the dependence of SCC mechanisms on NaCl concentration need to be performed.

There have been a limited number of studies which might lead to the clarification of the role of anions in the stress corrosion cracking of aluminum alloys. Due to the difference in testing material, specimen geometry, and testing condition, the experimental results obtained by different researchers are frequently inconsistent. Speidel [87] investigated the effect of concentration of anions on kinetics of SCC of aluminum alloys. It was demonstrated that SCC kinetics of aluminum alloys is accelerated by anions of Cl^-, Br^-, and I^- compared with distilled water. It was also found that the level of the plateau crack growth velocity rose monotonically with increasing iodide concentration [87]. The influence of environment and temperature on SCC crack growth rate of AA7075 was investigated by de Jong [90]. It was found that the crack growth rate increased with increasing chloride ion concentration, although the influence of the concentration was found to be less pronounced at the higher values of the stress intensity factor. There is a very distinct influence of the temperature on the chloride ion concentration influence. The concentration influence decreases with increasing temperature. Le et al. [91] investigated some anion effects on SCC of AA7075-T651 in various NaCl solutions. A five-fold increase in crack growth rate was observed from 0.01M to 0.6M NaCl, presumably by increasing the activation of the aluminum surface. A 30% decrease in crack growth rate was observed from 0.6M NaCl to 3M NaCl, perhaps because of lower solubility of oxygen. Connolly et al. [128, 134] compared stress corrosion crack growth rates for AA7040 and AA7150 alloys as a function of bulk aqueous chloride concentrations. DCB crack growth rates for AA7040 and AA7150 are relatively insensitive to bulk chloride content in chromate-inhibited solutions. Crack growth rates at higher chloride concentrations (i.e., bulk solutions containing 0.6M NaCl and 1.0M NaCl) were higher by only a factor of two on average compared to lower chloride contents. Connolly et al. [128, 134] attributed this insensitivity to the role of the critical crack tip chemistry: once this chemistry is established, the bulk solution chemistry has only a small influence on the crack tip behavior. In the current study, the crack growth rate in the solution with 0.1% NaCl can be a thousand times higher than that in the solution with 0.01% NaCl. It is apparent that the critical crack tip chemistry established during the stable crack growth stage is in fact significantly dependent on the bulk NaCl concentration, and operative SCC mechanisms may be varied in different bulk NaCl concentrations.

Connolly et al. [128, 134] also found that the incubation time in chromate-inhibited solution was strongly influenced by bulk chloride content and decreased with increasing chloride content for both AA7040-T7651 and AA7150-T7751. This is consistent with the studies of incubation effects where the crack tip chemistry was shown to play a role in the observance of an incubation time [139]. The development of the crack tip environment required for SCC is thought to begin with an increase in chloride and it is speculated that the higher bulk chloride solution levels expedite the development of the critical crack tip chemistry necessary for SCC initiation [128, 134]. However, the existence of non-monotonic relationship between the incubation time and NaCl concentration at an identical stress intensity factor requires further investigations.

II.4. MEASUREMENT OF K_{ISCC}

The threshold stress intensity factor for SCC (K_{ISCC}) is defined as a value of stress intensity factor below which the stress corrosion cracking would not occur. It is an important fracture mechanics parameter to evaluate the stress corrosion resistance of the material in a corrosive environment. Traditionally, this value can be obtained from K– incubation time, K– time to failure, or da/dt- K curves, as schematically shown in Fig. 49 [85]. Theoretically, K_{ISCC} would correspond to infinite incubation time or time to failure. In practice, this notion becomes unreasonable and often the determination of K_{ISCC} is based on the patience of the researcher. When the complete SCC rate curves are examined, it can be seen that the slope of stage I is still finite even at the slowest crack growth rates, which leads to a conclusion that there is still a possibility of crack growth below the practically identified threshold stress intensity. Additional challenge in correct determination of K_{ISCC} arises from the phenomenon of wedging of crack flanks by corrosion products. In constant COD controlled experiments, this leads to additional stresses at the crack tip even when theoretically the load approaches zero at the end of experiment. The accumulation of corrosion products is avoided in the present investigation by addition of sodium dichromate to the solution.

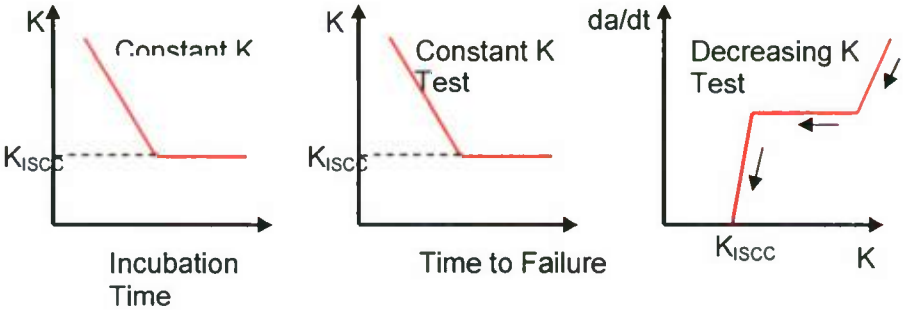

Fig. 49 Traditional methods to measure K_{ISCC}

In the current investigation, the threshold stress intensity factor for SCC (K_{ISCC}) was measured by incremental load tests. The load rate was 0.0002 N/s. The variations of crack length and the corresponding applied load with time were recorded. The continuous crack growth can be detected when the load reaches a certain value. From this critical point, the value of K_{ISCC} can be determined. Table 15 summarizes the seven specimens tested under incremental load condition for the determination K_{ISCC} at different NaCl concentrations. Two examples of the loading curve and the crack growth curve are shown in Fig. 50.

Table 15. Incremental load experiments for K_{ISCC} at different NaCl concentrations

Spec.#	NaCl, w%	*dP/dt*, N/sec	K_{ISCC} $MPa\sqrt{m}$	a_i, mm
SL92	3.50	2.14e-4	4.49	6.018
SL93	0.10	2.27e-4	6.37	14.607
SL94	0.35	2.26e-4	4.21	14.684
SL95	1.00	2.19e-4	4.60	14.100
SL96	0.035	2.24e-4	7.76	13.839
SL97	0.70	2.25e-4	4.21	14.523
SL98	5.00	2.24e-4	4.41	13.931

dP/dt - Rate of applied external load
K_{ISCC} – Threshold stress intensity factor in stress corrosion
a_i – Crack length at the beginning of the experiment measured from the line of applied load

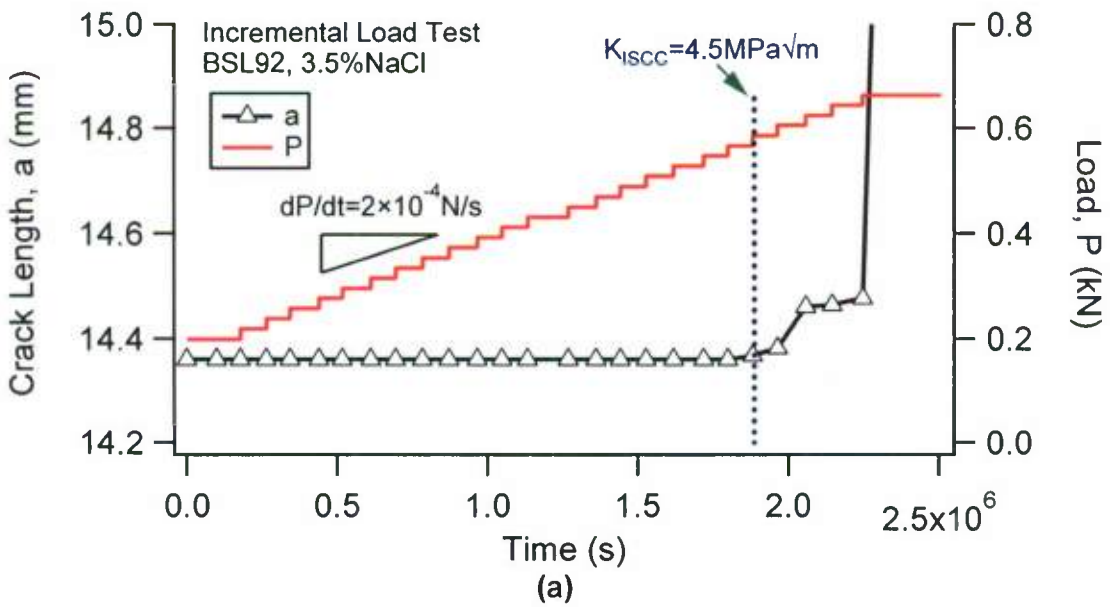

(a)

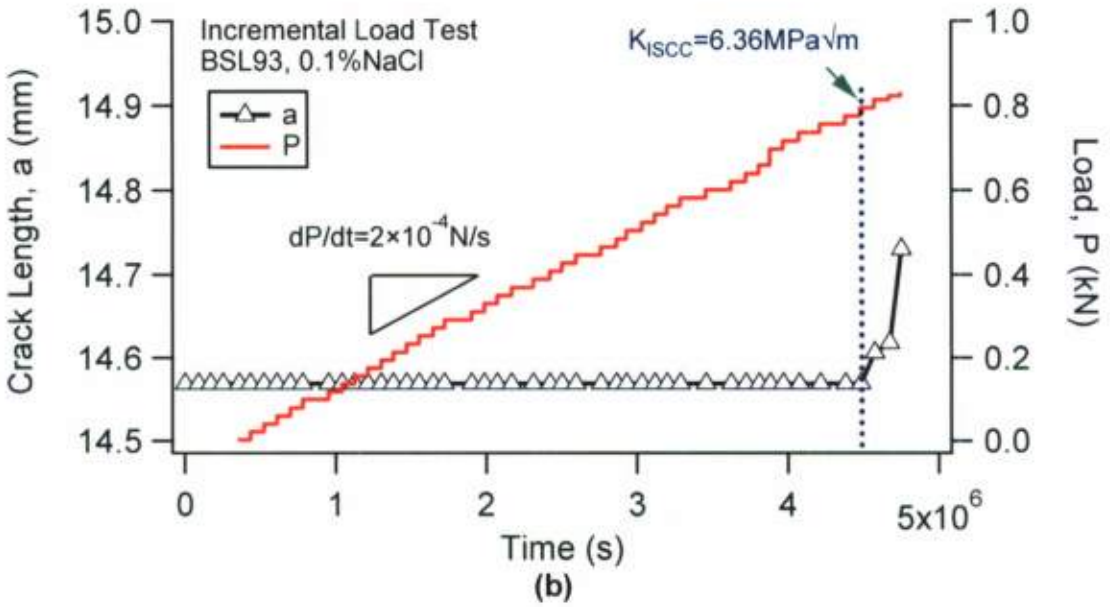

Fig. 50 Measurement of K_{ISCC} via an incremental load test

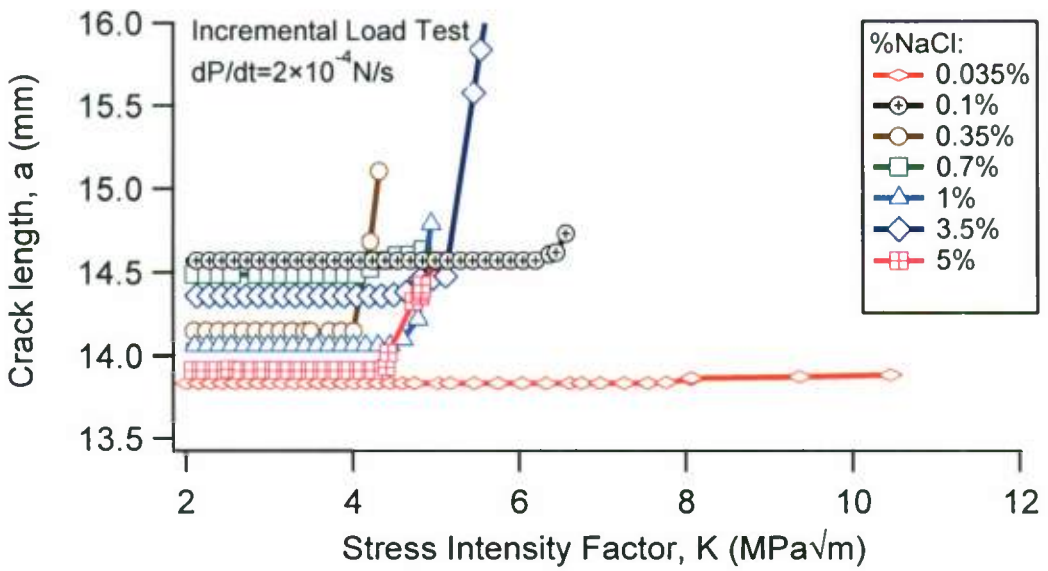

Fig. 51 Variations of crack length versus stress intensity factor at different NaCl concentrations during the incremental load tests

Figure 51 shows the variations of crack length with the stress intensity factor during incremental load tests in solutions with different NaCl concentrations. The critical point corresponding to the threshold stress intensity factor for SCC can be detected easily.

When the applied stress intensity factor is larger than K_{ISCC}, the crack length increases significantly with the increase of stress intensity factor.

Figure 52 shows the dependence of K_{ISCC} on NaCl concentration of the corrosive solution. When the concentration of NaCl of the solution is less than 0.35%, the threshold stress-intensity factor for stress-corrosion cracking increases significantly with the decrease of the NaCl concentration. When the concentration of NaCl of the solution is in the range of 0.35% to 5%, K_{ISCC} is approximately around 4.4 MPa$\sqrt{m}$, almost independent of NaCl concentration. K_{ISCC} in 3.5% NaCl aqueous solution measured in the current investigation agrees with the typical value reported in literature, which ranges from 4 to 7.75 MPa$\sqrt{m}$. It should be noted that the measured K_{ISCC} may be influenced by the loading rate applied in the test.

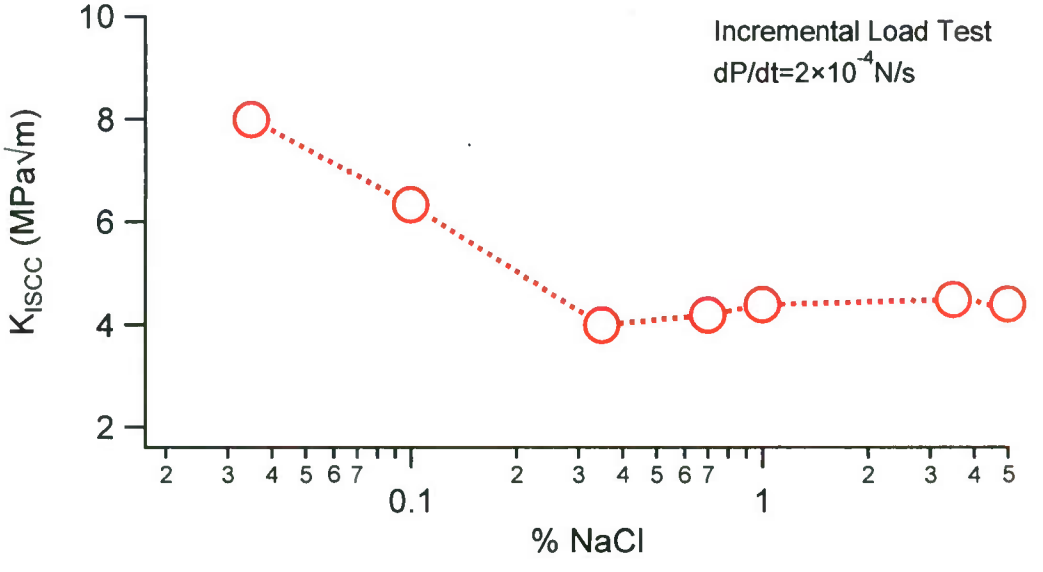

Fig. 52 Dependence of K_{ISCC} on NaCl concentration

II.5. INFLUENCE OF NACL CONCENTRATION ON FRACTURE STRESS INTENSITY FACTOR

Extensive stress corrosion experiments were conducted on 7075-T651 aluminum alloy in NaCl aqueous solutions of different concentrations. For some stress corrosion experiments, the applied load was increased gradually with time (raising load experiment) at different loading rates. The duration of each experiment ranged from 172 hours (one week) to as long as 6396 hours (9 months). The incubation time and crack growth were obtained. At the same time, several specimens were tested until

final fracture. Therefore, the fracture stress intensity factor (K_f) was obtained for these specimens. The results of the fracture K_f are listed in Table 16 and also shown in Fig.53. As a comparison, two identical specimens were tested in dry air for the fracture stress intensity factor. The average fracture K in dry air was found to be 24.2 $MPa\sqrt{m}$ for the material using the specimens with a thickness of 3.8 mm. It should be noticed that the term "fracture K" or "fracture stress intensity factor" is used here to distinguish it from the fracture toughness (K_{IC}). This is because K_{IC} is obtained using a thick specimen assuming plane strain condition while the fracture stress intensity factor, K_f, was determined using specimens with a small thickness (3.8 mm) (refer to Fig.25). Since identical specimens were used in all the experiments, the fracture K reflects the fracture strength for the material with the given thickness.

Table 16. Fracture stress intensity factor with different NaCl concentrations

Spec#	NaCl (%/M)	Time before fracture t_f (hours)	Crack length before fracture a_f(mm)	Stress Intensity Factor at fracture K_f ($MPa\sqrt{m}$)
SL114	0.01/0.0017	4367.7	18.41	24.77
SL116	0.01/0.0017	3473.9	19.15	24.88
SL106	0.035/0.006	6396.3	15.96	19.60
SL105	0.035/0.006	1108.4	31.90	22.02
SL104	0.035/0.006	1108.7	20.64	18.47
SL67	0.035/0.006	2422.8	26.48	20.50
SL69	0.07/0.012	322.2	28.57	22.63
SL63	0.10/0.017	172.0	26.50	22.50
SL72	0.10/0.017	48.3	22.10	22.10
SL61	0.35/0.06	203.1	32.12	30.19
SL99	0.35/0.06	372.5	32.38	22.93
SL100	0.35/0.06	267.0	27.22	25.98
SL101	0.35/0.06	178.4	24.32	23.63
SL102	0.35/0.06	318.6	33.75	21.52
SL62	1.00/0.17	206.6	26.64	21.30
SL64	2.00/0.34	251.0	29.38	26.60
SL65	3.00/0.513	304.7	26.07	21.60
SL77	3.50/0.60	167.9	17.36	18.37
SL37	3.50/0.60	218.2	28.52	25.66
SL66	5.00/0.855	286.1	29.76	29.86

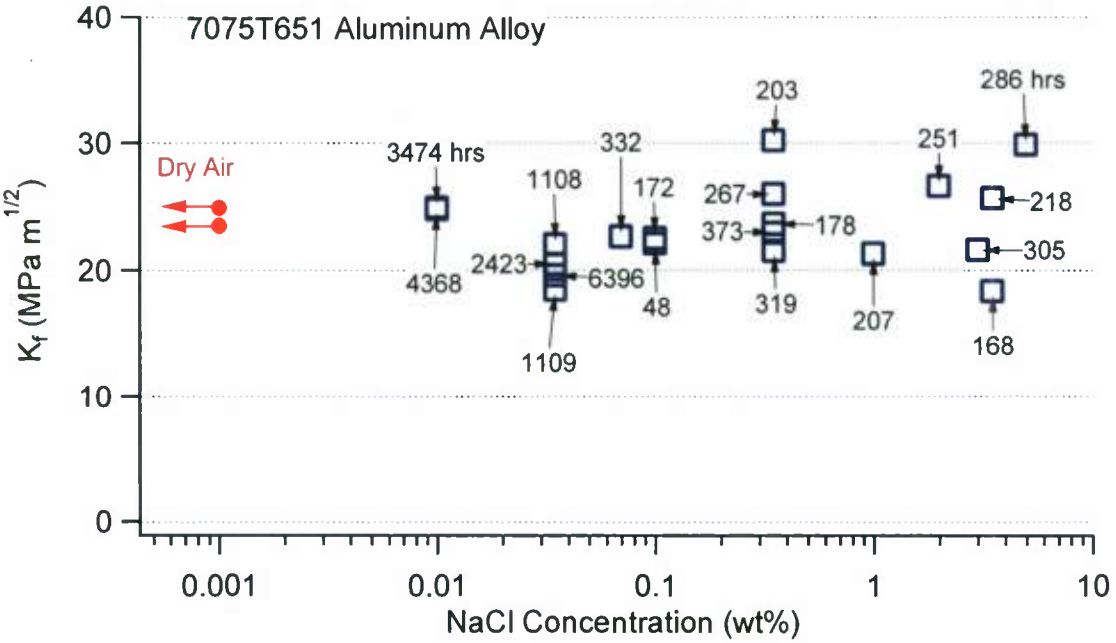

Fig. 53 Influence of NaCl concentration on the fracture stress intensity factor (the number next to a square marker indicates the time to fracture in hours)

The two red solid circles in Fig.53 are the results of fracture K obtained in dry air (12% relative humidity) at room temperature. Again, the average fracture K in dry air is 24.2 $MPa\sqrt{m}$. The fracture K values at different NaCl concentrations show a scatter with an average value of 22.83 $MPa\sqrt{m}$ which is close to the fracture K in dry air. There is no clear trend in the influence of the NaCl concentration of the fracture stress intensity factor. Therefore, the current experimental results listed in Table 16 and shown in Fig.53 reveal that the NaCl concentration has no influence on the fracture stress intensity factor from a statistics point view.

The time shown next to the blue square markers in Fig.53 (also listed in Table 16) is the total time that the specimen was submerged in the aqueous solution during the stress corrosion testing. The results suggest that the duration of the experiment in the NaCl solution has no influence on the fracture stress intensity factor considering the data scatter. It should be noticed that the maximum duration of a stress corrosion experiment in the current investigation was 9 months. A much longer duration of submerging time in the NaCl solution might influence the fracture strength.

II.6. DISCUSSION

From the fracture mechanics point of view, characterization of SCC behavior of a material is evident from the complete curve of crack growth rate versus stress intensity factor. Similar to fatigue crack growth, resistance of materials to SCC can be evaluated based on the comparison of crack growth velocities corresponding to specific range of values of stress intensity. Since rates of stress corrosion cracking are very low in aluminum alloys, the use of servo hydraulic testing equipment becomes unrealistic. Traditionally, double cantilever beam (DCB) specimens are widely used to evaluate the SCC behavior of an engineering component subjected to plane strain state in service. In this type of crack growth test, the COD of the specimen is kept constant and the stress intensity factor decreases with crack propagation. The applied load cannot be measured directly in experiment and is derived based on some empirical equations or pre-calibrated curves of load versus crack length. However, such relationships are not applicable when variable loading is introduced during the test. In the current investigation, the tendency of variation of stress intensity factor with crack length is adjustable and controllable by adding or removing the spring washers in the loading system. The load can be measured directly from the displacement of the O-ring and their relationship is inherent and consistent and is not relevant to the loading history of the specimen. Therefore, the testing technique in the current investigation is especially suitable for the study of the loading history effect on SCC behavior of the material.

For SCC of 7075-T651 aluminum alloy in 3.5% in NaCl aqueous solution, the main operating mechanisms can be grouped into anodic dissolution (AD) and hydrogen embrittlement (HE) [88]. Mueller [95] claimed that when HE was the predominant mechanism for SCC, extensive metal dissolution was not necessary for crack growth, and the crack tip radii were relatively sharp compared with AD situation that was characterized by blunt crack tips. In the current investigation, the plateau crack growth rate agrees well with the data reported in literature and is independent of the stress intensity factor between 10~22 MPa$\sqrt{m}$. The crack tip is observed to be sharp. The stable crack growth at this *K* level is most likely dominated by HE [88]. For the transient stage, the overall crack growth rate is much lower. This stage is possibly governed by AD mechanism. It should be mentioned that physically the crack tip blunting occurs due to delamination (grain boundary separation) as a result of combined action of stress and anodic dissolution [131].

In addition to average plateau velocity, another important fracture mechanics parameter, the threshold SCC stress intensity (K_{ISCC}), is determined from the experiments on pre-cracked specimens. The K_{ISCC} value was estimated from the decreasing K tests as 4.5 MPa$\sqrt{m}$, which is in agreement with the value measured from the incremental load test (Fig. 50), and also agrees with the previously obtained results ranging from 4 to 7.75 MPa$\sqrt{m}$ [92, 131, 137]. It should be mentioned that the

determination of the threshold stress intensity based on the crack growth data from the experiments under increasing K control can lead to erroneous result due to the consistent presence of the transient stage in SCC propagation (Fig. 35(b)). The present investigation reveals the existence of transient crack growth regardless of initially applied stress intensity factor. In other words, the crack growth rate curve does not immediately merge with the plateau regime when the applied stress intensity is within the plateau range. The presence of transient stage can mislead towards determination of "pseudo" threshold stress intensity.

After overloading (or underloading) followed by unloading, residual compressive stress (or tensile stress) is introduced at the crack tip. For specimens with different overload or underload percentages, the imposition of residual stress to the applied stress can results in different stress state at the crack tip although identical initial external load was applied in the subsequent SCC tests. As a result, different extent of HE may be involved for these loading cases. It is generally agreed that hydrogen enrichment is a necessary condition to hydrogen delayed cracking. A hydrostatic positive stress field enhances accumulation of hydrogen because of higher solubility. Mao et al. [138] pointed out that the presence of hydrogen together with applied stress made the anodic dissolution reaction more dominant. For the specimens having experienced underloading, the tensile residual stress leads to a higher hydrostatic positive stress in the SCC test. Therefore, the mechanisms governing the incubation of SCC can be different from the specimens subjected to overload prehistory.

The results of SCC experiments conducted in the present investigation under two-step high-low loading conditions reveal the effect similar to crack growth retardation observed in fatigue crack growth when the loading magnitude is reduced during the experiment. It was determined that reduction in stress intensity factor, i.e. transition from Step 1 to Step 2 in the high-low experiments, introduces the second period of stress corrosion crack incubation. The second incubation stage is more prolonged with a greater drop in the applied load at the onset of Step 2. The arguments stated above regarding effect of compressive residual stresses after overloading on incubation time can be extended to the case of the high-low sequence experiments. It can be suggested that compressive residual stress at the end of high-loading step results in dominance of anodic dissolution mechanism as opposed to hydrogen enhanced cracking typical for plateau regime which leads to the new incubation period in crack growth.

In SCC tests, a general requirement of all pre-cracked specimen configurations is that the dimensions be sufficient to maintain predominantly triaxial stress (plane strain) conditions, in which plastic deformation is limited to a very small region in the vicinity of the crack tip [85]. The specimen thickness should be larger than $2.5(K_{IC}/YS)^2$, where K_{IC} is the plane-strain fracture toughness and YS is the yield stress of material. For the

material in the S-L direction under the current investigation, $K_{IC} \approx 25$ MPa $\sqrt{m}$ and YS=430 MPa. Therefore, the specimen thickness is required to be larger than 8.5 mm. The specimen thickness used in the current investigation was 3.8 mm, which is approximately one half of the thickness satisfying the plane-strain condition. Such a thickness results in a plane stress condition during SCC tests. However, the obtained experimental results can reflect the general trends of the SCC behavior of the material under plane strain conditions, such as the influence of loading level on the incubation time, the overload/underload effects on the incubation time, and the stabilized crack growth behavior which is *K*-independent. Moreover, the stabilized crack growth rate and the threshold stress intensity factor for SCC under plane stress condition are consistent with those reported in literature measured under plane strain conditions. In the current study, the crack length is measured only on one side of the specimen surface due to the restriction of the experimental set-up. However, this operation has no influence on the determination of the incubation time. In addition, the crack front profile during steady propagation keeps unchanged. The selection of location to measure the crack length has minimal influence on the stabilized crack growth rate.

II.7. CONCLUSIONS

The stress corrosion cracking (SCC) experiments on 7075-T651 aluminum alloy support the following conclusions:

1. Three different stages were observed for SCC growth of 7075T651 aluminum alloy: incubation, transient growth, and stable growth. Incubation time increases significantly when stress intensity factor decreases, following a power law format similar to the *S-N* curve in fatigue. In the transient stage, the crack growth rate is low and generally slows down until stable growth stage starts. The curve of crack growth rate versus stress intensity factor exhibits a plateau when the stress intensity factor is in the range of 10~22 MPa $\sqrt{m}$.
2. Overloading significantly increases the incubation time while underloading significantly decreases the incubation time. The high-low sequence loading effect on SCC is similar to the overloading effect. Overloading/underloading has no apparent influence on the transient and stable growth behavior. In the high-low sequence loading, the transient stage can be very short or disappear completely.
3. The NaCl concentration has a significant influence on the incubation time and stable crack growth rate. The critical NaCl concentration is 0.1%, at which the incubation time is shortest and the stable crack growth rate is the fastest. When NaCl concentration is less than 0.1%, incubation time increases significantly and crack growth rate decreases significantly with the decrease of NaCl concentration.

4. The influence of NaCl concentration on the incubation time becomes more significant with the decrease of stress intensity factor. At a high stress intensity factor, the incubation time is mainly determined by the stress intensity factor and the influence of NaCl concentration is insignificant.
5. The threshold stress-intensity factor for stress-corrosion cracking (K_{ISCC}) in solutions with different NaCl concentrations were measured by incremental load tests. When the NaCl concentration of solution is less than 0.35%, K_{ISCC} increases significantly with the decease of the NaCl concentration. When the concentration of NaCl of the solution is in the range of 0.35% to 5%, K_{ISCC} is approximately around 4.4 MPa$\sqrt{m}$, almost independent of NaCl concentration.
6. Influence of NaCl concentration on the fracture stress Intensity factor was found to be insignificant.

ACKNOWLEDEMENTS

The work was financially supported by the Office of Naval Research (N00014-08-1-0646). Dr. Asuri K. Vasudevan provided valuable suggestions in the course of the research. Dr. Jixi Zhang and Dr. Sergiy Kalnaus performed the primary research tasks of the research. Mr. Qin Yu conducted some of the experiments and prepared all the results presented in the Appendices.

REFERENCES

1. Y. Hirose and T. Mura: *Eng. Fract. Mech.*, 1984, vol. 19(2), pp. 317-29.
2. S. Ramamurthy and A. Atrens: *Corr. Sci.*, 1993, vol. 34(9), pp. 1385-1402.
3. R.H. Jones, M.J. Danielson, and D.R. Baer: in *Fracture Mechanics: Perspectives and Directions (Twentieth Symposium)*, R.P. Wei and R.P. Gangloff, eds., ASTM STP 1020, ASTM, Philadelphia, 1989, pp. 209-232.
4. R.P. Wei and R.P. Gangloff: in *Fracture Mechanics: Perspectives and Directions (Twentieth Symposium)*, R.P. Wei and R.P. Gangloff, eds., ASTM STP 1020, ASTM, Philadelphia, 1989, pp. 233-264.
5. W.Y. Chu, C.M. Hsiao, and J.W. Wang: *Metall. Trans. A*, 1985, vol. 16, pp. 1663-70.
6. N. Taniguchi and A.R. Troiano: *Trans. Iron Steel Institute Japan*, 1969, vol. 9(4), pp. 306-12.
7. Y. Lee and R P. Gangloff: *Metall. Mater. Trans. A*, 2007, vol. 38A, pp. 2174-90.
8. S. Serebrinsky, E.A. Carter, and M. Ortiz: *J. Mech. Phys. Solids*, 2004, vol. 52, pp. 2403-30.
9. I. Scheider, M. Pluff, and W. Dietzel: *Eng. Fract. Mech.*, 2008, vol. 75, pp. 4283-91.
10. T. Boellinghaus and H. Hoffmeister: *Corrosion*, 2000, vol. 56(6), pp. 611-22.
11. V.K. Tewari: *Tool and Alloy Steels*, 1981, vol. 16(3-4), pp. 89-93.
12. U. Gramberg: in *Corrosion Cracking*, V.S. Goel, ed., Salt Lake City; Utah; USA; 2-6 Dec. 1985. pp. 147-50.
13. D.A. Berman and V.S. Agarwala: in *Hydrogen Embrittlement: Prevention and Control*, L. Raymond, ed., ASTM STP 962, 1988, pp. 98-104.
14. W. G. Clark Jr.: *J. Mater. Energy Syst.*, 1979, vol. 1(1), pp. 33-40.
15. Y. Takeda and C.J. McMahon Jr.: *Metall. Trans. A*, 1981, vol. 12, pp. 1255-66.
16. W. Dietzel: *Mater. Sci. (Russia)*, 2004, vol. 40(6), pp. 749-55.
17. N. Eliaz, A. Shachar, B. Tal, and D. Eliezer: *Eng. Failure Anal.*, 2002, vol. 9, pp. 167-84.
18. J.B. Leblond, D. Nejem, D. Dubois, and S. Talbot-Besnard: *Acta Metall.*, 1987, vol. 35 (7), pp. 1703-14.
19. S.I. Pyun, and H.K. Lee: *Metall. Trans. A.*, 1990, Vol. 21A(9), pp. 2577-83.
20. R.P. Wei and S.R. Novak: *J. Testing Eval., JTEVA*, 1987, vol. 15(1), pp. 38-75.
21. A.J. McEvily, Jr., ed.: *Atlas of Stress-Corrosion and Corrosion Fatigue Curves*, ASM International, Materials Park, OH, 1990, 541p.
22. H.C. Chu and R.P. Wei: *Corrosion*, 1990, vol. 46(6), pp.468-76.

23. R.O. Ritchie, M.H. Castro Cedeno, V.F. Zackay, and E.R. Parker: *Metall. Trans. A*, 1978, vol. 9A, pp. 35-40.

24. G.F. Li, R.G. Wu, and T.C. Lei: *Metall. Trans.* A, 1990, vol. 21A, pp. 503-505.

25. R.M. Rieck, A. Atrens, and I.O. Smith: *Materials Forum*, 1989, vol. 13(1), pp. 48-53.

26. R.H. Jones: *Stress-Corrosion Cracking: Materials Performance and Evaluation*, Materials Park OH: ASM International, 1992, 448 p.

27. W. Dietzel, and K. Ghosal: *Fatigue Fract. Engng Mater. Struct. (UK)*, 1998, vol. 21(10), pp. 1279-86.

28. A. Oehlert, and A. Atrens: *Corr. Sci.*, 1996, vol. 38(7), pp. 1159-69.

29. S. Liu and D.D. Macdonald: *Corrosion*, 2002, vol. 58(10), pp. 835 – 45.

30. Y. Hirose and T. Mura: *Eng.. Fract. Mech.*, 1989, vol. 34(3), pp. 729-42.

31. I.W. Kang, J.K. Choi, and S.I. Pyun: *Steel Research*, 1987, vol. 58(12), pp. 565-69.

32. D.D. Macdonald: in *Chemistry and Electrochemistry of Corrosion and Stress Corrosion Cracking: A Symposium Honoring the Contributions of R.W. Staehle*, 2001 TMS Annual Meeting; New Orleans, LA; USA; 11-15 Feb. 2001. pp. 193-210.

33. J.A. Hauser II, R.W. Judy, and T.W. Crooker: in *Corrosion Cracking*, Salt Lake City, Utah, USA, 2-6 Dec. 1985, American Society for Metals, Metals Park, Ohio 44073, USA pp. 215-20.

34. B.F. Brown and C.D. Beachem: *Corr. Sci.*, 1965, vol. 5(11), pp. 745-50.

35. C.S. Carter: *Corrosion*, 1971, vol. 27(11), pp. 471-77.

36. A.A. Sheinker and J.D. Wood: in *Stress Corrosion Cracking of Metals – A State of the Art*, ASTM STP 518, 1972, pp. 16-38.

37. P. Shahinian and R.W. Judy, Jr.: in: *Stress Corrosion--New Approaches*, ASTM STP 610, 1976, pp. 128-42.

38. Yu.A. Krupin and I.K. Kiselev: *Mater. Sci. Eng., A.*, 1990, vol. A130(1), pp. 29-35.

39. S. Yuyama, T. Kishi and Y. Hisamatsu: *J. Acoust. Emiss.*, 1983, vol. 2(1-2), pp. 71-93.

40. W.B. Lisagor: in *Environment-Sensitive Fracture: Evaluation and Comparison of Test Methods,* ASTM STP 821, 1984, pp. 80-97.

41. Y. Hirose and K. Tanaka: *J. Soc. Mater. Sci. Jpn.*, 1980, vol. 29(323), pp. 822-28.

42. M. Tsuda, Y. Hirose, Z. Yajima, and K. Tanaka: in *Proceedings of the Second International Conference on Residual Stresses*, Nancy, France, 23-25 November 1988, pp. 997-1002.

43. H.W. Chung: *Diss. Abstr. Int.*, 1983, vol. 44(4), p. 204.

44. R.M. Rieck, A. Atrens, and I.O. Smith: *Metall. Trans. A.*, 1989, vol. 20A(5), pp. 889-95.

45. E.M. Hackett, P.J. Moran, and J.P. Gudas: in *Fracture Mechanics: Seventeenth Volume*, ASTM STP 905, 1986, pp. 512-41.

46. Y. Hirose, Z. Yajima, and K. Tanaka: in *Advances in X-Ray Analysis*, 1984, vol. 27, pp. 213-20.

47. M. Tsuda, Y. Hirose, Z. Yajima, and K. Tanaka: *J. Soc. Mater. Sci. Jpn.*, 1988, vol. 37(417), pp. 599-605.

48. Y. Hirose and K. Tanaka: in *Metallic Corrosion. 8th International Congress on Metallic Corrosion*, Mainz, Federal Republic of Germany, 6-11 Sept. 1981. vol. I, pp. 553-558.

49. G. Sandoz: *Metall. Trans.*, 1972, vol. 3, pp. 1169 – 76.

50. V.K. Tewari, R. Winand, J. Charlier, J.P. Elinck, and J. Van Muylder: *Steel Research*, 1982, vol. 53(8), pp. 329-32.

51. F.P. Ford: in *Embrittlement by the Localized Crack Environment*, Philadelphia, PA, USA, 4-5 Oct., 1983, pp. 117-47.

52. W.G. Clark and J.D. Landes, Jr.,: in *Stress Corrosion – New Approaches*, ASTM STP 610, 1976, pp. 108-27.

53. K. Hirano, S. Ishizaki, H. Kobayashi, and H. Nakazawa: *J. Testing Eval., JTEVA*, 1985, vol. 13(2), pp. 162 – 68.

54. R.A. Mayville, T.J. Warren, and P.D. Hilton: *J. Eng. Mater. Techn.*, ASME Transactions, 1987, vol. 109(3), pp. 188-93.

55. R.A. Mayville, T.J. Warren, and P.D. Hilton: *J. Testing Eval., JTEVA*, 1989, vol. 17(4), pp. 203-11.

56. W. Dietzel, K.H. Schwalbe, and D. Wu: *Fatigue Fract. Eng. Mater. Struct.*, 1989, vol. 12(6), pp. 495-510.

57. N. Winzer, A. Atrens, W. Dietzel, G. Song, and K.U. Kainer: *Mater. Sci. Eng. A*, 2008, vol. 472, pp. 97-106.

58. W. Dietzel and J. Mueller-Roos: *Mater. Sci.*, 2001, vol. 37(2), pp. 264-71.

59. ISO 7539-9:2003 Corrosion of metals and alloys - Stress corrosion testing - Part 9: Preparation and use of pre-cracked specimens for tests under rising load or rising displacement.

60. R.P.M. Proctor and H.W. Paxton: *Trans. ASM*, 1969, vol. 62, pp. 989-99.

61. E.A. Steigerwald and W.D. Benjamin: *Metall. Trans.*, 1971, vol. 2, pp. 606-8.

62. V.A. Marichev: *Zashchita Metallov*, 1975, vol. 11(3), pp. 296-99.

63. A. Nadai: *Theory of Flow and Fracture of Solids*, vol. 1, Second ed. McGraw-Hill Book Company, Inc., New York, Toronto, and London, 1950, pp. 347-52.

64. J.C. Newman, Jr.: *Int. J. Fracture*, 1981, vol. 17, pp. 567-78.

65. A. Atrens and Z.F. Wang: *J. Mater. Sci.*, 1998, vol. 33, pp. 405-15.

66. D.L. Dull and L. Raymond: *Metall. Trans.*, 1972, vol. 3, pp. 2943-47.

67. I.M. Austen: *Int. J. Fracture*, 1976, vol. 12, pp. 253-63.

68. K. Nakasa and H. Takei: *Eng. Fract. Mech.*, 1983, vol. 18, pp. 879-85.

69. Yu.A. Krupin and I.K. Kiselev: *Scripta Metallurgica et Materialia*, 1990, vol. 24, pp. 2113-18.

70. C. Berger: in *Corrosion Cracking*, Salt Lake City, Utah, USA, 2-6 Dec. 1985, pp. 235-240.

71. Y. Hirose and T. Mura: *Eng. Fract. Mech.*, 1984, vol. 19(6), pp. 1057-67.

72. R.P. Wei and S.R. Novak: in *Environment-Sensitive Fracture: Evaluation and Comparison of Test Methods*, ASTM STP 821, 1984, pp. 75-79.

73. A.K. Wong, L. Milton, and W.F. Czyrklis: Report# AMMRC-MS-79-1, Army Materials and Mechanics Research Center, Watertown, MS, 1979, pp. 10-13.

74. W.G. Clark, Jr.: in *Flaw Growth and Fracture*, ASTM STP 631, 1977, pp. 331 – 44.

75. R.K. Singh Raman, R. Rihan, and R.N. Ibrahim: *Mater. Sci. Engng. A*, 2007, vol. 452-453, pp. 652-656.

76. R.N. Ibrahim, R. Rihan, and R.K. Singh Raman: *Eng. Frac. Mech.*, 2008, vol. 75(6), pp. 1623-34.

77. B.P. Somerday and R.P. Gangloff: *Mater. Sci. Eng.*, 1998, A254, pp. 166-78.

78. B.P. Somerday and R.P. Gangloff: *Mater. Sci. Eng.*, 1998, A254, pp. 179-88.

79. S. Yamamoto and T. Fujita: in *Proc. Fracture 1969*, Chapman and Hall, London, 1969, pp. 425-38.

80. W.W. Gerberich, P.G. Marsh, and J.W. Hoehn: in *Proc. Hydrogen Effects in Materials*, Moran, WY, USA, 1994, pp. 539-51.

81. W.W. Gerberich, R.A. Oriani, M.J. Lii, X. Chen, and T. Foecke: *Philos. Mag.*, 1991, vol. A63(2), pp. 363-76.

82. J.A. Wert: *Corrosion*, 1983, vol. 39(2), pp. 71-73.

83. A. Oehlert and A. Atrens: *J. Mater. Sci. (UK)*, 1998, vol. 33(3), pp. 775-81.

84. J.H. Underwood, J.C. Newman, Jr., and R.R. Seeley: *J. Testing Eval., JTEVA*, 1980, vol. 8(6), pp. 308-13.

85. D.O. Sprowls: *Evaluation of Stress-Corrosion Cracking*, ASM Metal Handbook, 9th Ed., vol. 13, B, J. R. Davis, J.D. Destefani, G.M. Crankovic Eds., Metal Park, OH, 1987, pp. 245-282.

86. M.O. Speidel: *Metall. Trans. A*, 1975, vol. 6A (4), pp. 631-651.

87. M.O. Speidel: *The Theory of Stress Corrosion Cracking in Alloys*, ed. by J.C. Scully, North Atlantic Treaty Organization (NATO), Scientific Affairs Division,

Brussels, 1971, pp. 289-344.

88. S.M. Lee, S.I. Pyun, and Y.G. Chun: *Metall. Trans. A*, 1991, vol. 22A (10), pp. 2407-2414.
89. K. Endo, K. Komai, and I. Yamamoto: *Bull. Jpn. Soc. Mech. Eng.*, 1981, vol. 24 (194), pp. 1326-1332.
90. H.F. de Jong: *Aluminium*, 1982, vol. 58 (9), pp. 526-531.
91. A.H. Le, B.F. Brown, and R.T. Foley: *Corrosion*, 1980, vol. 36 (12), pp. 673-679.
92. A.H. Le and R.T. Foley: *Corrosion*, 1983, vol. 39 (10), pp. 379-383.
93. Y. Miyagi and T. Eto: *Kobe Res. Dev.*, 1986, vol. 36 (2), pp. 117-120.
94. M Baydogan, H Cimenoglu, K. E. Sabri, and J Rasty: *Metall. Mater. Trans. A*, 2008, vol. 39A (10), pp. 2470-2476.
95. M.P. Mueller, A.W. Thompson, and I.M. Bernstein: *Corrosion*, 1985, vol. 41 (3), pp. 127-136.
96. C.P. Ferrer, M.G. Koul, B.J. Connolly, and A.L. Moran: *Corrosion*, 2003, vol. 59 (6), pp. 520-528.
97. J.K. Park: *Mater. Sci. Eng. A*, 1988, vol. 103 (2), pp. 223-231.
98. K. Ural: *J. Mater. Sci. Lett.*, 1994, vol. 13 (5), pp. 383-385.
99. Y. Reda, R. Abdel-Karim, and I. Elmahallawi: *Mater. Sci. Eng. A*, 2008, vol. 485 (1-2), pp. 468-475.
100. M. Talianker and B. Cina: *Metall. Trans. A*, 1989, vol. 20A (10), pp. 2087-2092.
101. R.T. Holt, V.R. Parameswaran, and W. Wallace: *Can. Aeronaut. Space J.*, 1996, vol. 42 (2), pp. 83-87.
102. K. Rajan, W. Wallace, and J.C. Beddoes: *J. Mater. Sci.*, 1982, vol. 17 (10), pp. 2817-2824.
103. D. Li, J. Liu, P. Liu, G. Zhu, and B. Guo: *Mater. Sci. Forum*, 2002, vol. 396-402 (3), pp. 1497-1504.
104. D. Yan, Y. Zhang, H. Wang, and S. Wang: *J. Mater. Eng.*, 1993, vol. 2, pp. 13-16.
105. M. Hua, C. Li, and H. Wang: *Acta Metall. Sin.*, 1988, vol. 24 (1), pp. A41-A46.
106. T.M. Yue, L.J. Yan, C.F. Dong, and C.P. Chan: *Mater. Sci. Technol.*, 2005, vol. 21 (8), pp. 961-966.
107. T.M. Yue, C.F. Dong, L.J. Yan, and H.C. Man: *Mater. Lett.*, 2004, vol. 58 (5), pp. 630-635.
108. T.M. Yue, L.J. Yan, and C.P. Chan: *Appl. Surf. Sci.*, 2006, vol. 252 (14), pp. 5026-5034.
109. L.M. Wu, W.H. Wang, Y.F. Hsu, and S. Trong: *Mater. Trans.*, 2007, vol. 48 (3), pp. 600-609.

110. W.Y. Chu, C.M. Hsiao, and J.W. Wang: *Metall. Trans. A*, 1985, vol.16A (9), pp. 1663-1670.

111. A.H. Hanisch, L.H. Burck: *Corrosion*, 1982, vol. 38 (6), pp. 330-335.

112. M.R. Chlistovsky, P.J. Heffernan, and D.L. DuQuesnay: *Int. J. Fatigue*, 2007, vol. 29 (9-11), pp. 1941-1949.

113. R. Hermann: *J. Mater. Sci.*, 1981, vol. 16 (9), pp. 2381-2386.

114. W.G. Clark: *ASTM STP 700*, 1980, pp. 97-111.

115. Gaillard, Chouvy, and Blechet: *Rev. Alum.*, 1982, vol. 513, pp. 30-35.

116. D. Rhodes and J.C. Radon: *Corr. Sci.,* 1981, vol. 21 (5), pp. 381-389.

117. H.P. Chu, G.A. Wacker: J. Basic Eng., 1969, vol. 91 (4), pp. 656-659.

118. B.F. Brown: Mater. Res. Stds, 1966, vol. 6 (3), pp. 129-133.

119. T. Saito and T. Tanaka: *J. Jpn. Inst. Light Met.*, 1975, vol. 25 (6), pp. 214-222.

120. R.C. Dorward and K.R. Hasse: *Corros. Sci.*, 1982, vol. 22 (3), pp. 251-257.

121. T. Ohnishi, H. Kojima, N. Seko, and K. Higashi: *J. Jpn. Inst. Light Met.*, 1985, vol. 35 (6), pp. 344-352.

122. A.C. Fraker and J.R. Ruff, Jr.: *Corrosion Sci.*, 1970, vol. 10 (4), pp. 191-195.

123. D.O. Sprowls, M.B. Shumaker, J.D. Walsh, and J.W. Coursen, *Evaluation of Stress Corrosion Cracking Susceptibility Using Fracture Mechanics Techniques. Pt. 1. Final Report*, Contract NAS 8-21487, Contract Report NASA CR-124469, May 1973.

124. R.C. Dorward and K.R. Hasse: *Corrosion*, 1978, vol. 34 (11), pp. 386-395.

125. ASTM E647-05: *Standard Test Method for Measurement of Fatigue Crack Growth Rates*. ASTM International.

126. B.W. Lifka: *ASTM STP 425*, 1966, pp. 82-83.

127. R.C. Dorward and K.R. Hasse: *Corrosion Sci.*, 1979, vol. 19 (2), pp. 131-140.

128. B.J. Connolly, M. G. Koul, and A.L. Moran: in *Corrosion 2003*, NACE International, Houston, TX, 2003, paper No. 03515.

129. P. Martin, J.I. Dickson, and J.P. Bailon: *Mater. Sci. Eng.*, 1985, vol. 69 (1), pp. L9-L13.

130. W.Y. Chu, C.M. Hsiao, and J.W. Wang: *Metall. Trans. A*, 1985, vol.16A (9), pp. 1663-1670.

131. M.O. Speidel and M.V. Hyatt: in *Advances in Corrosion Science and Technology*, M.G. Fontana, R.W. Staehle, eds., Plenum Press, New York, 1972, vol. 2, pp. 115-335.

132. A. Hartman, J.W. Lievers, and W.J. Vandervet, *Study of the growth of stress corrosion cracks in the aluminum alloy 7075. Part 1 Investigation on the corrosion medium*, Report No. NLR-TR-71090-U-PR-1, Sep. 1971.

133. L.M. Young: *Microstructural Dependence of Aqueous Environment-Assisted Crack Growth and Hydrogen Uptake in AA 7050*, Ph.D. Dissertation, University of Virginia, 1999.

134. B.J. Connolly, M. G. Koul, and A.L. Moran: *Corrosion*, 2005, vol. 61 (10), pp. 976-986.

135. M. Landkof and L. Gal-or: Corrosion, 1980, vol. 36 (5), pp. 241-246.

136. M.R. Bayoumi: *Eng. Fract. Mech.*, 1996, vol. 54 (6), pp. 879-889.

137. N.J.H. Holroyd, A.K. Vasudevan, and L. Christodoulou: in *Aluminum Alloys - Contemporary Research and Applications*, A.K. Vasudevan and R.D. Doherty, eds., Academic Press, Inc., 1989, vol. 31, pp. 463-483.

138. S.X. Mao, B. Gu, N.Q. Wu, and L. Qiao: *Phil. Mag. A*, 2001, vol. 81A (7), pp. 1813-1831.

139. K. Cooper, "Chemistry and electrochemistry of environment-assisted cracking of an Al-Zn-Mg-Cu alloy," Ph.D. Diss., University of Virginia, 2001.

APPENDIX A EXPERIMENTAL CRACK GROWTH DATA FOR STRESS CORROSION CRACKING OF AISI4340 STEEL

Table A1. Stress Corrosion Experimental Data for Specimen HT-24 (0% NaCl, Constant Load Control, $P = 3.40kN$)

$t(s)$	$a(mm)$	$K(MPa\sqrt{m})$	$da/dt(mm/s)$
0	8.004	25.70	0
122	8.192	26.19	0.003198
145	8.228	26.28	0.003939
165	8.311	26.49	0.004583
175	8.360	26.62	0.005307
191	8.420	26.78	0.006695
203	8.567	27.16	0.007079
216	8.632	27.34	0.007510
229	8.767	27.70	0.007597
248	8.882	28.00	0.007081
262	8.995	28.31	0.007449
283	9.076	28.53	0.008310
300	9.282	29.10	0.009828
321	9.475	29.64	0.012450
335	9.665	30.17	0.014090
347	9.849	30.70	0.015100
370	10.258	31.91	0.01524
385	10.506	32.66	0.01459
398	10.757	33.43	0.01350
432	11.011	34.24	0.01115
462	11.348	35.34	0.01074
497	11.642	36.32	0.01043
512	11.977	37.49	0.01092
546	12.285	38.59	0.01104
582	12.591	39.73	0.01084
605	12.918	41.00	0.01053
638	13.312	42.58	0.01122
669	13.552	43.59	0.01342
681	13.724	44.33	0.01344

704	14.047	45.77	0.01529
720	14.447	47.65	0.01684
746	14.738	49.08	0.01683
764	15.181	51.38	0.01692
788	15.563	53.50	0.01650
819	15.984	55.99	0.01701
835	16.304	58.00	0.01679
853	16.623	60.11	0.01690
876	17.034	63.02	0.01731
907	17.570	67.16	0.01657
931	17.916	70.07	0.01609
960	18.358	74.09	0.01588
981	18.760	78.07	0.01560
1,010	19.149	82.27	0.01548
1,032	19.536	86.82	0.01539
1,055	19.846	90.77	0.01530

P=applied load;
t=time in second;
a=crack length measured from the line of action of the external load;
K=applied stress intensity factor;
da/dt=crack growth rate.

Table A2. Stress Corrosion Experimental Data for Specimen HT-26 (0% NaCl, Constant Load Control, $P = 3.00kN$)

$t(s)$	$a(mm)$	$K(MPa\sqrt{m})$	$da/dt(mm/s)$
0	8.006	22.74	0
611	8.188	23.16	0.01086
631	8.406	23.66	0.01156
661	8.718	24.39	0.01260
675	8.959	24.96	0.01263
690	9.145	25.41	0.01286
704	9.345	25.90	0.01386
722	9.534	26.37	0.01365
740	9.786	27.00	0.01357
757	10.144	27.93	0.01283
782	10.401	28.61	0.01114
802	10.603	29.16	0.00949
834	10.802	29.70	0.00810
873	10.956	30.13	0.00859
894	11.311	31.15	0.00934
915	11.534	31.81	0.00944
946	11.769	32.52	0.00994
961	11.986	33.19	0.00991
991	12.183	33.82	0.01163
1,012	12.440	34.65	0.01309
1,032	12.754	35.70	0.01474
1,043	12.961	36.42	0.01470
1,061	13.199	37.26	0.01495
1,074	13.432	38.12	0.01444
1,107	13.828	39.63	0.01268
1,122	14.084	40.65	0.01303
1,144	14.297	41.52	0.01307
1,166	14.516	42.45	0.01371
1,182	14.868	44.01	0.01424
1,204	15.131	45.22	0.01483
1,222	15.429	46.66	0.01439
1,235	15.637	47.71	0.01445
1,255	15.891	49.03	0.01515
1,279	16.154	50.46	0.01676
1,295	16.578	52.91	0.01848

1,320	16.962	55.29	0.02079
1,333	17.330	57.73	0.02092
1,347	17.640	59.93	0.02039
1,359	17.855	61.52	0.02064
1,371	18.095	63.39	0.01910
1,389	18.442	66.26	0.01875
1,406	18.733	68.83	0.01919
1,429	19.113	72.43	0.01977
1,441	19.473	76.13	0.02008

P=applied load;
t=time in second;
a=crack length measured from the line of action of the external load;
K=applied stress intensity factor;
da/dt=crack growth rate.

Table A3. Stress Corrosion Experimental Data for Specimen HT-27 Step2 (3.5% NaCl, $\delta = 0.042mm$) and Step3 (3.5% NaCl, $P = 1.00kN$)

$t(s)$	$a(mm)$	$K(MPa\sqrt{m})$	$da/dt(mm/s)$
Step2 (3.5% NaCl, constant COD control, $\delta = 0.042mm$)			
0	10.309	15.67	0.0044235
32	10.454	15.37	0.0042395
65	10.576	15.19	0.0040497
100	10.752	14.97	0.0038483
148	10.930	14.64	0.0035722
203	11.062	14.27	0.0032468
269	11.285	14.06	0.0028975
343	11.510	13.90	0.0024611
422	11.666	13.40	0.0020556
522	11.875	13.41	0.0016701
677	12.010	13.25	0.0011818
890	12.177	13.29	0.0008148
1,160	12.332	13.24	0.0006024
1,368	12.390	13.20	0.0005046
1,621	12.463	13.07	0.0004446
1,730	12.579	13.11	0.0004138
1,966	12.707	13.02	0.0003665
2,469	12.826	12.82	0.0003240
2,868	12.957	12.50	0.0002942
3,468	13.016	12.28	0.0002435
4,068	13.242	12.17	0.0002034
4,416	13.389	12.05	0.0001858
5,016	13.408	11.89	0.0001553
7,424	13.536	11.85	0.0002327
8,029	13.629	11.85	0.0003131
8,419	13.925	11.83	0.0003229
8,549	14.130	11.73	0.0001721
8,952	14.198	11.87	0.0003318
9,334	14.199	11.83	0.0003168
9,748	14.325	11.80	0.0001857
Step3 (3.5% NaCl, constant load control, $P = 1.00kN$)			
13,138	14.562	14.22	0.00031787
13,170	14.663	14.36	0.0007822

13,227	14.846	14.64	0.0021169
13,277	15.085	15.00	0.0041558
13,333	15.349	15.42	0.0042518
13,404	15.631	15.89	0.004435
13,460	15.873	16.31	0.0045689
13,513	16.153	16.82	0.0045654
13,583	16.450	17.38	0.0045736
13,637	16.714	17.91	0.0046689
13,709	17.080	18.69	0.0047003
13,785	17.394	19.39	0.0047469
13,857	17.701	20.12	0.004817
13,921	18.074	21.08	0.0047653
13,985	18.368	21.88	0.0046748
14,040	18.657	22.71	0.0046467
14,101	18.945	23.60	0.004532
14,178	19.258	24.63	0.0042749
14,266	19.614	25.89	0.0040652
14,338	19.895	26.96	0.0040183
14,428	20.230	28.33	0.0040169
14,486	20.483	29.45	0.0040659
14,559	20.717	30.55	0.0041295
14,709	21.407	34.20	0.0042836
14,803	21.801	36.61	0.0043102
14,894	22.275	39.91	0.0041649
14,991	22.669	43.04	0.0040962
15,067	22.948	45.50	0.0040907
15,139	23.253	48.46	0.0040175
15,255	23.604	52.28	0.0038997
15,329	23.957	56.64	0.0038245
15,387	24.277	61.13	0.0037656

P=applied load;
t=time in second;
a=crack length measured from the line of action of the external load;
K=applied stress intensity factor;
da/dt=crack growth rate.
δ = COD=crack opening displacement

Table A4. Stress Corrosion Experimental Data for Specimen HT-33 Step2 (0% NaCl, $\delta = 0.062mm$) and Step3 (0% NaCl, $P = 0.8kN$)

$t(s)$	$a(mm)$	$K(MPa\sqrt{m})$	$da/dt(mm/s)$
Step2 (0% NaCl, constant COD control, $\delta = 0.062mm$)			
0	7.994	23.87	0.01102
33	8.316	23.76	0.01125
66	8.682	23.64	0.01147
92	9.017	23.53	0.01165
130	9.408	23.04	0.01191
162	9.779	22.67	0.01142
185	10.218	22.56	0.01121
217	10.588	22.01	0.01055
256	10.941	20.65	0.009692
313	11.306	19.08	0.008103
349	11.642	18.65	0.007243
400	11.965	17.99	0.006774
447	12.262	17.56	0.006629
501	12.534	17.12	0.006564
556	12.896	16.82	0.006526
605	13.284	16.45	0.006513
657	13.655	15.83	0.00655
714	13.988	15.55	0.00652
767	14.363	15.27	0.00634
832	14.712	14.92	0.006034
877	15.029	14.73	0.005998
930	15.325	14.10	0.00572
992	15.681	13.84	0.005205
1,046	15.947	13.93	0.004799
1,086	16.268	13.99	0.00435
1,178	16.548	13.69	0.002862
1,277	16.765	13.55	0.001881
1,400	16.916	13.47	0.001151
1,523	16.951	13.49	0.0004497
3,830	16.953	13.38	0.0005682
Step3 (0% NaCl, constant load control, $P = 0.8kN$)			
4,198	16.953	14.77	0.001539
4,277	17.159	15.13	0.002395

4,323	17.480	15.71	0.003064
4,374	17.793	16.32	0.005963
4,423	18.099	16.96	0.006541
4,478	18.454	17.74	0.0071
4,524	18.820	18.62	0.007372
4,565	19.157	19.48	0.007787
4,613	19.493	20.41	0.008221
4,661	19.878	21.57	0.008734
4,700	20.223	22.70	0.009277
4,734	20.593	24.03	0.009589
4,770	20.905	25.24	0.009788
4,799	21.224	26.60	0.01026
4,831	21.598	28.34	0.01066
4,868	21.936	30.09	0.01112
4,905	22.264	31.95	0.01173
4,936	22.753	35.09	0.0121
4,965	23.109	37.72	0.01249
5,003	23.598	41.88	0.01319
5,036	24.040	46.32	0.01383
5,058	24.300	49.32	0.01464
5,082	24.635	53.64	0.01544
5,104	24.992	59.00	0.01618
5,127	25.384	65.91	0.01694
5,141	25.701	72.55	0.01741

P=applied load;
t=time in second;
a=crack length measured from the line of action of the external load;
K=applied stress intensity factor;
da/dt=crack growth rate.
δ = COD=crack opening displacement

Table A5. Stress Corrosion Experimental Data for Specimen HT-34 step2 (0.35% NaCl, $\delta = 0.070mm$) and step3 (0.35% NaCl, $P = 1.10kN$)

$t(s)$	$a(mm)$	$K(MPa\sqrt{m})$	$da/dt(mm/s)$
Step2 (0.35% NaCl, constant COD control, $\delta = 0.070mm$)			
0	8.564	10.88	0.0045476
18	8.586	18.33	0.0045554
54	8.710	18.19	0.0045709
94	8.870	18.03	0.0045881
136	9.097	17.89	0.0046062
160	9.364	17.97	0.0047488
208	9.482	17.76	0.0047251
254	9.663	17.42	0.0045833
299	9.875	17.24	0.0042583
334	10.040	17.11	0.0039752
394	10.295	16.84	0.0039378
462	10.579	16.29	0.003596
547	10.811	16.00	0.0031899
607	11.002	15.76	0.0030248
707	11.204	15.29	0.0028926
781	11.447	15.09	0.0028452
857	11.653	14.84	0.0028807
987	12.062	14.40	0.0029618
1,074	12.337	14.70	0.0030657
1,163	12.598	13.92	0.003074
1,322	13.049	13.51	0.0030966
1,449	13.483	13.17	0.0029594
1,584	13.956	12.90	0.002737
1,710	14.302	12.92	0.0024199
1,831	14.648	13.02	0.0021358
1,998	14.869	12.86	0.0014589
2,135	15.090	12.95	0.0006776
2,479	15.175	12.96	0.0001979
3,035	15.177	12.84	0.0001108
3,787	15.180	12.75	5.1245e-05
5,918	15.188	12.39	1.7148e-05

Step3 (0.35% NaCl, constant load control, $P = 1.10kN$)

12,732	15.188	16.77	0.0001066
12,815	15.282	16.94	0.0002126
12,896	15.430	17.20	0.0004657
12,965	15.704	17.71	0.0028535
13,060	15.965	18.22	0.0028526
13,186	16.374	19.06	0.0030702
13,322	16.807	20.02	0.0031568
13,442	17.191	20.93	0.0032161
13,590	17.593	21.97	0.0030893
13,690	17.923	22.87	0.0030852
13,748	18.204	23.69	0.0031741
13,859	18.590	24.90	0.0032281
14,056	18.980	26.22	0.0033964
14,135	19.329	27.51	0.0034317
14,237	19.834	29.55	0.0035469
14,353	20.184	31.11	0.0038041
14,476	20.640	33.37	0.004129
14,585	21.041	35.59	0.0042435
14,690	21.518	38.54	0.0043371
14,747	21.849	40.83	0.0042526
14,831	22.264	44.04	0.004182
14,930	22.654	47.46	0.0038827
15,016	23.014	51.00	0.0036228
15,148	23.422	55.56	0.0032237
15,266	23.715	59.27	0.002867

P=applied load;
t=time in second;
a=crack length measured from the line of action of the external load;
K=applied stress intensity factor;
da/dt=crack growth rate.
δ = COD=crack opening displacement

Table A6. Stress Corrosion Experimental Data for Specimen HT-40 step2 (0.0035% NaCl, $\delta = 0.051mm$) and step3 (0.0035% NaCl, $P = 1.00kN$)

$t(s)$	$a(mm)$	$K(MPa\sqrt{m})$	$da/dt(mm/s)$
Step2 (0.0035% NaCl, constant COD control, $\delta = 0.051mm$)			
0	7.223	16.93	0.006929
86	7.763	16.38	0.006963
169	8.265	15.84	0.006996
231	8.741	15.40	0.007021
285	9.150	15.10	0.007043
352	9.713	14.75	0.006881
408	10.101	14.51	0.006716
470	10.495	14.09	0.006230
553	11.002	13.55	0.005524
634	11.364	13.05	0.005016
716	11.726	12.52	0.004600
782	11.980	12.21	0.004145
837	12.245	11.84	0.003757
903	12.595	11.82	0.003387
990	12.842	11.48	0.002780
1,070	12.970	11.29	0.002014
1,158	13.113	11.24	0.000823
1,286	13.190	11.24	0.000545
1,575	13.233	11.24	0.000296
2,021	13.267	11.12	9.645e-05
Step3 (0.0035% NaCl, constant load control, $P = 1.00kN$)			
5,514	13.405	12.64	0.000838
5,575	13.684	12.99	0.001777
5,647	14.047	13.46	0.003641
5,715	14.393	13.94	0.005569
5,811	14.922	14.71	0.005811
5,892	15.451	15.55	0.006155
5,978	16.009	16.51	0.00642
6,046	16.450	17.34	0.006636
6,121	16.895	18.24	0.006791
6,188	17.442	19.45	0.006957
6,260	17.899	20.57	0.007092
6,330	18.430	21.99	0.007133

6,407	18.953	23.56	0.007107
6,466	19.456	25.25	0.006996
6,539	19.956	27.13	0.006995
6,617	20.451	29.22	0.007
6,684	20.887	31.30	0.006862
6,760	21.392	34.02	0.00693
6,821	21.872	36.98	0.007244
6,864	22.241	39.56	0.007623
6,929	22.532	41.80	0.008124
6,965	22.913	45.05	0.008419
6,999	23.255	48.35	0.008698
7,050	23.730	53.63	0.009115
7,095	24.125	58.77	0.009484

P=applied load;
t=time in second;
a=crack length measured from the line of action of the external load;
K=applied stress intensity factor;
da/dt=crack growth rate.
δ = COD=crack opening displacement

Table A7. Stress Corrosion Experimental Data for Specimen HT-39 step2 (0.0105% NaCl, $\delta = 0.063mm$) and step3 (0.0105% NaCl, $P = 1.10kN$)

$t(s)$	$a(mm)$	$K(MPa\sqrt{m})$	$da/dt(mm/s)$
Step2 (0.0105% NaCl, constant COD control, $\delta = 0.063mm$)			
0	10.155	21.38	0.005373
29	10.236	21.54	0.005529
67	10.525	21.11	0.005734
121	10.858	20.38	0.006026
204	11.316	19.10	0.006347
294	11.938	18.60	0.006343
357	12.403	18.09	0.006418
449	12.867	17.07	0.006546
515	13.376	16.80	0.006841
581	13.793	16.23	0.007008
638	14.197	15.59	0.007169
707	14.790	15.27	0.006976
776	15.242	14.80	0.006612
846	15.678	14.40	0.006105
916	16.104	13.96	0.005479
993	16.433	13.38	0.005007
1,069	16.858	13.24	0.004534
1,168	17.255	12.82	0.003759
1,251	17.573	12.59	0.003203
1,350	17.884	12.23	0.00248
1,461	17.973	11.93	0.001873
1,611	18.186	11.68	0.001353
1,751	18.430	11.85	0.001048
1,921	18.517	11.83	0.000697
Step3 (0.0105% NaCl, constant load control, $P = 1.10kN$)			
3,431	18.622	24.80	0.001374
3,482	18.925	25.82	0.003444
3,582	19.250	26.99	0.004791
3,639	19.610	28.39	0.005155
3,704	19.954	29.84	0.005539
3,755	20.215	31.02	0.005784
3,806	20.546	32.62	0.005699
3,867	20.930	34.67	0.005359

3,921	21.209	36.29	0.005036
3,971	21.465	37.89	0.00488
4,032	21.639	39.04	0.004672
4,073	21.875	40.71	0.004532
4,119	22.163	42.89	0.004374

P=applied load;
t=time in second;
a=crack length measured from the line of action of the external load;
K=applied stress intensity factor;
da/dt=crack growth rate.
δ = COD=crack opening displacement

Table A8. Stress Corrosion Experimental Data for Specimen for HT-37 step1 (0.015% NaCl, $dP/dt = 0.100N/s$) and step2 (0.015% NaCl, $\delta = 0.24mm$)

$t(s)$	$a(mm)$	$K(MPa\sqrt{m})$	$da/dt(mm/s)$
Step1 (0.015% NaCl, constant load rate control, $dP/dt = 0.100N/s$)			
0	6.036	8.349	0
708	6.036	8.797	0
3,434	6.036	10.58	6.43e-05
3,960	6.036	10.77	8.62e-05
4,053	6.077	10.89	0.000153
4,481	6.105	11.17	0.000438
4,596	6.170	11.33	0.000981
4,665	6.248	11.47	0.001361
4,726	6.366	11.66	0.001612
4,848	6.529	11.96	0.002328
4,927	6.776	12.32	0.002589
5,021	7.071	12.76	0.002844
5,104	7.371	13.22	0.003166
5,236	7.726	13.80	0.003292
5,334	8.037	14.32	0.003547
5,415	8.371	14.86	0.004007
5,525	8.762	15.50	0.004721
5,593	9.105	16.11	0.005316
5,651	9.498	16.76	0.005487
5,714	9.818	17.34	0.005411
5,758	10.137	17.92	0.005312
5,829	10.487	18.57	0.004774
5,922	10.813	19.24	0.004333
5,998	11.139	19.91	0.004016
6,066	11.451	20.58	0.003909
6,158	11.780	21.33	0.003854
6,258	12.142	22.18	0.003713
6,344	12.474	22.98	0.003762
6,440	12.796	23.77	0.003918
6,513	13.085	24.58	0.003991
6,579	13.397	25.41	0.004068
6,650	13.683	26.23	0.004136
6,729	13.995	27.16	0.004214
6,811	14.349	28.23	0.004213

6,895	14.652	29.24	0.004559
6,958	15.024	30.47	0.004826
7,049	15.366	31.74	0.004995
7,120	15.859	33.57	0.004945
7,177	16.158	34.79	0.004892
7,249	16.440	36.00	0.005142
7,318	16.736	37.37	0.005376
7,411	17.216	39.70	0.006378
7,457	17.618	41.73	0.005280
7,504	17.979	43.73	0.005415
7,563	18.373	46.05	0.004871
7,832	18.691	39.99	0.003012
	Step2 (0.015% NaCl, constant COD control, $\delta = 0.24mm$)		
7,861	18.881	39.17	0.005362
7,901	19.189	38.46	0.006784
7,938	19.378	37.64	0.007135
7,971	19.703	37.45	0.007110
8,008	19.986	37.13	0.006989
8,095	20.515	37.83	0.006426
8,132	20.749	34.20	0.006454
8,185	21.139	33.44	0.006470
8,249	21.402	32.80	0.006484
8,298	21.900	31.66	0.006254
8,352	22.203	30.63	0.005929
8,398	22.455	30.27	0.005625
8,448	22.702	29.52	0.004741
8,501	22.974	28.71	0.004500
8,580	23.224	27.36	0.004441
8,631	23.438	26.03	0.004353
8,680	23.738	26.95	0.004134
8,736	23.983	26.25	0.004249
8,803	24.232	25.38	0.003968
8,883	24.457	23.97	0.003877
8,972	24.826	22.87	0.004301
9,030	25.065	22.09	0.004408
9,132	25.597	21.44	0.004602
9,174	25.844	21.37	0.004561

9,251	26.113	20.17	0.004424
9,307	26.373	19.27	0.004317
9,364	26.603	18.65	0.004414
9,421	26.868	17.83	0.004429
9,474	27.103	17.87	0.004313
9,522	27.356	17.66	0.004073
9,590	27.593	16.59	0.003499
9,641	27.787	16.88	0.002959
9,698	27.903	16.64	0.002289
9,759	28.046	16.61	0.001573

P=applied load;
t=time in second;
a=crack length measured from the line of action of the external load;
K=applied stress intensity factor;
da/dt=crack growth rate.
δ = COD=crack opening displacement

Table A9. Stress Corrosion Experimental Data for Specimen HT-29 (0% NaCl, constant displacement control, $\Delta = 0.191mm$)

$t(s)$	$a(mm)$	$K(MPa\sqrt{m})$	$da/dt(mm/s)$
0	8.048	26.81	0
197	8.081	26.20	0.005999
215	8.226	26.51	0.006977
232	8.357	26.73	0.007901
245	8.500	27.00	0.008607
265	8.741	27.37	0.009694
283	8.929	27.74	0.01067
299	9.188	28.18	0.01115
319	9.312	28.22	0.01131
331	9.457	28.45	0.01136
348	9.620	28.64	0.01099
360	9.853	29.02	0.01061
375	10.032	29.12	0.01021
394	10.215	29.09	0.009607
408	10.341	29.20	0.009515
422	10.507	29.31	0.009052
450	10.684	29.14	0.008424
472	10.782	28.82	0.008157
493	10.902	28.64	0.008441
507	11.044	28.69	0.008487
522	11.236	29.00	0.008442
541	11.386	28.94	0.008328
561	11.584	28.78	0.008324
583	11.765	28.89	0.008389
595	11.985	29.25	0.008485
614	12.074	29.26	0.008291
631	12.147	29.18	0.008085
650	12.229	28.88	0.007977
679	12.434	28.87	0.007815
699	12.677	29.11	0.007781
721	12.892	28.98	0.007814
742	13.088	29.01	0.008075
762	13.215	28.97	0.008228
778	13.319	28.94	0.00833
797	13.419	28.8	0.008222

815	13.601	28.86	0.007779
835	13.771	28.92	0.007629
856	13.981	29.01	0.007624
873	14.113	28.98	0.007734
893	14.286	29.01	0.007799
915	14.419	28.78	0.007818
949	14.527	28.19	0.007965
969	14.756	28.61	0.008285
989	14.964	28.84	0.008747
1,020	15.220	28.41	0.009571
1,042	15.424	28.32	0.01034
1,063	15.579	28.26	0.01096
1,075	15.783	28.69	0.01126
1,089	15.980	28.93	0.01123
1,106	16.189	28.67	0.01138
1,127	16.380	28.25	0.01146
1,140	16.610	28.55	0.01152
1,160	16.839	28.65	0.01133
1,179	17.081	28.74	0.0109
1,200	17.243	28.38	0.01054
1,216	17.427	28.40	0.01045
1,245	17.651	28.46	0.01031
1,261	17.818	28.42	0.01013
1,275	17.997	28.35	0.01002
1,292	18.184	27.87	0.00997
1,311	18.331	27.74	0.01007
1,331	18.597	28.26	0.01016
1,351	18.795	28.08	0.01024
1,371	18.961	27.51	0.009994
1,389	19.124	27.47	0.009692
1,411	19.348	27.63	0.009408
1,429	19.543	26.45	0.00922
1,447	19.771	26.80	0.008958
1,469	19.960	27.15	0.008903
1,492	20.082	27.33	0.008883
1,519	20.281	27.10	0.008866
1,536	20.422	25.87	0.008907
1,559	20.613	25.98	0.008988

1,583	20.829	26.26	0.009116
1,600	21.079	26.84	0.009267
1,623	21.277	26.53	0.009467
1,646	21.483	26.21	0.009556
1,662	21.680	26.11	0.009634
1,687	21.884	26.25	0.009613
1,720	22.208	25.40	0.009499
1,736	22.342	25.47	0.009259
1,758	22.512	25.65	0.00905
1,772	22.668	25.79	0.00898
1,789	22.879	25.31	0.008781
1,806	23.023	25.06	0.00873
1,822	23.160	25.36	0.008601
1,846	23.308	24.96	0.008522
1,859	23.404	24.46	0.008491
1,870	23.537	24.50	0.008329
1,892	23.683	24.03	0.008169
1,913	23.880	24.06	0.008206
1,933	24.022	23.39	0.008283
1,954	24.246	23.47	0.008337
1,976	24.428	23.40	0.008212
1,990	24.542	23.35	0.008162
2,009	24.638	22.52	0.008063
2,026	24.804	22.42	0.007969
2,047	24.999	22.55	0.007845
2,075	25.210	22.33	0.007585
2,100	25.373	21.63	0.007401
2,121	25.574	21.80	0.007301
2,149	25.700	21.04	0.007199
2,166	25.898	21.39	0.007108
2,193	26.053	20.58	0.007065
2,218	26.209	18.99	0.007071
2,245	26.357	19.24	0.006993
2,262	26.514	19.56	0.006918
2,283	26.683	19.16	0.00686
2,308	26.856	18.52	0.006646
2,328	27.021	17.70	0.006594
2,353	27.186	18.16	0.006425

2,370	27.244	17.86	0.006316
2,387	27.371	17.83	0.006077
2,413	27.511	14.89	0.00578
2,439	27.652	15.50	0.005492
2,459	27.778	16.05	0.005089
2,473	27.853	15.95	0.004871
2,495	27.980	15.89	0.004564
2,514	28.062	15.68	0.004228
2,528	28.121	15.33	0.004022
2,561	28.259	14.66	0.003328
2,598	28.313	15.15	0.002935
2,638	28.382	14.93	0.00251
2,656	28.440	15.25	0.002319
2,674	28.502	15.60	0.002128
2,708	28.542	15.72	0.001767

P=applied load;
t=time in second;
a=crack length measured from the line of action of the external load;
K=applied stress intensity factor;
da/dt=crack growth rate.
Δ =displacement at the loading point

Table A10. Stress Corrosion Experimental Data for Specimen HT-30 (3.5% NaCl, constant displacement control, $\Delta = 0.141mm$)

$t(s)$	$a(mm)$	$K(MPa\sqrt{m})$	$da/dt(mm/s)$
0	8.00	21.61	0
187	8.04	21.38	0.002908
215	8.199	21.62	0.00345
235	8.309	21.77	0.003837
246	8.414	21.92	0.00405
265	8.511	22.02	0.004418
287	8.640	22.10	0.005348
318	8.744	22.15	0.005016
335	8.901	22.31	0.004832
371	9.033	22.26	0.004588
406	9.177	22.29	0.004447
448	9.316	22.16	0.004334
493	9.512	22.12	0.00437
509	9.700	22.38	0.004356
558	9.828	22.17	0.004404
594	9.943	22.05	0.004415
623	10.104	22.08	0.004424
657	10.301	22.09	0.004286
698	10.498	22.07	0.004072
754	10.683	21.96	0.004004
797	10.875	21.93	0.003896
835	11.024	21.89	0.003739
893	11.171	21.60	0.003611
947	11.340	21.72	0.003555
990	11.505	21.69	0.003468
1,045	11.762	21.92	0.003284
1,093	11.913	21.90	0.003287
1,133	12.059	21.76	0.003266
1,169	12.161	21.74	0.003206
1,225	12.287	21.87	0.003052
1,301	12.458	21.67	0.00293
1,336	12.682	21.82	0.002963
1,404	12.808	21.66	0.00297
1,450	12.958	21.49	0.002995
1,490	13.092	21.57	0.003151

1,538	13.219	21.39	0.003283
1,569	13.360	21.47	0.003345
1,635	13.507	21.21	0.00361
1,675	13.642	21.26	0.003676
1,708	13.858	21.25	0.003702
1,758	14.038	21.32	0.003722
1,791	14.208	21.44	0.003713
1,837	14.334	21.31	0.003748
1,879	14.490	21.00	0.003646
1,925	14.647	21.11	0.003478
1,973	14.792	21.23	0.003377
2,012	14.940	21.28	0.003311
2,057	15.089	21.02	0.003317
2,131	15.352	20.96	0.003256
2,179	15.504	20.88	0.003206
2,249	15.663	20.64	0.003318
2,298	15.868	20.76	0.003335
2,346	16.020	20.43	0.003383
2,390	16.157	20.47	0.003409
2,433	16.259	20.36	0.003418
2,468	16.526	20.57	0.003448
2,542	16.702	20.32	0.003363
2,590	16.888	19.73	0.003395
2,632	17.027	19.92	0.003429
2,684	17.158	20.02	0.003494
2,735	17.279	19.98	0.003438
2,762	17.449	20.20	0.003507
2,809	17.629	19.86	0.003532
2,858	17.803	19.49	0.003591
2,904	18.001	19.70	0.003609
2,953	18.112	19.63	0.003513
3,000	18.324	19.74	0.003368
3,045	18.458	19.56	0.003382
3,090	18.622	19.46	0.003447
3,145	18.772	19.36	0.003587
3,192	18.891	19.10	0.003796
3,243	19.083	18.93	0.003889
3,285	19.305	19.09	0.003977

3,330	19.512	18.56	0.004067
3,364	19.670	18.71	0.004169
3,414	19.908	19.04	0.004184
3,468	20.075	19.08	0.004024
3,510	20.238	18.77	0.003895
3,559	20.448	18.60	0.00377
3,607	20.635	18.32	0.003696
3,658	20.810	18.40	0.003649
3,698	20.914	18.16	0.003648
3,741	21.110	17.99	0.003631
3,799	21.290	17.82	0.00367
3,853	21.502	17.26	0.003728
3,903	21.688	17.44	0.003764
3,947	21.832	17.38	0.00377
3,997	22.045	16.98	0.003779
4,055	22.313	17.08	0.003832
4,120	22.545	17.01	0.003822
4,170	22.697	16.60	0.003812
4,231	22.896	16.39	0.003777
4,267	23.095	16.44	0.003761
4,327	23.328	16.18	0.003759
4,399	23.580	15.97	0.003838
4,485	23.893	15.44	0.003924
4,544	24.090	15.28	0.004044
4,581	24.293	15.28	0.003961
4,630	24.490	14.72	0.003939
4,690	24.728	15.18	0.003960
4,748	24.967	14.99	0.003968
4,819	25.329	14.43	0.003845
4,910	25.590	14.44	0.003460
5,059	26.109	13.78	0.002694
5,197	26.448	13.77	0.001984
5,294	26.665	14.05	0.001485
5,446	26.751	13.75	0.000703

P=applied load; t=time in second;
a=crack length measured from the line of action of the external load;
K=applied stress intensity factor;
da/dt=crack growth rate.
Δ =displacement at the loading point

Table A11. Stress Corrosion Experimental Data for Specimen HT-31 (3.5% NaCl, constant displacement control, $\Delta = 0.122mm$)

$t(s)$	$a(mm)$	$K(MPa\sqrt{m})$	$da/dt(mm/s)$
0	8.009	18.05	0.000486
132	8.078	17.93	0.001406
182	8.206	18.03	0.001755
252	8.338	18.01	0.002242
324	8.543	18.04	0.002819
472	8.992	18.13	0.003376
568	9.392	18.40	0.003553
653	9.738	18.66	0.003637
746	10.029	18.70	0.003598
822	10.304	18.93	0.003483
912	10.652	19.35	0.003378
1,053	11.068	19.40	0.003267
1,142	11.399	19.86	0.003121
1,426	12.247	20.24	0.00274
1,561	12.522	19.67	0.002651
1,726	12.949	20.28	0.002716
1,838	13.258	20.53	0.002796
1,971	13.593	20.22	0.003034
2,088	14.026	20.79	0.003115
2,212	14.404	20.35	0.003198
2,379	15.010	21.04	0.003214
2,522	15.388	20.77	0.003146
2,672	15.887	20.14	0.003024
2,838	16.379	20.93	0.002968
2,993	16.878	20.24	0.003054
3,146	17.195	20.49	0.003123
3,319	17.814	20.36	0.003228
3,471	18.361	20.21	0.003149
3,635	18.930	19.96	0.003125
3,795	19.436	19.04	0.002996
4,019	19.919	19.70	0.002914
4,219	20.476	19.13	0.002935
4,531	21.536	18.61	0.003164
4,978	23.002	17.60	0.003388
5,169	23.678	17.01	0.003401

5,313	24.191	15.47	0.003364
5,448	24.605	16.30	0.003333
5,644	25.302	15.69	0.003205
5,817	25.835	14.96	0.003084
6,395	27.442	15.56	0.001539
6,639	27.645	16.23	0.000886
6,991	27.659	16.13	0

P=applied load;
t=time in second;
a=crack length measured from the line of action of the external load;
K=applied stress intensity factor;
da/dt=crack growth rate.
Δ =displacement at the loading point

Table A12. Stress Corrosion Experimental Data for Specimen HT-28 step5 (3.5% NaCl, constant displacement control, $\Delta = 0.121mm$)

$t(s)$	$a(mm)$	$K(MPa\sqrt{m})$	$da/dt(mm/s)$
38,444	9.715	17.44	0.003756
38,480	9.809	17.47	0.003689
38,500	9.905	17.54	0.003651
38,535	10.028	17.56	0.003586
38,591	10.258	17.70	0.003609
38,642	10.392	17.73	0.00349
38,701	10.603	17.81	0.003367
38,754	10.819	17.80	0.003226
38,821	11.014	17.64	0.00312
38,927	11.315	17.42	0.002801
39,056	11.640	17.31	0.002758
39,163	11.886	17.13	0.00289
39,253	12.171	17.05	0.002992
39,368	12.562	17.10	0.003116
39,470	12.891	17.02	0.0032
39,578	13.241	17.20	0.003264
39,699	13.592	17.09	0.003303
39,819	13.978	17.12	0.003447
39,992	14.663	16.70	0.003707
40,138	15.146	17.07	0.003792
40,222	15.543	17.33	0.003812
40,344	16.017	16.96	0.003806
40,462	16.422	16.47	0.003878
40,654	17.158	16.21	0.003942
40,774	17.624	16.65	0.003996
40,897	18.174	16.78	0.003989
41,010	18.627	16.28	0.003978
41,134	19.114	16.66	0.003875
41,327	19.833	16.46	0.003721
41,451	20.272	16.27	0.003773
41,572	20.691	15.91	0.003782
41,673	21.112	15.77	0.003839
41,813	21.682	15.59	0.003875
41,935	22.118	15.24	0.003818
42,031	22.533	15.21	0.003762

42,151	22.947	14.29	0.00367
42,267	23.353	14.60	0.003624
42,382	23.799	14.67	0.003417
42,496	24.176	14.09	0.003163
42,624	24.635	14.64	0.00277
42,763	24.957	14.32	0.002369
42,883	25.139	13.97	0.002052
43,006	25.365	13.58	0.001724
43,125	25.644	13.69	0.001478
43,281	25.826	13.26	0.001142
43,423	25.972	12.90	0.0007499
43,578	26.000	12.92	9.161e-05
43,849	26.000	12.92	1.844e-05
46,160	26.000	12.92	6.693e-05
48,303	26.272	12.18	0.0001119
48,754	26.272	11.85	0.0001213

P=applied load;
t=time in second;
a=crack length measured from the line of action of the external load;
K=applied stress intensity factor;
da/dt=crack growth rate.
Δ =displacement at the loading point

Table A13. Stress Corrosion Experimental Data for Specimen HT-36 Step2 (3.5% NaCl, constant displacement control, $\Delta = 0.150mm$)

$t(s)$	$a(mm)$	$K(MPa\sqrt{m})$	$da/dt(mm/s)$
0	8.041	16.02	0.004522
10	8.140	16.12	0.004584
39	8.261	16.20	0.004762
91	8.468	16.24	0.005082
134	8.287	18.21	0.005346
160	8.792	16.29	0.005506
183	9.052	16.56	0.005597
216	9.252	16.67	0.005903
272	9.651	16.89	0.00612
334	9.932	16.97	0.005846
396	10.184	16.94	0.004965
452	10.493	16.97	0.004604
512	10.710	17.04	0.004379
573	10.988	16.98	0.004195
627	11.229	16.94	0.004086
694	11.441	16.93	0.004029
753	11.701	16.97	0.003986
815	11.947	17.00	0.00409
877	12.197	16.85	0.00416
934	12.349	16.81	0.004264
996	12.674	16.62	0.004539
1,054	12.918	16.84	0.00473
1,114	13.268	16.90	0.004794
1,174	13.509	16.78	0.004874
1,237	13.817	16.80	0.004872
1,294	14.258	17.04	0.004729
1,353	14.537	17.00	0.004551
1,414	14.668	16.79	0.004382
1,476	15.003	16.87	0.004313
1,544	15.259	16.79	0.004156
1,599	15.436	16.64	0.003995
1,656	15.619	16.31	0.004097
1,718	15.939	16.49	0.004248
1,793	16.306	16.35	0.004512
1,838	16.447	16.22	0.00481

1,893	16.620	16.05	0.00503
1,921	16.864	16.06	0.004845
1,960	17.032	16.08	0.004796
1,989	17.243	16.20	0.004831
2,021	17.448	16.15	0.004974
2,075	17.694	16.15	0.004925
2,133	17.848	15.72	0.004697
2,179	18.090	15.78	0.004654
2,230	18.312	15.70	0.004622
2,284	18.587	15.55	0.004688
2,328	18.849	15.58	0.004732
2,377	19.035	15.43	0.004821
2,424	19.264	15.37	0.004782
2,474	19.512	15.33	0.004704
2,522	19.758	15.11	0.004604
2,581	20.004	15.11	0.004505
2,637	20.276	15.11	0.004456
2,697	20.552	14.86	0.004365
2,753	20.727	14.54	0.004267
2,808	20.979	14.37	0.004233
2,851	21.190	14.38	0.004246
2,896	21.364	14.26	0.004328
2,959	21.630	14.04	0.004465
3,013	21.825	13.79	0.004547
3,047	22.007	13.71	0.004569
3,086	22.187	13.62	0.004598
3,125	22.437	13.66	0.004683
3,167	22.611	13.61	0.004714
3,209	22.776	13.26	0.004687
3,266	23.060	13.35	0.004487
3,305	23.235	13.31	0.004411
3,347	23.453	13.19	0.004255
3,400	23.654	13.04	0.00416
3,455	23.843	12.83	0.003936
3,512	24.062	12.86	0.003593
3,559	24.309	12.79	0.003297
3,625	24.496	12.69	0.002871
3,667	24.660	12.82	0.002659

3,734	24.758	12.53	0.002249
3,803	24.856	12.58	0.001817
3,859	24.938	12.35	0.001477
3,917	25.038	12.62	0.001236
3,971	25.111	12.42	0.001095
4,039	25.169	12.47	0.000917
4,100	25.205	12.36	0.000758
4,249	25.218	12.33	0.000368
4,663	25.230	12.30	0

P=applied load;
t=time in second;
a=crack length measured from the line of action of the external load;
K=applied stress intensity factor;
da/dt=crack growth rate.
Δ =displacement at the loading point

Table A14. Stress Corrosion Experimental Data for Specimen HT-38 (0.0228% NaCl, constant loading rate control, $dP/dt = 0.278N/s$)

$t(s)$	$a(mm)$	$K(MPa\sqrt{m})$	$da/dt(mm/s)$
0	6.018	8.34	0
692	6.057	9.56	0.0002953
741	6.102	9.70	0.0003382
1,123	6.140	10.37	0.0006729
1,173	6.210	10.56	0.001165
1,314	6.374	11.00	0.001467
1,368	6.519	11.26	0.001738
1,468	6.719	11.70	0.001972
1,623	6.964	12.29	0.002383
1,689	7.200	12.73	0.002474
1,801	7.478	13.30	0.002805
1,883	7.734	13.81	0.003016
1,983	8.003	14.42	0.00303
2,062	8.310	15.02	0.003139
2,160	8.610	15.69	0.003305
2,290	8.988	16.59	0.003811
2,376	9.290	17.25	0.004178
2,452	9.679	18.11	0.004274
2,525	10.071	18.96	0.004399
2,610	10.457	19.88	0.004311
2,704	10.798	20.80	0.003903
2,817	11.188	21.91	0.003391
2,890	11.483	22.75	0.003181
2,990	11.777	23.70	0.00308
3,154	12.138	25.01	0.003378
3,281	12.514	26.29	0.003664
3,364	12.997	27.85	0.003705
3,446	13.382	29.18	0.003834
3,565	13.758	30.72	0.00363
3,668	14.109	32.19	0.00323
3,783	14.431	33.67	0.003144
3,914	14.797	35.53	0.003377
4,020	15.163	37.34	0.003782
4,131	15.589	39.54	0.00438
4,229	16.039	41.92	0.00500

4,327	16.573	45.02	0.005659
4,409	17.055	47.99	0.005956
4,488	17.569	51.45	0.006283
4,563	18.095	55.32	0.006595
4,615	18.325	57.31	0.006810

P=applied load;
t=time in second;
a=crack length measured from the line of action of the external load;
K=applied stress intensity factor;
da/dt=crack growth rate.
dP/dt=rate of applied external load

Table A15. Stress Corrosion Experimental Data for Specimen HT-43 (0.012% NaCl, constant loading rate control, $dP/dt = 0.100N/s$)

$t(s)$	$a(mm)$	$K(MPa\sqrt{m})$	$da/dt(mm/s)$
0	5.936	7.88	0
1,491	5.962	9.14	0.000226
2,297	6.074	9.75	0.000538
2,442	6.204	9.97	0.000594
2,650	6.352	10.26	0.000894
2,745	6.497	10.51	0.00103
3,053	6.735	10.97	0.001603
3,158	6.967	11.32	0.00200
3,313	7.253	11.76	0.00270
3,435	7.625	12.32	0.003383
3,518	7.929	12.76	0.003884
3,606	8.296	13.30	0.004426
3,692	8.703	13.92	0.004827
3,781	9.172	14.63	0.005118
3,857	9.585	15.27	0.005075
3,946	10.061	16.06	0.004961
4,026	10.484	16.78	0.00478
4,153	10.978	17.71	0.004462
4,253	11.429	18.58	0.004372
4,340	11.825	19.39	0.004333
4,425	12.165	20.09	0.004281
4,509	12.561	20.96	0.004159
4,599	12.935	21.85	0.004011
4,719	13.373	22.93	0.003877
4,837	13.812	24.10	0.003981
4,963	14.261	25.33	0.004437
5,048	14.625	26.44	0.004837
5,142	15.158	28.07	0.00526
5,259	15.817	30.30	0.005332
5,326	16.232	31.81	0.005219
5,401	16.645	33.48	0.004976
5,482	16.930	34.70	0.004562
5,570	17.371	36.74	0.003903
5,677	17.809	38.95	0.00292
5,821	18.194	41.21	0.00159
5,997	18.194	41.57	0

P=applied load; t=time in second;
a=crack length measured from the line of action of the external load;
K=applied stress intensity factor; da/dt=crack growth rate.
dP/dt=rate of applied external load

Table A16. Stress Corrosion Experimental Data for Specimen HT-42 (0.0% NaCl, constant loading rate control, $dP/dt = 0.100N/s$)

$t(s)$	$a(mm)$	$K(MPa\sqrt{m})$	$da/dt(mm/s)$
0	6.219	8.01	0
6,437	6.246	12.08	0.00430
6,458	6.336	12.21	0.00433
6,483	6.445	12.38	0.00437
6,506	6.532	12.51	0.00435
6,567	6.790	12.89	0.00444
6,599	6.979	13.17	0.00450
6,678	7.295	13.68	0.00475
6,731	7.568	14.11	0.00513
6,814	7.944	14.72	0.00617
6,857	8.244	15.20	0.00711
6,898	8.565	15.71	0.00847
6,947	8.951	16.35	0.01104
6,993	9.430	17.17	0.01295
7,015	9.817	17.78	0.01199
7,033	10.217	18.50	0.01274
7,064	10.502	19.03	0.01257
7,130	11.210	20.41	0.00929
7,177	11.524	21.07	0.00844
7,215	11.852	21.76	0.00856
7,258	12.126	22.42	0.00907
7,292	12.502	23.26	0.00925
7,324	12.828	23.99	0.00991
7,349	13.111	24.71	0.01039
7,393	13.461	25.61	0.01024
7,421	13.870	26.71	0.01025
7,456	14.200	27.64	0.01024
7,495	14.566	28.74	0.01044
7,522	14.860	29.65	0.01027
7,568	15.332	31.19	0.01049
7,590	15.585	32.14	0.01075
7,623	15.938	33.48	0.01105
7,667	16.386	35.19	0.01161
7,696	16.753	36.72	0.01184
7,725	17.133	38.45	0.01223

7,760	17.562	40.53	0.01284
7,794	17.965	42.62	0.01312
7,846	18.672	46.79	0.01363
7,880	19.189	50.27	0.01402
7,916	19.683	53.94	0.01444
7,951	20.163	58.00	0.01485

P=applied load;
t=time in second;
a=crack length measured from the line of action of the external load;
K=applied stress intensity factor;
da/dt=crack growth rate.
dP/dt=rate of applied external load

Table A17. Stress Corrosion Experimental Data for Specimen HT-41 (3.5% NaCl, constant loading rate control, $dP/dt = 0.100N/s$)

$t(s)$	$a(mm)$	$K(MPa\sqrt{m})$	$da/dt(mm/s)$
0	5.957	7.97	0
2,071	6.004	9.27	0.0001243
2,147	6.080	9.40	0.0001293
2,196	6.196	9.55	0.0001325
4,049	6.332	10.88	0.000866
4,143	6.496	11.14	0.001281
4,278	6.589	11.33	0.001609
4,376	6.771	11.63	0.001991
4,461	6.964	11.92	0.00239
4,545	7.177	12.24	0.002732
4,623	7.416	12.60	0.002997
4,719	7.757	13.11	0.003342
4,824	8.059	13.60	0.003817
4,900	8.353	14.05	0.004103
4,962	8.651	14.51	0.004349
5,037	9.019	15.10	0.004756
5,117	9.370	15.69	0.004887
5,196	9.788	16.39	0.005009
5,250	10.081	16.88	0.004833
5,332	10.452	17.58	0.00463
5,401	10.852	18.32	0.004263
5,506	11.184	19.01	0.003746
5,587	11.476	19.61	0.00351
5,688	11.754	20.23	0.003143
5,782	12.100	21.00	0.00315
5,859	12.380	21.67	0.003213
5,977	12.608	22.27	0.003635
6,088	13.051	23.41	0.004179
6,159	13.378	24.23	0.004389
6,244	13.866	25.52	0.004581
6,316	14.185	26.45	0.004519
6,403	14.569	27.58	0.004246
6,502	14.944	28.84	0.003897
6,625	15.347	30.25	0.003739
6,722	15.769	31.82	0.003614
6,801	16.048	32.94	0.003512

P=applied load; t=time in second;
a=crack length measured from the line of action of the external load;
K=applied stress intensity factor; da/dt=crack growth rate.
dP/dt=rate of applied external load

Table A18. Stress Corrosion Experimental Data for Specimen HT-44 step1 (0.0% NaCl, $dP/dt = 0.100N/s$) and step2 (0.0035% NaCl, $dP/dt = 0.100N/s$) and step3 (0.035% NaCl, $dP/dt = 0.037N/s$)

$t(s)$	$a(mm)$	$K(MPa\sqrt{m})$	$da/dt(mm/s)$
Step1 (0.0% NaCl, constant loading rate control, $dP/dt = 0.100N/s$)			
0	5.955	9.17	0
168	6.067	9.41	0
276	6.103	9.52	0
1,313	6.285	10.35	0.0007857
1,405	6.417	10.55	0.001286
1,606	6.599	10.90	0.001865
1,679	6.800	11.17	0.002759
1,725	6.977	11.42	0.003105
1,778	7.133	11.65	0.003492
1,837	7.354	11.95	0.003823
1,899	7.599	12.33	0.003886
1,968	7.866	12.69	0.001238
1,991	8.030	12.95	0.0001702
Step2 (0.0035% NaCl, constant loading rate control, $dP/dt = 0.100N/s$)			
16,788	8.290	8.58	8.4e-05
17,158	8.351	8.93	0.0001355
17,603	8.365	9.28	0.0001859
18,322	8.461	9.94	0.0005176
18,461	8.571	10.16	0.0009268
18,511	8.695	10.30	0.001163
18,591	8.862	10.56	0.001368
18,781	9.025	10.88	0.001409
18,867	9.196	11.13	0.001267
18,951	9.344	11.36	0.001201
19,124	9.531	11.74	0.001207
19,352	9.706	12.12	0.001461
19,481	9.880	12.44	0.00207
19,596	10.097	12.80	0.00287
19,667	10.368	13.19	0.003462
19,726	10.621	13.62	0.003629
19,793	10.861	13.96	0.004094
19,861	11.188	14.45	0.004359

19,943	11.445	14.88	0.004694
19,989	11.746	15.39	0.004814
20,037	12.011	15.83	0.004944
20,109	12.355	16.43	0.005162
20,170	12.653	16.99	0.005004
20,241	13.044	17.68	0.005177
20,301	13.293	18.19	0.005107
20,351	13.575	18.78	0.002312
20,392	13.852	19.37	0.0008092
	Step3 (0.035% NaCl, constant loading rate control, $dP/dt = 0.037N/s$)		
26,932	14.132	10.11	0.0001106
27,218	14.166	10.27	0.0005232
27,272	14.254	10.39	0.0002328
27,326	14.307	10.47	0.0004271
27,399	14.425	10.65	0.0004447
28,275	14.483	11.18	0.0008166
28,344	14.547	11.29	0.001389
28,468	14.656	11.47	0.001939
28,543	14.854	11.75	0.002409
28,617	15.091	12.05	0.002899
28,693	15.297	12.42	0.003321
28,748	15.501	12.69	0.003672
28,794	15.662	12.95	0.003899
28,855	15.905	13.34	0.004242
28,902	16.148	13.72	0.00445
28,953	16.366	14.09	0.004615
29,017	16.662	14.58	0.004659
29,083	17.000	15.22	0.00473
29,165	17.367	15.95	0.004916
29,231	17.630	16.50	0.005077
29,283	18.000	17.33	0.005204
29,350	18.314	18.12	0.005367

P=applied load;
t=time in second;
a=crack length measured from the line of action of the external load;
K=applied stress intensity factor;
da/dt=crack growth rate.
dP/dt=rate of applied external load

Table A19. Stress Corrosion Experimental Data for Specimen HT-47 step1 (0.35% NaCl, $dP/dt = 0.100N/s$) and step2 (0. 35% NaCl, $dP/dt = 0.044N/s$)

$t(s)$	$a(mm)$	$K(MPa\sqrt{m})$	$da/dt(mm/s)$
Step1 (0.35% NaCl, constant loading rate control, $dP/dt = 0.100N/s$)			
0	6.052	8.15	0.000731
118	6.136	8.30	0.001083
182	6.223	8.43	0.001274
273	6.349	8.60	0.001545
356	6.533	8.82	0.001691
451	6.644	8.99	0.001695
524	6.845	9.28	0.001708
617	6.958	9.39	0.001707
713	7.101	9.63	0.001877
793	7.252	9.83	0.002114
862	7.405	10.02	0.002265
928	7.580	10.26	0.002544
997	7.782	10.51	0.00275
1,114	8.058	10.91	0.003163
1,189	8.364	11.33	0.003806
1,279	8.630	11.67	0.004907
1,352	8.981	12.14	0.005847
1,392	9.343	12.59	0.005712
1,438	9.657	13.02	0.005959
1,498	10.040	13.55	0.005668
1,566	10.337	13.99	0.004642
1,652	10.660	14.52	0.003957
1,739	10.937	14.99	0.00358
1,815	11.233	15.48	0.003403
1,917	11.565	16.07	0.003282
2,010	11.886	16.68	0.003243
2,117	12.171	17.24	0.003232
2,206	12.468	17.81	0.003439
2,302	12.797	18.52	0.00346
2,403	13.154	19.31	0.003396
2,494	13.610	20.32	0.001389
Step2 (0. 35% NaCl, constant loading rate control, $dP/dt = 0.044N/s$)			
8,267	14.322	8.14	0
8,387	14.322	8.23	1.712e-05
8,720	14.322	8.49	2.150e-05
9,252	14.322	8.90	1.246e-05
9,740	14.322	9.31	5.606e-05

10,072	14.343	9.60	0.000109
10,608	14.372	10.02	0.000228
10,667	14.455	10.18	0.000285
10,749	14.487	10.25	0.000367
11,061	14.552	10.58	0.000656
11,247	14.673	10.86	0.001096
11,333	14.821	11.08	0.001416
11,452	14.953	11.31	0.00188
11,513	15.103	11.59	0.002118
11,578	15.263	11.85	0.002313
11,667	15.481	12.17	0.002762
11,740	15.688	12.49	0.002901
11,817	15.903	12.89	0.003033
11,871	16.137	13.27	0.003175
11,971	16.419	13.78	0.003363
12,037	16.624	14.18	0.003385
12,127	16.962	14.85	0.003294
12,195	17.230	15.36	0.003362
12,304	17.559	16.12	0.003266
12,390	17.792	16.68	0.003199
12,484	18.124	17.49	0.003146
12,593	18.462	18.42	0.003175
12,710	18.866	19.52	0.003158
12,869	19.330	21.05	0.003148
12,994	19.711	22.40	0.003212
13,132	20.112	24.01	0.003335
13,198	20.423	25.25	0.003404
13,326	20.826	27.12	0.003387
13,410	21.130	28.62	0.00341
13,523	21.545	30.94	0.003386
13,688	21.999	33.83	0.003833
13,823	22.441	37.10	0.004765
13,904	22.958	41.26	0.005734
13,995	23.428	45.78	0.006783
14,050	23.869	50.79	0.007417
14,119	24.441	58.45	0.008212

P=applied load; t=time in second;
a=crack length measured from the line of action of the external load;
K=applied stress intensity factor;
da/dt=crack growth rate.
dP/dt=rate of applied external load

Table A20. Stress Corrosion Experimental Data for Specimen HT-51 (3.5% NaCl, constant loading rate control, $dP/dt = 0.0325N/s$)

$t(s)$	$a(mm)$	$K(MPa\sqrt{m})$	$da/dt(mm/s)$
0	6.282	12.82	0
803	6.295	13.01	0.001002
912	6.353	13.11	0.001283
963	6.437	13.24	0.001414
1,044	6.551	13.43	0.001927
1,085	6.645	13.55	0.002056
1,140	6.766	13.77	0.002242
1,183	6.896	13.95	0.002442
1,273	7.095	14.28	0.002516
1,343	7.289	14.57	0.002479
1,390	7.399	14.74	0.002462
1,465	7.602	15.07	0.002521
1,565	7.813	15.42	0.002541
1,656	8.058	15.82	0.002774
1,717	8.253	16.14	0.002971
1,829	8.528	16.61	0.00346
1,908	8.872	17.20	0.003963
1,988	9.194	17.78	0.004251
2,072	9.556	18.42	0.004336
2,116	9.852	18.94	0.004465
2,190	10.108	19.43	0.004474
2,245	10.307	19.81	0.00442
2,286	10.579	20.35	0.004185
2,351	10.831	20.84	0.004123
2,411	11.088	21.37	0.003724
2,492	11.367	21.95	0.003014
2,570	11.543	22.33	0.002703
2,671	11.700	22.73	0.002613
2,797	12.046	23.52	0.002909
2,862	12.284	24.08	0.003023
2,945	12.570	24.77	0.003131
3,017	12.784	25.31	0.003227
3,094	13.020	25.94	0.003147
3,169	13.232	26.51	0.003149
3,238	13.509	27.26	0.003163

3,356	13.838	28.19	0.003069
3,406	14.027	28.76	0.003014
3,493	14.271	29.51	0.0028
3,667	14.743	31.04	0.00275
3,800	15.028	32.03	0.002718
3,990	15.632	34.23	0.002633
4,068	15.844	35.05	0.002689
4,175	16.099	36.11	0.002726
4,268	16.290	36.93	0.002433
5,029	18.410	48.11	0.003306
5,147	18.794	50.72	0.003748
5,230	19.099	52.90	0.004127
5,305	19.387	55.10	0.004522
5,368	19.733	57.92	0.004918
5,434	20.079	60.95	0.005333
5,504	20.430	64.35	0.005773

P=applied load;
t=time in second;
a=crack length measured from the line of action of the external load;
K=applied stress intensity factor;
da/dt=crack growth rate.
dP/dt=rate of applied external load

Table A21. Stress Corrosion Experimental Data for Specimen HT-52 step2 (3.5% NaCl, constant loading rate control, $dP/dt = 1.000N/s$)

$t(s)$	$a(mm)$	$K(MPa\sqrt{m})$	$da/dt(mm/s)$
9,373	8.191	3.10	0
9,505	8.191	4.15	0
10,095	8.191	8.69	0.000333
10,293	8.191	10.22	0.000556
10,363	8.244	10.84	0.000962
10,405	8.320	11.22	0.001914
10,430	8.409	11.50	0.001975
10,477	8.497	12.01	0.002388
10,527	8.635	12.57	0.002511
10,604	8.802	13.40	0.002674
10,664	8.998	14.16	0.002943
10,767	9.314	15.48	0.003379
10,855	9.573	16.65	0.003439
10,904	9.854	17.53	0.003439
10,976	10.107	18.64	0.003484
11,082	10.403	20.17	0.003268
11,192	10.777	22.01	0.002852
11,294	11.072	23.64	0.002781
11,412	11.339	25.48	0.00265
11,551	11.627	27.63	0.00248
11,646	12.036	29.82	0.002463
11,851	12.405	33.21	0.002638
12,015	12.791	36.43	0.002929
12,197	13.364	40.84	0.003122
12,287	13.730	43.47	0.003215
12,378	14.075	46.27	0.003288
12,506	14.370	49.41	0.00339
12,632	14.847	53.70	0.003491

P=applied load;
t=time in second;
a=crack length measured from the line of action of the external load;
K=applied stress intensity factor;
da/dt=crack growth rate.
dP/dt=rate of applied external load

Table A22. Stress Corrosion Experimental Data for Specimen HT-54 step1 (3.5% NaCl, $dP/dt = 0.05N/s$) and step2 (3.5% NaCl, $dP/dt = 3.00N/s$)

$t(s)$	$a(mm)$	$K(MPa\sqrt{m})$	$da/dt(mm/s)$
Step1 (3.5% NaCl, constant loading rate control, $dP/dt = 0.05N/s$)			
0	6.177	6.33	0
17,456	6.177	11.85	0.000380
18,313	6.217	12.18	0.000418
18,357	6.325	12.35	0.000420
18,412	6.414	12.47	0.001107
18,491	6.606	12.75	0.001549
18,689	6.764	13.04	0.001336
18,774	6.891	13.23	0.001393
18,846	7.022	13.46	0.00153
18,978	7.190	13.76	0.001874
19,054	7.338	13.98	0.002017
19,185	7.671	14.51	0.002309
19,315	7.994	15.02	0.002539
19,451	8.343	15.59	0.002643
19,565	8.677	16.18	0.002841
19,694	8.988	16.73	0.003136
19,834	9.406	17.46	0.003275
19,904	9.761	18.09	0.003224
20,004	10.126	18.77	0.003332
20,148	10.540	19.57	0.003137
20,300	10.944	20.40	0.002829
20,407	11.312	21.18	0.00269
20,604	11.764	22.20	0.002452
Step2 (3.5% NaCl, constant loading rate control, $dP/dt = 3.00N/s$)			
28,165	13.594	7.09	0
28,208	13.594	8.76	0
28,283	13.605	11.58	0.001107
28,317	13.649	12.98	0.001218
28,369	13.771	15.20	0.001657
28,444	13.900	18.36	0.00222
28,510	14.069	21.41	0.002567
28,562	14.185	23.74	0.002836
28,605	14.328	26.01	0.002803

28,662	14.518	28.79	0.002955
28,718	14.714	31.83	0.003043
28,824	14.896	37.19	0.003416
28,881	15.222	41.06	0.003653
28,927	15.322	43.67	0.003433
28,982	15.614	47.70	0.003846
29,038	15.807	51.38	0.003789
29,106	15.928	55.43	0.004325
29,189	16.355	62.42	0.004992
29,248	16.741	68.39	0.005965
29,296	17.015	73.35	0.006706
29,378	17.512	82.75	0.007972
29,425	18.020	90.95	0.008698

P=applied load;
t=time in second;
a=crack length measured from the line of action of the external load;
K=applied stress intensity factor;
da/dt=crack growth rate.
dP/dt=rate of applied external load

Table A23. Stress Corrosion Experimental Data for Specimen HT-55 step1 (3.5% NaCl, $dP/dt = 3.3N/s$), step2 (3.5% NaCl, $dP/dt = 7.1N/s$), step3 (3.5% NaCl, $dP/dt = 7.5N/s$) and step4 (3.5% NaCl, $dP/dt = 0.68N/s$)

$t(s)$	$a(mm)$	$K(MPa\sqrt{m})$	$da/dt(mm/s)$
Step1 (3.5% NaCl, constant loading rate control, $dP/dt = 3.3N/s$)			
0	5.957	11.19	0.00306
12	5.971	11.55	0.002961
39	6.082	12.23	0.002737
76	6.147	13.10	0.002345
109	6.239	13.91	0.001958
160	6.298	15.05	0.002216
186	6.380	15.76	0.002225
236	6.511	16.96	0.002899
301	6.686	18.73	0.003314
342	6.878	19.97	0.003441
388	7.016	21.35	0.003494
443	7.210	23.04	0.002847
481	7.319	24.18	0.002765
568	7.480	26.69	0.003024
611	7.662	28.20	0.002899
665	7.858	30.08	0.003545
Step2 (3.5% NaCl, constant loading rate control, $dP/dt = 7.1N/s$)			
7,379	9.136	11.47	0
7,403	9.176	12.99	0.002819
7,419	9.251	14.06	0.00292
7,439	9.298	15.29	0.003389
7,464	9.381	16.90	0.00366
7,483	9.462	18.28	0.003842
7,501	9.537	19.56	0.00355
7,516	9.585	20.49	0.002938
7,564	9.688	23.77	0.00255
7,604	9.787	26.47	0.002671
7,642	9.920	29.28	0.002906
7,697	10.060	33.35	0.003109
7,732	10.178	36.09	0.003229
7,767	10.299	38.75	0.003216
7,798	10.402	41.30	0.003112

7,838	10.508	44.28	0.002707
	Step3 (3.5% NaCl, constant loading rate control, $dP/dt = 7.5N/s$)		
13,812	11.550	12.64	0.000574
13,825	11.595	14.72	0.002313
13,859	11.671	17.59	0.00248
13,904	11.770	21.42	0.003153
13,923	11.851	23.12	0.00292
13,947	11.938	25.31	0.003019
13,976	11.995	27.78	0.002284
14,020	12.078	31.66	0.001916
14,072	12.168	36.34	0.002518
14,113	12.268	40.12	0.002817
14,143	12.402	43.33	0.002868
14,183	12.498	47.22	0.002667
14,236	12.608	52.22	0.002154
	Step4 (3.5% NaCl, constant loading rate control, $dP/dt = 0.68N/s$)		
16,391	14.784	6.54	0.000133
16,410	14.784	6.73	0.000283
16,719	14.784	9.83	0.002465
16,741	14.895	10.12	0.002841
16,764	14.931	10.44	0.002886
16,788	15.008	10.68	0.002367
16,809	15.055	10.92	0.002625
16,844	15.130	11.39	0.002622
16,877	15.252	11.88	0.003057
16,916	15.338	12.43	0.003239
16,945	15.480	12.95	0.003279
16,985	15.585	13.47	0.003355
17,013	15.691	13.96	0.003055
17,061	15.832	14.73	0.003234
17,102	15.954	15.34	0.003364
17,157	16.160	16.31	0.003373
17,197	16.314	17.07	0.003448
17,243	16.430	17.80	0.003278
17,282	16.591	18.58	0.003195
17,329	16.726	19.57	0.003313
17,378	16.884	20.46	0.003496

17,422	17.035	21.37	0.00344
17,468	17.242	22.55	0.003342
17,572	17.503	24.62	0.003114
17,660	17.797	26.71	0.003434
17,726	18.011	28.35	0.00411
17,767	18.195	29.64	0.003711
17,805	18.392	30.94	0.003837
17,871	18.549	32.58	0.003128
17,939	18.784	34.67	0.002397

P=applied load;
t=time in second;
a=crack length measured from the line of action of the external load;
K=applied stress intensity factor;
da/dt=crack growth rate.
dP/dt=rate of applied external load

Table A24. Stress Corrosion Experimental Data for Specimen HT-45 (3.5% NaCl, constant COD rate control, $d\delta/dt = 1.0e-04 mm/s$)

$t(s)$	$a(mm)$	$K(MPa\sqrt{m})$	$da/dt(mm/s)$
0	5.925	6.97	0
99	5.928	9.97	0.001543
113	6.034	10.64	0.001788
153	6.123	12.06	0.00249
197	6.221	13.63	0.003179
248	6.395	15.44	0.003217
280	6.554	16.39	0.003345
320	6.675	17.69	0.003359
371	6.821	19.36	0.003208
405	6.944	20.50	0.003145
468	7.109	22.37	0.003235
521	7.297	24.06	0.003328
568	7.512	25.69	0.003386
649	7.721	27.91	0.003583
705	7.943	29.54	0.003511
758	8.138	31.09	0.003414
813	8.369	32.54	0.003751
868	8.508	33.88	0.003912
943	8.753	35.64	0.004782
1,012	9.177	37.74	0.00617
1,076	9.494	38.75	0.006831
1,142	10.120	39.54	0.006526
1,164	10.383	39.33	0.006591
1,223	10.642	39.89	0.006205
1,303	11.027	41.56	0.005009
1,369	11.335	42.90	0.004587
1,439	11.675	44.12	0.004432
1,499	11.982	45.14	0.004258
1,606	12.342	46.33	0.003937
1,686	12.652	47.67	0.003916
1,739	12.851	48.43	0.003931
1,808	13.129	49.26	0.003871
1,864	13.379	50.02	0.00381
1,914	13.568	50.71	0.003673
1,986	13.789	50.92	0.003475
2,044	14.008	51.49	0.003316

P=applied load; t=time in second;
a=crack length measured from the line of action of the external load;
K=applied stress intensity factor; da/dt=crack growth rate;
δ =COD=crack opening displacement; $d\delta/dt$ **=COD rate**

Table A25. Stress Corrosion Experimental Data for Specimen HT-48 (3.5% NaCl, constant COD rate control, $d\delta/dt = 2.0e-05 mm/s$)

$t(s)$	$a(mm)$	$K(MPa\sqrt{m})$	$da/dt(mm/s)$
0	6.006	12.06	0.005242
35	6.224	12.27	0.004765
66	6.358	12.60	0.004343
110	6.524	12.91	0.003744
148	6.658	13.39	0.003107
216	6.818	13.64	0.002723
303	7.003	14.14	0.002687
369	7.205	14.46	0.002732
428	7.373	14.91	0.002799
487	7.564	15.17	0.002931
556	7.738	15.50	0.003044
642	7.987	15.87	0.003369
721	8.246	16.19	0.003859
788	8.561	16.56	0.004164
855	8.835	16.73	0.00414
890	9.031	16.74	0.004427
948	9.255	16.99	0.004648
1,012	9.467	17.13	0.004959
1,055	9.785	17.41	0.004905
1,109	10.098	17.71	0.00487
1,166	10.377	17.80	0.004671
1,226	10.604	18.05	0.003942
1,290	10.813	18.05	0.00353
1,375	11.081	18.38	0.003206
1,452	11.297	18.51	0.003004
1,500	11.537	18.60	0.00296
1,609	11.774	18.85	0.002794
1,706	12.011	18.93	0.002805
1,792	12.280	19.03	0.002879
1,887	12.514	19.18	0.003035
1,986	12.883	19.47	0.003173
2,063	13.136	19.68	0.003192
2,171	13.450	19.70	0.003126
2,234	13.680	19.72	0.003041
2,310	13.902	19.77	0.003045

2,407	14.166	19.92	0.00300
2,477	14.380	19.81	0.002785
2,541	14.610	20.06	0.002785
2,633	14.845	20.06	0.002817
2,739	15.033	19.91	0.002884
2,812	15.313	19.98	0.002925
2,891	15.602	20.17	0.002961
2,999	15.909	20.30	0.00307
3,073	16.131	20.32	0.00304
3,197	16.430	19.95	0.003183
3,261	16.695	19.91	0.003136
3,317	16.907	20.04	0.003242
3,403	17.180	20.15	0.003362
3,528	17.537	19.96	0.003038
3,598	17.838	18.18	0.002886
3,678	18.026	19.73	0.002712
3,771	18.244	19.56	0.002511

P=applied load;
t=time in second;
a=crack length measured from the line of action of the external load;
K=applied stress intensity factor;
da/dt=crack growth rate;
δ =COD=crack opening displacement
$d\delta / dt$ =COD rate

Table A26. Stress Corrosion Experimental Data for Specimen HT-49 (3.5% NaCl, constant COD rate control, $d\delta/dt = 2.0e-04mm/s$)

$t(s)$	$a(mm)$	$K(MPa\sqrt{m})$	$da/dt(mm/s)$
0	6.411	9.19	0.000747
46	6.450	12.91	0.001405
84	6.531	16.19	0.001948
128	6.618	19.91	0.002368
164	6.724	22.82	0.002404
212	6.842	27.14	0.002392
264	6.952	31.20	0.002263
312	7.056	35.18	0.002247
352	7.156	38.75	0.002222
405	7.272	42.86	0.002098
455	7.368	46.58	0.002126
525	7.493	51.73	0.002376
555	7.611	53.94	0.002483

P=applied load;
t=time in second;
a=crack length measured from the line of action of the external load;
K=applied stress intensity factor;
da/dt=crack growth rate;
δ =COD=crack opening displacement
$d\delta/dt$ =COD rate

Table A27. Stress Corrosion Experimental Data for Specimen HT-50 (3.5% NaCl, constant COD rate control, $d\delta/dt = 1.0e-05 mm/s$)

$t(s)$	$a(mm)$	$K(MPa\sqrt{m})$	$da/dt(mm/s)$
0	6.321	11.49	0.000410
9	6.350	11.55	0.000426
119	6.375	12.00	0.000627
199	6.429	12.42	0.000773
243	6.524	12.72	0.000822
366	6.584	13.09	0.001103
434	6.685	13.50	0.001338
533	6.791	13.68	0.001906
600	6.926	13.93	0.002326
658	7.091	13.96	0.002525
709	7.265	14.03	0.002793
775	7.450	14.15	0.002927
853	7.662	14.26	0.002906
920	7.854	14.32	0.002915
992	8.084	14.36	0.002977
1,071	8.300	14.49	0.002994
1,130	8.496	14.46	0.003072
1,193	8.687	14.62	0.003069
1,265	8.887	14.58	0.003121
1,311	9.072	14.65	0.003225
1,396	9.311	14.56	0.003582
1,455	9.505	14.66	0.003680
1,522	9.807	14.68	0.003635
1,580	10.079	14.76	0.003758
1,650	10.284	14.87	0.003647
1,740	10.567	14.79	0.003292
1,788	10.770	14.92	0.003097
1,852	10.987	14.82	0.003151
1,923	11.146	14.73	0.003127
2,010	11.373	14.59	0.003311
2,059	11.621	14.76	0.003281
2,133	11.844	14.70	0.003413
2,189	12.088	14.63	0.003366
2,272	12.308	14.49	0.003236
2,331	12.512	14.55	0.003310

2,392	12.650	14.31	0.003226
2,456	12.940	14.54	0.003314
2,522	13.168	14.38	0.003303
2,588	13.332	14.33	0.003360
2,654	13.564	14.26	0.003294
2,726	13.796	14.12	0.003375
2,805	14.082	14.06	0.003478
2,878	14.356	14.02	0.003512
2,952	14.597	14.09	0.003412
3,018	14.819	14.01	0.003350
3,077	15.050	14.10	0.003376
3,156	15.255	13.96	0.003315
3,214	15.469	13.98	0.003265
3,272	15.708	13.96	0.003197
3,344	15.884	13.71	0.003156
3,401	16.075	13.92	0.003124
3,457	16.244	13.89	0.003093

P=applied load;
t=time in second;
a=crack length measured from the line of action of the external load;
K=applied stress intensity factor;
da/dt=crack growth rate;
δ =COD=crack opening displacement
$d\delta / dt$ =COD rate

APPENDIX B EXPERIMENTAL CRACK GROWTH DATA FOR STRESS CORROSION CRACKING OF 7075T651

Table B1. Stress Corrosion Experimental Data for Specimen SL51 (3.5% NaCl, $K_i = 5.8 MPa\sqrt{m}$)

$t(s)$	$a(mm)$	$K(MPa\sqrt{m})$	$da/dt(mm/s)$
326,796	14.075	5.80	7.23e-07
350,629	14.095	5.81	8.16e-07
390,656	14.095	5.81	9.73e-07
425,045	14.135	5.82	1.11e-06
464,897	14.255	5.86	1.33e-06
496,586	14.255	5.86	1.26e-06
518,750	14.256	5.86	1.14e-06
554,091	14.347	5.89	7.40e-07
591,187	14.347	5.82	6.19e-07
605,702	14.363	5.83	5.70e-07
666,101	14.363	5.83	9.51e-08
688,888	14.366	5.83	1.15e-07
738,251	14.368	5.83	1.35e-07
755,806	14.368	5.83	1.42e-07
821,488	14.385	5.83	1.67e-07
924,246	14.958	5.96	7.33e-07
983,377	14.992	5.89	4.76e-07
1.03e+06	15.014	5.90	2.92e-07
1.07e+06	15.015	5.90	1.41e-07
1.21e+06	18.978	7.38	9.89e-07
1.25e+06	19.016	7.40	1.67e-06
1.28e+06	19.108	7.44	2.00e-06
1.30e+06	19.120	7.45	2.35e-06
1.35e+06	19.249	7.31	1.24e-06
1.46e+06	24.403	10.50	1.50e-05
1.50e+06	25.030	10.91	1.53e-05
1.59e+06	26.400	12.10	1.58e-05
1.63e+06	27.212	13.04	1.61e-05
1.68e+06	27.824	13.26	1.63e-05

K_i=Initial stress intensity factor at the start of the test; t=time in second;
a=crack length measured from the line of action of the external load;

K=applied stress intensity factor; da/dt=crack growth rate.

Table B2. Stress Corrosion Experimental Data for Specimen SL76 (3.5% NaCl, $K_i = 6.8 MPa\sqrt{m}$)

$t(s)$	$a(mm)$	$K(MPa\sqrt{m})$	$da/dt(mm/s)$
300,270	14.047	6.45	2.09e-05
347,534	15.060	6.76	2.20e-05
387,137	15.947	6.95	2.28e-05
387,137	15.947	6.95	1.49e-06
434,284	16.001	6.98	8.05e-07
471,677	16.021	6.65	2.65e-07
650,782	16.189	6.55	2.11e-06
695,479	16.296	6.51	1.43e-06
735,932	16.318	6.27	8.19e-07
778,062	16.329	6.19	3.10e-07
820,405	16.345	5.85	1.98e-07
864,190	16.347	5.86	1.00e-07
905,104	16.351	5.60	2.49e-06
953,537	16.513	5.66	2.27e-06
1.08e+06	16.714	5.21	1.69e-06
1.13e+06	16.803	5.24	1.47e-06
1.17e+06	16.871	5.26	1.29e-06
1.21e+06	17.224	5.37	1.01e-06
1.25e+06	17.253	5.29	5.20e-07
1.30e+06	17.263	5.20	4.68e-07
1.35e+06	17.298	4.86	9.89e-07
3.78e+06	32.492	1.83	6.24e-06
4.19e+06	37.622	3.81	1.24e-05

K_i=Initial stress intensity factor at the start of the test;
t=time in second;
a=crack length measured from the line of action of the external load;
K=applied stress intensity factor;
da/dt=crack growth rate.

Table B3. Stress Corrosion Experimental Data for Specimen SL39 (3.5% NaCl, $K_i = 8MPa\sqrt{m}$)

$t(s)$	$a(mm)$	$K(MPa\sqrt{m})$	$da/dt(mm/s)$
120,731	14.21	8.04	1.78e-06
143,741	14.24	8.06	1.75e-06
162,208	14.32	8.10	1.72e-06
173,210	14.32	8.10	1.71e-06
208,459	14.35	8.03	1.52e-06
237,546	14.39	8.05	1.26e-06
259,860	14.47	8.09	1.20e-06
294,231	14.47	8.09	1.42e-06
326,750	14.51	8.11	2.10e-06
345,308	14.51	8.03	2.06e-06
384,205	14.64	8.09	2.90e-06
413,423	14.82	8.18	3.38e-06
499,961	15.05	8.21	3.98e-06
516,722	15.13	8.25	4.16e-06
556,275	15.22	8.21	4.22e-06
595,093	15.53	8.36	4.81e-06
640,035	15.73	8.54	5.36e-06
663,015	15.75	8.72	5.70e-06
784,155	16.55	8.96	1.24e-05
808,541	16.81	9.01	1.43e-05
837,712	17.35	9.31	1.69e-05
1.02e+06	21.64	11.62	2.76e-05
1.03e+06	22.71	12.53	2.29e-05
1.07e+06	23.67	13.18	1.96e-05
1.12e+06	24.65	13.93	1.52e-05
1.17e+06	24.90	13.75	9.03e-06
1.18e+06	24.90	13.14	6.65e-06
1.21e+06	25.20	12.84	7.51e-06
1.25e+06	25.34	12.83	1.17e-05
1.27e+06	25.37	12.70	1.41e-05
1.31e+06	26.52	12.80	1.81e-05

K_i=Initial stress intensity factor at the start of the test;
t=time in second;
a=crack length measured from the line of action of the external load;
K=applied stress intensity factor;
da/dt=crack growth rate.

Table B4. Stress Corrosion Experimental Data for Specimen SL33 (3.5% NaCl, $K_i = 9.8MPa\sqrt{m}$)

$t(s)$	$a(mm)$	$K(MPa\sqrt{m})$	$da/dt(mm/s)$
141,655	14.120	9.88	3.02e-06
149,314	14.130	9.88	2.80e-06
169,863	14.210	9.93	2.21e-06
207,152	14.240	9.87	1.36e-06
234,480	14.280	9.82	8.52e-07
257,629	14.300	9.83	7.60e-07
487,826	15.010	9.39	1.00e-05
505,933	15.120	9.37	9.52e-06
515,594	15.370	9.43	9.25e-06
690,825	16.440	9.27	4.88e-06
721,561	16.620	9.12	4.44e-06
755,511	16.740	9.09	3.51e-06
775,103	16.810	9.04	2.79e-06
811,694	16.890	8.83	1.13e-05
861,157	17.500	8.88	9.63e-06
898,657	17.870	8.90	8.37e-06
946,824	18.080	8.73	6.76e-06
987,351	18.350	8.59	5.94e-06
1.01e+06	18.490	8.38	5.35e-06
1.03e+06	18.670	8.47	5.27e-06
1.07e+06	18.820	8.25	4.01e-06
1.10e+06	18.910	8.10	3.08e-06
1.12e+06	18.990	8.04	2.38e-06
1.19e+06	20.110	7.90	3.63e-05
1.21e+06	20.910	8.31	2.76e-05
1.24e+06	21.610	8.25	1.42e-05
1.51e+06	22.740	6.90	1.86e-06
1.54e+06	22.850	6.70	2.42e-06
1.56e+06	22.860	6.58	2.84e-06
1.62e+06	23.080	6.17	4.05e-06
1.64e+06	23.200	6.09	4.37e-06
1.68e+06	23.330	5.49	5.13e-06
1.72e+06	23.580	5.05	5.85e-06

K_i=Initial stress intensity factor at the start of the test;
t=time in second;
a=crack length measured from the line of action of the external load;
K=applied stress intensity factor;
da/dt=crack growth rate.

Table B5. Stress Corrosion Experimental Data for Specimen SL41 (3.5% NaCl, $K_i = 10MPa\sqrt{m}$)

$t(s)$	$a(mm)$	$K(MPa\sqrt{m})$	$da/dt(mm/s)$
129,976	14.19	9.85	6.82e-08
164,189	14.19	9.85	1.99e-07
196,848	14.19	9.85	3.29e-07
220,180	14.21	9.86	5.02e-07
260,166	14.23	9.87	8.00e-07
294,905	14.23	9.87	8.58e-06
334,467	14.89	10.26	1.00e-05
366,093	14.96	10.30	1.12e-05
388,251	15.19	10.44	1.20e-05
423,650	15.78	10.80	1.38e-05
460,757	16.12	10.94	1.63e-05
475,213	16.58	11.15	1.63e-05
535,601	17.84	11.93	1.44e-05
558,307	17.93	11.99	1.37e-05
607,715	18.45	12.28	1.19e-05
625,367	18.64	12.33	9.10e-06
691,131	19.05	12.55	1.22e-05
793,178	20.67	12.93	1.69e-05
853,062	21.81	12.90	1.97e-05

K_i=Initial stress intensity factor at the start of the test;
t=time in second;
a=crack length measured from the line of action of the external load;
K=applied stress intensity factor;
da/dt=crack growth rate.

Table B6. Stress Corrosion Experimental Data for Specimen SL37 (3.5% NaCl, $K_i = 12.2 MPa\sqrt{m}$)

$t(s)$	$a(mm)$	$K(MPa\sqrt{m})$	$da/dt(mm/s)$
76,133	14.365	12.21	4.01e-06
98,260	14.445	12.19	3.48e-06
135,022	14.605	12.23	2.59e-06
182,786	14.625	12.24	1.93e-06
239,132	14.715	12.23	2.97e-06
258,893	14.815	12.30	3.65e-06
270,380	14.835	12.24	4.04e-06
335,222	15.465	12.70	7.37e-06
356,589	15.645	12.75	1.27e-05
392,067	16.275	13.14	2.12e-05
423,336	17.065	13.68	2.86e-05
441,511	17.595	14.03	3.30e-05
480,739	17.805	14.12	1.01e-05
510,234	18.105	14.19	1.03e-05
532,442	18.335	14.39	1.04e-05
596,419	21.405	17.05	9.29e-06
613,124	21.595	17.15	1.35e-05
654,059	22.355	17.71	1.76e-05
691,600	22.985	18.01	1.59e-05
736,800	25.905	21.72	2.10e-05
760,393	26.775	22.92	5.27e-05
785,529	28.525	25.66	8.65e-05

K_i=Initial stress intensity factor at the start of the test;
t=time in second;
a=crack length measured from the line of action of the external load;
K=applied stress intensity factor;
da/dt=crack growth rate.

Table B7. Stress Corrosion Experimental Data for Specimen SL77 (3.5% NaCl, $K_i = 16MPa\sqrt{m}$)

$t(s)$	$a(mm)$	$K(MPa\sqrt{m})$	$da/dt(mm/s)$
19,957	14.161	15.9539	3.69e-07
52,927	14.221	15.8637	3.10e-06
66,520	14.246	15.8868	4.34e-06
87,302	14.374	15.9321	4.95e-06
95,625	14.427	16.0553	4.04e-06
106,839	14.456	16.0824	1.69e-06
138,148	14.468	16.0196	2.30e-06
171,319	14.612	16.1545	3.23e-06
193,361	14.678	16.2167	3.87e-06
225,954	14.804	16.185	3.98e-06
324,714	15.233	16.5946	3.72e-06
406,665	15.583	16.8578	5.62e-06
507,692	15.677	16.8711	9.10e-06
604,391	17.363	18.3717	1.24e-05

K_i=Initial stress intensity factor at the start of the test;
t=time in second;
a=crack length measured from the line of action of the external load;
K=applied stress intensity factor;
da/dt=crack growth rate.

Table B8. Stress Corrosion Experimental Data for Specimen SL49 (3.5% NaCl, 25% overload, $K_i = 10MPa\sqrt{m}$)

$t(s)$	$a(mm)$	$K(MPa\sqrt{m})$	$da/dt(mm/s)$
175,226	14.020	9.91	2.12e-06
206,799	14.080	9.94	1.68e-06
233,600	14.120	9.98	1.31e-06
293,508	14.120	9.97	7.51e-06
322,180	14.310	10.01	6.11e-06
350,457	14.540	10.22	4.72e-06
380,892	14.570	10.16	3.24e-06
405,743	14.650	10.20	2.41e-06
431,701	14.690	10.23	1.62e-06
466,131	14.710	10.24	1.47e-06
498,351	14.780	10.28	1.24e-06
518,347	14.810	10.22	1.22e-06
576,823	14.850	10.25	1.19e-06
643,266	14.940	10.22	1.16e-06
672,600	14.980	10.24	1.14e-06
757,719	15.220	10.39	8.71e-06
780,007	15.370	10.40	8.37e-06
814,182	15.610	10.55	7.85e-06
846,851	15.880	10.63	7.34e-06
870,206	16.190	10.83	7.46e-06
910,216	16.290	10.81	7.70e-06
944,756	16.560	10.90	8.17e-06
984,496	16.920	11.13	8.71e-06
1.02e+06	17.277	11.19	9.14e-06
1.02e+06	17.277	11.19	3.76e-05
1.04e+06	17.988	11.68	3.68e-05
1.07e+06	19.541	12.55	3.55e-05
1.11e+06	20.532	13.05	3.41e-05
1.19e+06	23.118	14.58	3.13e-05

K_i=Initial stress intensity factor at the start of the test;
t=time in second;
a=crack length measured from the line of action of the external load;
K=applied stress intensity factor;
da/dt=crack growth rate.

Table B9. Stress Corrosion Experimental Data for Specimen SL45 (3.5% NaCl, Step 1: 50% overload, $K_i = 10MPa\sqrt{m}$, $K_f = 15.34MPa\sqrt{m}$; Step 2: $K_i = 8.27MPa\sqrt{m}$)

$t(s)$	$a(mm)$	$K(MPa\sqrt{m})$	$da/dt(mm/s)$
Step 1: 50% overload, $K_i = 10MPa\sqrt{m}$, $K_f = 15.34MPa\sqrt{m}$			
457,877	14.57	10.25	4.60e-06
498,797	14.73	10.34	4.63e-06
522,318	14.90	10.52	4.65e-06
546,675	14.96	10.41	4.92e-06
585,332	15.16	10.53	4.36e-06
608,528	15.30	10.62	4.61e-06
646,961	15.41	10.69	4.05e-06
670,720	15.55	10.77	1.19e-05
698,607	16.23	11.13	1.53e-05
724,025	16.45	11.36	1.84e-05
761,356	17.00	11.73	2.03e-05
782,237	17.88	12.37	1.95e-05
808,424	18.18	12.51	1.90e-05
843,942	18.67	12.79	1.70e-05
880,303	19.18	13.11	1.52e-05
892,353	19.78	13.62	1.46e-05
932,964	20.02	13.73	1.28e-05
1.02e+06	20.32	13.89	1.19e-05
1.04e+06	20.63	14.18	1.51e-05
1.10e+06	21.50	14.69	1.77e-05
1.13e+06	22.01	15.34	2.07e-05
Step 2: $K_i = 8.27MPa\sqrt{m}$			
1154,539	22.01	8.27	0
1189,192	22.01	8.15	0
1218,047	22.01	8.15	0
1240,496	22.01	8.15	0
1274,718	22.01	8.15	0
1307,652	22.01	8.03	0
1325,497	22.01	8.03	0
1364,463	22.01	8.03	0
1394,454	22.01	8.03	0
1414,312	22.01	8.03	0

1450,481	22.01	7.91	0
1478,418	22.01	7.80	0
1498,930	22.01	7.80	0
1540,605	22.01	7.80	0
1566,354	22.01	7.68	0
1.63e+06	22.65	8.04	6.67e-07
1.66e+06	22.67	8.04	1.37e-06
1.67e+06	22.69	8.06	1.93e-06
1.67e+06	22.69	8.04	1.23e-05
1.71e+06	23.11	8.31	1.09e-05
1.73e+06	23.37	8.08	1.00e-05
1.76e+06	23.66	8.13	8.83e-06
1.85e+06	24.25	6.82	7.14e-06
1.94e+06	24.83	7.60	8.10e-06
1.97e+06	25.10	7.62	8.26e-06
1.99e+06	25.40	7.66	7.24e-06
2.02e+06	25.51	7.12	4.60e-06
2.05e+06	25.61	7.02	1.24e-06

K_i=Initial stress intensity factor at the start of the test;
K_f=Final stress intensity factor at the end of the current step loading;
t=time in second; a=crack length measured from the line of action of the external load;
K=applied stress intensity factor; da/dt=crack growth rate

Table B10. Stress Corrosion Experimental Data for Specimen SL50 (3.5% NaCl, 75% overload, $K_i = 10MPa\sqrt{m}$)

$t(s)$	$a(mm)$	$K(MPa\sqrt{m})$	$da/dt(mm/s)$
349,127	14.265	9.80	1.75e-05
372,476	14.695	10.05	1.51e-05
412,423	15.005	10.23	1.10e-05
447,404	15.655	10.63	6.85e-06
486,805	15.655	10.63	1.92e-06
710,694	15.665	10.64	1.62e-05
759,953	16.460	11.15	1.30e-05
777,587	16.704	11.23	1.18e-05
945,005	17.608	11.76	2.86e-06
1.28e+06	27.253	22.65	2.06e-05
1.30e+06	27.494	23.18	1.10e-05

K_i=Initial stress intensity factor at the start of the test;
t=time in second;
a=crack length measured from the line of action of the external load;
K=applied stress intensity factor;
da/dt=crack growth rate.

Table B11. Stress Corrosion Experimental Data for Specimen SL47 (3.5% NaCl, 100% overload, $K_i = 10MPa\sqrt{m}$)

$t(s)$	$a(mm)$	$K(MPa\sqrt{m})$	$da/dt(mm/s)$
893,934	14.175	9.57	9.18e-06
932,265	14.475	9.67	6.48e-06
957,296	14.615	9.75	4.71e-06
984,455	15.645	10.35	2.60e-05
1.02e+06	16.435	10.67	1.85e-05
1.04e+06	16.805	10.91	2.12e-05
1.07e+06	17.405	10.86	3.13e-05

K_i=Initial stress intensity factor at the start of the test;
t=time in second;
a=crack length measured from the line of action of the external load;
K=applied stress intensity factor;
da/dt=crack growth rate.

Table B12. Stress Corrosion Experimental Data for Specimen SL46 (3.5% NaCl, 125% overload, $K_i = 10MPa\sqrt{m}$)

$t(s)$	$a(mm)$	$K(MPa\sqrt{m})$	$da/dt(mm/s)$
929,309	17.10	9.71	6.76e-06
974,999	17.46	9.75	9.00e-06
1.01e+06	17.83	9.78	1.08e-05
1.04e+06	18.83	10.30	1.37e-05
1.06e+06	19.22	10.46	1.11e-05
1.10e+06	19.46	10.41	7.37e-06
1.13e+06	19.63	10.32	4.25e-06
1.15e+06	19.74	10.18	1.85e-06
1.15e+06	19.74	10.18	2.52e-05
1.18e+06	20.69	10.39	2.75e-05
1.22e+06	21.62	10.48	2.98e-05
1.23e+06	22.09	10.47	2.73e-05
1.27e+06	23.42	10.46	3.63e-05
1.30e+06	23.55	9.49	5.17e-05
1.32e+06	25.86	4.28	6.18e-05

K_i=Initial stress intensity factor at the start of the test;
t=time in second;
a=crack length measured from the line of action of the external load;
K=applied stress intensity factor;
da/dt=crack growth rate.

Table B13. Stress Corrosion Experimental Data for Specimen SL44 (3.5% NaCl, 50% underload, $K_i = 10MPa\sqrt{m}$)

$t(s)$	$a(mm)$	$K(MPa\sqrt{m})$	$da/dt(mm/s)$
187,050	14.19	9.78	3.78e-06
193,437	14.28	9.83	3.54e-06
199,860	14.28	9.83	3.31e-06
232,724	14.34	9.86	1.97e-06
263,310	14.41	9.90	1.72e-06
282,881	14.46	9.93	1.91e-06
319,170	14.48	9.94	1.68e-06
346,926	14.58	10.00	1.22e-06
367,970	14.58	10.00	1.69e-06
410,122	14.60	9.94	2.14e-06
435,290	14.74	10.02	2.41e-06
496,101	14.77	10.03	5.40e-05
528,671	16.13	10.87	2.95e-05
541,166	16.44	11.07	2.01e-05
579,534	16.71	11.16	2.44e-05
603,359	17.14	11.45	2.26e-05
632,674	17.81	11.92	2.03e-05
664,199	18.57	12.39	1.79e-05
690,853	18.84	12.51	1.59e-05
838,514	23.91	17.17	2.34e-05
863,105	24.46	17.79	2.14e-05
923,524	25.61	19.24	1.63e-05
955,443	26.06	19.51	1.39e-05
975,782	26.35	19.85	1.24e-05
1.01e+06	26.74	20.04	9.62e-06
1.03e+06	29.76	26.52	1.13e-05
1.06e+06	30.24	26.77	1.89e-05

K_i=Initial stress intensity factor at the start of the test;
t=time in second;
a=crack length measured from the line of action of the external load;
K=applied stress intensity factor;
da/dt=crack growth rate.

Table B14. Stress Corrosion Experimental Data for Specimen SL48 (3.5% NaCl, Step 1: 100% underload, $K_i = 10MPa\sqrt{m}$, $K_f = 12.27MPa\sqrt{m}$; Step 2: $K_i = 10.7MPa\sqrt{m}$)

$t(s)$	$a(mm)$	$K(MPa\sqrt{m})$	$da/dt(mm/s)$
Step 1: 100% underload, $K_i = 10MPa\sqrt{m}$, $K_f = 12.27MPa\sqrt{m}$			
95,318	14.205	9.61	4.02e-06
112,227	14.305	9.66	3.42e-06
122,710	14.345	9.69	3.05e-06
180,401	14.405	9.72	1.88e-06
204,214	14.475	9.76	2.03e-06
242,435	14.555	9.88	2.17e-06
267,461	14.615	9.92	1.81e-06
291,649	14.655	9.86	1.71e-06
326,462	14.695	9.81	1.53e-06
355,845	14.755	9.84	9.05e-06
377,983	15.155	10.08	1.24e-05
412,241	15.595	10.34	1.77e-05
445,510	16.085	10.56	1.58e-05
462,678	16.765	10.99	1.66e-05
501,918	17.005	11.15	1.53e-05
532,272	17.495	11.48	1.30e-05
551,898	17.945	11.70	1.36e-05
588,303	18.245	11.91	1.26e-05
614,919	18.395	11.93	1.38e-05
636,062	18.975	12.27	1.48e-05
Step 2: $K_i = 10.7MPa\sqrt{m}$			
679,244	20.765	10.69	0
703,797	20.765	10.69	0
726,397	20.765	10.69	0
765,160	20.765	10.69	0
797,369	20.765	10.69	6.81e-06
810,202	20.865	10.76	8.78e-06
848,568	21.315	11.09	1.33e-05
872,471	21.655	11.24	1.52e-05
933,629	22.615	11.90	1.29e-05
959,977	23.005	12.24	1.34e-05

983,321	23.345	12.55	1.38e-05
1.02e+06	23.735	12.92	1.17e-05
1.05e+06	24.265	13.32	9.11e-06
1.08e+06	24.305	13.22	8.61e-06
1.11e+06	24.485	13.41	2.01e-05
1.13e+06	24.855	13.52	3.55e-05
1.16e+06	26.345	15.00	5.13e-05

K_i=Initial stress intensity factor at the start of the test;
K_f=Final stress intensity factor at the end of the current step loading;
t=time in second; a=crack length measured from the line of action of the external load;
K=applied stress intensity factor; da/dt=crack growth rate

Table B15. Stress Corrosion Experimental Data for Specimen SL66 (5.0% NaCl, $K_i = 10MPa\sqrt{m}$)

$t(s)$	$a(mm)$	$K(MPa\sqrt{m})$	$da/dt(mm/s)$
211216	14.437	10.0297	1.00e-06
256917	14.437	10.0297	1.10e-06
297193	14.52	10.0037	5.57e-06
341891	14.943	10.2528	1.00e-05
381988	15.365	10.5076	1.10e-05
514493	15.369	10.5101	1.49e-05
596213	16.602	11.2118	1.53e-05
639168	17.261	11.6577	1.54e-05
688747	20.366	14.0221	1.57e-05
727494	21.033	14.5408	2.08e-05
773544	22.466	16.049	2.69e-05
813286	23.06	16.7522	2.86e-05
861259	25.145	19.5394	2.97e-05
896422	25.744	20.5421	3.23e-05
987797	28.831	27.243	2.83e-05
1.03e+06	29.757	29.8604	2.79e-05

K_i=Initial stress intensity factor at the start of the test;
t=time in second;
a=crack length measured from the line of action of the external load;
K=applied stress intensity factor;
da/dt=crack growth rate.

Table B16. Stress Corrosion Experimental Data for Specimen SL65 (3.0% NaCl, $K_i = 10MPa\sqrt{m}$)

$t(s)$	$a(mm)$	$K(MPa\sqrt{m})$	$da/dt(mm/s)$
147,472	14.223	10.08	2.24e-06
197,103	14.288	10.19	3.16e-06
233,518	14.678	10.42	3.20e-06
289,885	14.686	10.43	1.72e-06
321,955	14.726	10.53	4.81e-07
371,124	14.731	10.53	8.19e-07
407,711	14.761	10.47	1.13e-06
450,955	14.834	10.52	1.49e-06
536,025	16.869	11.85	1.27e-05
582,315	17.337	12.19	7.49e-06
752,836	20.126	14.28	8.74e-06
796,303	20.737	14.98	1.12e-05
884,617	23.285	17.78	2.26e-05
927,914	24.550	19.46	1.81e-05
966,547	24.767	19.81	1.42e-05
1.01e+06	25.335	20.76	9.59e-06
1.06e+06	25.832	21.49	9.37e-06
1.10e+06	26.076	21.62	9.20e-06

K_i=Initial stress intensity factor at the start of the test;
t=time in second;
a=crack length measured from the line of action of the external load;
K=applied stress intensity factor;
da/dt=crack growth rate.

Table B17. Stress Corrosion Experimental Data for Specimen SL64 (2.0% NaCl, $K_i = 10MPa\sqrt{m}$)

$t(s)$	$a(mm)$	$K(MPa\sqrt{m})$	$da/dt(mm/s)$
87,476	14.328	9.93	1.62e-06
129,368	14.392	9.89	2.47e-06
168,000	14.514	10.04	3.25e-06
213,090	14.700	9.92	3.90e-06
262,124	14.906	10.27	3.24e-06
297,201	15.032	10.34	2.65e-06
344,699	15.087	10.30	2.10e-06
383,860	15.160	10.35	2.20e-06
435,218	15.299	10.35	3.03e-06
470,380	15.411	10.42	2.33e-05
519,819	16.764	11.28	2.97e-05
557,444	17.510	11.70	3.45e-05
598,893	19.250	13.01	3.99e-05
648,213	21.562	15.03	4.26e-05
690,634	24.189	18.20	4.08e-05
731,069	25.401	19.76	3.55e-05
752,349	25.807	20.30	3.26e-05
776,598	26.783	22.12	2.67e-05
817,738	27.874	24.33	2.32e-05
866,307	28.771	25.58	1.91e-05
903,583	29.377	26.61	1.60e-05

K_i=Initial stress intensity factor at the start of the test;
t=time in second;
a=crack length measured from the line of action of the external load;
K=applied stress intensity factor;
da/dt=crack growth rate.

Table B18. Stress Corrosion Experimental Data for Specimen SL62 (1.0% NaCl, $K_i = 10MPa\sqrt{m}$)

$t(s)$	$a(mm)$	$K(MPa\sqrt{m})$	$da/dt(mm/s)$
127,161	14.118	9.95	1.43e-06
176,928	14.172	10.06	1.16e-06
227,646	14.233	10.02	8.78e-07
268,606	14.266	10.11	1.15e-06
324,655	14.288	10.05	1.55e-06
351,616	14.405	10.20	1.75e-06
406,531	14.464	10.38	1.17e-05
435,585	14.730	10.47	1.77e-05
468,025	15.428	10.59	2.44e-05
513,395	16.596	11.60	3.38e-05
557,921	18.394	12.74	4.30e-05
605,100	21.414	15.26	4.21e-05
637,832	22.171	15.96	4.26e-05
668,660	24.431	18.63	3.91e-05
722,649	25.316	19.58	3.30e-05
743,889	26.647	21.31	3.07e-05

K_i=Initial stress intensity factor at the start of the test; t=time in second;
a=crack length measured from the line of action of the external load;
K=applied stress intensity factor; da/dt=crack growth rate.

Table B19. Stress Corrosion Experimental Data for Specimen SL79 (1% NaCl, $K_i = 15MPa\sqrt{m}$)

$t(s)$	$a(mm)$	$K(MPa\sqrt{m})$	$da/dt(mm/s)$
60,885	14.154	14.61	6.10e-06
98,867	14.520	15.00	1.01e-05
109,299	14.697	15.15	9.88e-06
143,931	15.061	15.09	7.79e-06
177,054	15.168	15.42	4.06e-06
240,443	15.238	15.56	4.40e-06
230,174	15.334	15.25	4.00e-06
263,883	15.491	15.71	6.57e-06
278,019	15.542	15.76	7.65e-06

K_i=Initial stress intensity factor at the start of the test; t=time in second;
a=crack length measured from the line of action of the external load;
K=applied stress intensity factor;
da/dt=crack growth rate.

Table B20. Stress Corrosion Experimental Data for Specimen SL102 (0.35% NaCl, $K_i = 6MPa\sqrt{m}$)

$t(s)$	$a(mm)$	$K(MPa\sqrt{m})$	$da/dt(mm/s)$
511,562	13.909	5.72	8.21e-06
557,522	13.956	5.88	9.71e-06
593,829	14.992	6.17	1.17e-05
641,323	15.070	6.20	1.56e-05
815,640	18.776	7.64	2.37e-05
862,412	19.954	8.24	1.97e-05
880,988	20.026	8.17	2.10e-05
902,299	20.550	8.46	1.86e-05
941,374	21.485	8.89	1.87e-05
962,016	21.666	8.89	3.44e-05
980,813	22.072	9.02	3.99e-05
1.02981e+06	25.477	11.59	6.11e-05
1.06713e+06	27.709	13.25	6.62e-05
1.11558e+06	30.898	17.47	7.93e-05
1.13024e+06	32.102	19.15	8.46e-05
1.14679e+06	33.742	21.52	9.06e-05

K_i=Initial stress intensity factor at the start of the test;
t=time in second;
a=crack length measured from the line of action of the external load;
K=applied stress intensity factor;
da/dt=crack growth rate.

Table B21. Stress Corrosion Experimental Data for Specimen SL99 (0.35% NaCl, $K_i = 8MPa\sqrt{m}$)

$t(s)$	$a(mm)$	$K(MPa\sqrt{m})$	$da/dt(mm/s)$
44,810	14.312	8.11	3.15e-07
82,570	14.347	8.20	1.03e-06
100,849	14.341	8.19	1.37e-06
118,005	14.376	8.36	1.48e-06
132,420	14.418	8.36	1.68e-06
169,777	14.496	8.42	1.8e-06
189,919	14.508	8.42	1.63e-06
210,999	14.537	8.44	1.41e-06
260,019	14.628	8.48	1.19e-06
277,839	14.628	8.48	1.52e-06
300,906	14.642	8.49	1.63e-06
339,543	14.695	8.44	1.84e-06
391,415	14.869	8.60	1.94e-06
426,363	14.934	8.56	1.70e-06
474,866	15.020	8.68	1.24e-06
511,788	15.024	8.60	8.02e-07
557,949	15.039	8.69	6.27e-07
593,998	15.072	8.70	4.22e-07
641,758	15.074	8.70	5.48e-07
815,791	15.198	8.77	1.64e-06
862,868	15.342	8.84	3.49e-06
881,166	15.388	8.79	4.08e-06
902,806	15.390	8.79	6.57e-06
941,375	15.724	8.96	1.23e-05
962,431	15.800	8.92	1.58e-05
980,930	16.444	9.26	1.92e-05
1.03027e+06	17.647	9.86	2.64e-05
1.06717e+06	18.619	10.36	3.27e-05
1.11621e+06	19.92	11.04	4.09e-05
1.14721e+06	21.673	12.05	4.22e-05
1.20264e+06	24.600	14.24	4.68e-05
1.23345e+06	26.412	15.92	5.20e-05
1.28821e+06	27.945	16.82	5.44e-05
1.31695e+06	30.072	18.88	5.56e-05
1.34091e+06	32.379	22.93	5.67e-05

K_i=Initial stress intensity factor at the start of the test; t=time in second;
a=crack length measured from the line of action of the external load;

K=applied stress intensity factor; da/dt=crack growth rate.

Table B22. Stress Corrosion Experimental Data for Specimen SL61 (0.35% NaCl, $K_i = 10MPa\sqrt{m}$)

$t(s)$	$a(mm)$	$K(MPa\sqrt{m})$	$da/dt(mm/s)$
0	14.043	10.06	0
38,444	14.059	10.06	4.48e-07
87,564	14.121	9.89	2.76e-06
125,046	14.229	9.94	3.48e-06
174,092	14.541	10.12	3.42e-06
211,888	14.606	10.16	2.69e-06
260,016	14.676	10.13	1.44e-06
299,663	14.733	10.24	1.76e-06
345,805	14.789	10.27	2.41e-06
385,461	14.931	10.36	4.02e-06
428,233	15.078	10.37	8.95e-06
476,435	15.489	10.54	2.31e-05
525,828	16.785	11.20	4.27e-05
573,187	19.794	13.47	5.82e-05
587,956	20.343	13.74	5.65e-05
601,330	21.011	14.37	4.99e-05
643,375	23.528	16.92	5.38e-05
653,734	24.176	17.50	7.61e-05
665,769	24.613	18.12	7.82e-05
688,335	27.261	22.08	1.03e-04
695,439	27.964	23.44	1.08e-04
731,262	32.123	30.19	1.31e-04

K_i=Initial stress intensity factor at the start of the test;
t=time in second;
a=crack length measured from the line of action of the external load;
K=applied stress intensity factor;
da/dt=crack growth rate.

Table B23. Stress Corrosion Experimental Data for Specimen SL78 (0.35% NaCl, $K_i = 15MPa\sqrt{m}$)

$t(s)$	$a(mm)$	$K(MPa\sqrt{m})$	$da/dt(mm/s)$
14,147	14.104	14.92	6.08e-08
21,348	14.104	14.92	9.23e-08
60,552	14.114	14.71	6.83e-07
69,052	14.114	14.71	1.16e-06
75,496	14.127	14.80	1.07e-06
104,020	14.181	14.85	3.24e-06
145,209	14.384	14.80	4.22e-06
176,157	14.528	15.07	4.45e-06
228,697	14.761	15.21	4.53e-06
274,740	14.899	15.33	5.43e-06
319,129	15.219	15.61	7.25e-06
340,673	15.364	15.75	8.38e-06
365,681	15.581	15.95	9.69e-06

K_i=Initial stress intensity factor at the start of the test;
t=time in second;
a=crack length measured from the line of action of the external load;
K=applied stress intensity factor;
da/dt=crack growth rate.

Table B24. Stress Corrosion Experimental Data for Specimen SL100 (0.35% NaCl, $K_i = 12MPa\sqrt{m}$)

$t(s)$	$a(mm)$	$K(MPa\sqrt{m})$	$da/dt(mm/s)$
44,304	14.577	11.96	5.44e-07
82,223	14.620	11.91	1.36e-06
100,349	14.644	11.93	1.74e-06
117,025	14.674	11.95	2.26e-06
132,003	14.708	11.98	2.51e-06
168,760	14.814	11.98	3.16e-06
189,313	14.920	12.13	3.30e-06
208,833	14.953	12.30	3.31e-06
259,466	15.156	12.29	2.71e-06
277,488	15.184	12.39	2.50e-06
299,938	15.237	12.43	2.34e-06
339,020	15.293	12.39	1.72e-06
390,430	15.382	12.46	1.74e-06
425,721	15.448	12.51	1.96e-06
473,818	15.501	12.55	2.65e-06
511,218	15.617	12.55	3.76e-06
556,906	15.770	12.67	6.34e-06
593,610	15.989	12.83	8.37e-06
640,720	16.436	13.17	1.17e-05
815,430	19.817	15.70	3.33e-05
861,673	21.539	17.38	4.25e-05
880,598	22.701	18.74	4.85e-05
901,613	23.392	19.73	5.25e-05
941,125	25.623	22.98	6.02e-05
961,371	27.215	25.98	6.41e-05

K_i=Initial stress intensity factor at the start of the test;
t=time in second;
a=crack length measured from the line of action of the external load;
K=applied stress intensity factor;
da/dt=crack growth rate.

Table B25. Stress Corrosion Experimental Data for Specimen SL101 (0.35% NaCl, $K_i = 14 MPa\sqrt{m}$)

$t(s)$	$a(mm)$	$K(MPa\sqrt{m})$	$da/dt(mm/s)$
45,131	14.310	13.99	8.67e-07
77,776	14.319	13.63	6.11e-06
101,051	14.363	13.96	1.05e-05
118,670	14.817	14.26	8.77e-06
132,346	14.874	14.31	1.02e-05
170,503	14.978	14.32	3.28e-06
190,195	15.038	14.37	2.98e-06
211,570	15.128	14.45	3.14e-06
260,367	15.243	14.54	2.68e-06
278,455	15.307	14.52	2.29e-06
339,859	15.442	14.55	1.83e-06
392,002	15.442	14.55	8.37e-06
426,744	15.594	14.44	1.32e-05
475,472	16.760	15.39	3.19e-05
512,136	17.626	15.94	4.21e-05
558,580	20.951	19.47	4.76e-05
594,236	22.245	20.82	4.65e-05
642,352	24.315	23.63	4.50e-05

K_i=Initial stress intensity factor at the start of the test;
t=time in second;
a=crack length measured from the line of action of the external load;
K=applied stress intensity factor;
da/dt=crack growth rate.

Table B26. Stress Corrosion Experimental Data for Specimen SL63 (0.1% NaCl, $K_i = 10MPa\sqrt{m}$)

$t(s)$	$a(mm)$	$K(MPa\sqrt{m})$	$da/dt(mm/s)$
20,339	14.059	10.16	6.51e-06
60,675	14.264	10.29	2.58e-06
76,635	14.265	10.29	1.03e-06
90,029	14.265	10.29	6.53e-07
107,601	14.269	10.29	2.07e-06
149,890	14.433	10.39	3.97e-06
188,293	14.461	10.48	6.84e-06
233,460	15.071	10.78	8.06e-06
282,340	15.525	11.15	6.45e-06
317,448	15.614	11.13	4.03e-06
365,036	15.718	10.96	1.94e-06
404,138	15.799	11.17	1.47e-06
455,457	15.846	11.20	8.47e-07
490,718	16.123	11.30	1.73e-05
540,056	17.630	12.36	5.37e-05
577,727	20.316	14.51	1.09e-04
619,149	26.502	22.55	1.90e-04

K_i=Initial stress intensity factor at the start of the test;
t=time in second;
a=crack length measured from the line of action of the external load;
K=applied stress intensity factor;
da/dt=crack growth rate.

Table B27. Stress Corrosion Experimental Data for Specimen SL72 (0.1% NaCl, $K_i = 15MPa\sqrt{m}$)

$t(s)$	$a(mm)$	$K(MPa\sqrt{m})$	$da/dt(mm/s)$
0	14.352	15.22	8.33e-06
45,228	14.410	15.12	1.09e-05
77,125	14.974	15.47	1.29e-05
87,086	15.087	15.57	9.45e-06
105,284	15.196	15.67	3.13e-05
133,579	17.197	17.63	8.99e-05
165,344	20.734	21.55	1.52e-04
173,729	22.102	23.54	1.74e-04

K_i=Initial stress intensity factor at the start of the test;
t=time in second;
a=crack length measured from the line of action of the external load;
K=applied stress intensity factor; da/dt=crack growth rate.

Table B28. Stress Corrosion Experimental Data for Specimen SL69 (0.07% NaCl, $K_i = 10MPa\sqrt{m}$)

$t(s)$	$a(mm)$	$K(MPa\sqrt{m})$	$da/dt(mm/s)$
122,072	14.378	9.94	6.07e-07
139,852	14.379	9.94	7.24e-07
170,155	14.411	9.96	9.23e-07
207,902	14.453	9.98	1.20e-06
249,423	14.503	10.01	1.54e-06
296,641	14.577	10.05	1.68e-06
338,703	14.689	10.12	1.72e-06
385,029	14.732	10.14	1.76e-06
425,287	14.785	10.18	5.66e-06
467,985	15.050	10.33	6.75e-06
514,889	15.395	10.54	7.03e-06
552,833	15.652	10.70	6.51e-06
903,784	16.106	10.83	9.91e-06
945,006	16.442	11.04	1.89e-05
985,385	17.695	11.89	2.48e-05
1.05e+06	19.852	13.28	2.49e-05
1.10e+06	20.741	13.74	1.89e-05
1.12e+06	21.123	14.09	1.65e-05
1.16e+06	28.573	22.63	1.80e-04

K_i=Initial stress intensity factor at the start of the test;
t=time in second;
a=crack length measured from the line of action of the external load;
K=applied stress intensity factor; da/dt=crack growth rate.

Table B29. Stress Corrosion Experimental Data for Specimen SL67 (0.035% NaCl, $K_i = 10MPa\sqrt{m}$)

$t(s)$	$a(mm)$	$K(MPa\sqrt{m})$	$da/dt(mm/s)$
250,200	14.411	10.41	3.87e-07
297,100	14.433	10.42	2.64e-07
339,256	14.433	10.42	1.54e-07
385,538	14.441	10.43	8.53e-08
426,025	14.441	10.43	9.92e-08
468,288	14.447	10.43	1.14e-07
515,685	14.566	10.51	6.02e-07
553,361	14.596	10.52	5.34e-07
600,386	14.600	10.45	4.50e-07
639,917	14.636	10.48	3.79e-07
684,634	14.641	10.48	3.12e-07
727,102	14.658	10.49	2.74e-07
771,390	14.661	10.49	2.54e-07
818,468	14.675	10.50	2.84e-07
859,152	14.677	10.50	2.61e-07
904,228	14.711	10.52	2.37e-07
945,765	14.715	10.52	1.74e-07
985,871	14.715	10.52	1.12e-07
1.12e+06	14.862	10.61	3.00e-07
1.16e+06	14.881	10.62	2.61e-07
1.21e+06	14.885	10.70	2.19e-07
1.25e+06	14.895	10.56	1.82e-07
1.30e+06	14.896	10.56	1.11e-07
1.48e+06	14.909	10.72	2.12e-07
1.51e+06	14.939	10.74	2.39e-07
1.55e+06	14.940	10.74	2.94e-07
1.59e+06	14.950	10.59	3.05e-07
1.64e+06	14.967	10.68	2.55e-07
1.68e+06	14.983	10.61	2.14e-07
1.72e+06	14.985	10.84	1.65e-07
1.76e+06	15.046	10.73	9.50e-07
1.85e+06	15.122	10.85	7.97e-07
1.89e+06	15.160	10.95	7.20e-07
1.94e+06	15.178	10.73	6.74e-07
1.99e+06	15.217	10.91	6.63e-07
2.03e+06	15.243	10.93	6.54e-07
2.07e+06	15.418	11.04	7.99e-07
2.15e+06	15.502	11.02	1.20e-06
2.20e+06	15.556	10.97	1.40e-06
2.33e+06	15.616	11.17	9.55e-07
2.42e+06	15.703	11.15	8.52e-07

2.51e+06	15.753	11.26	7.48e-07
2.54e+06	15.802	11.21	6.94e-07
2.68e+06	15.878	11.34	7.53e-07
2.80e+06	15.986	11.41	1.18e-06
2.89e+06	16.080	11.40	1.30e-06
2.98e+06	16.160	11.45	1.43e-06
3.06e+06	16.389	11.60	1.48e-06
3.15e+06	16.451	11.82	1.37e-06
3.24e+06	16.578	11.90	1.28e-06
3.33e+06	16.666	12.05	1.32e-06
3.42e+06	16.869	12.11	1.21e-06
3.51e+06	16.906	12.14	1.11e-06
4.04e+06	19.077	13.85	6.70e-07
4.24e+06	19.409	14.04	6.70e-07
4.37e+06	19.415	14.05	7.98e-07
4.45e+06	19.419	14.05	8.93e-07
4.55e+06	19.517	14.04	1.01e-06
4.65e+06	19.546	14.06	1.05e-06
4.74e+06	19.567	14.08	9.98e-07
4.79e+06	19.871	14.25	1.10e-06
4.88e+06	19.892	14.06	1.14e-06
4.95e+06	20.046	14.31	9.94e-07
5.07e+06	20.125	14.28	9.97e-07
5.34e+06	20.437	14.69	1.11e-06
5.77e+06	20.758	14.77	1.30e-06
6.18e+06	21.392	15.30	1.48e-06
7.04e+06	23.006	16.51	1.80e-06
7.21e+06	23.457	17.21	1.80e-06
7.38e+06	23.634	17.44	1.90e-06
7.69e+06	23.993	17.93	1.99e-06
7.92e+06	24.666	18.76	2.06e-06
8.12e+06	25.038	19.03	2.12e-06
8.36e+06	25.418	19.33	2.19e-06
8.72e+06	26.484	20.53	2.30e-06

K_i=Initial stress intensity factor at the start of the test;
t=time in second;
a=crack length measured from the line of action of the external load;
K=applied stress intensity factor;
da/dt=crack growth rate.

Table B30. Stress Corrosion Experimental Data for Specimen SL81 (0.035% NaCl, $K_i = 15MPa\sqrt{m}$)

$t(s)$	$a(mm)$	$K(MPa\sqrt{m})$	$da/dt(mm/s)$
42,730	13.937	14.93	0
83,464	13.937	14.85	2.14e-06
128,316	14.139	15.03	2.73e-06
168,986	14.185	15.07	1.15e-06
1.68127e+06	17.084	17.51	2.68e-06

K_i=Initial stress intensity factor at the start of the test;
t=time in second;
a=crack length measured from the line of action of the external load;
K=applied stress intensity factor;
da/dt=crack growth rate.

Table B31. Stress Corrosion Experimental Data for Specimen SL103 (0.035% NaCl, $K_i = 12MPa\sqrt{m}$)

$t(s)$	$a(mm)$	$K(MPa\sqrt{m})$	$da/dt(mm/s)$
118,720	14.232	12.14	5.78e-08
205,007	14.232	12.14	1.43e-07
248,266	14.239	12.14	1.95e-07
272,760	14.239	12.14	1.84e-07
329,032	14.264	12.09	2.95e-07
364,114	14.271	12.09	3.69e-07
415,176	14.277	12.10	5.01e-07
443,965	14.307	12.12	5.30e-07
537,240	14.366	12.23	6.18e-07
590,808	14.422	12.28	4.86e-07
626,317	14.437	12.29	3.64e-07
674,971	14.438	12.29	2.61e-07
715,398	14.445	12.22	1.85e-07
761,049	14.445	12.22	2.63e-07
798,090	14.460	12.23	3.07e-07
846,064	14.479	12.24	3.49e-07
893,803	14.511	12.34	3.14e-07
933,507	14.511	12.34	2.27e-07
969,348	14.523	12.35	3.28e-07
1.02028e+06	14.523	12.27	3.54e-07
1.05000e+06	14.523	12.27	4.60e-07
1.12791e+06	14.616	12.34	6.04e-07
1.22811e+06	14.649	12.36	1.11e-06
1.29834e+06	14.650	12.37	1.17e-06
1.38725e+06	15.024	12.64	1.51e-06
1.48588e+06	15.049	12.66	1.66e-06
1.57951e+06	15.078	12.68	1.58e-06
1.65755e+06	15.479	12.98	1.24e-06
1.83964e+06	15.586	13.06	1.05e-06
2.05516e+06	15.680	12.98	6.43e-07
2.23396e+06	15.768	13.12	3.93e-07
2.51083e+06	15.802	13.15	3.83e-07
2.69340e+06	15.835	13.18	3.69e-07
2.95425e+06	16.078	13.45	3.31e-07
3.29813e+06	16.158	13.51	4.05e-07

3.98844e+06	16.291	13.53	6.02e-07
4.84388e+06	17.090	14.19	8.45e-07
6.05492e+06	18.280	15.16	1.19e-06

K_i=Initial stress intensity factor at the start of the test;
t=time in second;
a=crack length measured from the line of action of the external load;
K=applied stress intensity factor;
da/dt=crack growth rate.

Table B32. Stress Corrosion Experimental Data for Specimen SL104 (0.035% NaCl, $K_i = 14 MPa\sqrt{m}$)

$t(s)$	$a(mm)$	$K(MPa\sqrt{m})$	$da/dt(mm/s)$
37,127	14.358	13.22	1.06e-05
72,909	14.678	13.39	1.07e-05
99,262	15.081	13.71	1.08e-05
121,334	15.883	14.37	1.21e-05
158,401	15.947	14.34	9.65e-06
207,516	16.290	14.71	4.81e-06
250,054	16.291	14.63	3.10e-06
275,723	16.291	14.63	2.94e-06
330,935	16.434	14.76	2.41e-06
366,725	16.733	14.93	2.55e-06
417,056	16.742	15.03	2.31e-06
446,599	16.747	15.03	1.90e-06
539,069	16.892	15.07	1.08e-06
628,123	17.044	15.21	1.04e-06
717,298	17.061	15.23	9.96e-07
799,875	17.119	15.28	9.49e-07
848,672	17.192	15.35	9.43e-07
895,693	17.276	15.42	7.52e-07
936,050	17.276	15.42	6.77e-07
971,304	17.294	15.44	5.18e-07
1.02289e+06	17.294	15.44	4.37e-07
1.05194e+06	17.331	15.47	5.50e-07
1.13069e+06	17.348	15.49	8.42e-07
1.22997e+06	17.503	15.63	1.08e-06
1.30116e+06	17.570	15.70	1.11e-06
1.38909e+06	17.698	15.73	1.09e-06
1.48860e+06	17.794	15.82	1.08e-06
1.58132e+06	17.881	15.90	1.05e-06
1.66032e+06	17.905	15.92	9.57e-07
1.84164e+06	18.226	16.14	1.21e-06
2.05780e+06	18.279	16.10	1.43e-06
2.23570e+06	18.823	16.65	1.38e-06

2.51356e+06	19.294	17.14	1.27e-06
2.69530e+06	19.393	17.25	1.26e-06
2.95697e+06	19.460	17.32	1.15e-06
3.29999e+06	19.995	17.93	9.94e-07
3.99115e+06	20.640	18.47	6.86e-07

K_i=Initial stress intensity factor at the start of the test;
t=time in second;
a=crack length measured from the line of action of the external load;
K=applied stress intensity factor;
da/dt=crack growth rate.

Table B33. Stress Corrosion Experimental Data for Specimen SL105 (0.035% NaCl, $K_i = 8MPa\sqrt{m}$)

$t(s)$	$a(mm)$	$K(MPa\sqrt{m})$	$da/dt(mm/s)$
36,130	14.490	7.88	9.36e-10
72,246	14.491	7.88	4.64e-09
98,538	14.491	7.88	7.34e-09
330,217	14.495	7.88	3.13e-08
365,728	14.495	7.88	2.52e-07
416,276	14.499	7.89	7.91e-07
445,589	14.499	7.89	9.59e-07
538,428	14.571	7.84	5.86e-06
592,430	14.780	7.94	9.13e-06
627,414	15.609	8.25	9.05e-06
676,606	16.072	8.48	9.13e-06
716,571	16.613	8.75	7.79e-06
762,615	16.703	8.71	4.79e-06
799,191	16.753	8.74	3.65e-06
847,722	16.864	8.80	2.57e-06
894,876	17.014	8.88	2.38e-06
935,085	17.181	8.96	3.84e-06
970,466	17.229	8.99	4.76e-06
1.02184e+06	17.251	9.00	7.77e-06
1.05126e+06	17.890	9.35	9.98e-06
1.12960e+06	18.458	9.59	1.42e-05
1.22922e+06	21.2000	11.31	1.23e-05
1.29997e+06	21.781	11.77	9.15e-06
1.38834e+06	21.995	11.83	5.81e-06
1.48744e+06	22.049	11.87	1.75e-06
1.58062e+06	22.128	11.94	9.55e-07
1.65927e+06	22.151	11.96	7.85e-07
1.84091e+06	22.310	12.09	1.45e-06
2.05677e+06	22.623	12.12	3.71e-06
2.23498e+06	23.064	12.38	4.52e-06
2.51300e+06	26.459	15.78	4.91e-06
2.69462e+06	26.740	15.84	5.21e-06
2.95592e+06	27.271	16.27	4.77e-06
3.29930e+06	28.613	17.11	4.19e-06
3.99016e+06	31.898	22.02	3.02e-06

K_i=Initial stress intensity factor at the start of the test;
t=time in second;
a=crack length measured from the line of action of the external load;
K=applied stress intensity factor;
da/dt=crack growth rate.

Table B34. Stress Corrosion Experimental Data for Specimen SL106 (0.035% NaCl, $K_i = 6MPa\sqrt{m}$)

$t(s)$	$a(mm)$	$K(MPa\sqrt{m})$	$da/dt(mm/s)$
2.6936e+06	14.093	5.95	5.44e-08
2.9547e+06	14.129	6.03	4.91e-08
3.2981e+06	14.164	5.97	4.20e-08
3.9889e+06	14.179	5.98	2.78e-08
4.8441e+06	14.159	5.97	1.24e-08
6.0552e+06	14.176	5.98	2.77e-08
6.5733e+06	14.176	5.98	3.84e-08
8.3718e+06	14.292	6.16	9.47e-08
8.4521e+06	14.308	6.17	1.32e-07
8.4919e+06	14.315	6.17	7.86e-08
8.5352e+06	14.330	6.18	8.24e-08
9.9217e+06	14.312	6.32	1.02e-08
1.0180e+07	14.310	6.32	1.19e-08
1.0902e+07	14.330	5.95	1.64e-08
1.1086e+07	14.332	5.96	1.40e-08
1.1511e+07	14.343	5.96	8.20e-09
1.1990e+07	14.344	6.04	1.48e-09
1.2289e+07	14.336	6.18	1.18e-09
1.5908e+07	14.336	6.33	1.01e-08
1.6010e+07	14.333	6.33	3.69e-08
1.6118e+07	14.344	6.41	5.03e-08
1.6617e+07	14.353	6.41	7.98e-08
1.7484e+07	14.464	6.45	5.76e-08
1.9783e+07	14.503	8.34	8.39e-08
1.9925e+07	14.524	8.87	2.05e-07
2.0058e+07	14.533	9.25	1.84e-07
2.0110e+07	14.587	9.73	1.63e-07
2.0258e+07	14.587	10.41	1.57e-07
2.0304e+07	14.596	10.87	1.47e-07
2.0463e+07	14.602	11.32	9.69e-08
2.0645e+07	14.641	11.73	9.02e-08
2.0726e+07	14.649	12.26	9.23e-08
2.0897e+07	14.649	12.79	1.16e-07
2.1273e+07	14.649	13.32	2.98e-07
2.1277e+07	14.700	13.89	2.71e-07

2.1366e+07	14.781	14.33	3.63e-07
2.1543e+07	14.798	14.50	6.41e-07
2.1625e+07	14.823	14.98	7.56e-07
2.1773e+07	14.952	15.09	6.91e-07
2.1839e+07	15.060	16.35	6.59e-07
2.1973e+07	15.087	16.99	1.95e-07
2.2147e+07	15.090	17.23	1.85e-07
2.2565e+07	15.255	18.34	6.39e-07
2.2727e+07	15.255	18.73	8.45e-07
2.3026e+07	15.686	19.60	1.22e-06

K_i=Initial stress intensity factor at the start of the test;
t=time in second;
a=crack length measured from the line of action of the external load;
K=applied stress intensity factor;
da/dt=crack growth rate.

Table B35. Stress Corrosion Experimental Data for Specimen SL114 (0.01% NaCl, $K_i = 8MPa\sqrt{m}$)

$t(s)$	$a(mm)$	$K(MPa\sqrt{m})$	$da/dt(mm/s)$
1.0084e+06	14.101	8.02	1.988e-08
1.5303e+06	14.108	8.03	1.883e-07
1.6307e+06	14.150	8.05	2.856e-07
1.7886e+06	14.199	8.07	3.425e-07
1.9009e+06	14.226	8.08	3.418e-07
2.0467e+06	14.326	8.06	2.429e-07
2.1640e+06	14.343	8.14	1.532e-07
2.2469e+06	14.332	8.13	1.552e-07
2.3358e+06	14.326	8.21	1.511e-07
2.4268e+06	14.341	8.14	1.101e-07
2.5010e+06	14.383	8.16	1.291e-07
2.5111e+06	14.383	8.23	1.597e-07
2.6951e+06	14.380	8.16	4.039e-08
2.9520e+06	14.378	8.16	3.054e-09
3.1195e+06	14.377	8.16	2.451e-08
3.2879e+06	14.381	8.17	3.684e-08
3.5988e+06	14.397	8.09	5.477e-08
3.8983e+06	14.440	8.19	5.779e-08
4.2409e+06	14.440	8.19	5.845e-08
4.6710e+06	14.455	8.20	6.618e-08
6.2331e+06	14.586	8.26	8.423e-08
7.1713e+06	14.698	8.31	8.425e-08
7.5163e+06	14.691	8.31	5.859e-08
7.6188e+06	14.706	8.31	6.561e-08
7.7263e+06	14.714	8.39	4.580e-08
8.2262e+06	14.724	8.40	5.366e-08
9.0933e+06	14.785	8.42	5.129e-08
1.1249e+07	14.866	9.01	7.770e-08
1.1302e+07	14.881	9.48	9.536e-08
1.1348e+07	14.958	10.07	2.133e-07
1.1392e+07	14.958	10.46	3.945e-07
1.1533e+07	14.966	10.93	2.653e-07
1.1667e+07	14.974	11.32	4.289e-07
1.1718e+07	15.000	11.81	3.517e-07
1.1867e+07	15.145	12.61	3.377e-07

1.1912e+07	15.145	13.01	4.078e-07
1.2072e+07	15.145	13.48	1.680e-07
1.2254e+07	15.145	13.95	1.859e-08
1.2334e+07	15.155	14.51	3.774e-08
1.2505e+07	15.155	14.67	6.846e-08
1.2885e+07	15.167	15.70	2.089e-07
1.2974e+07	15.242	16.80	2.035e-07
1.3151e+07	15.263	17.21	3.638e-07
1.3234e+07	15.296	17.88	5.215e-07
1.3381e+07	15.312	18.37	6.556e-07
1.3447e+07	15.437	19.07	7.167e-07
1.3576e+07	15.582	19.63	7.445e-07
1.3755e+07	15.705	20.26	6.297e-07
1.3904e+07	15.761	20.65	3.862e-07
1.4173e+07	15.781	21.17	3.879e-07
1.4336e+07	15.791	21.67	6.745e-07
1.4634e+07	15.811	22.02	1.198e-06
1.5723e+07	18.412	24.77	3.112e-06

K_i=Initial stress intensity factor at the start of the test;
t=time in second;
a=crack length measured from the line of action of the external load;
K=applied stress intensity factor;
da/dt=crack growth rate.

Table B36. Stress Corrosion Experimental Data for Specimen SL115 (0.01% NaCl, $K_i = 10MPa\sqrt{m}$)

$t(s)$	$a(mm)$	$K(MPa\sqrt{m})$	$da/dt(mm/s)$
419,236	14.240	10.18	1.365e-08
513,408	14.249	10.18	2.232e-08
747,822	14.248	10.18	2.573e-08
843,947	14.239	10.17	2.024e-08
1.0081e+06	14.239	10.17	3.537e-08
1.5302e+06	14.298	10.21	1.208e-07
1.6302e+06	14.297	10.21	1.614e-07
1.7885e+06	14.318	10.22	1.710e-07
1.9002e+06	14.344	10.24	1.925e-07
2.0465e+06	14.394	10.19	1.902e-07
2.1635e+06	14.394	10.19	1.553e-07
2.2467e+06	14.428	10.29	1.435e-07
2.3352e+06	14.422	10.28	2.308e-07
2.4265e+06	14.432	10.29	2.409e-07
2.5004e+06	14.450	10.30	2.369e-07
2.5109e+06	14.514	10.11	3.053e-07
2.6909e+06	14.521	10.11	2.688e-07
2.9518e+06	14.589	10.15	2.378e-07
3.1189e+06	14.626	10.10	1.811e-07
3.2876e+06	14.696	10.22	1.846e-07
3.5980e+06	14.712	10.15	1.514e-07
3.8982e+06	14.710	10.23	1.569e-07
4.2403e+06	14.797	10.28	1.715e-07
4.6708e+06	14.911	10.43	2.073e-07
6.2329e+06	15.273	10.49	2.753e-07
7.1710e+06	15.537	10.73	3.065e-07
7.5157e+06	15.697	10.75	2.359e-07
7.6187e+06	15.679	10.74	1.868e-07
7.7257e+06	15.716	10.76	1.244e-07
8.2260e+06	15.747	10.87	5.937e-08
9.0932e+06	15.782	10.89	8.110e-08
1.1249e+07	15.971	11.42	1.951e-07
1.1301e+07	16.016	11.87	3.068e-07
1.1348e+07	16.139	12.54	7.137e-07
1.1391e+07	16.159	13.06	9.946e-07

1.1533e+07	16.239	13.71	6.930e-07
1.1666e+07	16.309	14.28	5.018e-07
1.1718e+07	16.368	14.92	4.257e-07
1.1867e+07	16.417	15.73	2.811e-07
1.1912e+07	16.417	16.32	2.228e-07
1.2071e+07	16.417	16.84	9.325e-08
1.2253e+07	16.427	17.36	7.657e-08
1.2334e+07	16.427	18.21	9.260e-08
1.2505e+07	16.470	18.85	1.267e-07
1.2881e+07	16.514	19.59	2.014e-07

K_i=Initial stress intensity factor at the start of the test;
t=time in second;
a=crack length measured from the line of action of the external load;
K=applied stress intensity factor;
da/dt=crack growth rate.

Table B37. Stress Corrosion Experimental Data for Specimen SL116 (0.01% NaCl, $K_i = 12MPa\sqrt{m}$)

$t(s)$	$a(mm)$	$K(MPa\sqrt{m})$	$da/dt(mm/s)$
845,038	14.033	12.14	9.619e-08
1.0087e+06	14.032	12.14	1.326e-07
1.5304e+06	14.140	12.21	2.490e-07
1.6313e+06	14.157	12.22	3.193e-07
1.7887e+06	14.224	12.27	5.613e-07
1.9015e+06	14.245	12.29	6.729e-07
2.0469e+06	14.335	12.35	7.691e-07
2.1645e+06	14.553	12.51	7.387e-07
2.2471e+06	14.599	12.62	6.514e-07
2.3363e+06	14.591	12.61	4.740e-07
2.4270e+06	14.655	12.51	3.735e-07
2.5014e+06	14.672	12.67	3.297e-07
2.5112e+06	14.688	12.61	3.961e-07
2.6525e+06	14.734	12.64	2.237e-07
2.9522e+06	14.782	12.60	2.821e-07
3.1202e+06	14.821	12.63	3.104e-07
3.2881e+06	14.915	12.78	3.274e-07
3.5995e+06	15.015	12.47	3.584e-07
3.8985e+06	15.150	12.88	3.246e-07
4.2414e+06	15.239	13.02	2.979e-07
4.6712e+06	15.295	13.06	3.067e-07
6.2334e+06	15.898	13.45	4.200e-07
7.1711e+06	16.349	13.81	4.683e-07
7.5170e+06	16.494	13.93	3.238e-07
7.6188e+06	16.531	13.96	4.285e-07
7.7270e+06	16.548	13.98	4.432e-07
8.2261e+06	16.588	14.01	4.271e-07
9.0933e+06	17.217	14.46	3.482e-07
1.1250e+07	17.493	16.01	1.179e-07
1.1302e+07	17.532	16.57	1.020e-07
1.1349e+07	17.764	17.78	9.941e-07
1.1392e+07	17.805	18.36	1.675e-06
1.1534e+07	17.938	19.05	7.677e-07
1.1667e+07	17.938	19.50	3.442e-07
1.1719e+07	17.949	20.32	4.793e-07

1.1867e+07	17.952	20.86	5.453e-07
1.1913e+07	18.038	21.33	7.017e-07
1.2072e+07	18.223	22.40	1.308e-06
1.2254e+07	18.333	23.01	2.108e-06
1.2334e+07	18.696	24.28	2.459e-06
1.2505e+07	19.149	24.88	3.209e-06

K_i=Initial stress intensity factor at the start of the test;
t=time in second;
a=crack length measured from the line of action of the external load;
K=applied stress intensity factor;
da/dt=crack growth rate.

Table B38. Stress Corrosion Experimental Data for Specimen SL70 (0.01% NaCl, $K_i = 10MPa\sqrt{m}$)

$t(s)$	$a(mm)$	$K(MPa\sqrt{m})$	$da/dt(mm/s)$
1.65567e+06	14.051	10.14	7.83e-08
1.69815e+06	14.058	10.00	6.57e-08
1.74479e+06	14.058	10.15	5.18e-08
1.78665e+06	14.061	10.22	3.93e-08
1.83338e+06	14.061	10.22	2.51e-08
1.87338e+06	14.062	10.15	2.80e-08
2.00841e+06	14.062	10.22	1.69e-07
2.04474e+06	14.074	10.08	1.88e-07
2.09163e+06	14.080	10.23	1.91e-07
2.13671e+06	14.104	10.18	1.96e-07
2.18176e+06	14.106	10.18	1.60e-07
2.22172e+06	14.107	10.18	1.12e-07
2.26442e+06	14.111	10.25	1.62e-07
2.39113e+06	14.119	10.11	1.36e-07
2.87469e+06	14.198	10.53	8.17e-08
3.47838e+06	14.197	10.45	3.97e-08
3.95263e+06	14.201	10.45	2.05e-08
4.05431e+06	14.224	10.47	4.81e-08
4.29616e+06	14.231	10.40	7.33e-08
4.37936e+06	14.231	10.40	7.97e-08
4.84169e+06	14.270	10.42	1.16e-07
5.27127e+06	14.35	10.47	1.90e-07
5.68349e+06	14.401	10.43	2.29e-07
6.54002e+06	14.745	10.64	2.68e-07
6.71307e+06	14.766	10.65	2.60e-07
7.19105e+06	14.802	10.75	2.11e-07
7.42569e+06	14.946	10.92	3.30e-07
7.61823e+06	14.967	10.93	3.61e-07
7.86259e+06	14.988	10.94	4.52e-07
8.22431e+06	15.315	11.23	4.91e-07
8.57473e+06	15.414	11.30	4.90e-07
8.95977e+06	15.773	11.46	4.42e-07
9.59604e+06	15.783	11.46	2.89e-07
9.95264e+06	15.970	11.59	2.40e-07
1.04345e+07	16.077	11.66	2.03e-07

1.07767e+07	16.080	11.67	1.92e-07
1.09641e+07	16.143	11.71	3.39e-07
1.11211e+07	16.161	11.72	3.97e-07
1.13146e+07	16.249	11.78	4.70e-07
1.14648e+07	16.413	11.90	5.26e-07

K_i=Initial stress intensity factor at the start of the test;
t=time in second;
a=crack length measured from the line of action of the external load;
K=applied stress intensity factor;
da/dt=crack growth rate.

Table B39. Stress Corrosion Experimental Data for Specimen SL83 (0.01% NaCl, $K_i = 15MPa\sqrt{m}$)

$t(s)$	$a(mm)$	$K(MPa\sqrt{m})$	$da/dt(mm/s)$
524,926	14.008	14.87	7.16e-08
626,672	14.008	14.87	1.19e-07
1.10308e+06	14.008	14.73	7.51e-07
1.19523e+06	14.220	14.98	7.48e-07
1.29659e+06	14.239	15.07	8.98e-07
1.36156e+06	14.254	15.09	5.54e-07
1.44707e+06	14.393	14.92	5.00e-07
1.89685e+06	14.475	15.28	1.93e-07
2.60458e+06	14.489	15.29	9.92e-08
3.12444e+06	14.508	15.31	3.17e-07
3.86747e+06	14.684	15.40	6.61e-07
4.93626e+06	16.160	16.71	8.79e-07
6.9217e+06	17.639	18.06	7.24e-07
1.16635e+07	20.160	20.73	3.52e-07

K_i=Initial stress intensity factor at the start of the test;
t=time in second;
a=crack length measured from the line of action of the external load;
K=applied stress intensity factor;
da/dt=crack growth rate.

Table B40. Incremental load experiment for the determination of K_{ISCC} (Specimen SL92, 3.5% NaCl, $dP/dt = 2.14e-4N/s$)

$t(s)$	$a(mm)$	$K(MPa\sqrt{m})$	$da/dt(mm/s)$
0	14.360	1.54	0
1.79735e+06	14.360	4.34	0
1.88072e+06	14.367	4.49	2.49e-07
1.96340e+06	14.382	4.65	3.43e-07
2.05722e+06	14.461	4.82	3.40e-07
2.14388e+06	14.464	4.97	2.78e-06
2.24535e+06	14.477	5.12	5.01e-06
2.31094e+06	15.577	5.46	5.24e-06
2.39976e+06	15.838	5.54	4.58e-06
2.50844e+06	16.109	5.63	3.77e-06

P=applied load
dP/dt=rate of applied load
t=time in second;
a=crack length measured from the line of action of the external load;
K=applied stress intensity factor;
da/dt=crack growth rate.

Table B41. Incremental load experiment for the determination of K_{ISCC} (Specimen SL93, 0.1% NaCl, $dP/dt = 2.27e-4N/s$)

$t(s)$	$a(mm)$	$K(MPa\sqrt{m})$	$da/dt(mm/s)$
1.03905e+06	14.569	1.08	0
4.48388e+06	14.569	6.20	0
4.57515e+06	14.607	6.37	4.23e-07
4.67168e+06	14.618	6.45	4.49e-07
4.74997e+06	14.730	6.57	5.62e-07
5.19993e+06	14.742	6.72	3.88e-06
5.27081e+06	15.947	7.38	4.57e-06

P=applied load
dP/dt=rate of applied load
t=time in second;
a=crack length measured from the line of action of the external load;
K=applied stress intensity factor;
da/dt=crack growth rate.

Table B42. Incremental load experiment for the determination of K_{ISCC} (Specimen SL94, 0.35% NaCl, $dP/dt = 2.26e-4 N/s$)

$t(s)$	$a(mm)$	$K(MPa\sqrt{m})$	$da/dt(mm/s)$
950,908	14.15	1.07	0
3.19821e+06	14.15	4.01	0
3.28797e+06	14.684	4.21	5.94e-06
3.45495e+06	15.104	4.32	2.52e-06

P=applied load
dP/dt=rate of applied load
t=time in second;
a=crack length measured from the line of action of the external load;
K=applied stress intensity factor;
da/dt=crack growth rate.

Table B43. Incremental load experiment for the determination of K_{ISCC} (Specimen SL95, 1.0% NaCl, $dP/dt = 2.19e-4 N/s$)

$t(s)$	$a(mm)$	$K(MPa\sqrt{m})$	$da/dt(mm/s)$
0	14.064	1.52	0
2.07339e+06	14.064	4.45	0
2.16806e+06	14.100	4.60	3.80e-07
2.31080e+06	14.222	4.78	8.55e-07
2.42196e+06	14.788	4.95	5.09e-06

P=applied load
dP/dt=rate of applied load
t=time in second;
a=crack length measured from the line of action of the external load;
K=applied stress intensity factor;
da/dt=crack growth rate.

Table B44. Incremental load experiment for the determination of K_{ISCC} (Specimen SL96, 0.035% NaCl, $dP/dt = 2.24e-4N/s$)

$t(s)$	$a(mm)$	$K(MPa\sqrt{m})$	$da/dt(mm/s)$
80,828	13.835	1.15	0
3.45584e+06	13.835	7.54	0
3.53601e+06	13.839	7.76	4.99e-08
3.62116e+06	13.858	8.06	2.23e-07
3.70496e+06	13.866	8.06	9.55e-08
4.05658e+06	13.872	9.36	1.71e-08
4.31201e+06	13.883	10.4	4.31e-08

P=applied load
dP/dt=rate of applied load
t=time in second;
a=crack length measured from the line of action of the external load;
K=applied stress intensity factor;
da/dt=crack growth rate.

Table B45. Incremental load experiment for the determination of K_{ISCC} (Specimen SL97, 0.7% NaCl, $dP/dt = 2.25e-4N/s$)

$t(s)$	$a(mm)$	$K(MPa\sqrt{m})$	$da/dt(mm/s)$
0	14.486	1.05	0
1.80702e+06	14.486	4.05	0
1.89614e+06	14.523	4.21	4.04e-07
1.99526e+06	14.572	4.37	5.04e-07
2.06105e+06	14.598	4.53	3.95e-07
2.15572e+06	14.604	4.68	5.28e-08
2.24590e+06	14.634	4.84	3.44e-07

P=applied load
dP/dt=rate of applied load
t=time in second;
a=crack length measured from the line of action of the external load;
K=applied stress intensity factor;
da/dt=crack growth rate.

Table B46. Incremental load experiment for the determination of K_{ISCC} (Specimen SL98, 5.0% NaCl, $dP/dt = 2.24e-4N/s$)

$t(s)$	$a(mm)$	$K(MPa\sqrt{m})$	$da/dt(mm/s)$
0	13.915	1.80	0
1.56677e+06	13.915	4.26	0
1.65207e+06	13.931	4.41	1.99e-07
1.74066e+06	14.020	4.43	9.93e-07
1.90568e+06	14.326	4.73	1.86e-06
2.08674e+06	14.360	4.82	1.82e-07
2.17779e+06	14.360	4.82	0
2.25424e+06	14.380	4.82	2.62e-07
2.33831e+06	14.399	4.83	2.26e-07
2.51506e+06	14.425	4.83	1.53e-07
2.60848e+06	14.572	5.03	1.56e-06

P=applied load
dP/dt=rate of applied load
t=time in second;
a=crack length measured from the line of action of the external load;
K=applied stress intensity factor;
da/dt=crack growth rate.